Case Study of Foehn Events Over Alborz Mountains in Iran

By: Jafar (Jeff) Sepehri

Supervisors: Peter Taylor

Chair: Yongsheng Chen

Committee Member: Gary Klaassen

Internal Member: Ronald Hanson

Graduated Program in Earth and Space Science

York University

Toronto, Ontario

August 2022

Abstract

Warm and dry foehn winds can significantly affect human life in mountainous regions worldwide. Foehn's features include rising temperature, dropping relative humidity, and a fixed direction high wind commencement. Iran, a mountainous country, is affected by foehn in many places. The northern area of Iran is bordered by the Caspian Sea in the north and the Alborz Mountains in the south. The southwest part of the Caspian Sea coastal area is studied here. Large-amplitude Mountain waves have occurred and caused severe wildfires in the Caspian forests.

This study demonstrates that foehn events can occur due to high pressure over the interior regions and a lee cyclone over the southern Caspian Sea, with a strong south-north pressure gradient across the Alborz Mountains. Four typical 2021 wind events will be used to illustrate this foehn situation. Sample simulation results indicate the performance of WRF in predicting the variations of meteorological quantities.

Dedication

To my teachers and their teachers

Acknowledge

Firstly, I would like to express my sincere gratitude to my supervisor, Prof. Peter Taylor, for support of my MSc study and related research, his patience, motivation, and knowledge. His guidance helped me during the time of research and writing of this thesis. I could not have imagined having a better advisor and mentor for my MSc study.

Besides my advisor, I would like to thank Prof. Yongsheng Chen, a member of my supervisory committee, for his insightful comments, invaluable advice, and encouragement, but also for the hard questions which incented me to widen my research from various perspectives. I must also thank my examiners for taking the time to carefully review the thesis.

My sincere thanks also go to Prof. Mark D Gordon and Prof. Gary Klaassen, who provided me with an opportunity to progress my research. Without their precious support, conducting this research in the last two years would not be possible.

My special thanks to Ms. Marcia Gaynor, graduate program assistant, for her guidance and orientation.

I am grateful to Copernicus Climate Change Service (C3S) Climate Data Store for providing ERA5 data. Moreover, meteorological station data were gathered from IRIMO, which the author is grateful for.

I appreciate York University, Lassonde School of Engineering, and the Department, which allowed me to continue my studies in the field of my choice.

I am incredibly grateful to “my teachers and their teachers” from the first step of preschool. Also, I would like to thank professors M.T. Zamanian, M. Azarakhsh, M. Zadeh, and E. Taghizadeh.

Not forgetting, my appreciation also goes to my friends, classmates and colleagues for their encouragement and support throughout my studies.

Last but certainly not least, I would like to thank my wife and my family for spiritually supporting me through writing this thesis and my life in general.

Table of Contents

Chapter 1

Introduction

1.1 Introduction

When air flows over a mountain ridge, moisture-depleted drier air occasionally accelerates down the lee slope, producing arid and strong downslope wind, known as foehn wind. As (Lin 2007) wrote, it has been almost two centuries that scientists have paid attention to it from a scientific view. Foehn wind is a meteorological phenomenon in all mountain areas in the world. Due to its importance, WMO in 1992 published the following definition for this warm and dry wind. "Wind [which is] warmed and dried by descent, in general on the lee side of a mountain." It has a considerable impact on human life positively and negatively. Besides, it affects traffic, aviation, and even marine transportation near mountains and cliffs.

The name was originated in the middle of Europe where Alpine Mountains have a significant effect on the inhabitant's life. In etymology, the word Foehn has a Latin root, "Faonius," which means the wind coming from the west. But it doesn't mean that the wind occurs only in this region. In other parts of the world, it has different names. As Brinkman (1971) wrote, "the wind has also local names such as *Chinook* of the Rocky Mountains, the *South Foehn* north of Alps, the *North Foehn* south of Alps, the *Germich* (or *Garmij*) of the south-western part of the Caspian Sea, the *Santa Ana* of Southern California".

Foehn wind has a significant effect on local weather phenomena including humidity and surface air temperature. Richner and Hächler (2013) mentioned that "the Foehn wind has both affirmative and negative momentous impacts on indwelling life".

1.2 Background

"Foehn occurrence has been attributed to two main mechanisms" (Sharples et al., 2010). "The first involves the forced ascent of moist air over a mountain barrier. As the moist air rises, adiabatic cooling ultimately results in condensation and precipitation. The precipitation removes moisture from the air mass and the latent heat of condensation raises the temperature of the air. The drier air is then warmed further because of adiabatic compression as it descends the lee slopes" (Hann 1866, 1867; Barry 1992; Whiteman 2000). "This type of foehn can be referred to as thermodynamically driven. The second mechanism involves the upstream blocking of lower-level air by a mountain barrier, with drier upper air flowing down to replace it in the lee of the mountains. As the drier air from above descends the lee slopes it is warmed by adiabatic compression. Given the role of mechanical blocking, this type of foehn can be referred to as mechanically driven."

“Instances of mechanically driven foehn winds have been studied by Cook and Topil (1952), Brinkmann (1973, 1974), Lockwood (1962), Seibert (1990), and Ustrnul (1992). It is typical for the mechanically driven foehn to occur in association with a vertically propagating lee mountain wave (Lockwood 1962; Drobinski et al. 2007; Drechsel and Mayr 2008).”

For research on foehn-type winds in different parts of the world, see e.g. Brinkmann (1974) (Rocky Mountains), McGowan et al. (2002) (New Zealand Apls), Raphael (2003) (Santa Ana Winds), or Richner and Hächler (2013) (Alpine regions). Gaffin (2007) studied a 30-yr (1971-2000) period over the Appalachian Mountains. He found that “foehn wind events on the western side typically occurred as southeasterly winds developed ahead of a low-pressure system over the mid-Mississippi River Valley. In contrast, foehn wind events on the eastern side were usually the result of northwesterly winds behind the passage of the shallow cold front”. He also mentioned “the rise in surface dewpoints at the foehn stations during nearly three-fourths of the events on the western side and around one-third of the events on the eastern side”. Comparing the “dewpoint-rise composites to the composites from all foehn wind events near the southern Appalachians revealed that the rise in surface dewpoints was mainly the result of a drier initial surface (compared with the 850-hPa air mass) and not necessarily a moister 850-hPa air mass”.

Plavcan et al. (2014) presented an “automatic classification scheme” to obtain information about the (un)certainty of “diagnosing foehn winds from weather station data downwind of topographic obstacles”. They also used a statistical mixture model to separate foehn and no-foehn currents in a measured time series of wind. In addition, it accommodated other physically meaningful classifiers to wind speed and direction, such as the (potential) temperature difference to an upwind station or relative humidity. They explained that using only wind information gave nearly identical foehn frequencies when using additional covariables. It is from the point of view of climatology. “The suitability of mixture models for objective classification of foehn at other locations will have to be tested in future studies”.

Mofidi et al. (2015) investigated a “southerly foehn in the Alborz Mountains in northern Iran by using a combination of observations, reanalysis, and simulation data”. Their results indicate “a mechanically driven foehn occurred in the Alborz chain Mountains during December 16-18, 2005”. They mentioned “the foehn event occurred due to high pressure over the interior regions of Iran and lee cyclone over the southern Caspian Sea, with a robust south-north pressure gradient across the Alborz chain Mountains”. Taghavi et al. (2015) explored foehn characteristics and its

temporal evolution events, which had caused an extensive and high-intensify fire in the Gilan province and Mazandaran province "Caspian Hyrcanian mixed forests" in northern Iran. They concluded that a mechanically driven foehn event occurred in Alborz chain Mountains during December 4-5, 2012, and January 3-9, 2013.

Sprenger et al. (2017) used a "machine learning algorithm" (called AdaBoost, short form for Adaptive Boosting). Three years (from 2000 to 2002) of hourly simulations of the Consortium for Small-Scale Modeling's (COSMO) numerical weather prediction (NWP) model for foehn prediction and corresponding foehn wind observations were used to train the algorithm to distinguish between foehn and non-foehn events. The concise outcome of their results was "the probability of detection (88.2%), probability of false detection (2.9%), missing rate (11.8%), correct alarm ratio (66.2%), false alarm ratio (33.8%), and missed alarm ratio (0.8%). They also discussed the predictability of foehn events during the four seasons. They mentioned that the correct alarm ratio was highest in winter (86.5%), followed by spring (79.6%), autumn (69.2%), and the lowest ratio found in summer (48.8%)".

Mayr et al. (2018) set out the "Community Foehn Classification Experiment to quantify the uncertainly of human foehn classifications, compare them to machine classification, and provide a dataset for the development of foehn classification algorithms". Three groups of human experts and two objective algorithms faced the task of identifying foehn periods. Different points were results from that work, such as, uncertainly is largest for onset and even more so for the ending of a foehn event and also larger during the night; combining advance statistical and/or machine learning models with physically based concepts for choosing their input variables yields similar results to those of human experts. It is highly recommended to develop objective classification, ideally without resorting to manually specified and hard limits.

In the Southern Hemisphere, foehn research has been conducted in New Zealand (McGowan and Sturman, 1996; McGowan et al., 2002), the Antarctic Peninsula (Speirs et al., 2010, Turton et al., 2018; Cape et al., 2015) and South America (Garreaud, 2009; Norte, 2015; Temme et al., 2020).

"While most studies of foehn events have focused on a few selected regions, such as the European Alps and Rocky Mountains in the western most part of North America, similar events in northern Iran are not well represented in the meteorological literature. Many forest fires occur in Iran. For example, approximately 5,357 ha of Iran's forests burned during the period from 1990

to 1992, of which 2,155 ha were in the north of Iran" (Jazirehei, 1995). In addition, "about 1,258 wildfire events occurred in the northern forests of Iran between 1998 and 2005, burning 7,623 ha of forests. According to some reports, forty-six foehn events, locally known as Garmij[1], caused wildfires from 1976 to 1990 over the northern regions of Iran and account for approximately 44% of the total forest fires and other environmentally damaging events in the country" (Parnian 1999). Shirzadi (1992) studied "the synoptic and physical conditions of the foehn phenomenon and its destructive effects using different techniques such as the Nesterov index" (Nesterov, 1949), the Franssila index (Franssila, 1959), and other methods, which use the reduction in humidity for the northern parts of Iran. She concluded that the "domination of extra-tropical cyclones moving eastward through the Caspian Sea region should be the main reason for the occurrence of foehn in the lee of the Alborz Mountains. She also noted that the number of hectares burned increases during foehn wind events". Parnian (1999) investigated "foehn occurrence conditions in Gilan and Mazandaran provinces and obtained the same results".

Khashjan (2019) studied the effect of meteorological variables and occurrence of foehn phenomena on forest fires investigated using a combination of time series observations analysis, synoptic analysis, and simulation data in Zagros Mountains, in northwestern Iran and roughly follows Iran's western border. He used WRF numerical model to clarify the effect of meteorological variables on forest fires. He found that both sides of the Zagros Mountains are hot and dry, and these conditions are far more severe on the windward side. The results from the output of the WRF model showed that the surface pressure gradient between the windward and leeward Zagros Mountains is very low. The prevailing conditions in the region indicate the absence of the foehn phenomena in the region. His results suggest that "the mountain waves excited over the southern slopes of the Zagros Mountains are the primary source of the localized wind maximum around the lee side of Zagros".

1.3 Characteristics of Foehn

Foehn is an outstanding example to explain thermodynamic processes and the role of latent heat in the atmosphere. A simple graph of it, like Figure 1-1 could be seen in nearly every textbook. Hann (1901) displays the downslope of warm foehn flow on the Northside of the Alpine mountains when the southern region has resting cold air. In his book "Lehrbuch der Meteorologie," he

[1] Garmij is a local name for a foehn event in north of Alborz Mountains that means an extremely warm wind.

describes two kinds of Foehn wind (Figure 1-1 and Figure 1-2). In addition, he mentioned that there are other kinds of foehn wind besides these two. As explained by nearly every classical textbook, foehn could illustrate the role of latent heat in the atmosphere. Flowing of humid air towards a mountain range, causes dry-adiabatic ascent by forced convection, then cooling and reaching saturation. After that, until the top of the mountain range, the air rises wet-adiabatically, clouds are formed, and precipitation occurs. On the other hand, on the lee side, by descent the air and dry-adiabatic heating, it becomes dry (reduced RH) and the temperature is higher than the original temperature on the windward at the same elevation. Over the crest, the piled-up clouds can be seen (foehn wall[1]), and in the lee side clear, visibility is excellent (foehn window[2]).

However, in reality, foehn winds do not always follow this theory, and other researchers challenged this classical approach (Seibert, 2005). Scorer (1978) mentioned "two mechanisms for the warming of air masses without requiring the heat of condensation on the windward slope of the mountain ridge". In the first case, "the lower part becomes warmer, and the upper part cools when mixing produces a constant potential temperature, mentioned as the mechanical stirring of a stably stratified air mass". In the second, "a more important case block occurs upwind over potentially warmer air subsides in the lee".

The Alpine Experiment ALPEX in 1982 made an excellent opportunity to study foehn. During and after it was analyzed, the collected data confirmed that "there was blocked air during most foehn cases", at least in the Brenner field study. In the Alps mountains, a large-scale mesoscale south foehn wind happened on November 8, 1982. Unfortunately, this "century foehn" was too strong, affecting the program flights across the Alps, mostly between northern Italy and southern Germany, destroyed many boats and yachts, also the pier of the town of Sisikon. It is worthy of note that light precipitation was reported towards the end of this great foehn event (Richner and Hächler, 2013).

It is unfortune that most textbooks only mention the theory shown in Figure 1-1 as the foehn mechanism, without considering other forms of foehn. One of the accepted beliefs is the foehn winds occurs without precipitation. If the mountain crest is not too heigh, the advected air can pass

[1] "A cloud-free gap or clearance in the lee of the mountain range over which a foehn flow occurs. This gap is caused by the descending foehn air that is dry-adiabatically heated and becomes dry".

[2] In those situations where "foehn occurs with precipitation on the windward side of the mountain range, the clouds can be seen from the lee side as a "wall" topping the mountain ridge. Depending on the characteristics of the foehn flow, the clouds can be dragged over the ridge. It means that they are dissolved while sinking. Under these conditions, the foehn wall looks like a cap".

the ridge easily, and then descends, as shown in Figure 1-2, which is confirmed by trajectory analyses (Baumann et al., 2001, Richner and Hächler, 2013).

Topography is the main feature of the foehn areas. If a valley situation be such that its axis is aligned with the flow, so airflow penetrates the valley more easily, and the fewer ridges further downwind which could hinder the flow. The flow in this situation is diffluent, depending on topography, the degree of the diffluence being controlled. The topography defines the foehn areas, based on these principles. Ridges with "valleys perpendicular to them, mainly, represent the areas with the highest foehn frequency" (Richner and Hächler, 2013).

By considering the channeling effect of the valleys, as the flow further penetrates the valley, since the cross section decreases, the wind speeds can be higher near the ground than they are above. Observations demonstrate that, by determining the direction of the flow, the channeling effect can reach up to heights well above the crest of the mountains bordering the given valley.

Generally, foehn winds rarely descend more than 2,000 m behind the ridge over which they flow. Therefore, when discussing about foehn frequency at a given location, defining what is meant by saying, "There is Foehn", is essential. Sometimes an airflow above the location without reaching the ground, could be defined as foehn, but sometimes the winds must really touch down. In climatology, the definition of foehn can become more challenging. Some examples of definition of different foehn climatologies are given at Barry (2008).

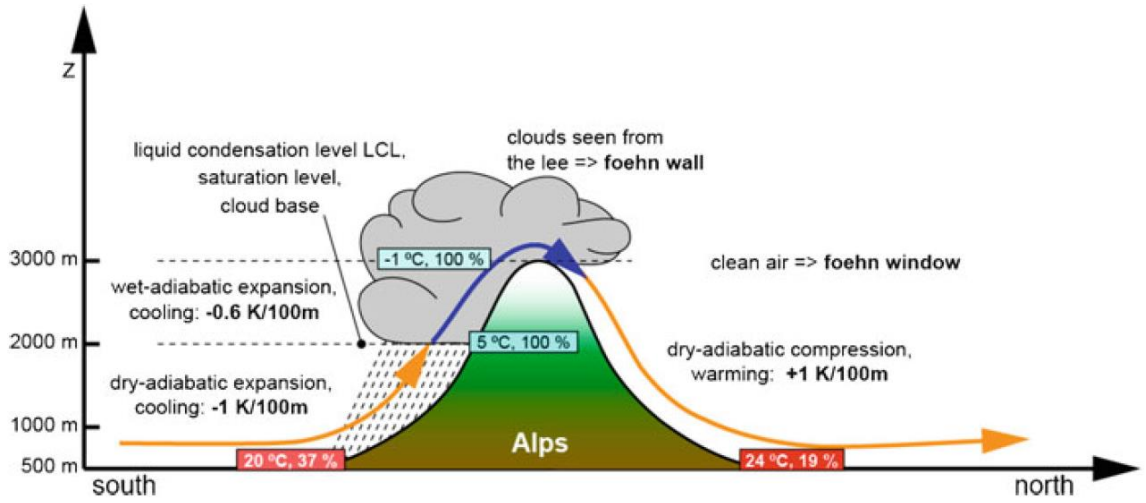

Figure 1-1. "Schematic description of the "textbook theory" of foehn. Diagrams similar to this one is found in many textbooks on meteorology", e.g. Richner and Hächler (2013).

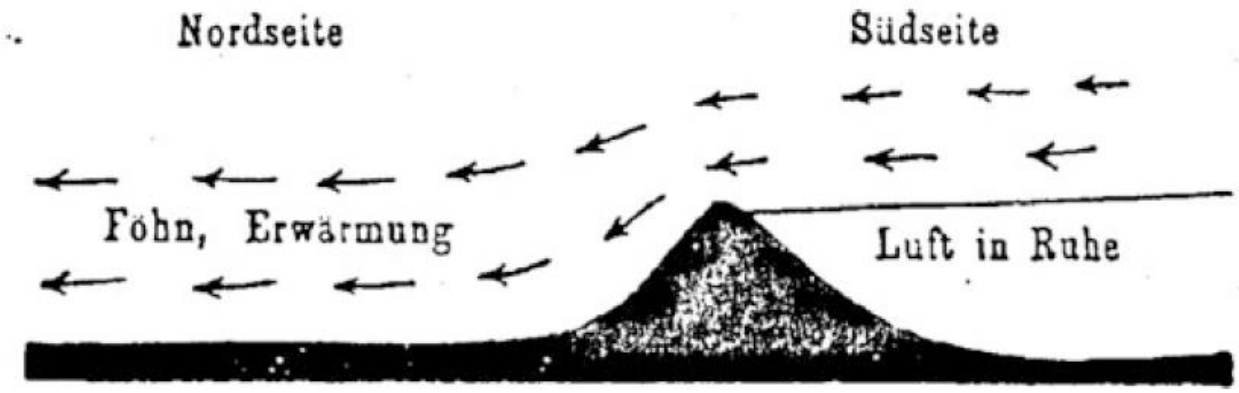

Figure 1-2. "The "proof" that Hann was aware of the two types of foehn: Original illustration depictingHann's (1866) foehn theory in Ficker (1920). "Nordseite": north side; "Südseite": south side; "Föhn, Erwärmung": foehn, warming; "Luft in Ruhe": air at rest. Note that north–south is reversed" with respect to Figure 1-1.

Literatures mentioned four mechanisms for foehn events (Elvidge and Renfrew, 2016,).

a. "Upwind of the mountain, cool, moist air can be blocked allowing potentially warmer, drier air to be advected isentropically down the lee slopes". This mechanism termed *isentropic drawdown*. "Flow blocking is characteristic of a nonlinear flow regime, where the speed of the approaching stably stratified flow is insufficient for ascent from low levels over the mountain" (Smith 1990).
b. "Without flow blocking, there is ascent on the windward slopes so the air cools, leading to condensation and latent heat release that reduces the cooling; precipitation removes the condensed water so that descent on the lee side is dry, which increase the (pressure related) warming leading to higher leeside temperatures (the *latent heating and precipitation* mechanism). Considerable orographic uplift and cloud formation are characteristic of a linear flow regime, where the approaching flow is strong enough to overcome buoyancy forces and ascend from low levels over the mountain" (Smith 1990). "These two mechanisms have been widely discussed in the literature" (e.g., Scorer 1978; Seibert 1990; Richner and Hächler 2013). However, two other foehn mechanisms also exist.
c. "As cool, moist air passes over the mountain, it will mix mechanically with the overlying air mass; for a statically stable atmosphere, this is potentially warmer (and usually drier) and so corresponds to a turbulent flux of sensible heat into the foehn flow (and a turbulent flux of moisture out of it)" (Scorer 1978; Ólafsson 2005).
d. "Associated with the mechanisms described in a – c, there is often clear, dry air on the downwind slopes, the "*Foehn Clearance*", and cloud on the upwind slopes; this situation

encourages radiative flux convergence and thus warmer air on the lee side" (Hoinka 1985a; Ólafsson 2005). "The importance of each mechanism depends upon the orographically forced flow dynamics and meteorological conditions and so varies from case to case" (Elvidge and Renfrew, 2016).

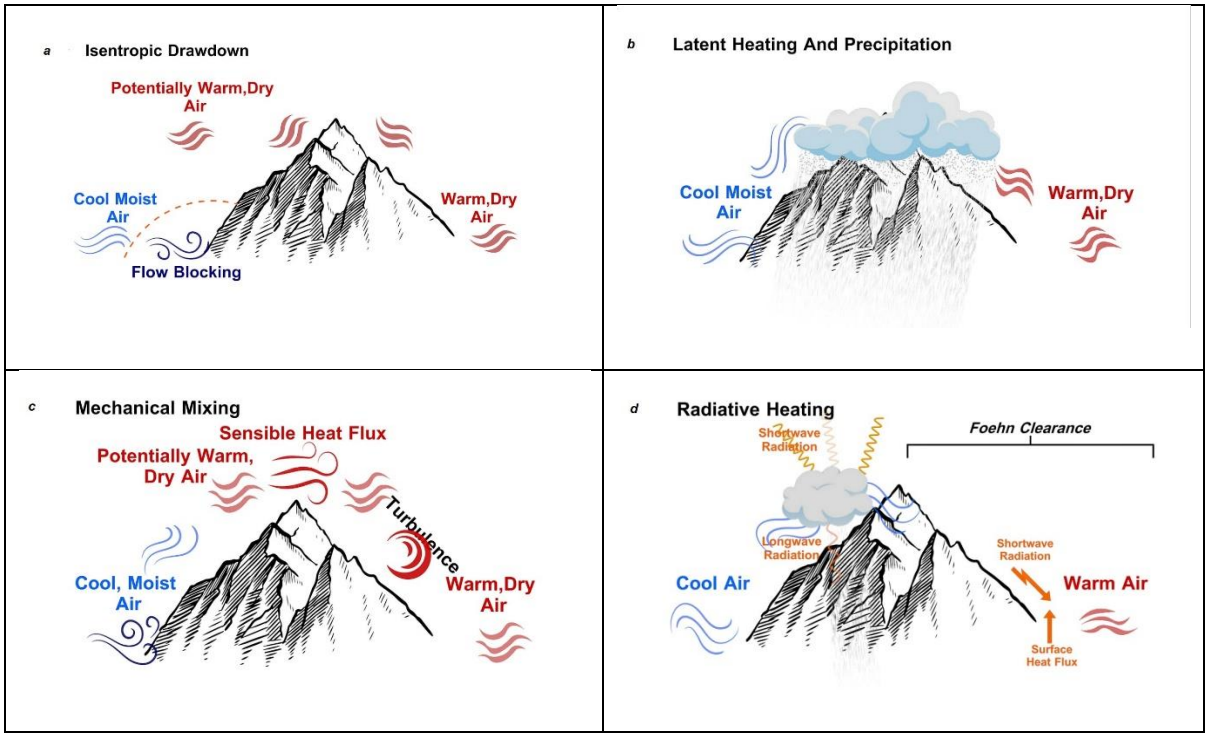

Figure 1-3. Foehn warming mechanisms.(a: Isontropic Drawdown, b: Latent Heating and Precipitation, c: Mechanical Mixing, d: Radiative Heating) (adapted from Elvidge and Renfrew, 2016)

"Throughout the literature a number of criteria have been used to distinguish reasons of "*Foehn Conditions*"" (Drobinski et al. 2007; Sharples 2009). "Commonly though, three criteria are used to distinguish Foehn conditions at stations in the lee of mountains" (Osmond 1941; Frey 1957). "They are surface winds blowing from the direction of the mountains, an abrupt rise in air temperature in the lee of the mountains, and an accompanying reduction in atmospheric moisture. Synoptic criteria can also be used to distinguish Foehn conditions" (Brinkmann 1970, 1971; Vergeiner 1971; Beer 1974; Hoinka 1985a; Barry 1992; McGowan and Sturman 1996; Gohm et al. 2004).

For all meteorologists, prediction of foehn is still a challenge. The general foehn situation can be predicted in an accurate way, however, today's numerical models still often imperfectly simulate the sudden onset of potentially damaging foehn events in the lee. Foehn winds have a

considerable societal impact like threats to transportation systems and a massive increase of fire danger (Richner and Hächler, 2013).

1.4 Societal Impact of Foehn

1.4.1 Climate Impact

“Regions under the influence of foehn experience warmer, drier climates and a longer crop growing season than they otherwise would. However, it is the foehn's adverse effects that grab the headlines. The warmth it brings can increase the risk of avalanches in ski resorts, cause glacial melt and downstream flooding, and contribute to the disintegration of ice shelves in the polar regions” (Richner and Hächler, 2013).

1.4.2 Air Quality

Mountains’ view with foehn occurrences are outstanding. Precipitation on the windward side resulted to, usually, clean air, without haze, which makes objects seen to be much closer (Burri et al., 1999). In some foehn types, the air mass originating at high levels has much lower aerosol concentrations than the air it replaces in the valleys and makes a stunning view of the mountain that is not usual. However, an augmentative effect on ozone concentration is a negative side of these fantastic mountain panoramas. Without reaching alarm levels of the values, foehn simply affects the growth of ozone concentrations up to triple (Baumann et al. 2001). Descending of air with richer ozone from about 4,000 m over the Mediterranean region, causes the higher concentrations, proved by trajectory calculations and aircraft measurements (Richner and Hächler, 2013).

1.4.3 Fires and Traffic Accidents

Some less well-known severe fire weather conditions are associated with synoptic events that can occur in connection with the topography of the region. These can lead to abrupt spatiotemporal changes in fire weather variables that ultimately result in locally elevated fire danger (Sharples et al., 2010). In some of these cases, the warm and very dry air flow accompanied with high wind speed on the lee side of mountain ranges, including mountain waves and foehn-like occurrences, supports and grows fire dangers, efficiently. “The warmth and dryness of the air being due to adiabatic compression of the air descending the mountain slopes” (Huschke 1959; WMO 1992).

So Foehn wind can spread fire severely, and it is a most dangerous effect. There are several

examples of towns were completely devastated by fire. In 1861, about 600 houses of the canton capital Glarus, Switzerland, have burned down completely. The other disaster occurred in 2001; foehn winds more than 15 ms^{-1} damaged some houses in Balzers, Principality of Liechtenstein (Richner and Hächler, 2013). Precautions must be considered during foehn situations in some mountain regions, like prohibition of igniting fire outside specially designated fire areas.

A study by Marsh (1987) on the extreme fire weather of 6 November 1982 in southeast Tasmania, showed "the feasibility of a large-scale ''foehn-type'' downslope flow related to the extreme fire weather of the day". Foehn effects, with their naturally warm, dry, relatively high-speed downslope winds (foehn winds), have been broadly studied in the United States and Europe. Worthy of mention, in the conditions of fire weather, are the Santa Ana winds of Southern California. Keeley (2004) concluded that "the autumn foehn (Santa Ana) in southern California was a main driver in determining the area burned, overriding most other climate factors".

Foehn winds are also key drivers of severe fire weather in Europe. Carrega (1991) found that "occurrences of disastrous fires near the French–Italian border driven by westerly foehn winds", and Conedera et al. (1996) discussed that "in southern Switzerland, the major time for forest fires is during north foehn events. The 1997 fire season serves as an example" (Conedera et al. 1998). Another example is New Zealand fire weather assessments, in which "foehn winds affect the humidity levels in the lee of the main mountain ranges" (Salinger et al. 2000; Salinger and Porteous 2002; Gosai and Salinger 2003, 2004, 2005). "Foehn winds have also been linked with high forest fire danger in Japan" (Kondo and Kuwagata 1992; Ninomiya et al. 1985), "certain parts of Korea" (Lim 2002), despite the "more moderate topography located there, and Iran" (Shirzadi 1992; Jazirehei, 1995; Parnian, 1999).

Mofidi et al. (2015) modelled an exceptional southerly Foehn (Garmij) in the Alborz Mountains in northern Iran, which resulted in an extensive and high-intensity fire in the Gilan and Mazandaran forests in the north of Iran. On the other hand, Khashjan (2019) studied three forest fires that occurred on 16-18 May 2015, in the Zagros Mountains, in northwestern Iran and roughly followed Iran's western border. He noted that the seasonal and dry conditions of the region, starting from late in May, cause drying of fields and pastures in the area and provided the conditions for fire. The prevailing conditions in the region indicate the absence of the Foehn phenomena in the region.

Flying objects can be affected by danger of the foehn winds. Local airports and skillful pilots

always pay attention to this flow and issued warnings related to it. For example, at Innsbruck airport, due to particular foehn measurements to increase safety and passenger comfort, climb out and approach to the most turbulence prone parts of the valley are prohibited . However, with increasing interest in sports like hot-air ballooning and paragliding, in recent decades, the number of severe accidents due to high winds and large shears was increased remarkably. Some procedures, including specific safety courses, training and special information and improved forecasts have decreased, but not gotten rid of this issue (Richner and Hächler, 2013).

Strong and gusty foehn winds cause cable car accidents and even train accidents. It required that all cable transportation systems are equipped to monitor wind speed and ~~to~~ have an alarm system. However, “sometimes gusts and shears that slide between the different anemometers can make trouble for operators” (Richner and Hächler, 2013).

1.4.4 Biometeorological Effects

There is much debating about the biometeorological effect of foehn winds. The effect of foehn on mental well-being is the subject of folk law in Alpine regions: the phenomenon has been linked to almost any ailment, depression, suicide, madness, accident, headaches, sleeplessness and crime waves. The likely explanations of foehn-related ailments might be pressure fluctuations, ion concentrations, and sferics (electromagnetic radiation originating in the atmosphere). However, some measurements show that neither sferics nor ion concentrations are related to foehn events, pressure variations caused by gravity waves on the cold pool remain a possible relation between foehn and man mood.

Although there is no proof of any cause-and-effect mechanism of correlation between pressure fluctuations and mental well-being, some statistical analyses show such a statistically significant correlation between the two. A survey of the short-term pressure fluctuations could not take into account the actual weather situation. Since fronts also cause high amplitude pressure fluctuations, the positive correlation might easily reflect that people feel mentally better when the weather is good. “An isolated direct analysis of the frequency of headaches and the occurrence of could not produce any definite result” (Richner and Hächler, 2013).

It seems that in recent years, after a long delay, “the research about biometeorology has become more popular in America. Multiple research projects related to Chinook winds and some diseases like headache, and strokes have been done, but no momentous advancement achieved, yet in

associating ailments to foehn-type winds or weather in general" (Cooke et al. 2000; Field and Hill 2002).

1.5 Scope of the Study

While most studies of foehn events have focused on a few selected regions, such as the European Alps and the Rocky Mountains in the western part of North America, similar events in northern Iran are not well represented in the meteorological literature. In this study, to learn more about foehn in the Alborz Mountains, time series of quantities such as wind speed, surface temperature, relative humidity and synoptic factors on the intensity and variability of foehns are studied. The abrupt temperature rise, drop in relative humidity, the onset of high winds and the constant wind direction are characteristics of foehn winds in the region. Given the influence of large-scale synoptic systems on mentioned components, these could be used for forecasting foehn winds in the area. Also, this could have significant application in issues related to forest fire forecasting.

In this survey, I try to represent an analysis of the characteristics of the candidate foehn events observed in the Alborz chain Mountains in Northern Iran for some selected dates, based on weather observation recorded at a number of weather stations, as well as analyses of the broader scale atmospheric structure using ERA5 reanalysis data.

Chapter 2

Data and Methods

2.1 Study area

Iran is a mountainous, arid, and ethnically diverse country of southwestern Asia. Much of Iran consists of a central desert plateau, which is ringed on all sides by lofty mountain ranges that afford access to the interior through high passes. Iran is bounded to the north by Azerbaijan, Armenia, Turkmenistan, and the Caspian Sea, to the east by Pakistan and Afghanistan, to the south by the Persian Gulf and the Gulf of Oman, and to the west by Turkey and Iraq. Iran also controls about a dozen islands in the Persian Gulf. About one-third of its 7,680-km boundary is seacoast (Figure 2-1).

Figure 2-1. Goegraphical position of Iran country (from Encyclopedia Britannica, Accessed on 10 Nov. 2021).

"The arid interior plateau, which extends into Central Asia, is bounded on the west by the Zagros Mountains, on the north by the Alborz Mountains and the Koppeh Dāgh Range, and on the

south by the Bashagard Range, which extends east from the Strait of Hormuz into the Baluchistan region of Iran. The plateau is cut by several smaller mountain ranges. In the flatlands lie the plateau's most-remarkable features, the Kavīr and Lūt deserts, also called the Dasht-e Kavīr and Kavīr-e Lūt. At the lowest elevations, series of basins in the poorly drained soil remain dry for months at a time; the evaporation of any accumulated water produces the salt wastes known as *kavīr*s. As elevation rises, surfaces of sand and gravelly soil gradually merge into fertile soil on the hillsides and mountain slopes" (Encyclopedia Britannica, Accessed on 10 Nov. 2021).

A series of massive, heavily eroded mountain ranges surround Iran's high interior basin. Most of the country is above 460 metres, with one-sixth of it over 1,980 metres. In sharp contrast are the coastal regions outside the mountain ring. In the north a strip 650 km long bordering the Caspian Sea and never more than 115 km wide (and frequently narrower) falls sharply from 3,000-metre summits to the marshy sea edge, some 30 metres below sea level. Along Iran's southern coast the land drops away from a 600-metre plateau, backed by a rugged escarpment three times as high, to meet the Persian Gulf and the Gulf of Oman.

The Zagros Mountains stretch in a northwest-southeast direction, from Iran's borders with Turkey and Iraq in the northwest to the Strait of Hormuz in the southeast. Farther to the south the range broadens into a band of parallel ridges 200 km wide that lies between the plains of Mesopotamia and the great central plateau of Iran. The range is drained on the west by streams that cut deep narrow gorges and water fertile valleys. The land is extremely rugged and difficult to access and is populated largely by pastoral nomads.

The Alborz Mountains run along the south shore of the Caspian Sea to meet the border ranges of the Khorāsān region to the east. The tallest peak in the chain is the snow-clad Mount Damāvand, which is also Iran's highest point. Many parts of Iran are isolated and poorly surveyed, and the elevation of many of its peaks are still in dispute; the height of Mount Damāvand is generally given as 5,671 metres.

Given the complex topography of the Alborz, the local climatic conditions not only quickly respond to changes in the surface energy budget but are also shaped by the interaction between the topography and persistent westerlies. The interaction can initiate foehn events—dry and warm downslope winds—in the lee of mountain ranges. The warm, gusty winds together with the increase in solar radiation caused by the evaporation of low-level clouds, can lead to an energy surplus that can be critical for ablation. At the same time, cloudy sky can be observed on the

windward side through orographically induced precipitation. In this region, the influence of foehn winds is poorly investigated (Mofidi, et al., 2015; Taghavi, et al., 2015). The characteristics and impact of foehn winds have been studied extensively in the Northern Hemisphere, such as the European Alps (Gohm and Mayr, 2004; Gohm et al., 2004; Armi and Mayr, 2007), the Rocky Mountains in North America or the Dinaric Alps by the Mediterranean Sea (Gohm et al., 2008). In this study we focused on western Alborz Mountains.

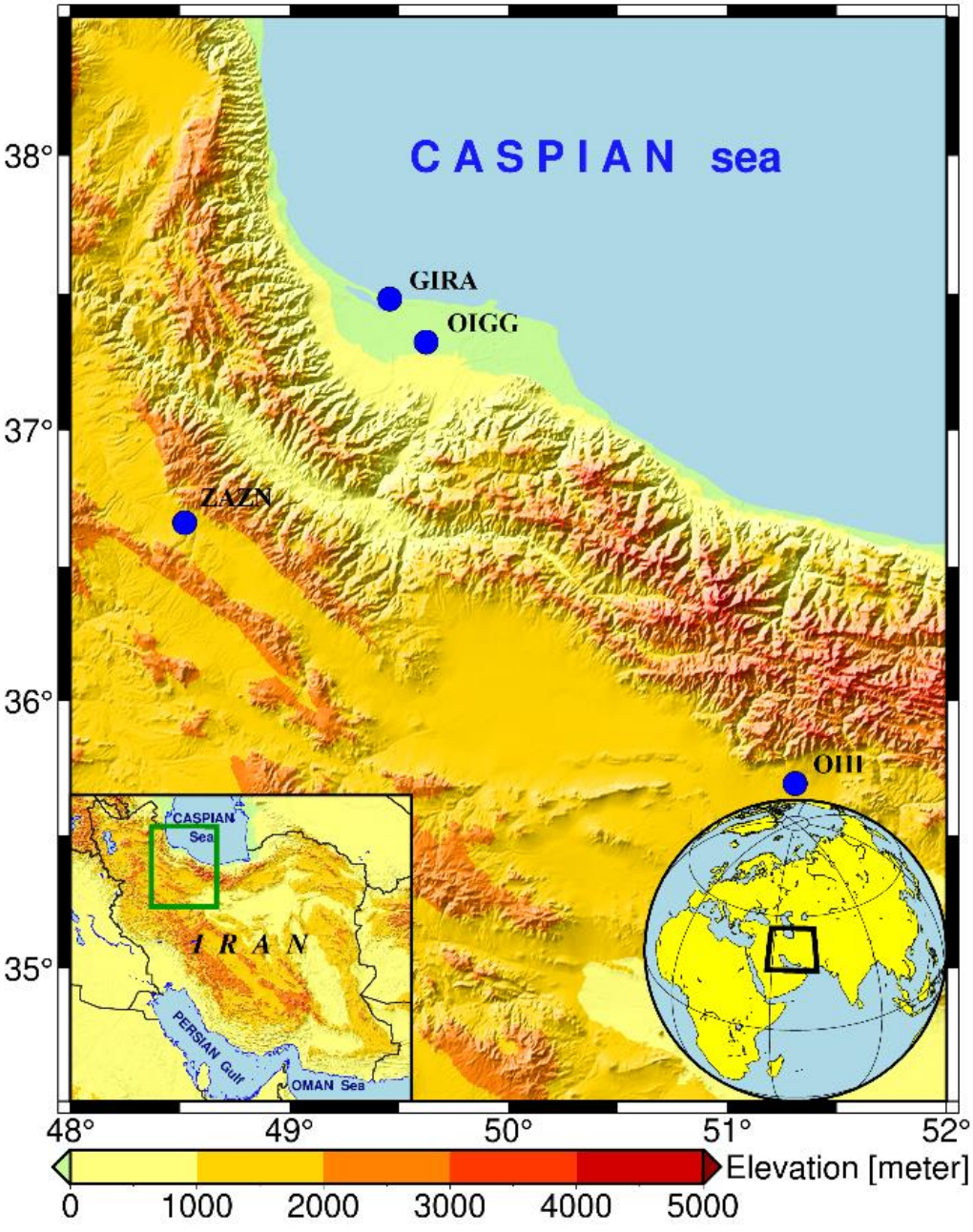

Figure 2-2. Topography of Iran (based on the color bar) and considered stations (blue bullets).

2.2 Data

2.2.1 Observational Data

This study focuses on a region in the North of Iran between 34.5-38.5° N and 48-52° E (Figure 2-2). Meteorological observational data from IRIMO stations, located along south-north transect across the Alborz Mountains (Figure 2-2), were used. The conditions on the windward side were represented by Tehran and Zanjan stations, located at the southern foot of Alborz Mountains with altitudes of ~1200m and ~1700m. For leeward stations Rasht-Airport and Anzali stations, on the northern side of Alborz Mountains, were chosen with altitude below sea level (Table 2-1). The difference of altitude between windward and leeward is considerable.

Table 2-1. Characteristics of considered stations

Station name	Station ID	windward/leeward	Lon (°)	Lat (°)	Height (m)
Rasht (Airport)	OIGG	leeward	49.62	37.32	-8.6
Anzali	GIRA	leeward	49.46	37.48	-23.6
Tehran	OIII	windward	51.31	35.69	1191.0
Zanjan	ZAZN	windward	48.52	36.66	1659.4

In order to have a consistent time series, we consider 3-hourly synoptic data in addition to necessary hourly/half-hourly METAR[1] and also SPECI[2] reports for the period 10 January to 10 February 2021, including all four-case study predesign, 14-15 January, 18 January, 28-29 January, and 5 February 2021. In METAR and SPECI reports, 9999 in visibility code means visibility is more than 10 km, NSC in cloudiness code means No Significant Cloud, also VV in cloudiness code means Vertical Visibility[3]. It should be pointed out that in METAR and SPECI reports values of meteorological quantities are rounded and there is no digit after decimal point.

2.2.2 Reanalysis Data

The ERA5 dataset from the European Center for Medium-Range Weather Forecasts (ECMWF) "is the fifth generation ECMWF reanalysis for the global climate and weather for the past 4 to 7 decades. ERA5 is the highest resolution globally available reanalysis dataset existing, with an

[1] Meteorological Terminal Air Report
[2] the name of the code for an aviation selected *special* weather report, will be reported when weather changes of significance to aviation are observed.
[3] A subjective or instrumental evaluation of the vertical distance into a surface- based obscuration that an observer is able to see. The height ascribed to vertical visibility is always a ceiling height.

approximate spatial resolution of 31 km, 137 vertical levels and hourly output" (Hersbach et al., 2019; Hersbach et al., 2020). "Currently data is available from 1950, split into Climate Data Store entries for 1950-1978 (preliminary back extension) and from 1979 onwards (final release plus timely updates). ERA5 replaces the ERA-Interim reanalysis" (Hersbach, 2018a and 2018b)

"Reanalysis combines model data with observations from across the world into a globally complete and consistent dataset using the laws of physics. This principle, called data assimilation, is based on the method used by numerical weather prediction centers, where every so many hours (12 hours at ECMWF) a previous forecast is combined with newly available observations in an optimal way to produce a new best estimate of the state of the atmosphere, called analysis, from which an updated, improved forecast is issued. Reanalysis works in the same way, but at reduced resolution to allow for the provision of a dataset spanning back several decades. Reanalysis does not have the constraint of issuing timely forecasts, so there is more time to collect observations, and when going further back in time, to allow for the ingestion of improved versions of the original observations, which all benefit the quality of the reanalysis product" (Hersbach, 2018a and 2018b)

"ERA5 provides hourly estimates for a large number of atmospheric, ocean-wave and land-surface quantities. An uncertainty estimate is sampled by an underlying 10-member ensemble at three-hourly intervals. Ensemble mean and spread have been pre-computed for convenience. Such uncertainty estimates are closely related to the information content of the available observing system which has evolved considerably over time. They also indicate flow-dependent sensitive areas. To facilitate many climate applications, monthly-mean averages have been pre-calculated too, though monthly means are not available for the ensemble mean and spread" (Hersbach, 2018a and 2018b)

ERA5 is updated daily with a latency of about 5 days (monthly means are available around the 6th of each month). "Data has been re-gridded to a regular lat-lon grid of 0.25 degrees for the reanalysis and 0.5 degrees for the uncertainty estimate (0.5 and 1 degree respectively for ocean waves). There are four main subsets: hourly and monthly products, both on pressure levels (upper airfields) and single levels (atmospheric, ocean-wave and land surface quantities). Recent studies have shown that it yields an overall improvement compared to other reanalysis datasets and previous versions" (Albergel, et al., 2018; Olauson, 2018, Taghizadeh et al., 2021).

In this study, variables of U and V component of wind at 10 m height, temperature and dewpoint temperature at 2 m height, and mean sea level pressure (MSLP) were obtained from

ERA5 hourly data on single levels from 1959 to present dataset (Hersbach et al., 2018a) in NetCDF format. On the other hand, geopotential, relative humidity, U and V component of wind variables on different pressure levels were extracted from *ERA5 hourly data on pressure levels from 1959 to present* dataset (Hersbach et al., 2018b) in NetCDF format.

2.3 Numerical Simulation

Due to the importance of prediction of the foehn, a case study of the event has been done using the Weather Research and Forecasting (WRF) model. "WRF model is a mesoscale numerical weather prediction system which offers operational forecasting a flexible and computationally efficient platform, while reflecting recent advances in physics, numeric, and data assimilation contributed by developers from the expansive research community" (Skamarock et al., 2019). WRF is currently in operational use at NCEP and other national meteorological centers as well as in real-time forecasting configurations at laboratories, universities, and companies.

2.4 Methodology

"The two most well-known mechanisms responsible for heating and drying the foehn air are thermodynamic warming and isentropic drawdown" as described further by Elvidge and Renfrew (2016). The former describes "an air parcel orographically lifted over a mountain barrier and cooling at the saturated adiabatic lapse rate, which causes the formation of clouds and precipitation on the windward side of the mountains. After the obstacle is passed, the air descends and warms dry adiabatically leading to drier and warmer air masses in the lee than upstream of the range. The second mechanism suggests that the low-level flow is blocked by the mountain. Hence, potentially warmer air is isentropically advected upwind and subsides down the lee slope, warming at the dry adiabatic lapse rate" (Elvidge and Renfrew 2016; Richner and Hächler, 2013).

"Foehn winds can be classified according to the prevailing flow regime upstream of the mountains. Often the Froude number (Fr) is used, denoting the ratio of kinetic to potential energy in a hydrodynamic system. In a supercritical flow regime ($Fr >> 1.0$), an air parcel with a high wind speed and/or in a less stable stratified environment is able to flow over the barrier. foehn events occurring under these conditions are often associated with the formation of linear mountain waves (linear type). A Fr just above 1.0 ($Fr \sim 1.1$) describes a critical or transitional flow regime, in which an internal hydraulic jump may form which is usually accompanied by a strong lee-side downslope wind (hydraulic jump-type). In a subcritical flow regime ($Fr < 1.0$), the kinetic energy

of a stably stratified air mass is insufficient to overcome the obstacle. In such a case, referred to as a blocking-type foehn, the mountain range blocks the upwind low-level air masses and the flow regime becomes nonlinear" (Temme et al., 2020).

Here, we provide a first quantification of the spatial and temporal extent of foehn winds and associated local-scale processes in the western Alborz Mountains. We used in-situ observations and numerical modeling to study the processes and phenomenology of foehn events over Alborz Mountains. Based on the phenomenological character of foehn types, inferences may be drawn on the spatial variability of the local climate and thus also on the Caspian Sea impact. With observational data from I.R. of Iran Meteorological Organization (IRIMO) stations windward and leeward of the Alborz, we detected four foehn events over January and February 2021. By using ERA5 data and plotting required maps of meteorological parameter, we assessed the synoptic characteristics and local conditions of four case study foehn events.

Chapter 3

Results

3.1 Introduction

The Alborz Mountains present a consistently high (up to ~5600 m), broad (60-130 km), and long (~900 km) quasi-2D barrier to the flow. Four foehn events examined have southerly flow across the Alborz onto the coastal area they occurred during the winter January and February 2021, caused by establishment of low pressure over the North of Alborz Mountains and a pressure difference between Southern and Northern Alborz.

3.2 Detection of foehn events

For detection of foehn events in regions with the potential of this event, we consider some meteorological stations located ~~at~~ leeward of the Alborz Mountains in the North of Iran. Time series (3-hourly) of temperature, dewpoint temperature, wind speed and surface pressure during 10 January to 10 February 2021 over Rasht-Airport station, (Lon 49.62E, Lat 37.32N) with ICAO[1] code OIGG, have been shown on Figure 3-1. In Figure 3-1(a), the left vertical axis shows temperature (°C), the right vertical axis shows wind speed unit (m/s), and the horizontal axis shows dates with hour. Blue, red, and gray lines are related to temperature, dewpoint temperature and wind speed, respectively. Based on this figure, we could detect four foehn events during this period; these occurred on 14-15 January, 18 January, 28-29 January, and 5 February 2021. It can be seen that on all of these dates, temperature increased, dewpoint temperature decreased, and wind speed rose. It is noteworthy that southerly wind in Rasht-Airport (Lon 49.62E, Lat 37.32N) means this station is located leeward of the mountain (Table 2-1). Southerly wind in this area shows a downslope wind which crosses the Alborz Mountains reaches the stations located on the Norther Alborz. So, foehn events on the above dates must be accompanied with southerly winds, which will be investigated more in the next section. Besides that, southerly wind in the study area means wind from coast to sea (Figure 2-2) and consequently decreasing of humidity. Decreasing the surface pressure on the station can also be seen during these foehn occurrences, based on Figure 3-1(b). This pressure decreasing could result the southerly winds, as will be discussed later.

[1] International Civil Aviation Organization

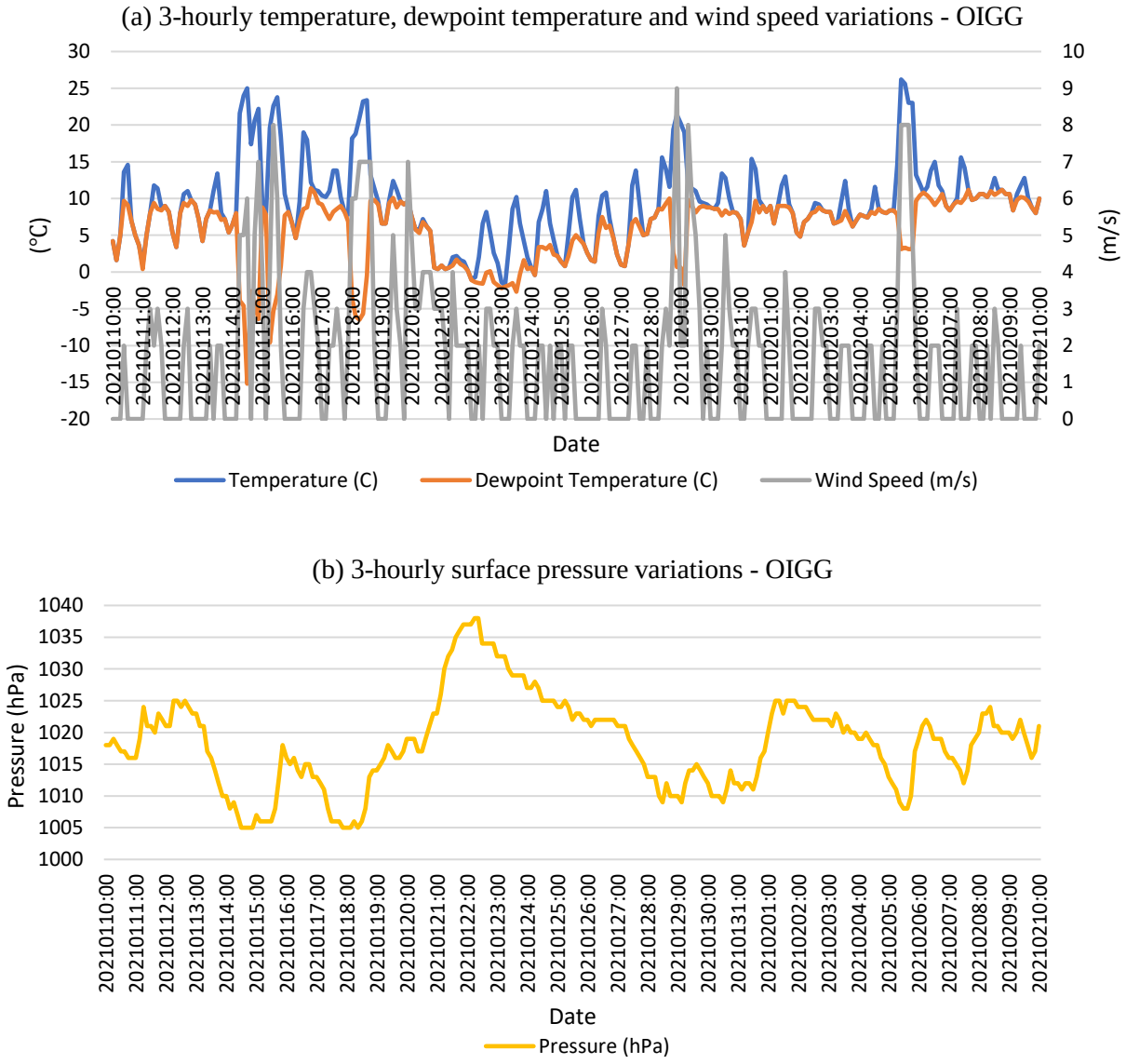

Figure 3-1. (a) 3-hourly temperature (°C) (blue line), dewpoint temperature (°C) (red line) and wind speed (m/s) (gray line), (b) 3-hourly pressure (hPa) of Rasht-Airport station from 00:00 UTC 10th January to 00:00 UTC 10th February 2021.

Time series of temperature, dewpoint temperature, wind speed and surface pressure of Anzali station with ICAO[1] code GIRA, (Lon 49.46E, Lat 37.48N), leeward of Alborz Mountains, from 00:00 UTC January 10 to 00:00 UTC February 10 was plotted at Figure 3-2. This figure depicts the same foehn events as Rasht-Airport station, (Lon 49.62E, Lat 37.32N), so that temperature increasing, dewpoint decreasing, rising wind speed, and falling pressure could be seen for the same dates as mentioned above. The values of the quantities in dates with foehn events have been given

[1] International Civil Aviation Organization

in the appendix (Table a-1, Table a-2, Table a-3 and Table a-4).

(a) hourly temperature, dewpoint temperature and wind speed variations - GIRA

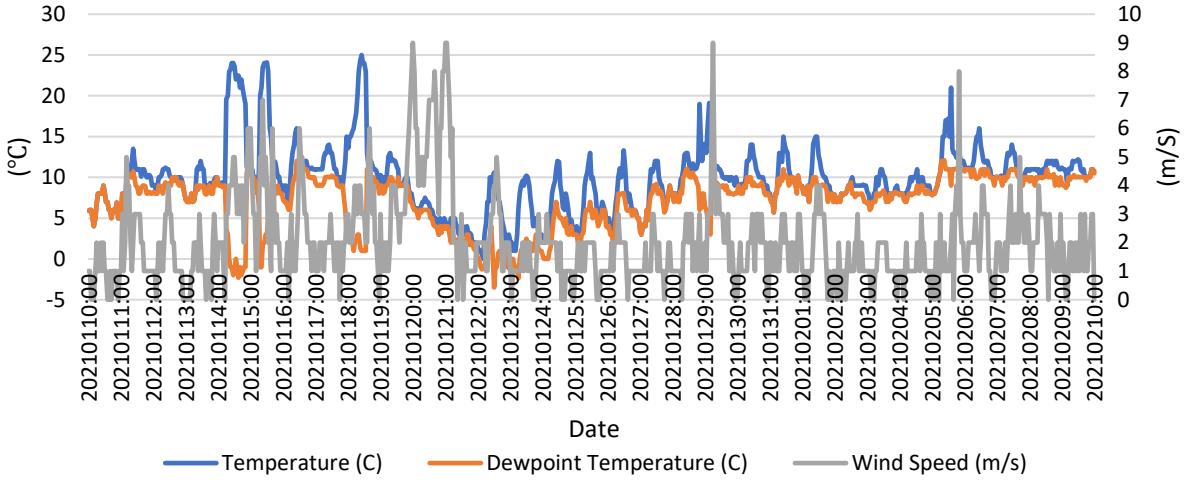

(b) hourly Pressure variations - GIRA

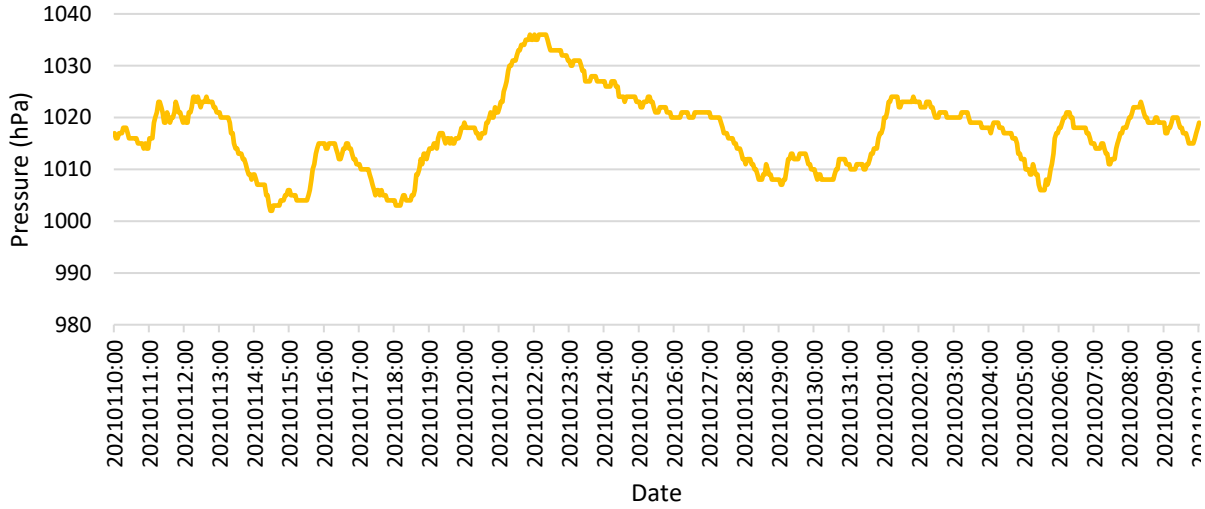

Figure 3-2. (a) Hourly temperature (°C) (blue line), dewpoint temperature (°C) (red line) and wind speed (m/s) (gray line), (b) hourly pressure (hPa) of Anzali station (GIRA) from 00:00 UTC 10th January to 00:00 UTC 10th February 2021.

Table 3-1. Dates on which foehn is detected and will be discussed.

dates
14-15 January 2021
18 January 2021
28-29 January 2021
5 February 2021

Table 3-1 shows dates with foehn based on the above discussion and which will be studied the next sections. In the following, we discussed on synoptic and analysis maps during these dates. For this purpose, geopotential height, temperature, wind was plotted in 500 mb level, also MSLP and 10-m wind were plotted using ERA5 data. We also gathered some available analysis maps plotted in IRIMO using observed data in synoptic stations and some upper air stations.

3.2.1 Wind Rose

As mentioned previously, Rasht-Airport station (Lon 49.62E, Lat 37.32N) is located north of the Alborz Mountains and south of Caspian Sea (Figure 3-3(a)). The wind rose of this station for different time periods is shown in Figure 3-3(b-g). WRPLOT View Version 8.0.2 has been used to plot wind rose (WRPLOT, 2018). In accordance with Figure 3-2, the wind rose plot for 10 January to 10 February 2021 has been shown in Figure 3-3(b). It could be seen the dominant wind in this area is calm (wind speed less than 1 knot). To better considering the wind direction, the calm wind was removed in Figure 3-3(c). Based on the legend about 47% of the time wind was calm. The wind rose shows that during this particular studied period the wind blew from the west 8% of the time. The yellow color shows wind speed equal or more than 18 knot and the direction of this wind speed is mostly southerly or southeasterly. To focus on foehn events only, the wind rose has been plotted for the dates on Table 3-1 separately (Figure 3-3(d-g)).

It could be seen in Figure 3-3(d) that wind with speed equal or more than 12 knot is from southerly or southeasterly for more than 40% of the time, which indicate a foehn event in 14-15 January 2021. Figure 3-3(e) shows wind rose plot for 18 January 00-23 UTC with wind from the south-southeast 48% of the time with speed more equal or more than 12 knot, which again shows foehn event at this date. Same plot for 28-29 January 2021 has been shown in Figure 3-3(f) which indicates that winds are from west for about 30% of the time. However, as will be discussed later (section 3.2.4), foehn occurred only during some hours of these dates; as it can be seen in this figure, wind with speed more than 6 knot from south and southeast. The wind rose for the last event of Table 3-1 has been shown on Figure 3-3(g) with wind speed more than 6 knot from south-southeast at more than 45% of the time; 13% of the time wind speed is equal or more than 18 knot, consistent with foehn occurrence.

(a)


Location of Rasht-Airport Station
Google Earth
300 mi
N

(b)


Rasht-Airport Wind Rose
Legend
>= 18
0 - 1
1 - 6
12 - 18
6 - 12
Google Earth
1000 ft
N

(c)

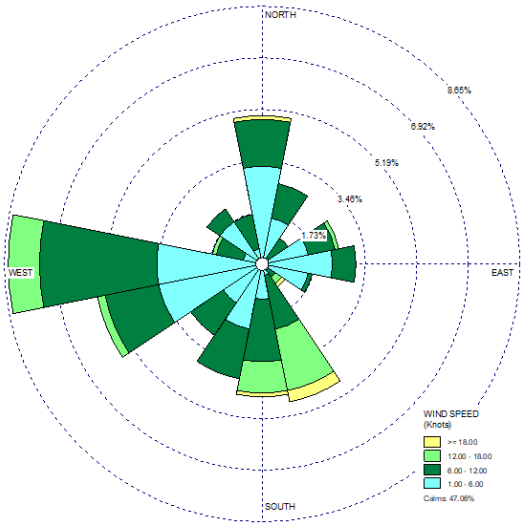
NORTH
8.65%
6.92%
5.19%
3.46%
1.73%
WEST
EAST
SOUTH
WIND SPEED
(Knots)
>= 18.00
12.00 - 18.00
6.00 - 12.00
1.00 - 6.00
Calms: 47.06%

(d)

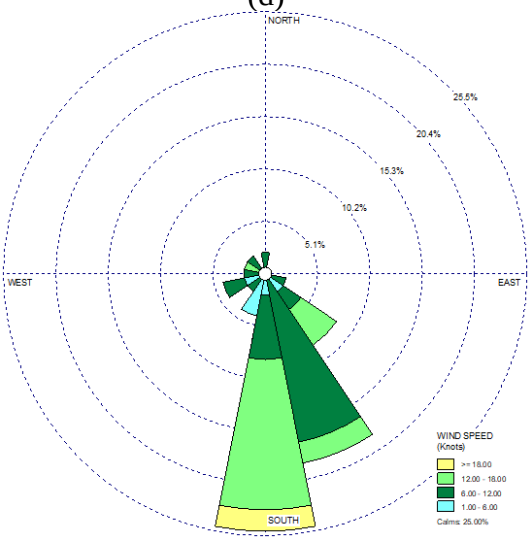
NORTH
25.5%
20.4%
15.3%
10.2%
5.1%
WEST
EAST
SOUTH
WIND SPEED
(Knots)
>= 18.00
12.00 - 18.00
6.00 - 12.00
1.00 - 6.00
Calms: 25.00%

(e)

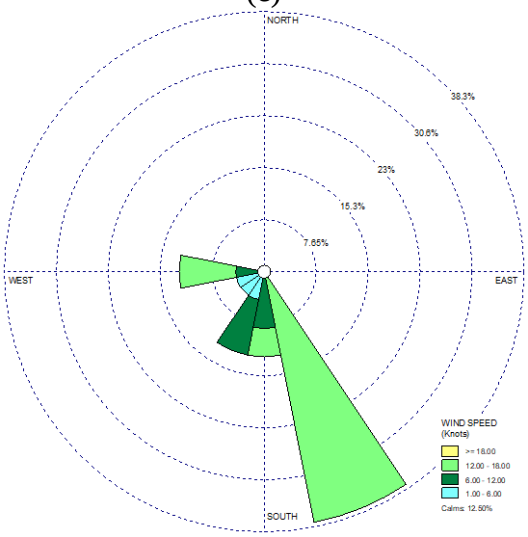
NORTH
38.3%
30.6%
23%
15.3%
7.65%
WEST
EAST
SOUTH
WIND SPEED
(Knots)
>= 18.00
12.00 - 18.00
6.00 - 12.00
1.00 - 6.00
Calms: 12.50%

(f)

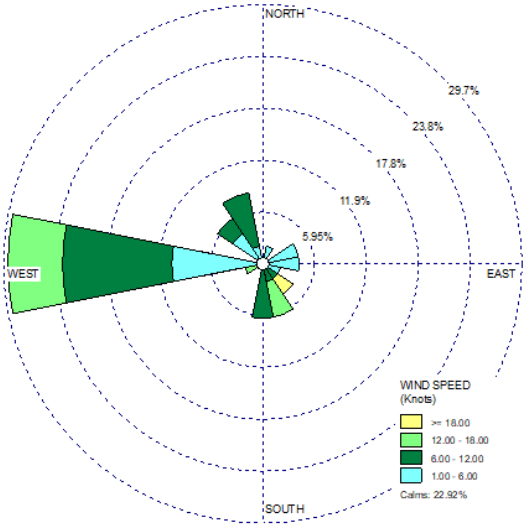
NORTH
29.7%
23.8%
17.8%
11.9%
5.95%
WEST
EAST
SOUTH
WIND SPEED
(Knots)
>= 18.00
12.00 - 18.00
6.00 - 12.00
1.00 - 6.00
Calms: 22.92%

(g)

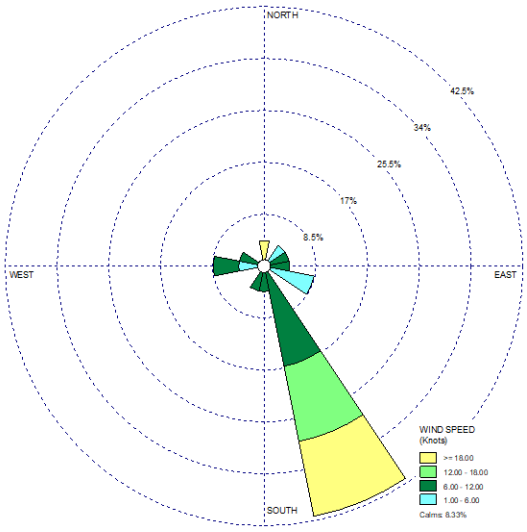

Figure 3-3. (a) Location of Rasht-Airport station has been shown on Google Earth by tiny orange dot. (b) Wind Rose of Rasht-Airport Station from 10 January to 10 February 2021, with considering calm wind plotted on Google Earth. (c) Wind Rose of Rasht-Airport Station from 10 January to 10 February 2021, without considering calm wind. (d) Wind Rose of Rasht-Airport Station for 14-15 January 2021, without considering calm wind. (e) Wind Rose of Rasht-Airport Station for 18 January 2021, without considering calm wind. (f) Wind Rose of Rasht-Airport Station for 28-29 January 2021, without considering calm wind. (g) Wind Rose of Rasht-Airport Station for 5 February 2021, without considering calm wind.

3.2.2 Analysis of foehn event on 14-15 January 2021

In this subsection foehn events that occurred during 14-15 January 2021 are reviewed. For more convenient querying of the changing trend of meteorological quantities, as mentioned in subsection 2.2.1, Table 3-2 shows 3-hourly synoptic data plus some hourly/half-hourly METAR and also SPECI reports over Rasht-Airport station. As mentioned in subsection 2.2.1, 9999 in visibility column means visibility is more than 10 km, NSC in cloudiness column means No Significant Cloud and also VV in cloudiness column means Vertical Visibility[1]. It should be pointed out that cloudiness column is filled from METAR and SPECI reports. Times with foehn conditions shaded gray in this table. Sometimes without foehn events are presented in Table 3-2 to show somehow ordinary conditions over the Rasht-Airport station. Beside that we gathered daily maximum temperature, maximum wind speed, direction of maximum wind speed and minimum pressure data from IRIMO over this station for this period (Table 3-3).

Considering Table 3-2, on 14 January, pressure dropped from 1010 to 1008 mb from 00:00 to 03:00 UTC, which will be discussed in the following analysis maps (Figure 3-4). This pressure

[1] A subjective or instrumental evaluation of the vertical distance into a surface-based obscuration that an observer is able to see. The height ascribed to vertical visibility is always a ceiling height.

drops over the Caspian shores of Iran could motivate southerly wind (150 degree) with speed about 5 m/s at 05:00 UTC. As mentioned above, southerly wind in this area satisfies foehn conditions. It is notable that wind was not detected (clam) (0 m/s) till 04:30 UTC at this date. This southerly wind can be the cause of 14 ℃ temperature increase, from 8 to 22 ℃, in the half-hour (04:30-05:00 UTC). At the same time, there is dewpoint falling by about 15 ℃, from 8 to -7 ℃. So, we could conclude that foehn conditions have prevailed in this area 04:30-05:00 UTC. It is worth noting that visibility improved from 600 m at 00:00 UTC to 2000 m at 03:00 UTC. It also improved to 6000 m at 05:00 UTC and finally to more than 10 km in 05:30 UTC, simultaneously with southerly wind. Also, low-level clouds reports were removed gradually as it was shown in Table 3-2. The reported low-level cloud in 00:00 UTC was BKN009, which means 5-7 oktas of sky above the station covered by cloud with the height of the cloud base in 900 ft; at 03:00 UTC the height of the cloud base rose to 2500 ft and at 04:30 UTC the sky is less cloudy which low-level cloud at this time covered 3-4 oktas (SCT025TCU). At 06:00 UTC low-level cloud covered 1-2 oktas (FEW025), which is consistent with what is mentioned in section 2.1 about evaporation of low-level clouds during foehn events.

On the other hand, a change in direction of wind has occurred from southeasterly-southerly (140 degree) to southwesterly-westerly (230-260 degree) with reducing speed from 7 to 3 m/s in 21-23:00 UTC. Also, temperature decreasing from 22 to 10 ℃ with humidity increasing (dewpoint increasing from -8 to 9 ℃) in an hour (22-23:00 UTC) shows disappearing foehn conditions. Since pressure variations at this station don't show a special result, this item should be queried out of the station, as discussed in the following about pressure gradient between southern and northern Alborz Mountains (Figure 3-4).

Similar conditions could be expressed for 15 January; wind turned from northerly (350 degree) in 04:00 UTC to southerly (200-180 degree) in 04:30-05:00 UTC. Temperature rose from 7 ℃ in 04:30 up to 14 ℃ at 05:00 and 19.6 ℃ at 06:00 UTC. Coincide with this rising temperature there is dropping of dewpoint from 7 to -9.6 ℃ in 04:30-06:00 UTC. So again, at Rasht-Airport station (Lon 49.62, Lat 37.32) located in the leeward area, temperature increased more than 12 ℃ and dewpoint decreased more than 16 ℃ in about an hour and a half, satisfying foehn conditions. Improvement of visibility from 3000 m to more than 10 km in an hour (04:00-05:00 UTC) could be from the effects of foehn event. Low-level cloud with the height of the base at 2000 ft which covered 3-4 oktas (SCT020) was removed at 06:00 UTC.

Foehn conditions was weakened with turning of wind from southerly-southwesterly (210 degree) to westerly-northwesterly (300-320 degree) between 15:00-17:00 UTC. Temperature dropped more than 7 ℃ (from 18.4 to 11 ℃) and dewpoint increased from 0.8 up to 9 ℃ in this interval. The other noteworthy point is increasing pressure at the station from 1008 to 1011 mb in 15:00-17:00 UTC, and also 1018 mb in 21:00 UTC.

Based on Table 3-3 daily minimum pressure in 14 and 15 January, which showed foehn conditions, about 5-8 mb was less than 13 and 16 January. Daily maximum temperature on 13 January was about 14 ℃, but on 14 and 15 January reached up to 23 ℃. Maximum wind speed was also higher in 14 and 15 January than 13 and 16 January, about 2-7 m/s. One point is that the wind direction with maximum speed was completely southerly (170-180 degree) for 14-15 January; again, considering the orientation of the Alborz Mountains (west-east) shows direction of wind from windward (south) to leeward (north), however, in 13 and 16 January direction of maximum wind speed was northerly (30 degree) and westerly (270 degree), respectively. It is worth noting that wind speed reaches to more than 7 m/s in some hours during these two foehn events (7 m/s at 21:00 UTC 14 January, and about 10 m/s at 08:00 UTC 15 January). So, in summary this table confirms foehn conditions in 14-15 January.

Table 3-2. 3-hourly and some half-hourly temperature, dewpoint temperature, wind speed and wind direction over Rasht-Airport station (Lon 49.62, Lat 37.32) (leeward) from 00:00 UTC 13 January to 21:00 UTC 16 January 2021. Foehn conditions were shaded gray.

date	Wind direction (degree)	Wind speed (m/s)	Temperature (℃)	Dewpoint (℃)	Visibility (m)	Cloudiness	Pressure (mb)
1/13/2021 00:00	0	0	4.2	4.2	500	VV003	1023
1/13/2021 03:00	0	0	7.2	7.2	700	VV004	1021
1/13/2021 06:00	60	2	8.4	8.4	2000	BKN012	1021
1/13/2021 09:00	0	0	11.0	8.1	4000	BKN012	1017
1/13/2021 12:00	220	2	13.4	8.2	5000	NSC	1016
1/13/2021 15:00	360	2	8.0	7.1	3000	FEW100	1014
1/13/2021 18:00	0	0	7.2	7.2	1500	NSC	1012
1/13/2021 21:00	0	0	5.4	5.4	100	NSC	1010
1/14/2021 00:00	0	0	6.4	6.4	600	BKN009	1010
1/14/2021 03:00	0	0	8.0	8.0	2000	BKN025	1008
					2000	SCT025TCU	
1/14/2021 04:30	0	0	8	8		BKN080	1008

					6000	SCT025TCU	
1/14/2021 05:00	150	5	22	-7		BKN080	1008
					9999	SCT025TCU	
1/14/2021 05:30	180	6	23	-4		BKN080	1009
					9999	SCT025TCU	
1/14/2021 06:00	170	5	21.6	-3.9		BKN070	1009
					9999	FEW025	
						SCT070	
1/14/2021 09:00	160	5	24.0	-4.6		BKN180	1007
					9999	FEW025	
						SCT080	
1/14/2021 12:00	170	6	25.0	-15.2		BKN180	1005
					9999	FEW025	
						SCT080	
1/14/2021 15:00	0	0	17.4	-2.6		BKN170	1005
					9999	SCT070	
1/14/2021 18:00	150	5	20.6	-4.4		SCT170	1005
					9999	FEW030	
1/14/2021 21:00	140	7	22.2	-6.4		SCT200	1005
					9999	FEW080	
1/14/2021 22:00	230	5	22	-8		SCT200	1005
					7000	FEW080	
1/14/2021 23:00	260	3	10	9		SCT200	1007
1/15/2021 00:00	240	4	9.2	8.8	2500	SCT010	1007
1/15/2021 00:11	250	4	9	9	400	NSC	1007
1/15/2021 03:00	0	0	7.8	7.8	900	NSC	1006
1/15/2021 04:00	350	3	8	8	3000	SCT020	1006
					5000	FEW020	
1/15/2021 04:30	200	2	7	7		SCT180	1006
					9999	FEW020	
1/15/2021 05:00	180	2	14	2		BKN180	1006
					9999	FEW090	
1/15/2021 06:00	150	4	19.6	-9.6		BKN200	1006
					9999	FEW090	
1/15/2021 08:00	180	9.5 (19 kt)	22	-10		BKN200	1006
					9999	FEW090	
1/15/2021 09:00	180	8	22.6	-5.3		SCT200	1006

1/15/2021 12:00	170	6	23.8	-3.1	9999	FEW030	1006
1/15/2021 15:00	210	2	18.4	0.8	9999	FEW100	1008
1/15/2021 16:00	300	6	13	9	9999	FEW100	1008
1/15/2021 17:00	320	3	11	8	9999	NSC	1012
1/15/2021 18:00	0	0	10.6	7.7	9999	NSC	1013
1/15/2021 21:00	0	0	8.6	8.2	9999	NSC	1018
1/16/2021 00:00	0	0	6.6	6.6	4000	NSC	1016
1/16/2021 03:00	0	0	4.6	4.6	4000	NSC	1015
1/16/2021 06:00	0	0	9.6	7	7000	NSC	1016
1/16/2021 09:00	70	3	19.0	8.6	9999	NSC	1014
1/16/2021 12:00	40	4	18.0	8.8	9999	NSC	1013
					4000	FEW015CB	
						SCT020	
1/16/2021 15:00	250	4	12.2	11.4		OVC080	1015
					7000	SCT020	
1/16/2021 18:00	240	3	11.2	10.8		BKN080	1015
					8000	SCT020	
1/16/2021 21:00	240	2	11.0	9.4		BKN080	1013

Table 3-3. Maximum Temperature, wind speed, direction of maximum wind, and minimum pressure over Rasht-Airport station (Lon 49.62, Lat 37.32) (leeward) from 13 to 16 January 2021.

date	Maximum Temperature (°C)	Maximum wind speed (m/s)	Direction of maximum wind speed	Minimum pressure (mb)
1/13/2021	13.6	3	30	1010.8
1/14/2021	25.2	8	170	1005.2
1/15/2021	23.8	10	180	1006.2
1/16/2021	20.4	6	270	1013.5

For more consideration, same quantities (temperature, dewpoint, wind speed and direction and surface pressure) for Anzali station (Lon 49.46E, 37.48N) and January 13-16 are gathered in Table a-1; times with foehn conditions were shaded gray in this table. A drop of surface pressure could be seen in this table from 13 January, which that its value at 00:00 UTC January 13 was about 1020 hPa, and at the same time January 14 was about 1009 hPa. This surface pressure falling continued till 11:00 UTC January 14 which the reported surface pressure was about 1002 hPa. Deployment of the low pressure over the Caspian Sea caused southerly wind over leeward stations

including Anzali; 05-06:00 UTC wind speed rose from calm to 3 m/s with southerly direction (210 degree), caused the temperature increasing more than 10 ℃, from 9 to 19.6 ℃, in about one hour; at the same time dewpoint decreased from 9 to 3.7 ℃, then reached to -1 ℃ at 09:00 UTC January 14, showing the foehn condition from 06:00 UTC. The visibility improved from 7000 to more than 10 km from 05:00 to 06:00 UTC January 14.

Based on data in Table a-1, foehn conditions in Anzali station can be seen till 20:00 UTC January 14, which the southerly wind continued. At 21:00 UTC wind turned westerly (300 degree), temperature decreased to 11.3 ℃, which means about 8 ℃ (from 19 ℃ at 20:00 UTC to 11.3 ℃ at 21:00 UTC) decreasing of temperature in about 1 hour; at the same time dewpoint increased more than 11 ℃ (from -1 ℃ to 10.5 ℃). Visibility decreased from more than 10 km to 3000 m in one hour (from 21:00 to 22:00 UTC), also reached to 100 m at 24:00 UTC January 14.

The westerly-northwesterly wind (260-320 degree) continued till 04:00 UTC January 15; at 05:00 UTC wind turned again southerly (210 degree), wind speed reached to 5 m/s, temperature increased about 10 ℃ and dewpoint decreased about 8 ℃ from 06:00 to 07:00 UTC, indicating foehn condition at Anzali station. This condition continued till 13:00 UTC January 15.

From 14:00 UTC January 15 surface pressure at the station took increasing trend. At this time wind turned northwesterly (330 degree), temperature decreased about 7 ℃ in about one hour (from 13:00-14:00 UTC), and dewpoint increased 3 ℃; so, the foehn conditions was removed from the station after 14:00 UTC.

To survey the windward condition, Tehran station (Lon 51.31E, Lat 35.69N) reports from 13-16 January were gathered in Table a-5, time with foehn condition in leeward, shaded gray in this table. In January 13 and 16, when foehn didn’t occur, comparing weather reports of leeward and windward stations (Table 3-2, Table a-1 and Table a-5) resolved no significant pressure gradient between the south (windward) and north (leeward) of the Alborz Mountains, and the sky of Tehran station was reported clear. In January 14 and 15, when foehn occurred north of the Alborz Mountains, pressure gradient could be seen between the leeward and windward side; the surface pressure over the Tehran station during the foehn event was more than 1014 hPa, while Rasht-Airport and Anzali station reported less than 1009 hPa. The wind direction of Tehran in January 13-16 from 06-18:00 UTC was about southeasterly-southwesterly, which somehow shows cross wind over the Alborz Mountains, however, the reports of cloudiness of sky in January 14-15 over Tehran station (windward of Alborz Mountains) matches the foehn condition.

Another windward station is Zanjan (Lon 48.52E, Lat 36.66E), which its data for January 13-16 were gathered in Table a-9, with shaded gray for foehn times. Unlike Tehran station, Zanjan didn't report any cloudiness in January 14. The surface pressure in this station is less than Tehran and wind for this date is easterly (100-120 degree), which didn't cross the Alborz Mountains. But wind in Zanjan station for January 15 is southerly-southwesterly (200-240 degree), which crossed the Alborz Mountains and cloudiness of sky was reported.

Reanalysis maps of for 14-15 January 2021 have been shown on Figure 3-4. The analysis maps have been plotted by the NCAR Command Language (NCL, 2019). For convenience in tracking the context, it is suggested to consider southwest of Caspian Sea as the study area. The approximate location of Rash-Airport station, in the study area has been shown by a blue dot in analysis maps. In Figure 3-4(a), related to 00:00 UTC 14 January 2021, it can be seen that the study area is downstream of the upper trough. In Figure 3-4(b), showing MSLP at this time, a high pressure 1016-1020 mb area expanded from Saudi Arabi to the Iranian Plateau. A tongue of this high-pressure system is stretched to the south of Alborz Mountains. On the other hand, a low-pressure system with two closed centers, 1000 mb, could be seen, one over the east of Ukraine and the other one over the north of Caspian Sea. Considering the mentioned upper trough (Figure 3-4(a)), dynamical structure of the low pressure over Caspian Sea could be concluded. At 03:00 UTC 14 January the upper trough moved slightly eastward (Figure 3-4(c)). At this time the 1008 mb contour expanded over the Caspian Sea and stretched to the shores of Iran including the study area, as pressure value entered at 03:00 UTC in Table 3-2 confirms. The 1016 mb contour is still stationed over the south of Alborz Mountains (Figure 3-4(d)). This layout of high and low pressure over two sides of Alborz Mountains, caused southerly wind with direction of 150-180 degree and speed of 5-6 m/s over the Rash-Airport station, from 05:00-06:00 UTC 14 January (Table 3-2), and then caused about a 12 °C temperature increasing and also 12 °C dewpoint decreasing, as mentioned above for Rasht-Airport station (Lon 49.62E, Lat 37.32N). One of the indications of a foehn event is simultaneous reduction of absolute humidity with temperature rising. Generally, low pressure over the Caspian Sea with a high pressure over south of Alborz Mountains seems the most appropriate pattern for foehn events over north coasts of Iran (Mofidi, et al., 2015).

As discussed previously, from 22:00 UTC 14 January foehn conditions disappeared. However, pressure at the Rasht-Airport station didn't change considerably (Table 3-2), indicating pressure variations should be sought out of the station. Considering the 500 mb map at 21:00 UTC 14

January (Figure 3-4(e)), a trough over Iraq and approaching the Caspian sea over the next hours (00:00-03:00 UTC 15 January, Figure 3-4(g, i)), caused a reducing pressure gradient between windward and leeward of Alborz Mountains; as the 1008 mb contour could be seen over Alborz Mountains and the 1016 mb contour settled down just over the south half of Iran (Figure 3-4(f, h, j)). It is necessary to note that there is a climatological low pressure over the sea at this time of year, respecting the temperature contrast between land and sea. This weakening of pressure gradient is the reason that without having specific pressure variations in Rasht-Airport station (Lon 49.62E, Lat 37.32N), after 21:00 UTC 14 January, as mentioned above, the wind turned and foehn conditions were removed. General climatological conditions have ruled in a 1-2 hours period (21:00-23:00 UTC); temperature decreased by about 12 ℃ and dewpoint increased about 17 ℃; visibility changing is also sharp, from over 10 km in 21-22:00 UTC to 400 m in a SPECI report issued at 00:11 UTC 15 January for Rasht-Airport station (Table 3-2).

Taking into account Table 3-2, it is explained that the wind turned southerly in 04:30-05:00 UTC 15 January, providing foehn conditions at Rasht-Airport station. The synoptic analysis is that reaching the trough receives the Caspian Sea at 06:00 and 09:00 UTC 15 January (Figure 3-4(k, m)), high pressure behind the trough axis settles over the Alborz Mountains and low pressure over Caspian Sea strengthened (Figure 3-4 (l, n)).

As the trough cross over the Caspian Sea at 12-18:00 UTC (Figure 3-4(o, q, s)), low pressure passed the sea and pressure over the sea increased (Figure 3-4(p, r, t)), so that 1012 mb contour could be seen over the Caspian Sea at 15:00 UTC; Rasht-Airport station reported 1011 mb and northerly wind (with direction 320 degree and speed 3 m/s) at 17:00 UTC 15 January (Table 3-2). So, low pressure trough passes over the Caspian Sea, foehn conditions disappeared at about 18:00 UTC 15 January. In this case, pressure variations with approaching a trough to the study area and its position respect to the Caspian Sea created, reduced and again created foehn conditions over the north of Alborz Mountains.

(a)

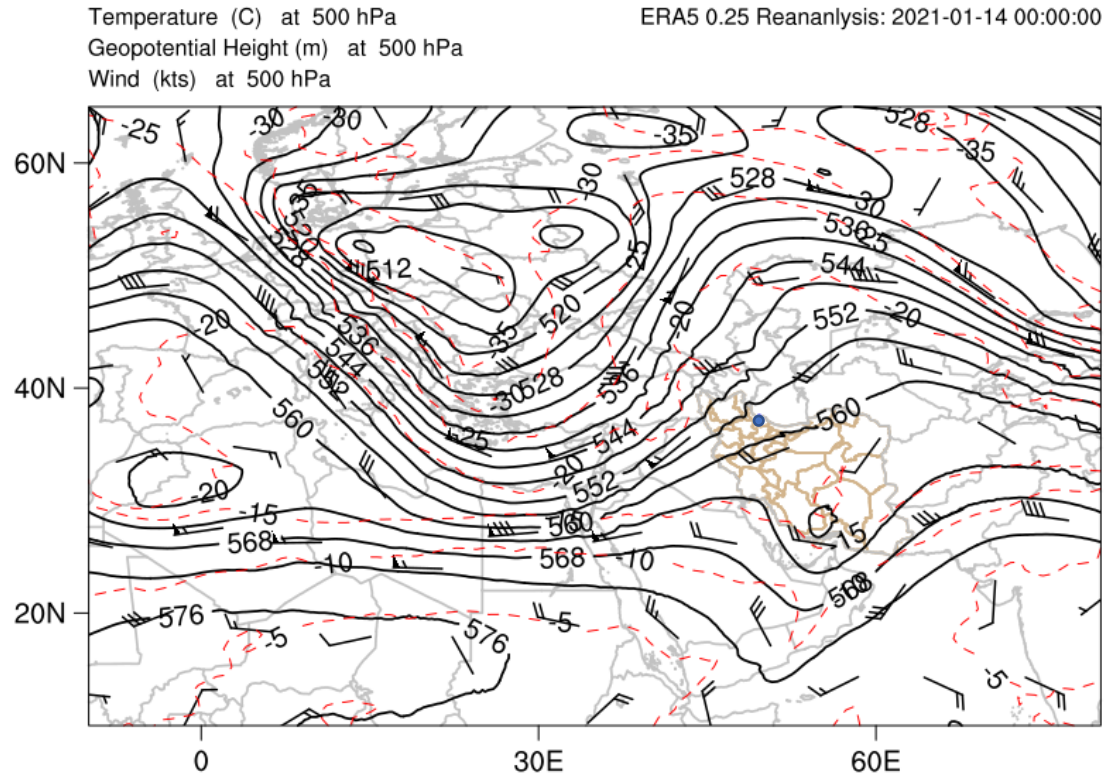
Temperature (C) at 500 hPa
Geopotential Height (m) at 500 hPa
Wind (kts) at 500 hPa
ERA5 0.25 Reananlysis: 2021-01-14 00:00:00
60N
40N
20N
0
30E
60E

(b)

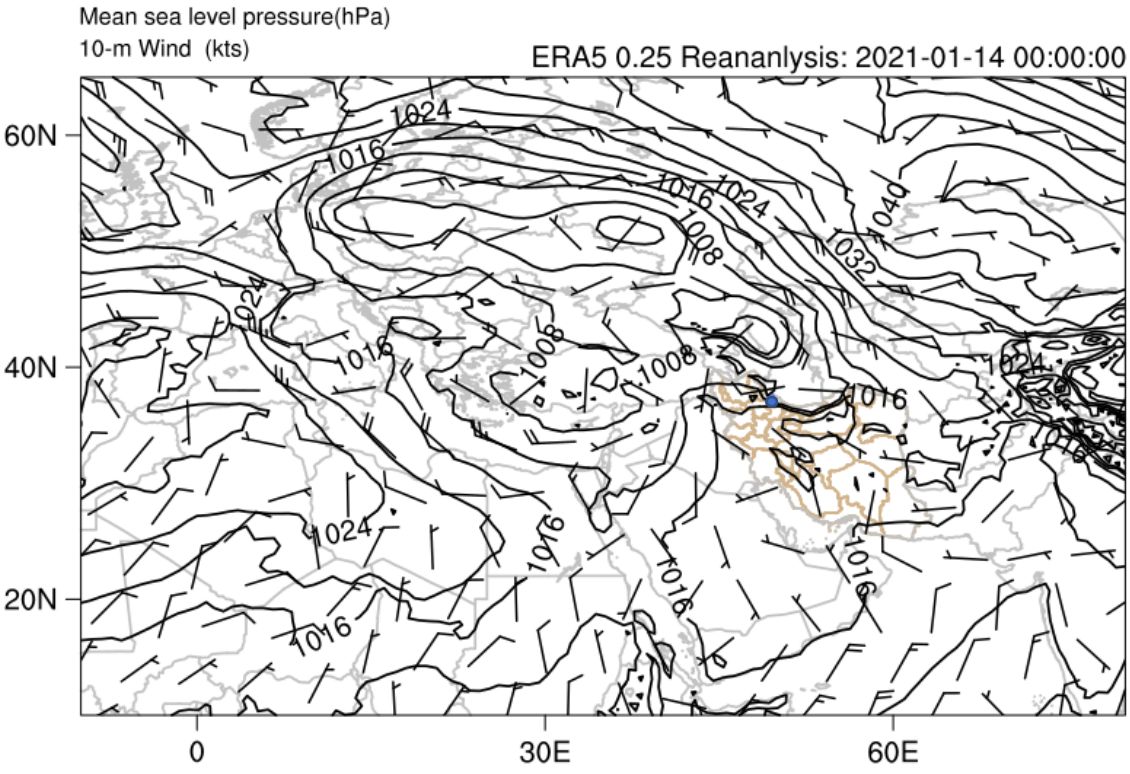
Mean sea level pressure(hPa)
10-m Wind (kts)
ERA5 0.25 Reananlysis: 2021-01-14 00:00:00
60N
40N
20N
0
30E
60E

(c)

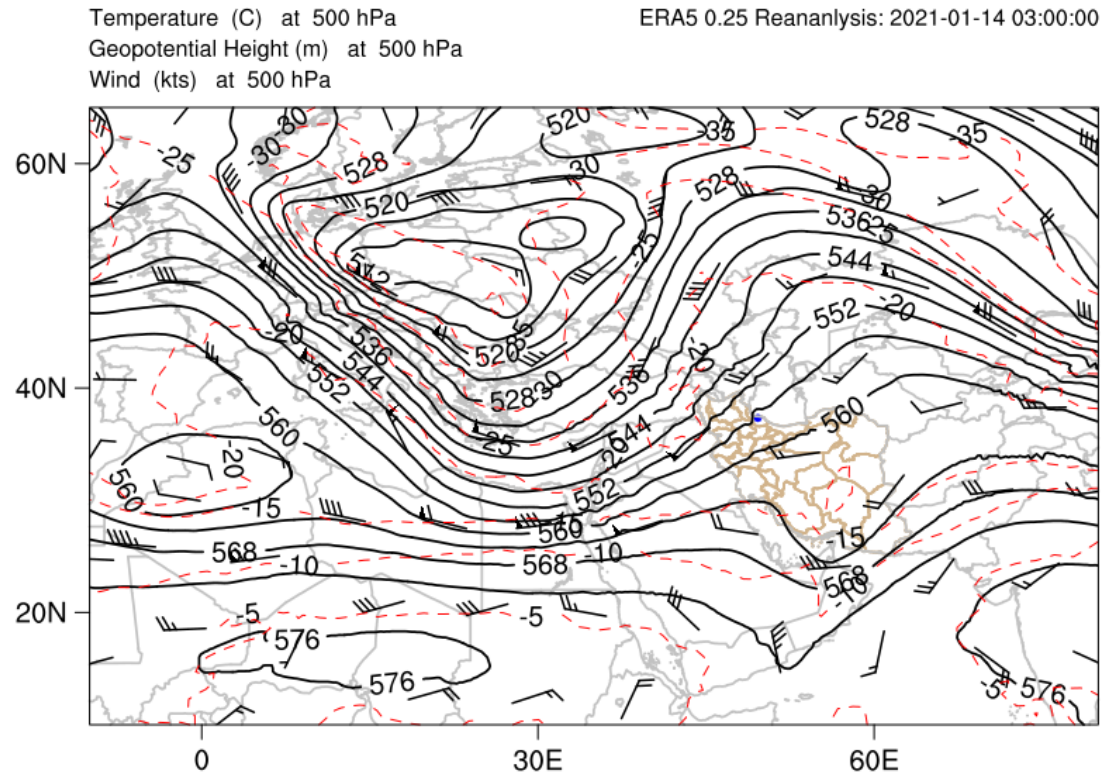
Temperature (C) at 500 hPa
Geopotential Height (m) at 500 hPa
Wind (kts) at 500 hPa
ERA5 0.25 Reananlysis: 2021-01-14 03:00:00
60N
40N
20N
0
30E
60E

(d)

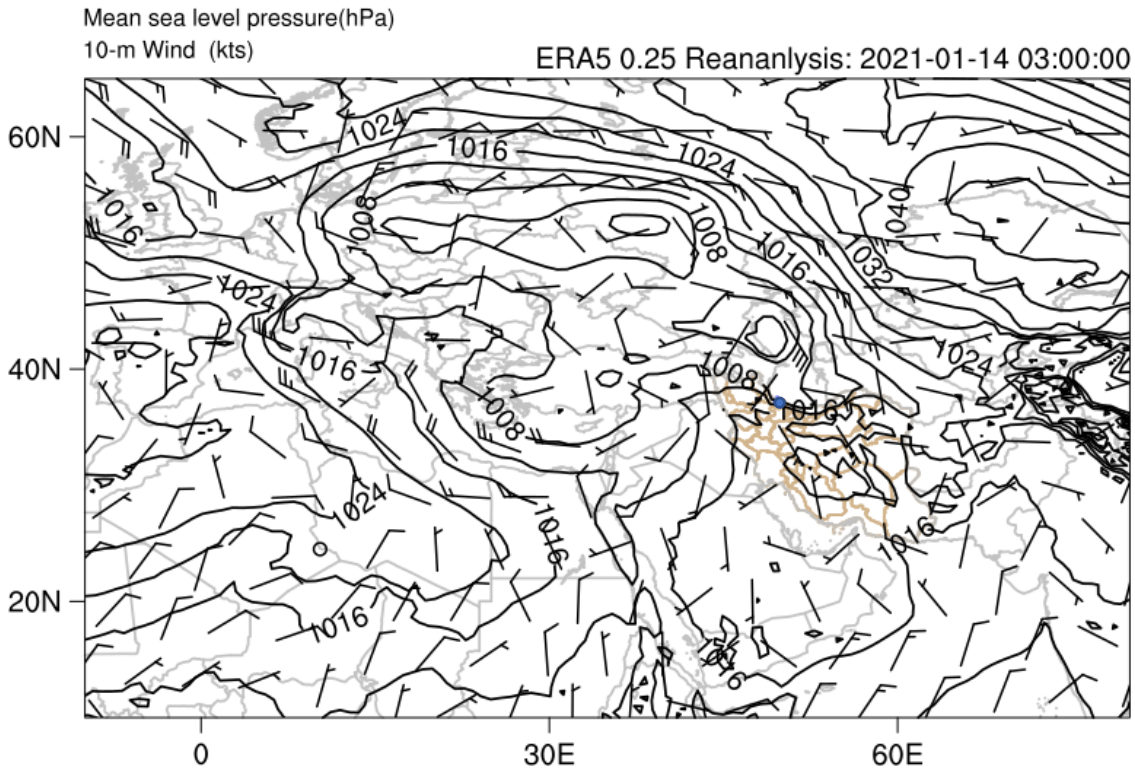
Mean sea level pressure(hPa)
10-m Wind (kts)
ERA5 0.25 Reananlysis: 2021-01-14 03:00:00
60N
40N
20N
0
30E
60E

(e)

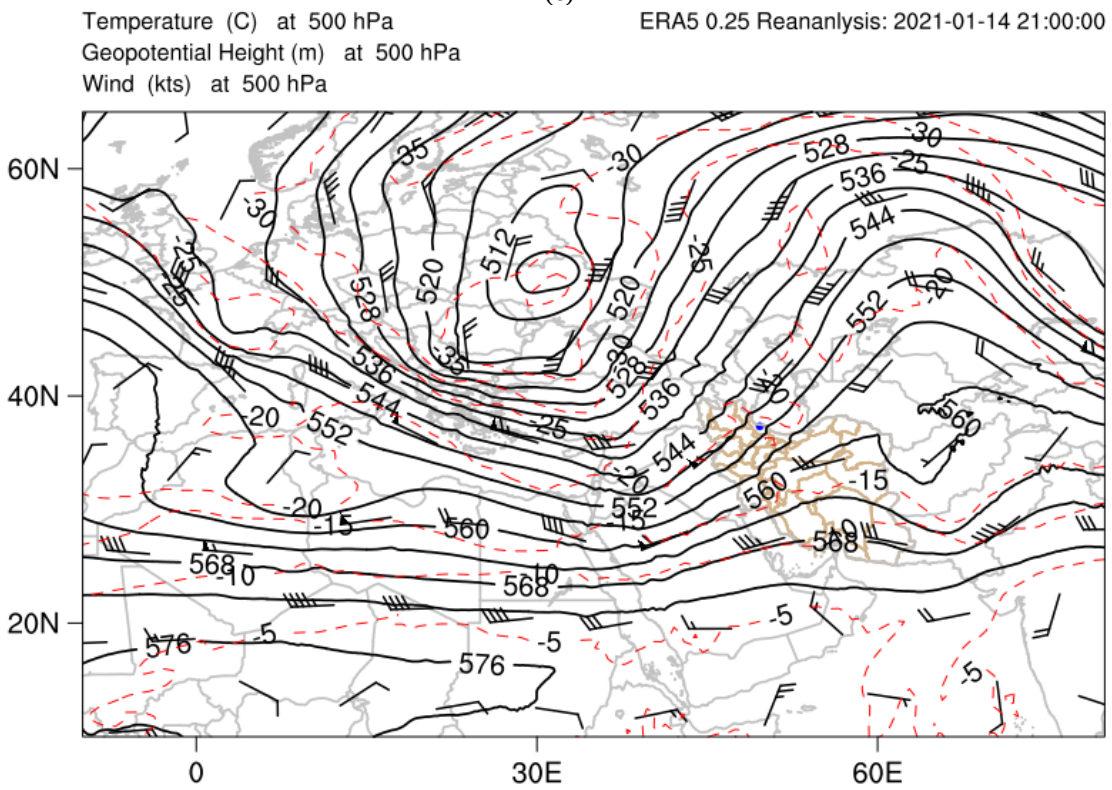
Temperature (C) at 500 hPa
Geopotential Height (m) at 500 hPa
Wind (kts) at 500 hPa
ERA5 0.25 Reananlysis: 2021-01-14 21:00:00
60N
40N
20N
0
30E
60E

(f)

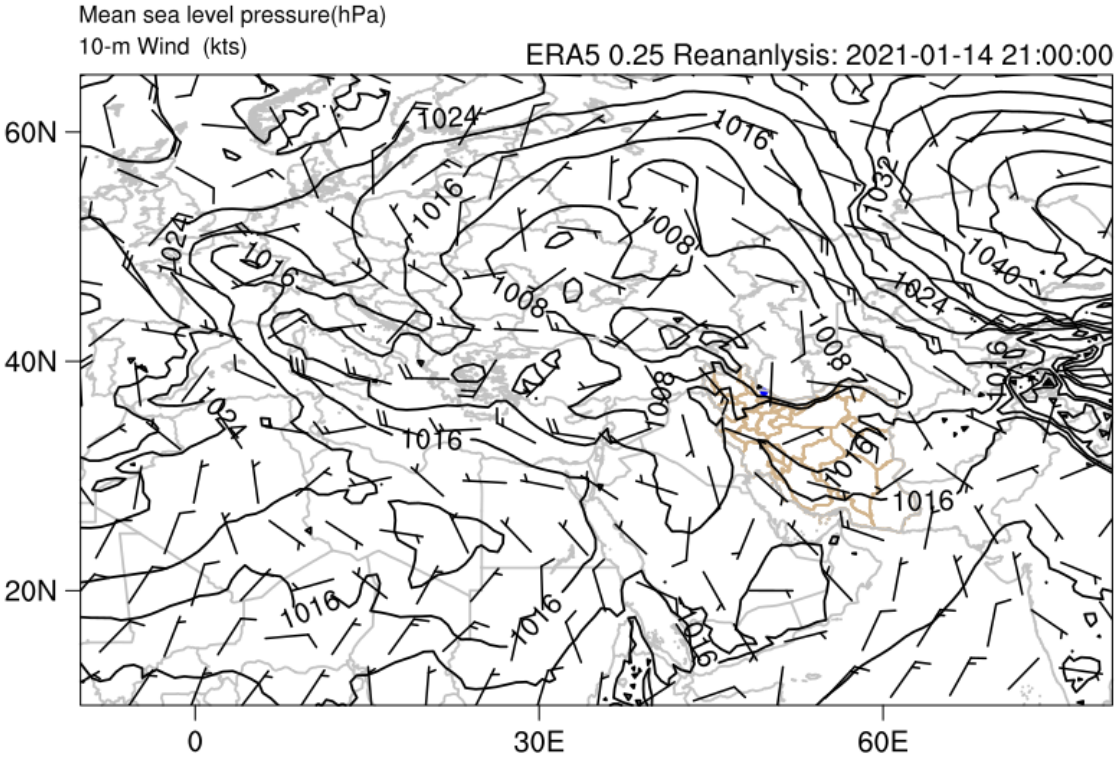
Mean sea level pressure(hPa)
10-m Wind (kts)
ERA5 0.25 Reananlysis: 2021-01-14 21:00:00
60N
40N
20N
0
30E
60E

(g)

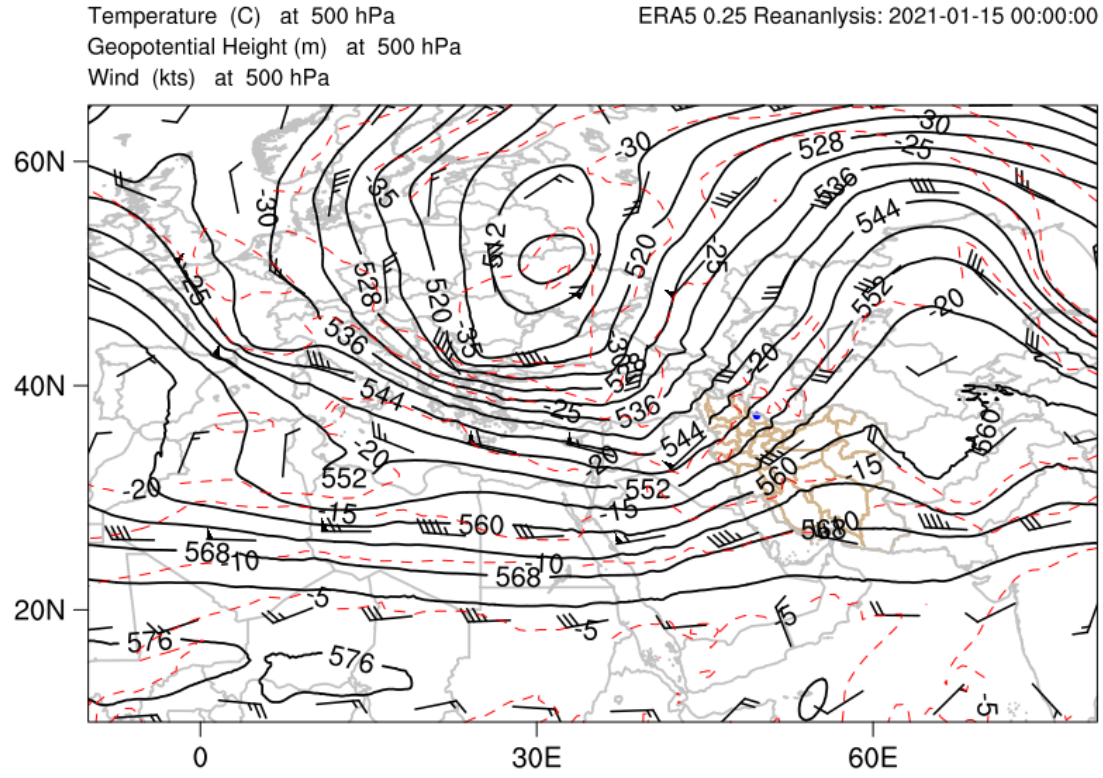
Temperature (C) at 500 hPa
Geopotential Height (m) at 500 hPa
Wind (kts) at 500 hPa
ERA5 0.25 Reananlysis: 2021-01-15 00:00:00
60N
40N
20N
0
30E
60E

(h)

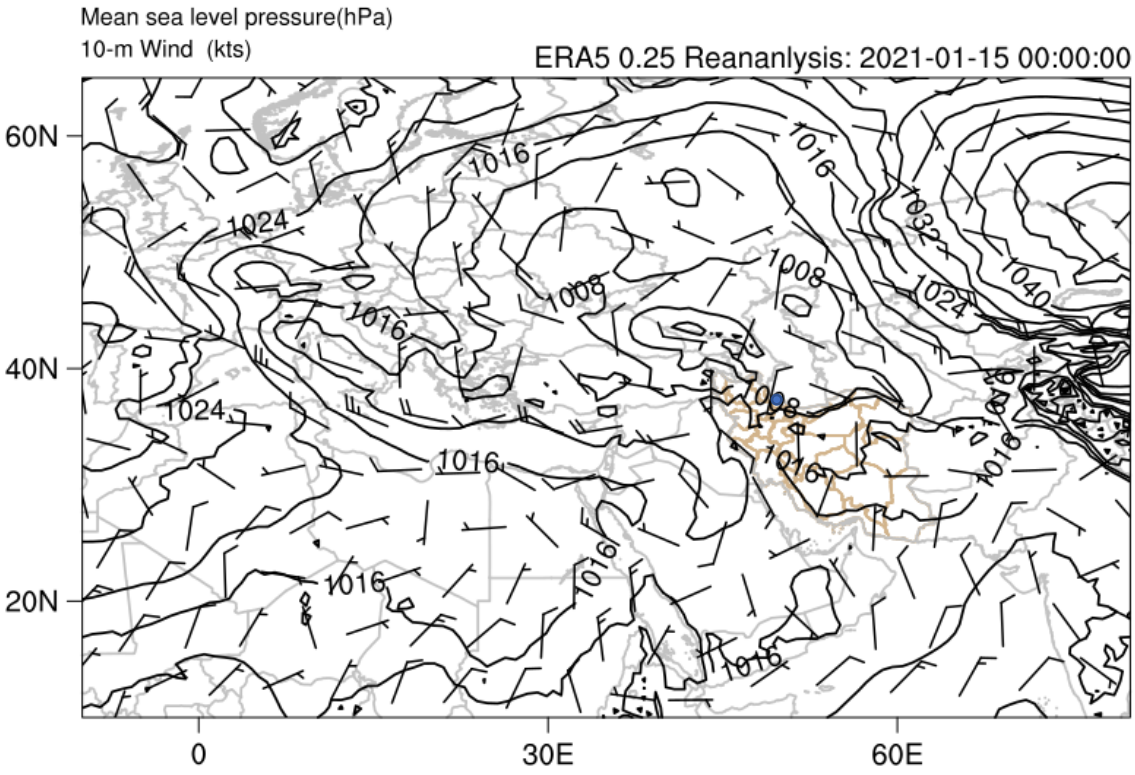
Mean sea level pressure(hPa)
10-m Wind (kts)
ERA5 0.25 Reananlysis: 2021-01-15 00:00:00
60N
40N
20N
0
30E
60E

(i)

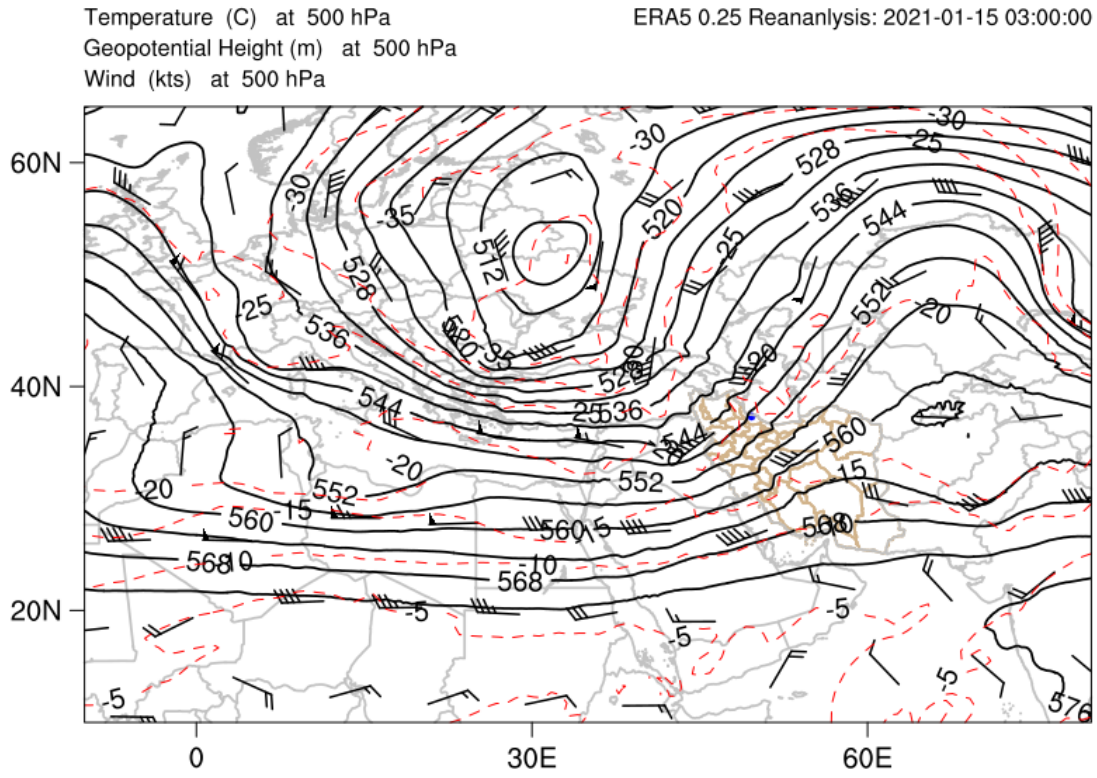
Temperature (C) at 500 hPa
Geopotential Height (m) at 500 hPa
Wind (kts) at 500 hPa
ERA5 0.25 Reananlysis: 2021-01-15 03:00:00
60N
40N
20N
0
30E
60E

(j)

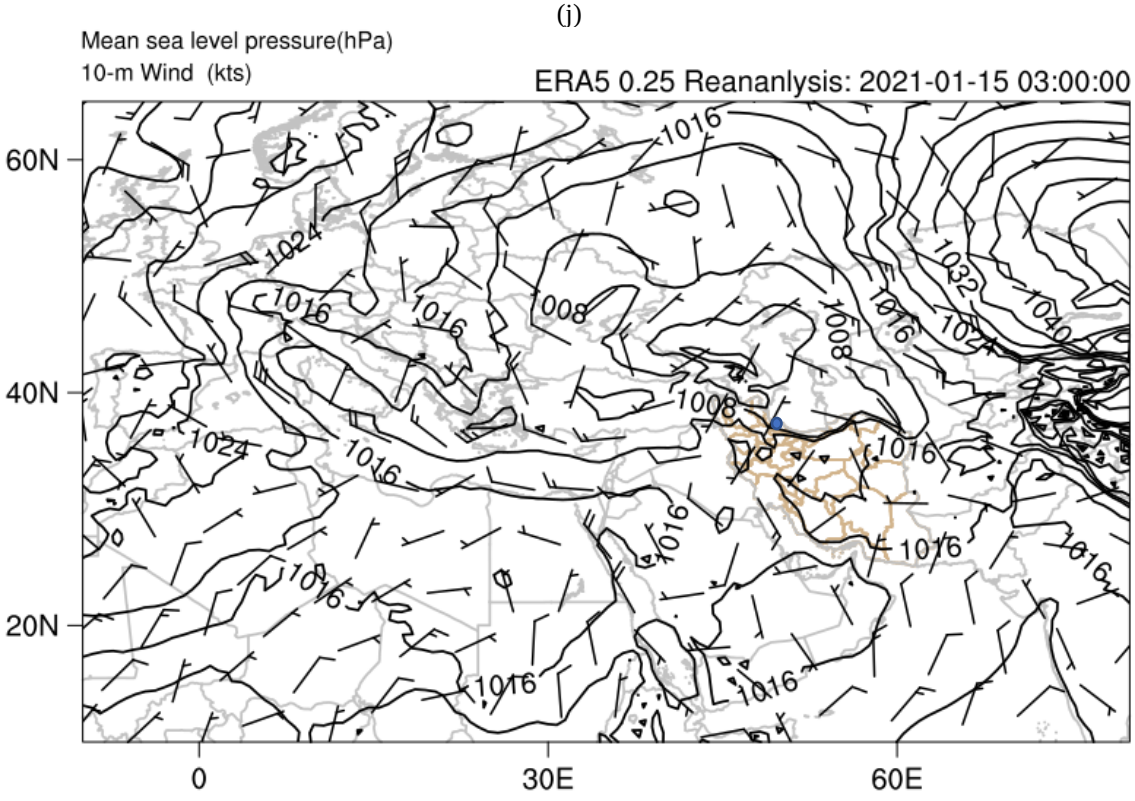
Mean sea level pressure(hPa)
10-m Wind (kts)
ERA5 0.25 Reananlysis: 2021-01-15 03:00:00
60N
40N
20N
0
30E
60E

(k)

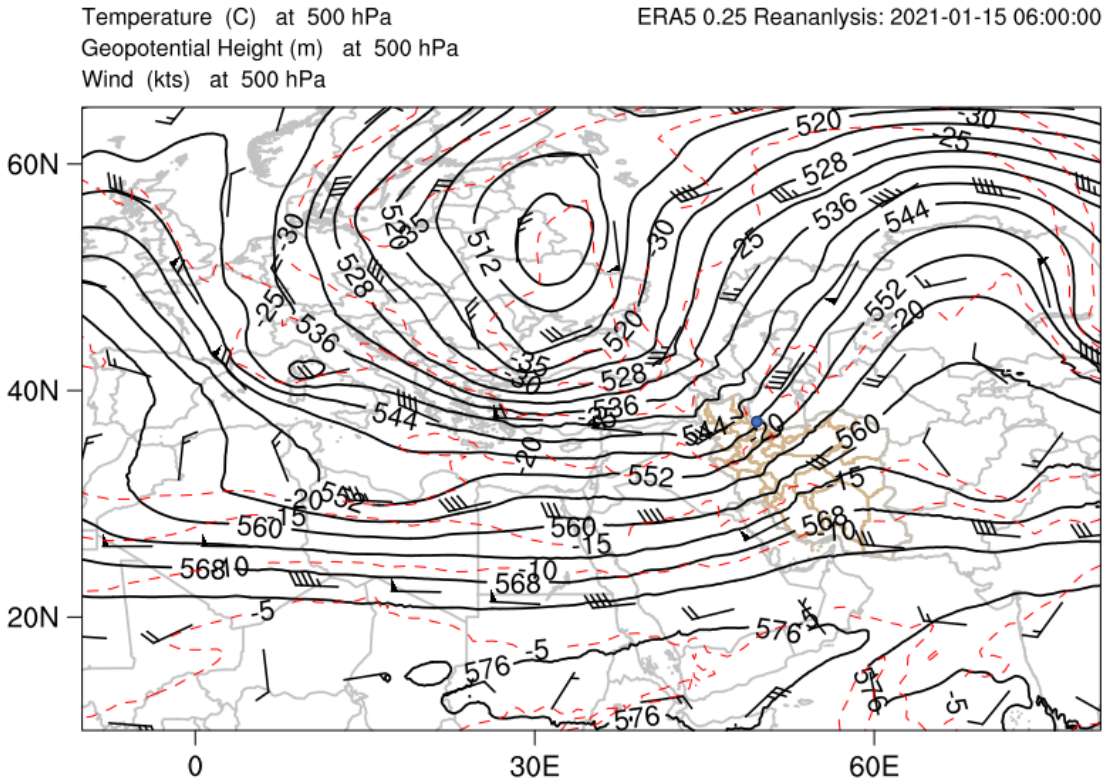
Temperature (C) at 500 hPa
Geopotential Height (m) at 500 hPa
Wind (kts) at 500 hPa
ERA5 0.25 Reananlysis: 2021-01-15 06:00:00
60N
40N
20N
0
30E
60E

(l)

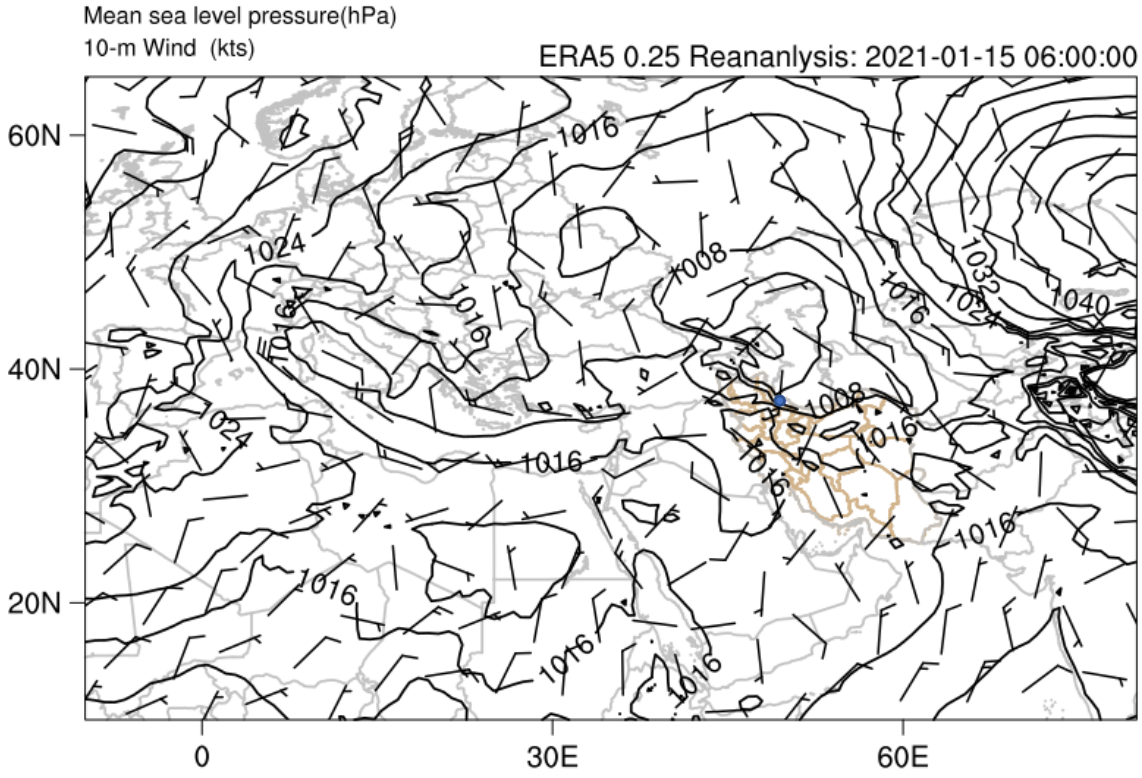
Mean sea level pressure(hPa)
10-m Wind (kts)
ERA5 0.25 Reananlysis: 2021-01-15 06:00:00
60N
40N
20N
0
30E
60E

(m)

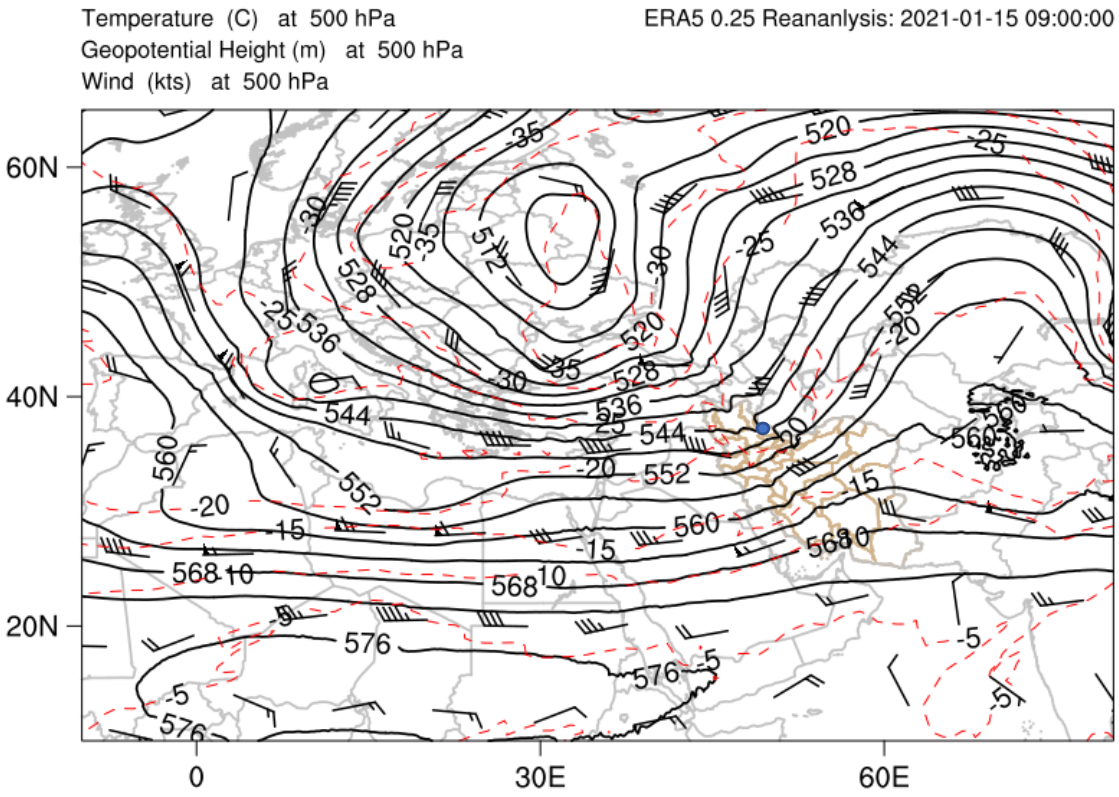
Temperature (C) at 500 hPa
Geopotential Height (m) at 500 hPa
Wind (kts) at 500 hPa
ERA5 0.25 Reananlysis: 2021-01-15 09:00:00
60N
40N
20N
0
30E
60E

(n)

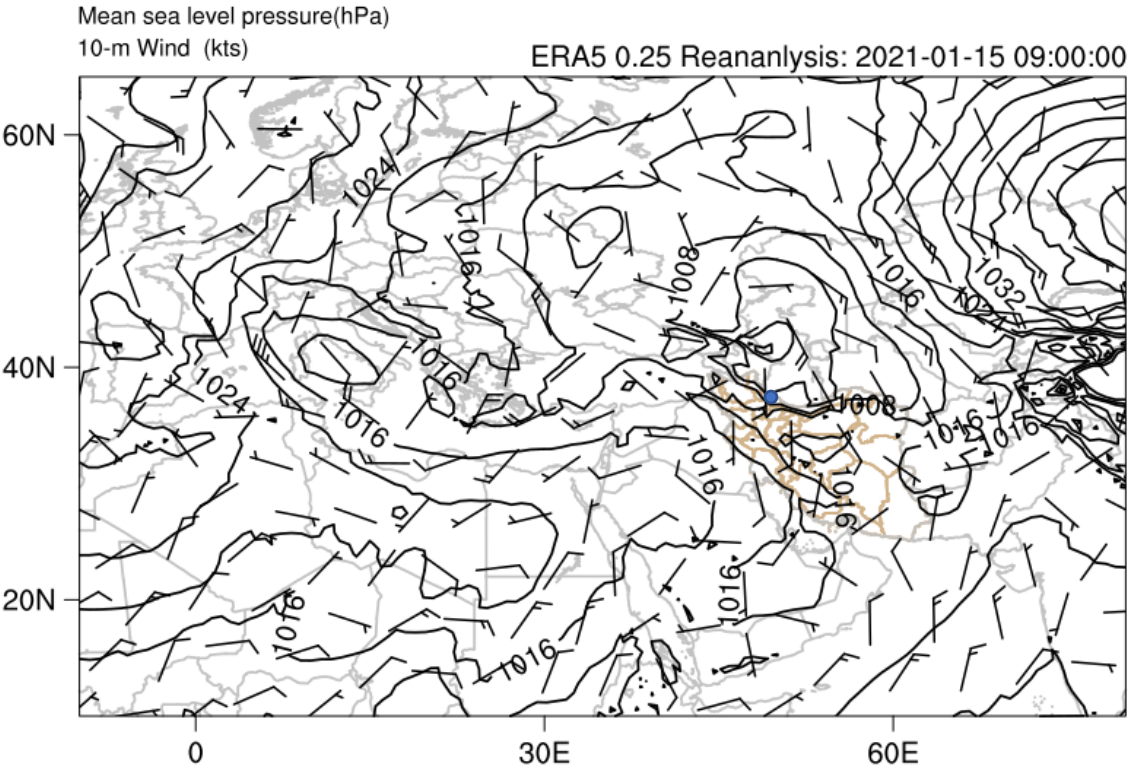
Mean sea level pressure(hPa)
10-m Wind (kts)
ERA5 0.25 Reananlysis: 2021-01-15 09:00:00
60N
40N
20N
0
30E
60E

(o)

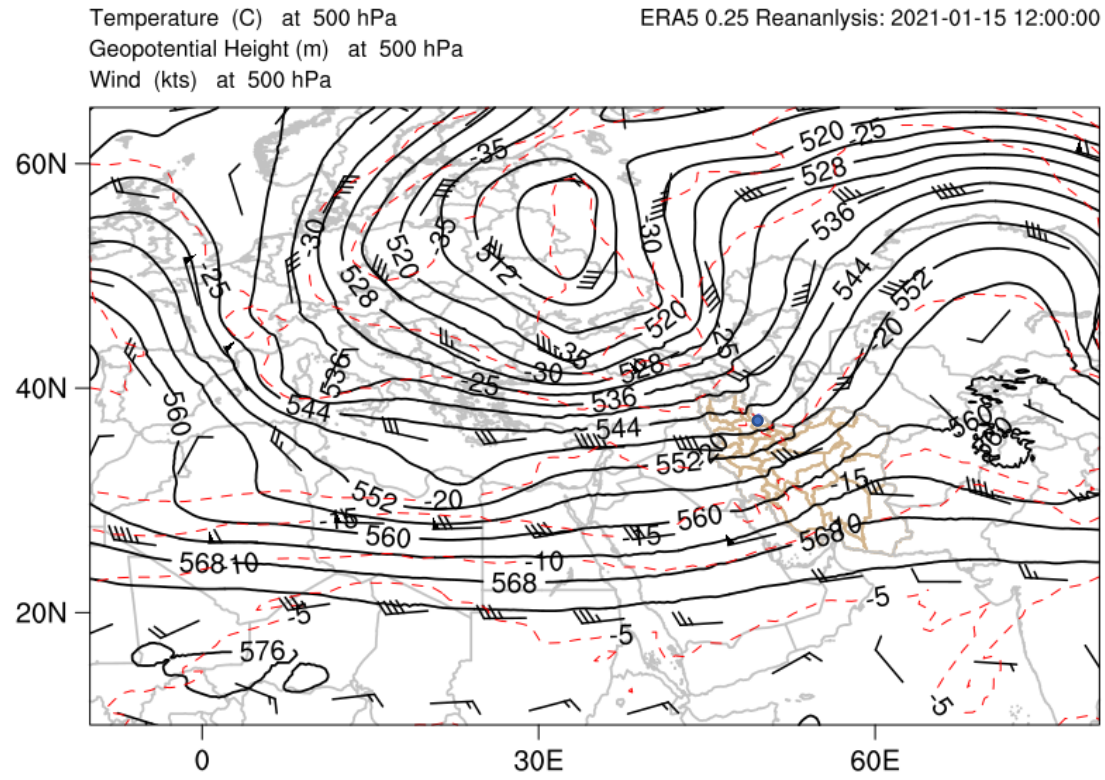
Temperature (C) at 500 hPa
Geopotential Height (m) at 500 hPa
Wind (kts) at 500 hPa
ERA5 0.25 Reananlysis: 2021-01-15 12:00:00
60N
40N
20N
0
30E
60E

(p)

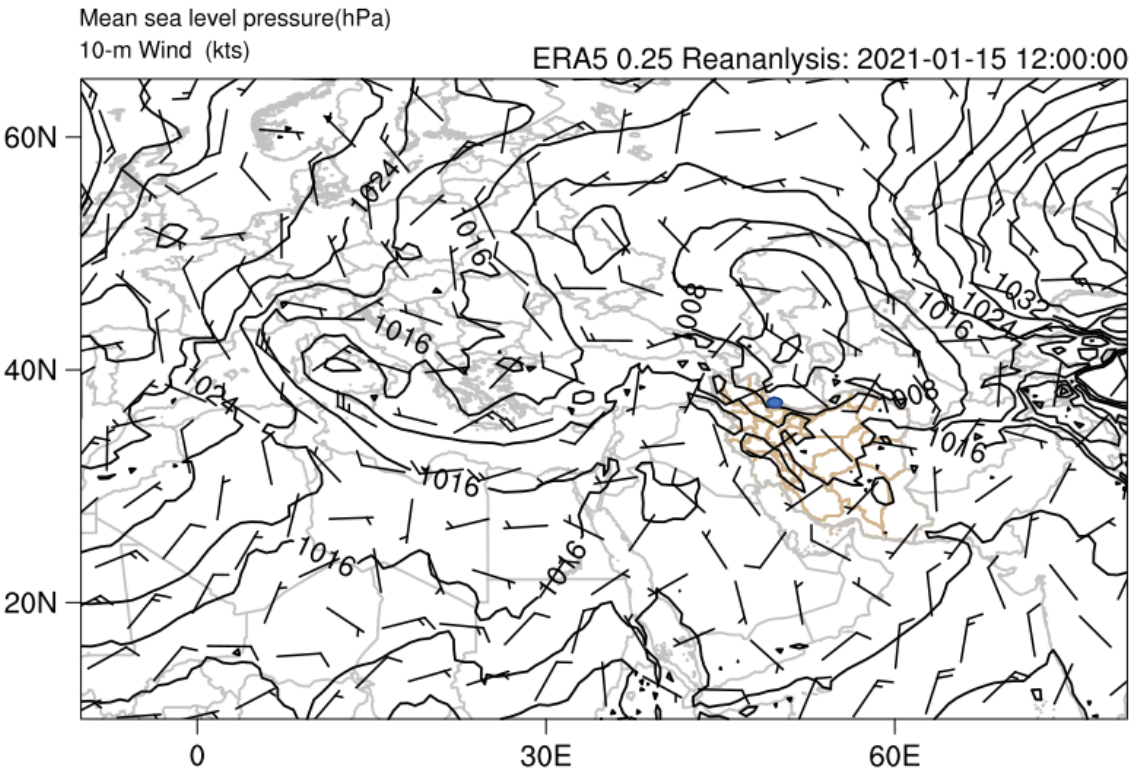
Mean sea level pressure(hPa)
10-m Wind (kts)
ERA5 0.25 Reananlysis: 2021-01-15 12:00:00
60N
40N
20N
0
30E
60E

(q)

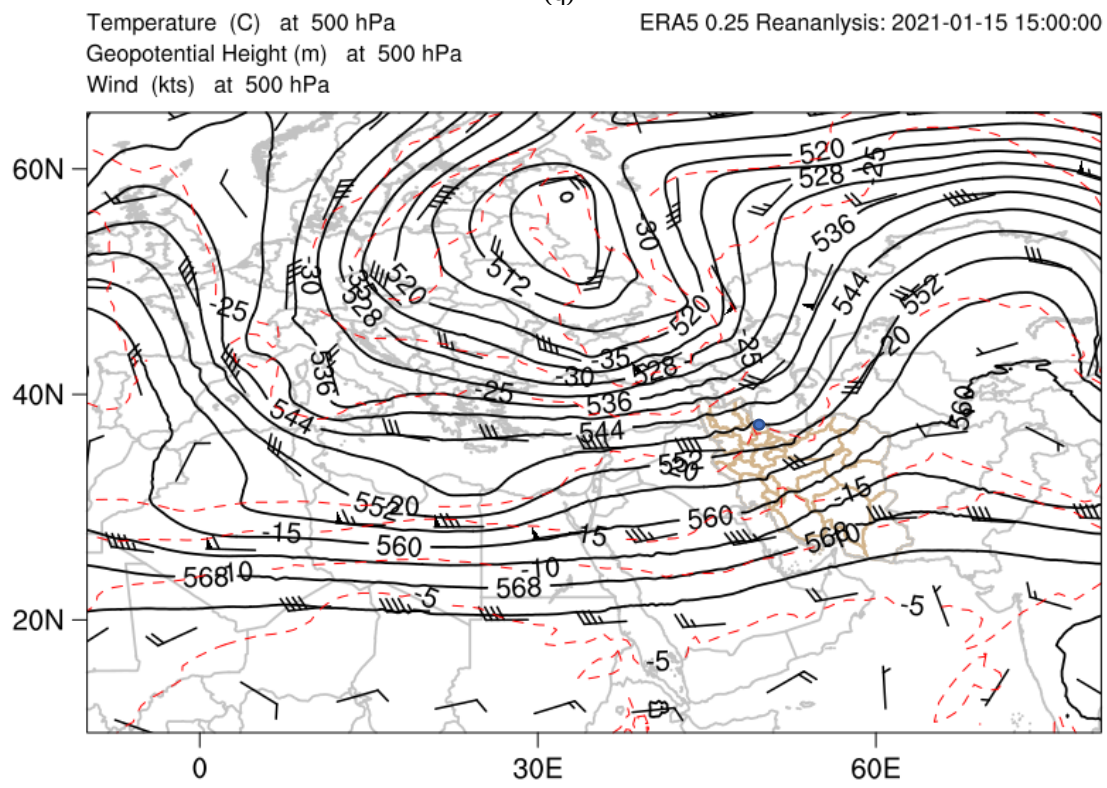
Temperature (C) at 500 hPa
Geopotential Height (m) at 500 hPa
Wind (kts) at 500 hPa
ERA5 0.25 Reananlysis: 2021-01-15 15:00:00
60N
40N
20N
0
30E
60E

(r)

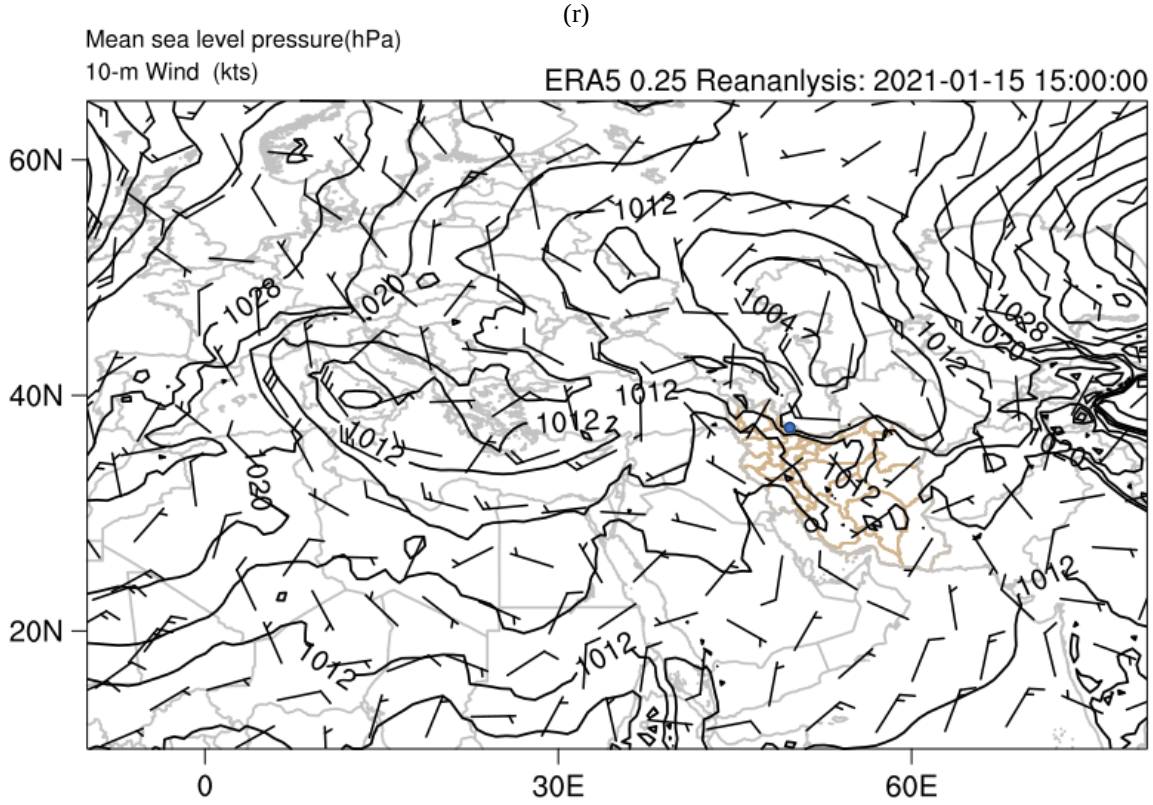
Mean sea level pressure(hPa)
10-m Wind (kts)
ERA5 0.25 Reananlysis: 2021-01-15 15:00:00
60N
40N
20N
0
30E
60E

(s)

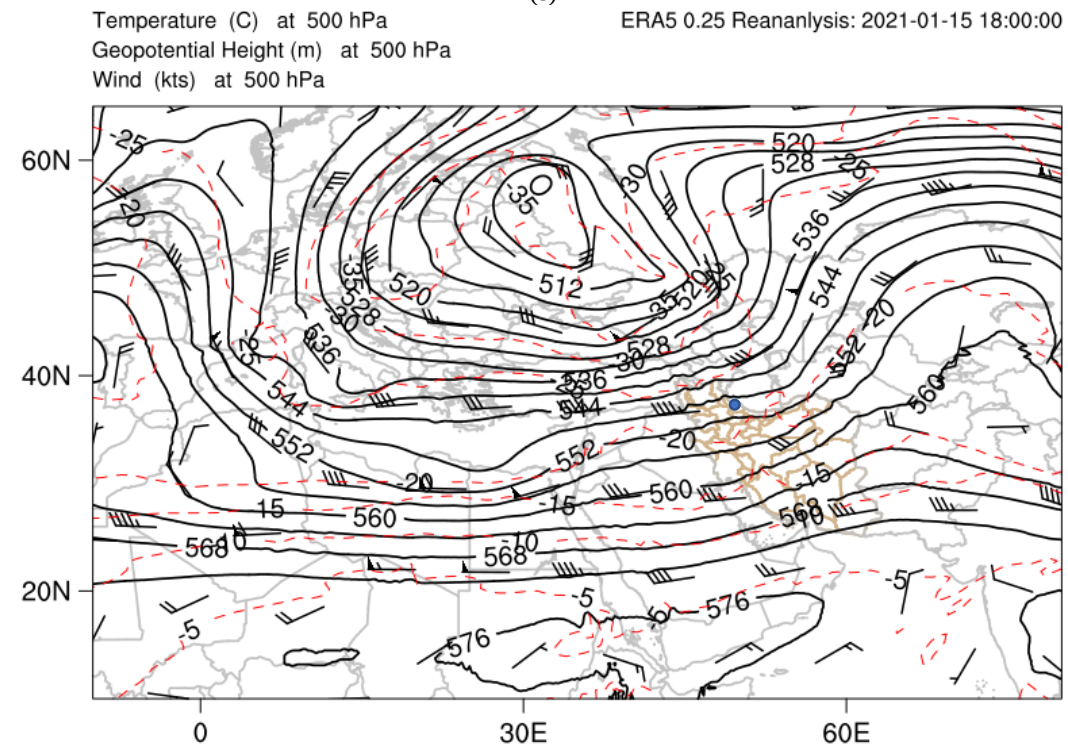

(t)

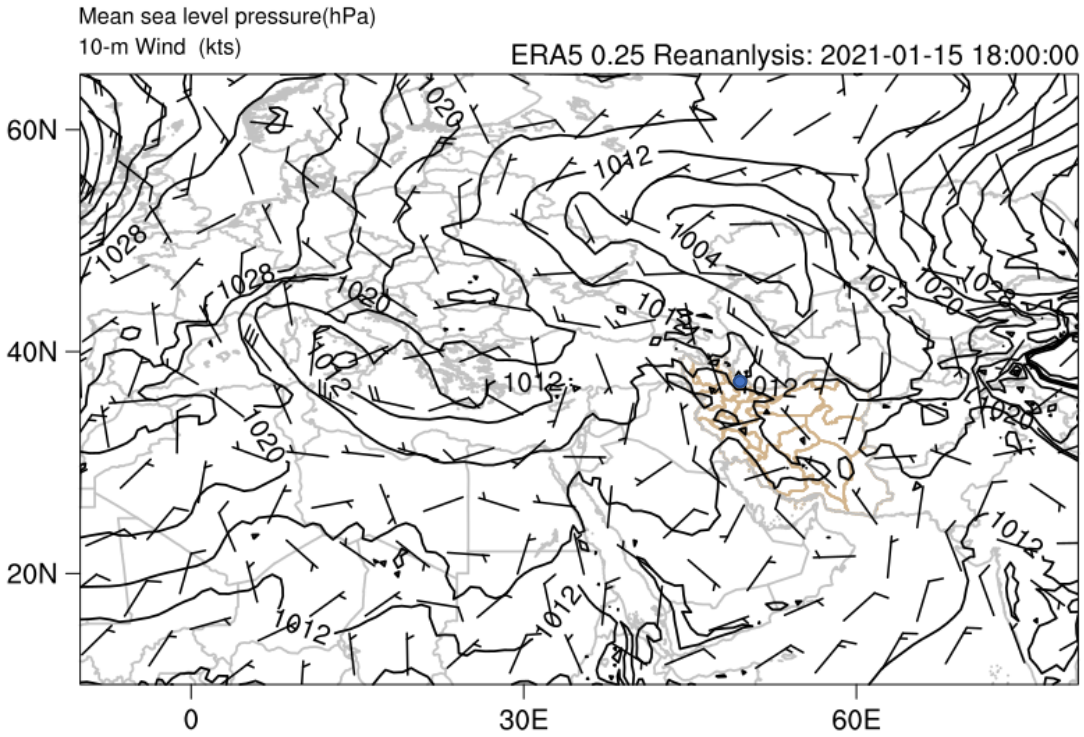

Figure 3-4. Analysis maps for (a, c, e, g, i, k, m, o, q, s) geopotential height (m) (black contours), temperature (℃) (red contoures) and wind barbs at 500 mb pressure level, (b, d, f, h, j, l, n, p, r, t) mean sea level pressure (mb) (black contours) with wind barbs at 10-m height above ground for14-15 January, different hours as the headers.

Skew-T plots of Tehran station (Lon 51.31E, Lat 35.69N) at 00:00 UTC January 13-15, obtained from the University of Wyoming (https://weather.uwyo.edu/upperair/sounding.html) and have been shown in Figure 3-5. As mentioned before the ridge of Alborz Mountains is about 5600-5700 m which is about 500 hPa. The wind direction in the column of atmosphere below the 500 hPa is expected to be southwesterly-northwesterly, normally, as can be seen in January 13 (Figure 3-5(a)). At 00:00 UTC January 13 the wind speed at the height range of ridge is about 10 kt. For January 14 (Figure 3-5(b)) the wind speed below the 500 hPa is mostly southwesterly-westerly; northwesterly direction is not seen at this column of atmosphere. The wind speed at about 500 hPa is about 25kt which is higher with respect to January 13. In January 15 (Figure 3-5(c)) wind speed below 500 hPa is mostly southwesterly with speed about 45 kt at about ridge height, providing the upstream conditions for foehn development.

(a) (b)

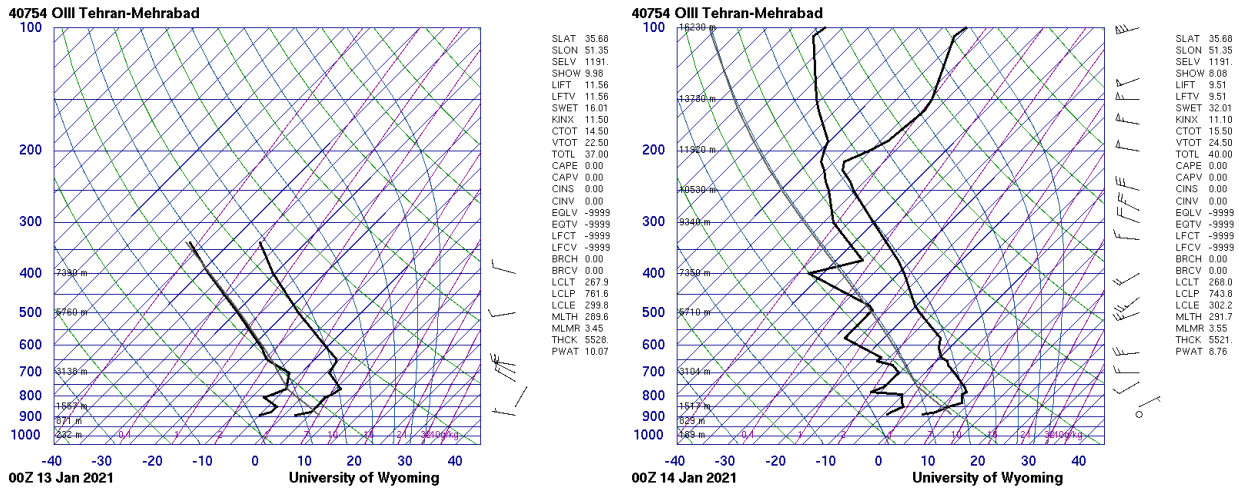

(c)

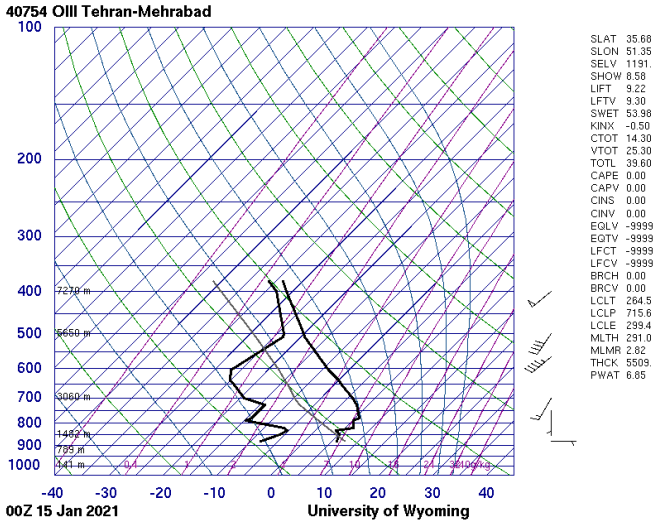

Figure 3-5. Skew-T diagram of Tehran Station (windward) at 00:00 UTC (a) 13, (b) 14, (c) 15 January derived form Univeristy of Wyoming.

3.2.3 Analysis of foehn event on 18 January 2021

In this section another foehn event which occurred on 18 January 2021 is reviewed. As in the previous section, for considering meteorological parameter variations, values of temperature (℃), dewpoint temperature (℃), wind speed (m/s) and direction, and pressure (mb) variables from 17 to 19 January 2021 are gathered in Table 3-4. This table shows a sharp temperature increase from 7.8 to 18.2 ℃ in a 3-hour interval from 21:00 UTC 17 January to 00:00 UTC 18 January 2021. It should be noted that generally minimum temperature in Iran occurs between 00:00-03:00 UTC (early morning), so it is interesting that temperature is rising. Concurrent with the about 10 ℃ temperature rise, dewpoint fell from 6.9 to -3.5 ℃. Wind speed increased by about 4 m/s in this 3 hourly interval. Wind direction rotated from northwesterly (320 degree) at 12:00 UTC 17 January to easterly (90 degree) at 15:00 UTC and then southerly (1800 degree) at 21:00 UTC; so foehn criteria were satisfied. This southerly wind continued to about 14:30 UTC 18 January, which caused falling of absolute humidity and decreasing of dewpoint. It is worth mentioning that visibility improved from 6000 m at 21:00 UTC 17 to more than 10 km at 00:00 UTC 18 January. Times with foehn conditions were shaded gray in Table 3-4.

These conditions continued till 14:30 UTC 18 January. Looking at pressure it has an increasing trend from 09:00 UTC 18 January. Its values rose about 2 mb in about 6 hours, from 09:00-14:30 UTC, were reached 1007 mb. Then it increased to 1013 mb at 18:00 UTC, showing a 6 mb rise in

about 4 hours. Wind turned from southerly (170 degree) at 14:30 UTC to westerly (270 degree) at 15:00 UTC 18 January, in about half an hour. With this wind turning, temperature decreased about 8 ℃ and dewpoint increased about 10 ℃, indicating that the foehn condition is over. Low level cloud with sky cover about 5-7 oktas and a base at about 600 feet (BKN006) was reported at 15:30 UTC.

Table 3-4. Same as Table 3-2 except from 00:00 UTC 17 January to 21:00 UTC 19 January 2021. Foehn conditions were shaded gray.

Date	Wind direction (degree)	Wind speed (m/s)	Temperature (℃)	Dewpoint (℃)	Visibility (m)	Cloudiness	Pressure (mb)
1/17/2021 00:00	0	0	10.4	9.2	9999	SCT020 BKN090	1013
1/17/2021 03:00	0	0	10.2	8.1	9999	SCT020 BKN090	1012
1/17/2021 06:00	260	2	11.0	7.2	9999	FEW020 BKN090	1011
1/17/2021 09:00	310	2	13.8	8.2	9999	FEW090	1008
1/17/2021 12:00	320	3	13.8	8.6	9999	NSC	1006
1/17/2021 15:00	90	2	10.2	9	9999	NSC	1006
1/17/2021 18:00	0	0	8.2	8.2	4000	NSC	1006
1/17/2021 19:00	0	0	7	7	2000	NSC	1005
1/17/2021 20:00	0	0	8	8	5000	NSC	1005
1/17/2021 21:00	180	2	7.8	6.9	6000	NSC	1005
1/18/2021 00:00	150	6	18.2	-3.5	9999	SCT070	1005
1/18/2021 03:00	150	6	18.8	-6	9999	SCT070	1005
1/18/2021 06:00	150	7	21.0	-6.5	9999	BKN170 FEW020 SCT080	1006
1/18/2021 09:00	160	7	23.2	-5.7	9999	FEW080	1005
1/18/2021 12:00	160	7	23.4	-0.5	9999	FEW030	1006
1/18/2021 14:30	170	4	21	0	9999	FEW040	1007
1/18/2021 15:00	270	7	13.2	9.7	9999	FEW080	1008
1/18/2021 15:30	280	6	12	11	9999	BKN006	1009
1/18/2021 18:00	240	2	11.4	9.8	9999	OVC010	1013
1/18/2021 21:00	0	0	9.6	9.2	9999	SCT015	1014
1/19/2021 00:00	0	0	6.6	6.6	2500	NSC	1014

1/19/2021 03:00	0	0	6.6	6.6	2500	NSC	1015
1/19/2021 06:00	230	2	9.8	9.4	6000	NSC	1016
1/19/2021 09:00	350	5	12.4	10.1	8000	FEW020CB SCT025 BKN080	1018
1/19/2021 12:00	10	3	11.2	8.8	9999	FEW015CB SCT020 OVC070	1017
1/19/2021 15:00	240	2	9.6	9.6	4000	BKN010 FEW015CB OVC070	1016
1/19/2021 18:00	0	0	9.2	9.2	8000	BKN010 FEW015CB OVC070	1016
1/19/2021 21:00	280	7	9.6	9.6	8000	BKN010 OVC070	1017

Some daily quantities have been shown in Table 3-5. Maximum temperature between 17 and 18 January, rose about 9 ℃ and then dropped about 12 ℃ between 18 and 19 January 2021. Maximum wind speed on 18 January increased about 5 m/s compared to the previous day. Direction of this maximum wind speed was southerly on 18 January, however, maximum wind on 19 January was westerly with speed about 7 m/s. Minimum pressure on 17-18 January was about 1005 mb and on 19 January was about 1014 mb, which shows almost a 9 mb increase (Table 3-5).

Table 3-5. Same as Table 3-3 except from 17 to 19 January 2021.

date	**Maximum Temperature (℃)**	**Maximum wind speed (m/s)**	**Direction of maximum wind speed**	**Minimum pressure (mb)**
1/17/2021	15.5	3	320	1005.7
1/18/2021	24.2	8	180	1005.6
1/19/2021	12.6	7	280	1014.5

A similar query was performed over Anzali station (Lon 49.46E, Lat 37.48N) (Table a-2). The trend of pressure falling is visible from 17 to 18 January; pressure at 00:00 UTC January 17 was about 1011 hPa and at 00:00 January 18 was about 1004 hPa. From 15:00 UTC January 17 wind was southerly, and dewpoint was decreasing. At 22-23:00 UTC southerly wind speed increased

little, temperature increased about 3 ℃, and dewpoint decreased about 3 ℃. The rising trend of temperature in January 18 continued till 13:00 UTC. However, from 13:00 to 14:00 UTC temperature decreased about 10 ℃. It is worthy of note that in Iran maximum temperature normally happens between 10-13:00 UTC, but this sharp decreasing of temperature is abnormal, as can be compared with 17 and 19 January. The sudden rise of dewpoint from 13-14:00 UTC should also be mentioned. The wind turned westerly (250 degree) and surface pressure has an increasing trend. In summary the foehn condition could be concluded for Anzali station, same as Rasht-Airport station, both leeward. Visibility has no limitation during the foehn hours in these stations.by reporting more than 10 km visibility.

Station reports of Tehran (Lon 51.33E, Lat 35.72N), representing windward condition, for January 17-19 have been gathered in Table a-6, with shaded gray for foehn conditions. Comparing the column of surface pressure of this table with those in Table 3-4 and Table a-2 indicating presence of pressure gradient over south and north of Alborz Mountains, from 06:00 UTC January 17, especially during foehn event (21:00 UTC January 17 to 15:00 UTC January 18). The sky is partly cloudy, and wind is southerly (160 degree) to northwesterly (320 degree) over Tehran station (windward situation) in this period.

Similar reports were gathered for Zanjan station (Lon 48.52E, Lat 36.66N), as a windward station, in Table a-10; times with foehn conditions were shaded gray. Again, surface pressure at this station confirms a pressure gradient over south and north of Alborz Mountains during foehn event times. The sky was cloudy, and wind crossed the mountain with southerly to southwesterly direction. After January 19 the cloudiness of sky reduced, and wind turned southerly to southeasterly.

Reanalysis maps at 500 mb and surface level are shown in Figure 3-6. Taking into account 500 mb level in 12:00 UTC 17 January, a cutoff low can be seen over the Black Sea, sending waves to the east, and forming significant diffluence over the Caspian Sea. Also, a trough is discernible over the Alborz Mountains moving eastward, can be seen in the Figure 3-6(a). Corresponding to the dynamical structure of the deep trough (with cutoff low) over the Black Sea, in sea level map, a low pressure formed over the Black Sea, tending to east, as its tongue reaches the Caspian Sea (Figure 3-6(b)).

At 18:00 UTC, following on eastward movement of the deep trough and its cutoff low, the western Alborz Mountains (including Rasht region, Lon 49.62E, Lat 37.32N) was affected by its

minor troughs. It seems low pressure expanded more toward the Caspian Sea (Figure 3-6(d)).

At 21:00 UTC the minor troughs existed over the western Alborz Mountains, yet (Figure 3-6(e)). The important point at this time is a pressure gradient that formed over the desired area; a 1004 mb contour could be seen over the west of northern coastal of Iran, on the other hand, a 1012 mb contour affected the western Alborz Mountains (Figure 3-6(f)). This pressure gradient caused the southerly wind reported at this time (Table 3-4).

At 00:00 UTC 18 January, minor troughs affect the western Alborz Mountains, yet, showing the slow movement of the deep trough (Figure 3-6(g)). The pressure gradient over the western Alborz Mountains could be seen at this time as well (Figure 3-6(h)). So, again in this case pressure gradient caused by low pressure over the northern Alborz Mountain and high pressure over the southern Alborz Mountains prepared foehn conditions.

At 15:00 and 18:00 UTC 18 January, the deep trough, with cutoff low moved eastward (Figure 3-6(i and k)). The low pressure corresponding to it, also moved eastward and passed the Caspian Sea. So, the pressure gradient were removed over the northern coast of Iran, as 1010 mb pressure contour could be seen over the southern coast of Caspian Sea at 15:00 UTC and extended over the Caspian Sea at 18:00 UTC ((Figure 3-6(j and l)). Pressure increased over the Rasht-Airport station from 1006 mb at 12:00 UTC to 1008 mb at 15:00 UTC and 1013 mb at 18:00 UTC. Also, wind rotated from southerly at 12:00 UTC to westerly at 15:00 UTC (Table 3-4).

The noticeable point in this case is the short lifetime of the foehn event, as at 15:00 UTC 18 January, foehn conditions were destroyed and a remarkable decrease in temperature (from about 23 to 13 ℃) and increase in dewpoint (from less than 0 to above 9 ℃) is obvious (Table 3-4). To explain this, it can be stated that low amplitude waves (minor trough) may provide foehn conditions for a short time (a few hours).

Given that the considered time is winter, the contrast in temperature between land and sea caused amplification of high pressure over the mountain area and a deepening low pressure over the sea; so, this contrast temperature could be the second amplifier factor for the pressure gradient for this foehn event.

(a)

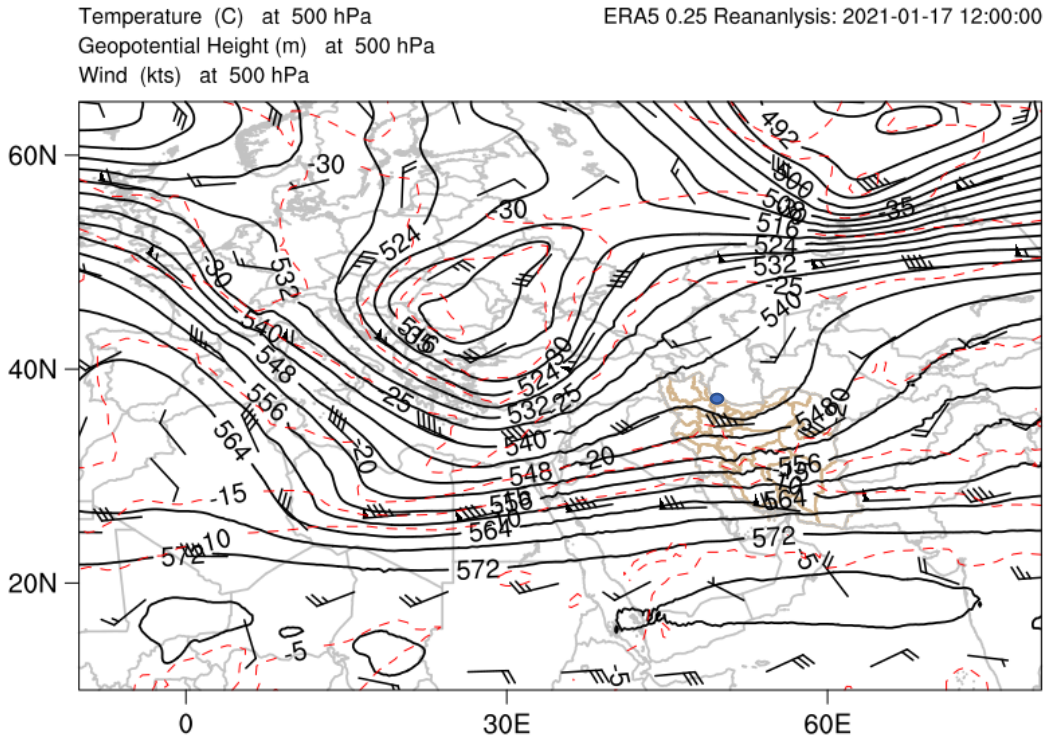
Temperature (C) at 500 hPa
Geopotential Height (m) at 500 hPa
Wind (kts) at 500 hPa
ERA5 0.25 Reananlysis: 2021-01-17 12:00:00
60N
40N
20N
0
30E
60E

(b)

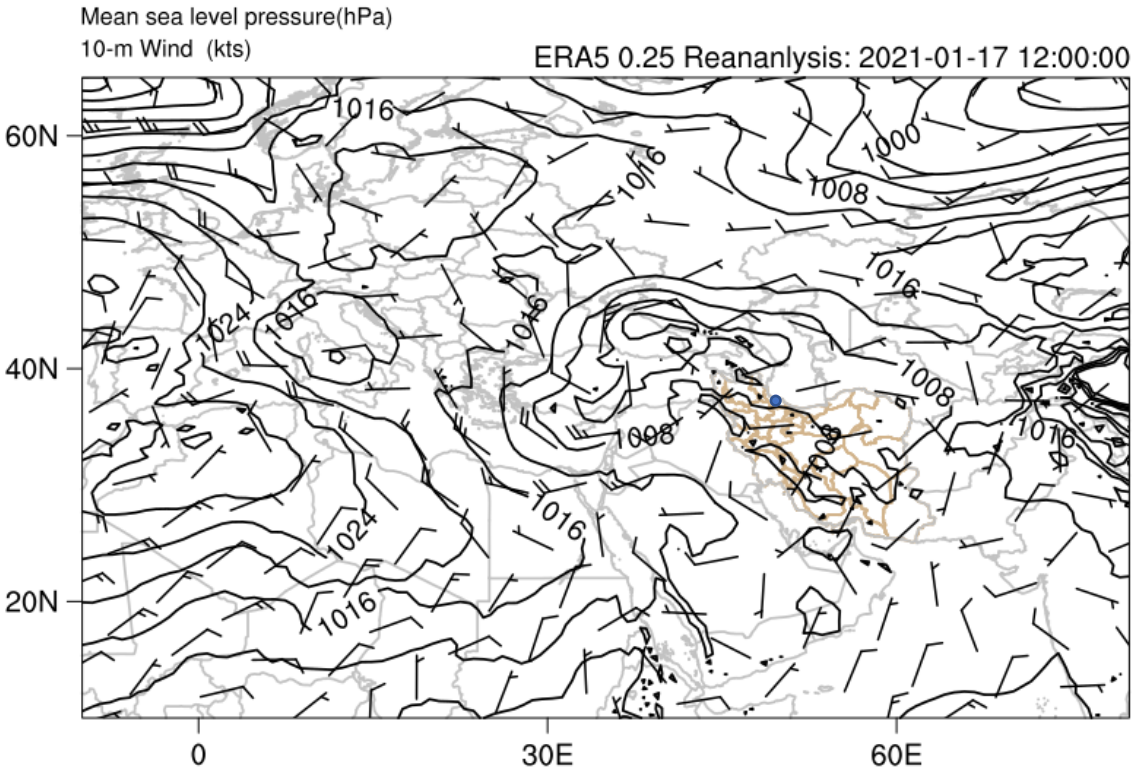
Mean sea level pressure(hPa)
10-m Wind (kts)
ERA5 0.25 Reananlysis: 2021-01-17 12:00:00
60N
40N
20N
0
30E
60E

(c)

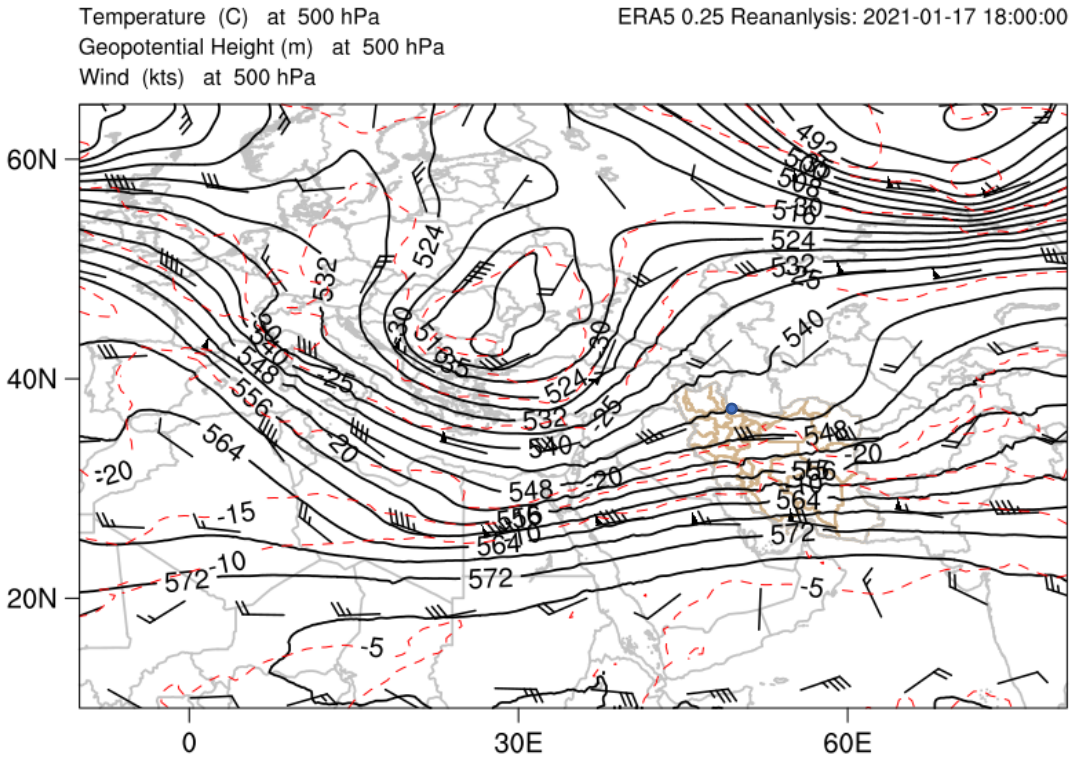
Temperature (C) at 500 hPa
Geopotential Height (m) at 500 hPa
Wind (kts) at 500 hPa
ERA5 0.25 Reananlysis: 2021-01-17 18:00:00
60N
40N
20N
0
30E
60E

(d)

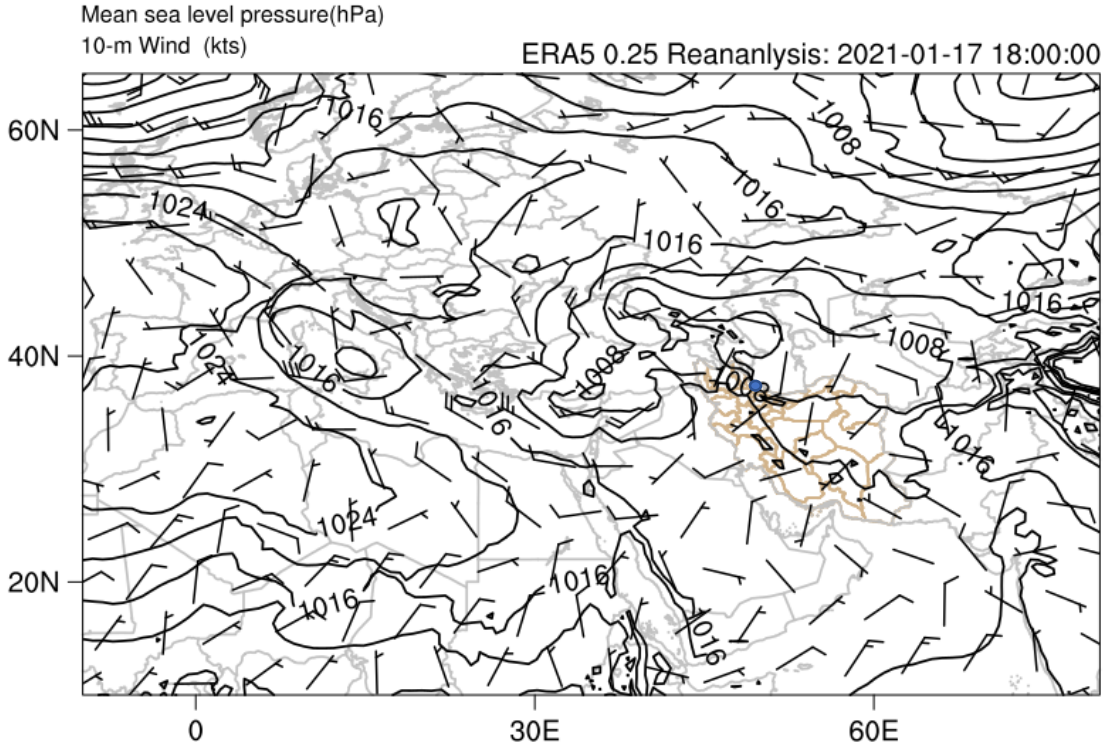
Mean sea level pressure(hPa)
10-m Wind (kts)
ERA5 0.25 Reananlysis: 2021-01-17 18:00:00
60N
40N
20N
0
30E
60E

(e)

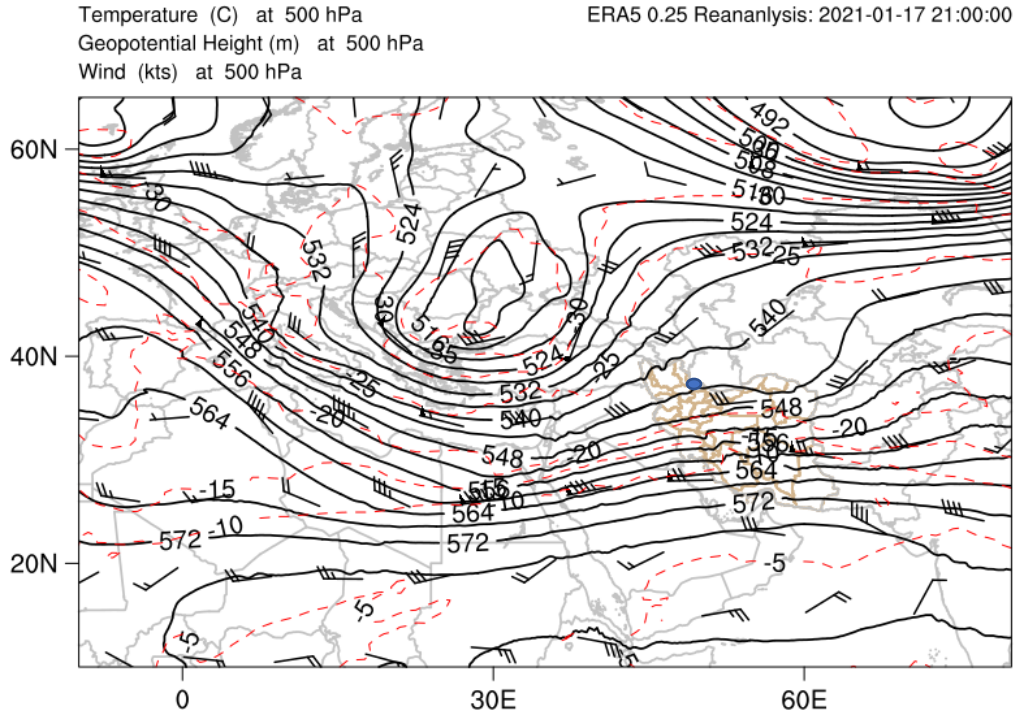
Temperature (C) at 500 hPa
Geopotential Height (m) at 500 hPa
Wind (kts) at 500 hPa
ERA5 0.25 Reananlysis: 2021-01-17 21:00:00
60N
40N
20N
0
30E
60E

(f)

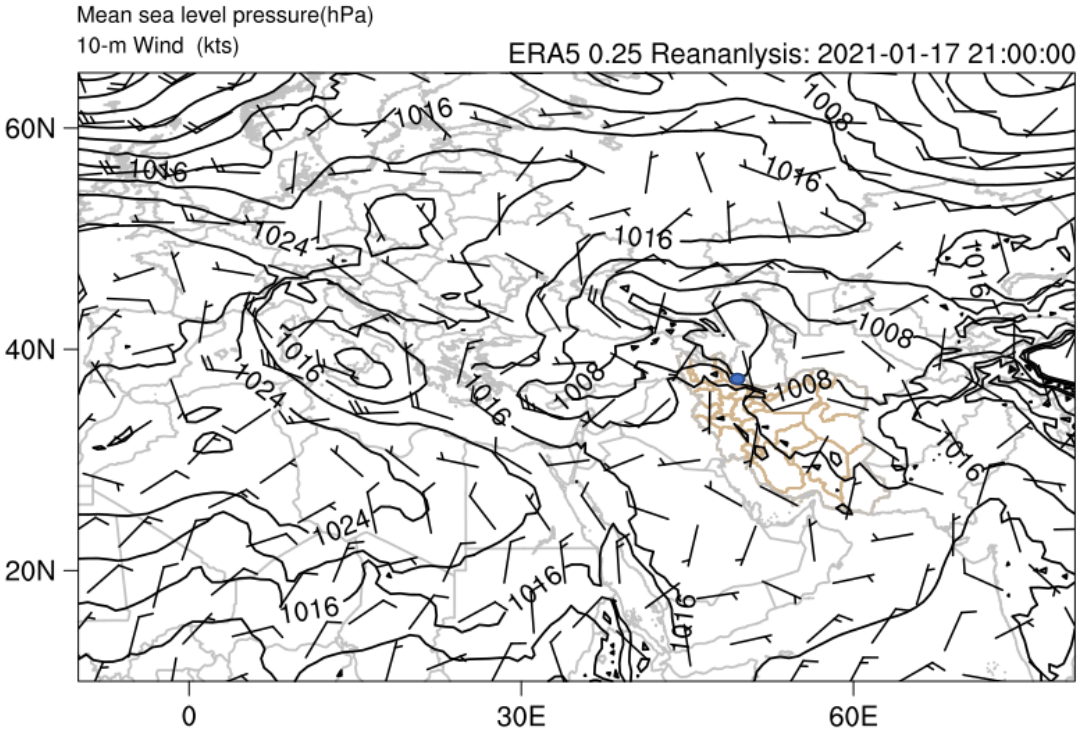
Mean sea level pressure(hPa)
10-m Wind (kts)
ERA5 0.25 Reananlysis: 2021-01-17 21:00:00
60N
40N
20N
0
30E
60E

(g)

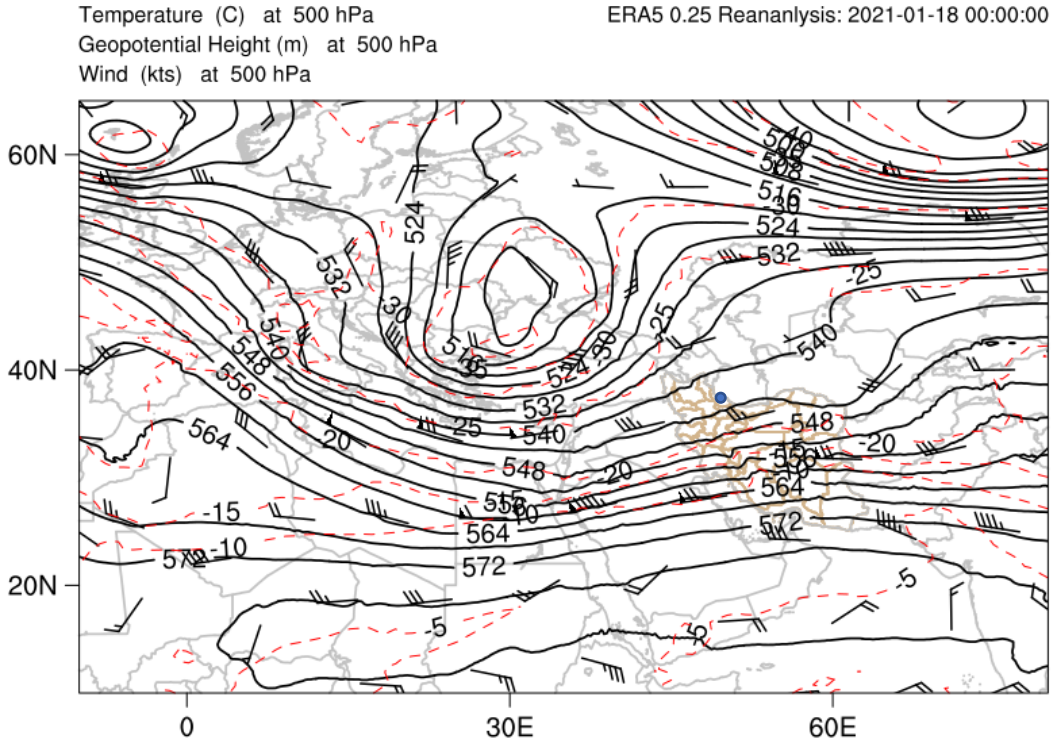
Temperature (C) at 500 hPa
Geopotential Height (m) at 500 hPa
Wind (kts) at 500 hPa
ERA5 0.25 Reananlysis: 2021-01-18 00:00:00
60N
40N
20N
0
30E
60E

(h)

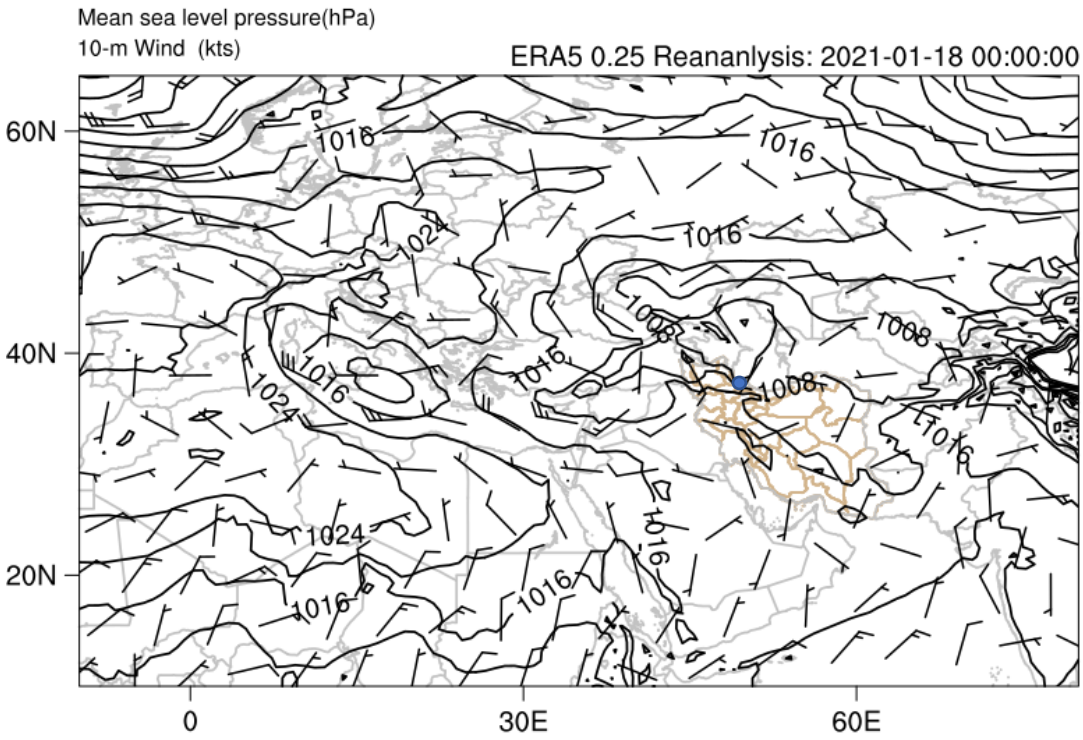
Mean sea level pressure(hPa)
10-m Wind (kts)
ERA5 0.25 Reananlysis: 2021-01-18 00:00:00
60N
40N
20N
0
30E
60E

(i)

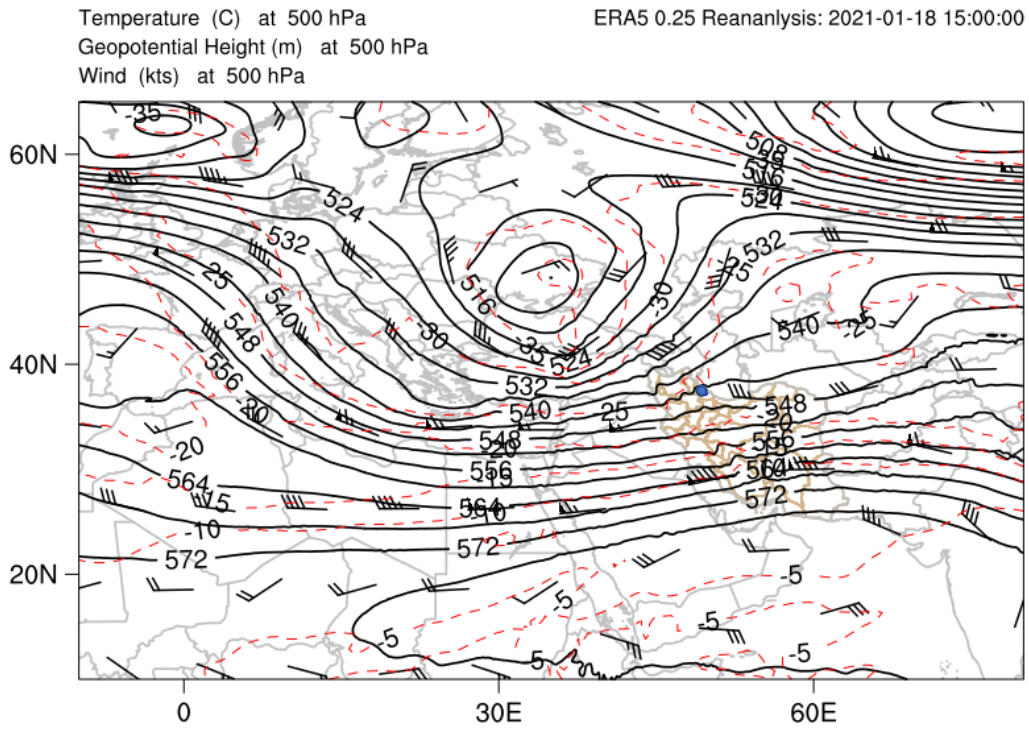
Temperature (C) at 500 hPa
Geopotential Height (m) at 500 hPa
Wind (kts) at 500 hPa
ERA5 0.25 Reananlysis: 2021-01-18 15:00:00
60N
40N
20N
0
30E
60E

(j)

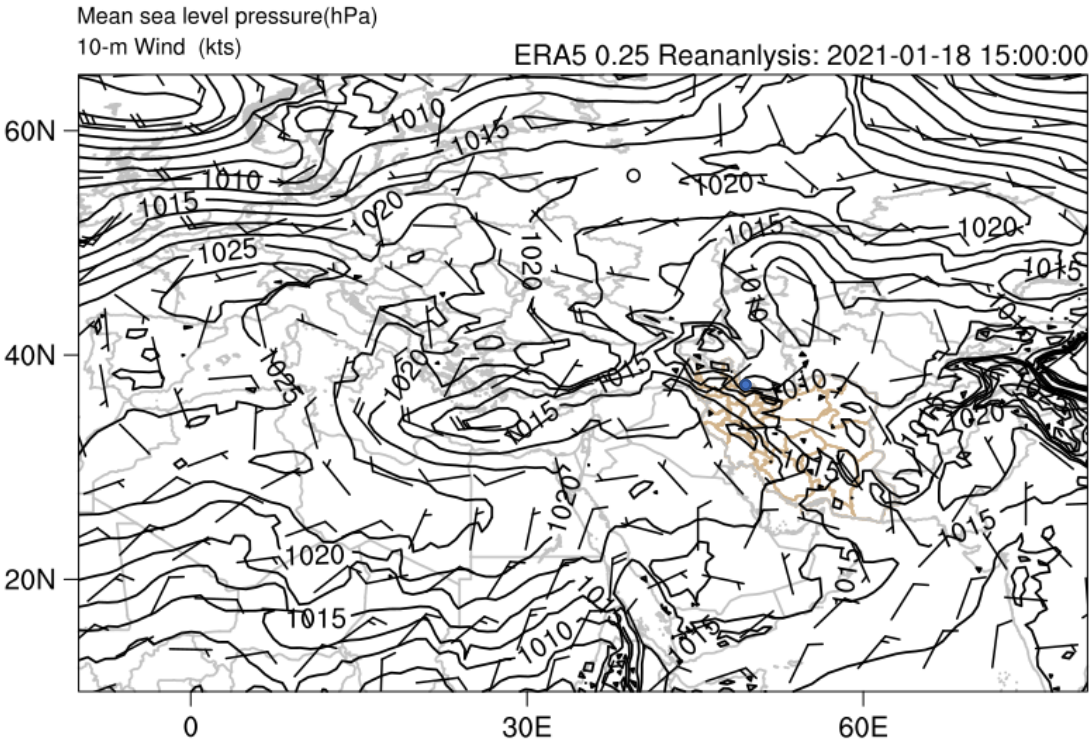
Mean sea level pressure(hPa)
10-m Wind (kts)
ERA5 0.25 Reananlysis: 2021-01-18 15:00:00
60N
40N
20N
0
30E
60E

(k)

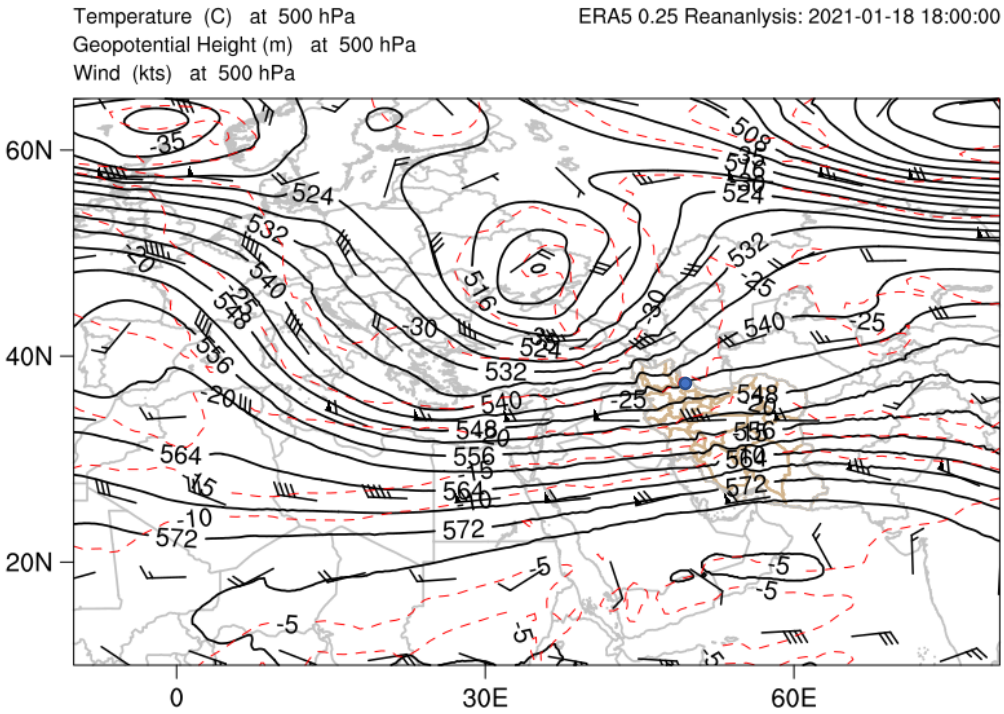

(l)

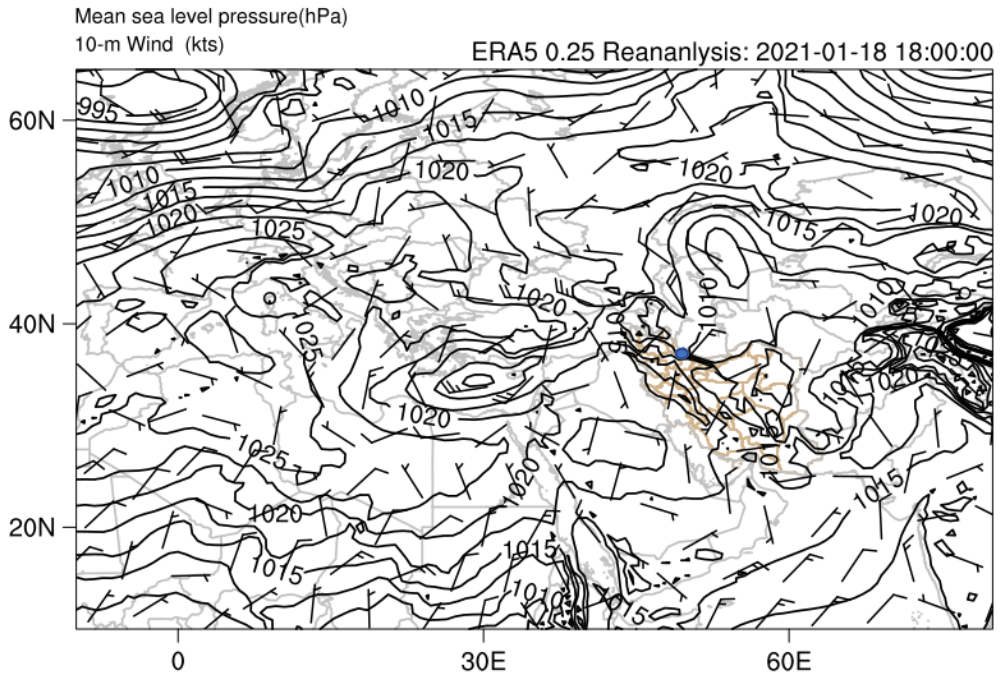

Figure 3-6. Analysis maps for (a, c, e, g) geopotential height (m) (black contours), temperature (℃) (red contoures) and wind barbs at 500 mb pressure level, (b, d, f, h) mean sea level pressure (mb) (black contours) with wind barbs at 10-m height above ground for17-18 January, different hours as the headers.

Skew-T plots over Tehran station for 00:00 and 12:00 UTC January 17 have been shown in Figure 3-7. Wind direction below the 500 hPa, which is approximately the pressure height of the ridge of the Alborz Mountains, is southerly to southwesterly with speed of 40 kt over the ridge. At 12:00 UTC wind is westerly to northwesterly from 700 to 600 hPa and mostly southwesterly from 550 to 500 hPa. In both 00:00 and 12:00 UTC skew-T plots, condition of crossing wind from south to north side of the Alborz Mountains at low levels can be concluded.

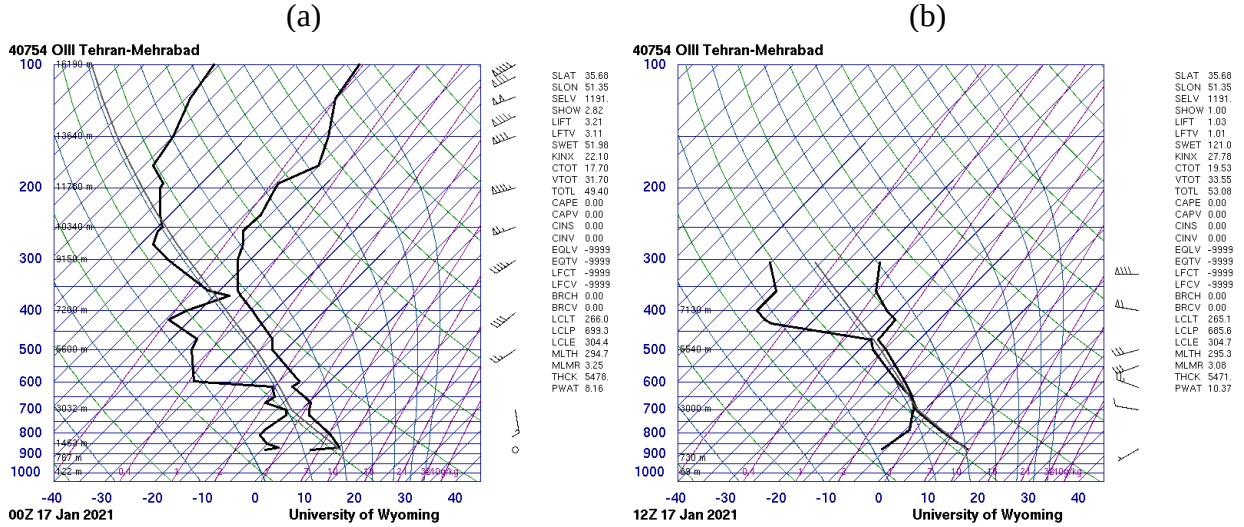

Figure 3-7. Skew-T diagram of Tehran Station (windward) at (a) 00:00 and (b) 12:00 UTC January 17 derived form Univeristy of Wyoming.

3.2.4 Analysis of foehn event on 28-29 January 2021

Another foehn event that occurred on 28-29 January 2021 will be discussed. Same as two previous subsections, temperature, dewpoint, wind speed and direction, and pressure values are gathered from Rasht-Airport station, for the desired dates in Table 3-6. Considering trends of values of parameters in this table, from 15:00 UTC 28 January, pressure decreased from 1012 at 15:00 UTC to 1010 mb at about 16:00 UTC; also 1009 mb reported at 03:00 UTC 29 January. Wind direction changed from westerly (270 degree) at 15:00 UTC to southerly (170 degree) at 18:00 UTC; and wind speed increased from 2 to 5 m/s from 17:00 to 18:00 UTC, reached to 9 m/s at 21:00 UTC 28 January. However, the wind was almost calm at 00:00-03:00 UTC 29 January with speed about 2 m/s and approximate easterly (60-120 degree), which did not match completely with foehn characteristics. Temperature increased from about 11 to 19.4 ℃, about 8 ℃ rise in just one hour from 17:00 to 18:00 UTC 28 January, this temperature rising is counter of diurnal variations. Meanwhile dewpoint decreased from about 11 to 2.6 ℃ in this one-hour interval, and then reaches

-1.8 ℃ at 03:00 UTC 29 January. It is worth noting that visibility at 17:00 UTC was about 4000 m which improved to more than 10 km at 18:00 UTC. Also, clouds in different levels of sky at 17:00 UTC were removed as no cloud was reported at 18:00 UTC. These changes, falling of pressure, increasing of temperature, decreasing of dewpoint, rising of wind speed with direction from downslope of mountains, indicate foehn conditions, from 18:00 UTC 28 January to 05:00 UTC 29 January, cells which ones were shaded gray in Table 3-6.

However, from 05:00 UTC 29 January, inverse trend of the mentioned variations of these parameters could be seen, i.e., pressure increased from about 1010 at 05:00 UTC to 1012 mb at 05:30 UTC; temperature decreased about 9 and dewpoint increased about 11 ℃ in this half-hour. Wind turned from southerly (180 degree) to westerly (250 degree); though relatively high wind speed was reported for some hours from 06:00-12:00 UTC 29 January. Visibility decreased from more than 10 km at 05:30 UTC 29 January to about 6000 m at 06:00 UTC. Cloudiness increased from almost sky cloud free at 05:00 UTC to 5-7 oktas low level cloud. Except for wind speed, other variations indicate that from about 05:30 UTC 29 January foehn conditions were removed.

Table 3-6. Same as Table 3-2 except from from 00:00 UTC 27 January to 21:00 UTC 30 January 2021. Foehn conditions were shaded gray.

Date	Wind direction	Wind speed (m/s)	Temperature (°C)	Dewpoint (°C)	Visibility (m)	Cloudiness	Pressure (mb)
1/27/2021 00:00	0	0	1.0	1.0	400	NSC	1021
1/27/2021 03:00	0	0	0.8	0.8	250	VV003	1021
						FEW025	
1/27/2021 06:00	0	0	3.6	3.6	2000	BKN180	1021
						FEW100	
1/27/2021 09:00	300	2	11.8	6.7	7000	SCT180	1019
1/27/2021 12:00	280	2	13.8	7.2	9999	NSC	1018
1/27/2021 15:00	0	0	9.2	6.1	9999	NSC	1017
1/27/2021 18:00	0	0	5.0	5.0	4000	NSC	1016
1/27/2021 21:00	250	2	5.2	5.2	400	NSC	1015
1/28/2021 00:00	0	0	7.2	7.2	800	BKN004	1013
1/28/2021 03:00	0	0	7.4	7.4	250	VV003	1013
1/28/2021 06:00	0	0	8.6	8.6	800	SCT005	1013
						BKN160	
1/28/2021 09:00	30	2	15.6	8.5	4000	FEW015	1010
1/28/2021 12:00	260	3	14	9.3	4000	FEW015	1009
						BKN170	
1/28/2021 15:00	270	2	11.6	10.0	5000	FEW010CB	1012
						SCT020	
						BKN170	
1/28/2021 16:00	270	2	11	11	5000	FEW010CB	1010
						SCT020	
						BKN170	
1/28/2021 17:00	60	2	11	11	4000	FEW010CB	1010
						SCT020	
						BKN170	
1/28/2021 18:00	170	5	19.4	2.6	9999	NSC	1010
1/28/2021 21:00	130	9	21.4	0.7	9999	NSC	1010
1/29/2021 00:00	120	2	20.2	0.6	9999	FEW100	1010
						SCT180	
1/29/2021 03:00	60	2	19	-1.8	9999	NSC	1009
1/29/2021 05:00	180	4	21	-2	9999	FEW100	1010

1/29/2021 05:30	250	5	12	9	9999	FEW025	1012
1/29/2021 06:00	270	8	11.8	9.8	6000	BKN007	1012
1/29/2021 09:00	260	6	11.4	9.0	6000	SCT010 BKN020	1014
1/29/2021 12:00	280	5	11.0	8.1	9999	SCT010 FEW015CB BKN025 OVC060	1014
1/29/2021 15:00	280	3	9.6	8.8	5000	BKN012 FEW015CB OVC060	1015
1/29/2021 18:00	0	0	9.4	9.0	8000	BKN015 OVC070	1014
1/29/2021 21:00	280	2	9.2	8.8	9999	OVC070	1013
1/30/2021 00:00	0	0	8.8	8.8	9999	FEW020 OVC070	1012
1/30/2021 03:00	0	0	8.6	8.6	6000	SCT015 OVC070	1010
1/30/2021 06:00	0	0	9.4	8.6	4000	SCT015 BKN070	1010
1/30/2021 09:00	310	2	13.4	7.7	9999	FEW015	1010
1/30/2021 12:00	280	5	12.8	8.4	9999	SCT020	1009
1/30/2021 15:00	40	3	10.0	7.9	9999	FEW020	1011
1/30/2021 18:00	180	2	8.2	8.2	6000	FEW080	1014
1/30/2021 21:00	240	2	8.0	8.0	4000	NSC	1012

Diurnal values of maximum temperature and wind speed, direction of maximum wind speed and minimum pressure are gathered on Table 3-7. Based on values in this table, maximum temperature on 27 January was about 14.2 ℃, and on 28 January was about 18.4 ℃. The point is that daily maximum temperature in IRIMO meteorological stations usually occurred before 15:00 UTC and is reported at 15:00 UTC; so. 18.4 ℃ at January 28 was occurred before that time. However, as discussed in Table 3-6, temperature with value more than 21 ℃ could be seen at 21:00 UTC 28 January, i.e., after the time of reporting the daily maximum temperature (15:00 UTC), showing an unusual condition; as discussed above, foehn has occurred after 18:00 UTC 28 January. Maximum temperature in this table for 29 January was about 21.6 ℃ which occurred

during morning times, again due to foehn conditions. Maximum temperature for 30 January, a day without foehn event, was only about 15.6 ℃. The direction of maximum wind speed on 28 January was southeasterly (130 degree), in accordance with downslope wind.

Table 3-7. Same as Table 3-3 except from 27 to 30 January 2021.

date	Maximum Temperature (℃)	Maximum wind speed (m/s)	Direction of maximum wind speed	Minimum pressure (mb)
1/27/2021	14.2	3	270	1015.3
1/28/2021	18.4	9	130	1009.3
1/29/2021	21.6	8	270	1009.9
1/30/2021	15.6	5	280	1009.3

Considering reports of Anzali station (Table a-3), indicated similar results. Times with foehn event were shaded gray in this table. Southerly wind blew from about 16:00 UTC (120 degree), however, the sharp temperature increase happened in 19:00-20:00 UTC which was about 7 ℃ in one hour. Decreasing of dewpoint is gentle, 3 ℃ at this one hour. Visibility, also, improved from 7000 m to more than 10 km in this one hour, another indicating of foehn condition. These relative conditions could be concluded till about 04:00 UTC 29 January. But in 04:00-05:00 UTC surface pressure at the station rose about 2 hPa; wind turned from southerly (200 degree) in 04:00 UTC to northwesterly (310 degree) at 05:00 UTC; temperature decreased about 8 ℃ and dewpoint increased about 7 ℃ in this one-hour interval, indicating removing foehn condition. It is worth noting that visibility was reduced to 5000 m in 05:00-06:00 UTC, simultaneous with northerly wind (330-350 degree) which bring humidity from the sea to the coastal city of Anzali, although sun rise also happened.

For querying windward condition, reports of Tehran station for 27-30 January were gathered on Table a-7, with shaded gray during foehn times. Reported surface pressure on January 27 was more than 1020 hPa and sky was clear; from 15:00 UTC January 28 the pressure gradient from south to north of the Alborz Mountains existed (considering reports of Tehran station in Table a-7 and Rasht-Airport station in Table 3-6, at the south and north of the Alborz Mountains, respectively). During foehn conditions sky over Tehran station was cloudy; the wind was southerly to westerly (170-290 degree). The weather condition over Zanjan station, as a windward station, is also written in Table a-11, again with shaded gray for foehn times. The cloudiness of sky over

the station was started from 06:00 UTC January 28.

Surface analysis map for 18:00 UTC January 28 and 00:00 UTC January 29 have been shown on Figure 3-8. The cloudiness of windward station is obvious, besides, the rain shower report (▽) could also be seen to windward at 18:00 UTC January 28 (Figure 3-8(a)). The cloudiness of sky over the windward station existed also at 00:00 UT January 29 (Figure 3-8(b)).

(a)

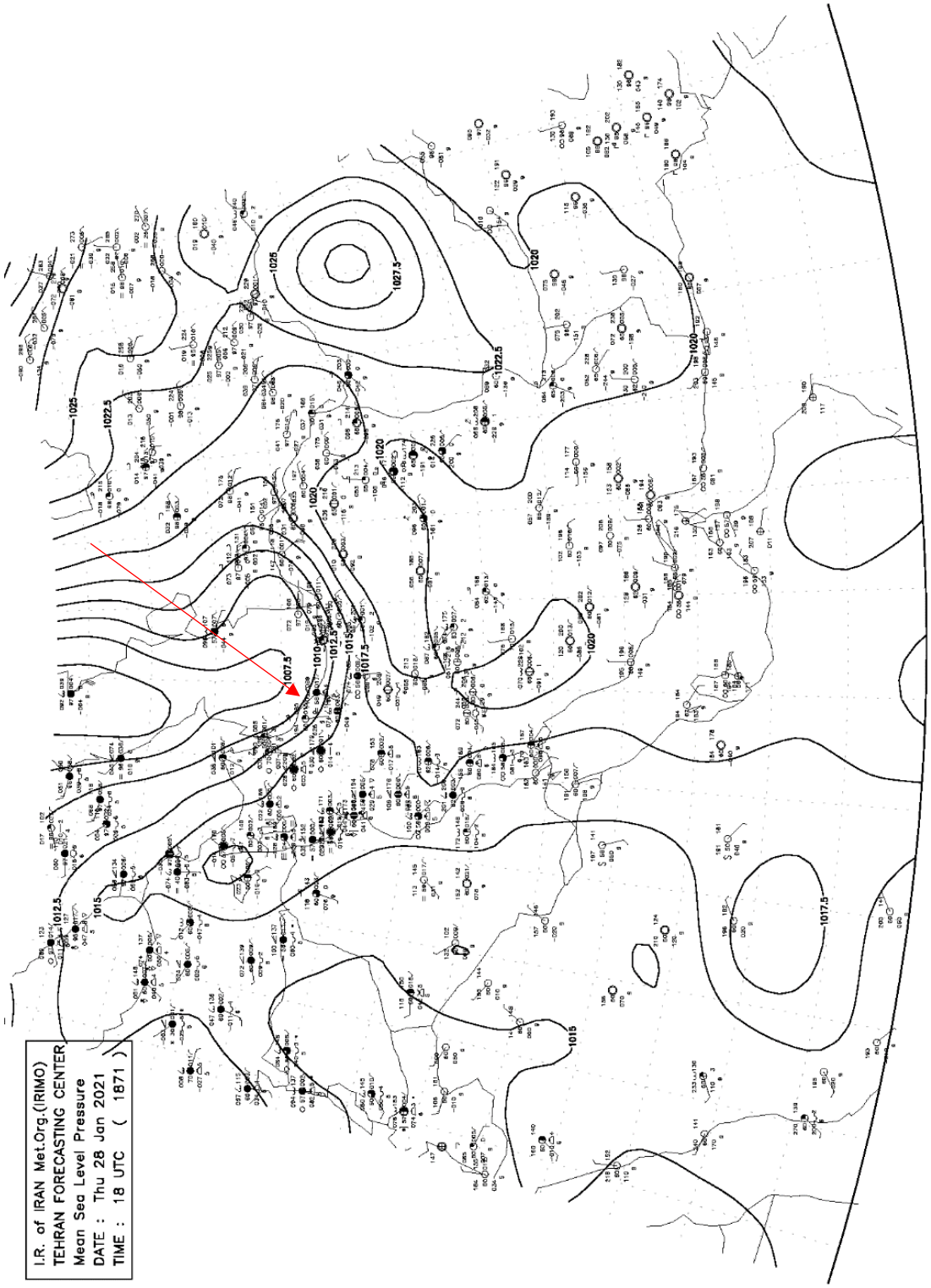
I.R. of IRAN Met.Org.(IRIMO)
TEHRAN FORECASTING CENTER
Mean Sea Level Pressure
DATE : Thu 28 Jan 2021
TIME : 18 UTC (1871)

(b)

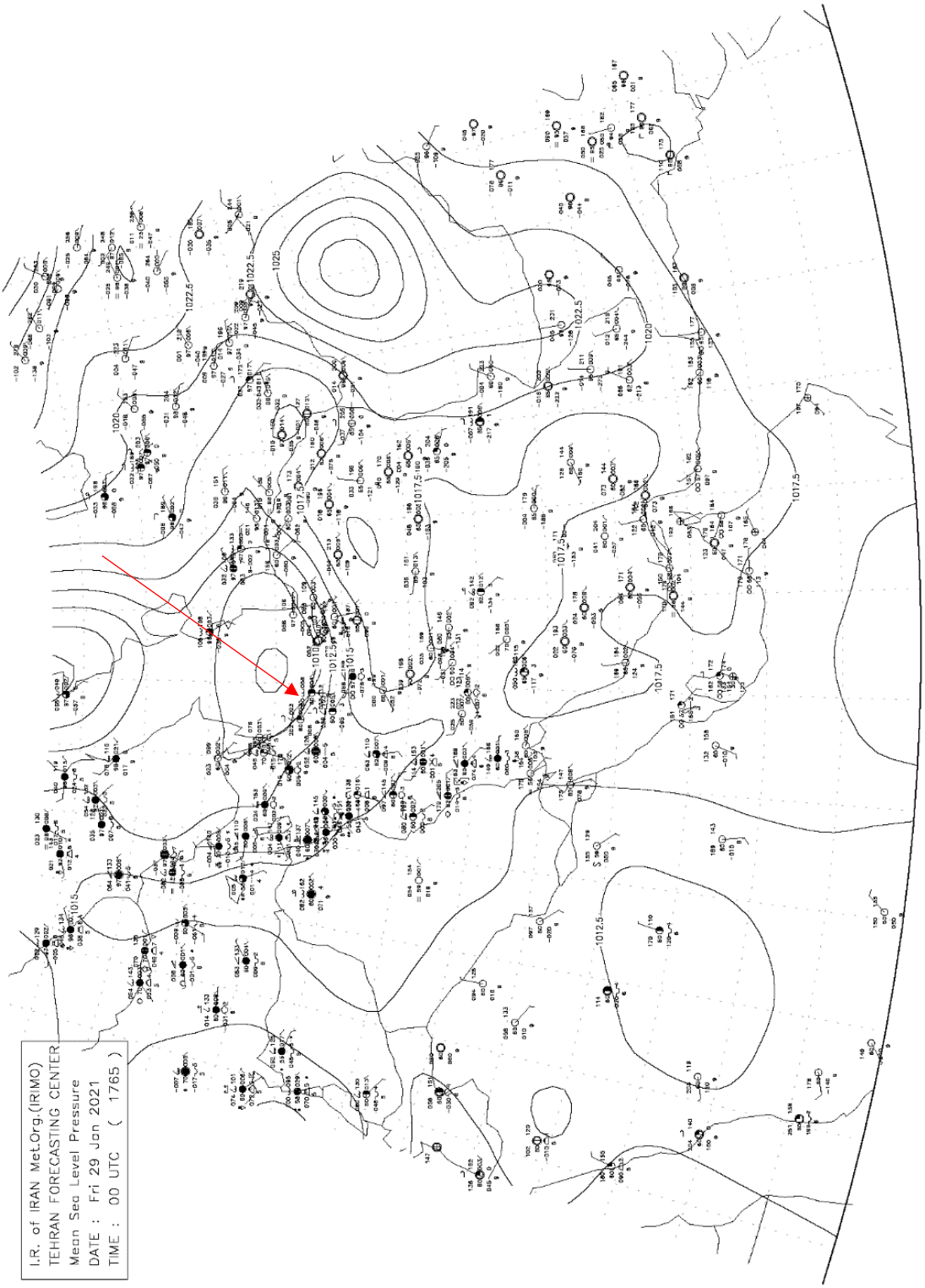

Figure 3-8. Analysis maps of mean sea level pressure provided by IRIMO for (a) 18:00 UTC January 28 and (b) 00:00 UTC January 29. The weather condition for stations have been exhibited at this figure with weather symbols.

In the following, synoptic analysis of the occurred foehn will be presented. At 12:00 UTC 28 January, a minor trough at the 500 hPa level could be seen over the west of Iran. Also, a cutoff low with 516 hPa closed contour could be seen over the north of the Black Sea (Figure 3-9(a)). Related to this trough there is a low pressure closed center with about 1000 hPa contour over the north of the Black Sea with extension to the north of Caspian Sea, as 1004 hPa pressure contour is recognizable over the Caspian Sea. The Siberian High with 1036 hPa contour is also visible (Figure 3-9(b)). At 15:00 UTC, the minor trough moved towards the Alborz Mountains (Figure 3-9(c)). The low pressure over the Caspian Sea expanded more (Figure 3-9(d)).

With eastward moving of the mentioned trough, its axis reaches to the Alborz Mountains at 18:00 UTC (Figure 3-9(e)). Its accompanying low pressure extended to south of the Caspian Sea. On the other hand, the Siberian High penetrates more over the Iranian Plateau, as a 1020 hPa closed pressure contour could be seen over the central Iranian Plateau. There is also pressure increasing upstream of the trough; so, that the mass accumulation of both the penetration of the Siberian High and high pressure on the upstream of the trough, could trigger the foehn mechanism. The pressure gradient between southern and northern Alborz Mountains, with 1016 hPa contour over the southern and 1008-1012 hPa contour over the northern Alborz Mountains could be seen (Figure 3-9(f)). In addition to this dynamical factor, there is a thermodynamical cause for the pressure gradient, related to seasonal and diurnal contrast between land and the Caspian Sea.

The aforementioned trough over the Alborz Mountains, and low pressure with 1008 hPa contour over the Caspian Sea, could be seen at 21:00 UTC (Figure 3-9(g) and (h)), as wind speed with value 9 m/s was reported at this time (Table 3-6). At 00:00 UTC 29 January, the minor trough somehow passed the Alborz Mountains (Figure 3-9(i)). The low pressure over the Caspian Sea has been weakened, as 1008 hPa contour moved to the northeast of the Caspian Sea (Figure 3-9(j)). Wind speed at this time was about 2 m/s over the Rasht-Airport Station (Table 3-6).

It seems that at 03:00 UTC the minor trough over the Alborz Mountains and low pressure over the Caspian Sea were weakened (Figure 3-9(k) and (l)), as northeasterly wind (60 degree) was reported at this time (Table 3-6). At 06:00 UTC for 500 hPa level, weakening of the mentioned minor trough could be noted (Figure 3-9(m)). Pressure over the Caspian Sea increased and at sea level 1012 hPa contour could be seen (Figure 3-9(n)), as the reported pressure at Rasht-Airport station was also 1012 hPa (Table 3-6). As mentioned above, the foehn characteristics were removed at 05:00 UTC.

(a)

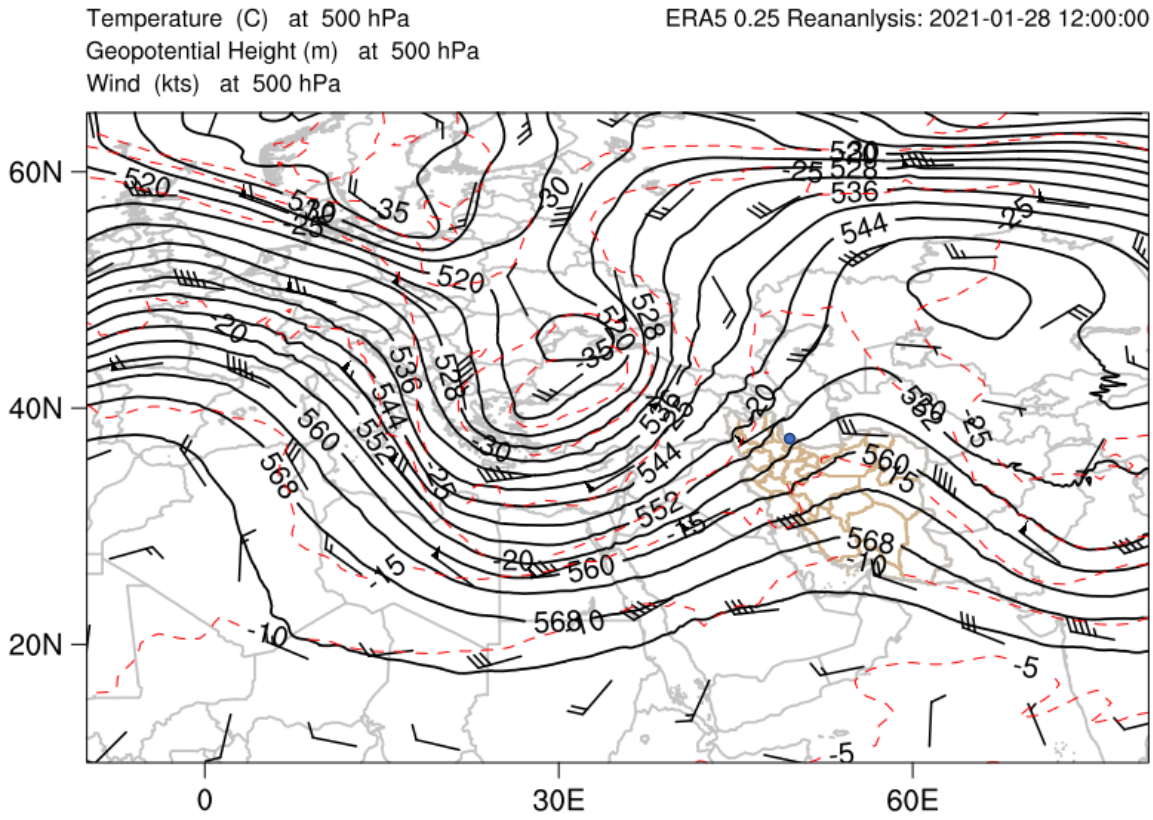
Temperature (C) at 500 hPa
Geopotential Height (m) at 500 hPa
Wind (kts) at 500 hPa
ERA5 0.25 Reananlysis: 2021-01-28 12:00:00
60N
40N
20N
0
30E
60E

(b)

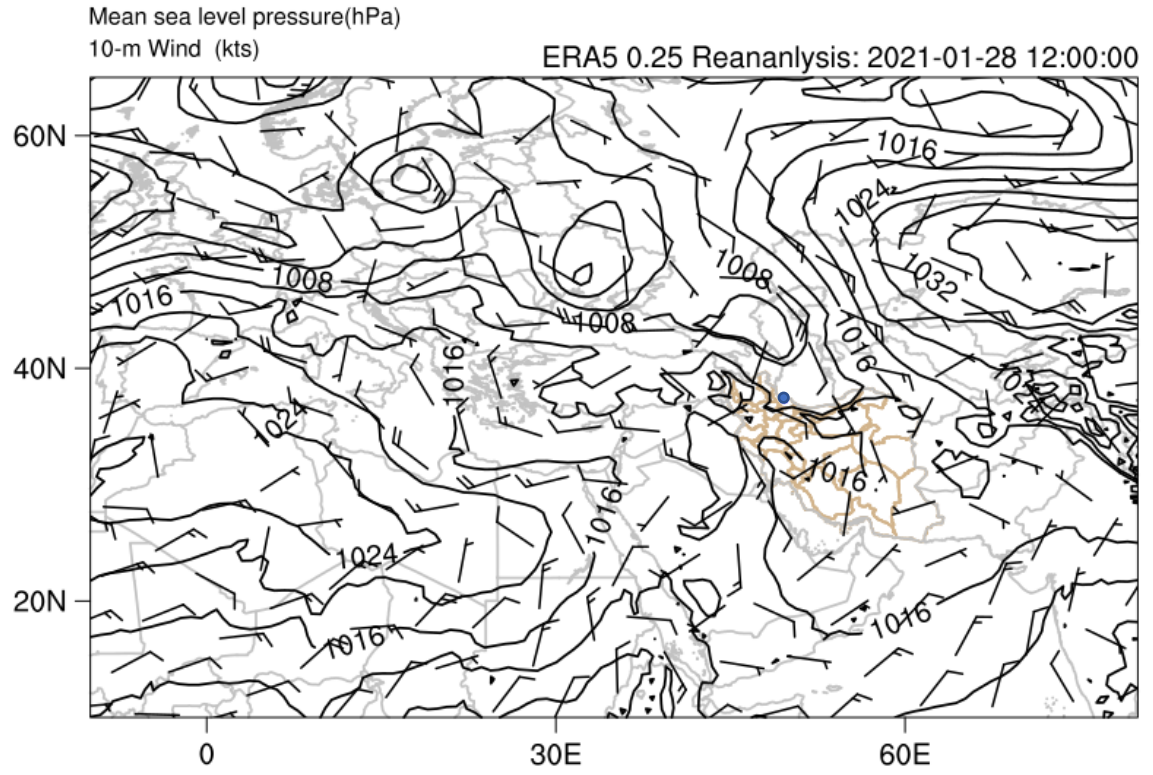
Mean sea level pressure(hPa)
10-m Wind (kts)
ERA5 0.25 Reananlysis: 2021-01-28 12:00:00
60N
40N
20N
0
30E
60E

(c)

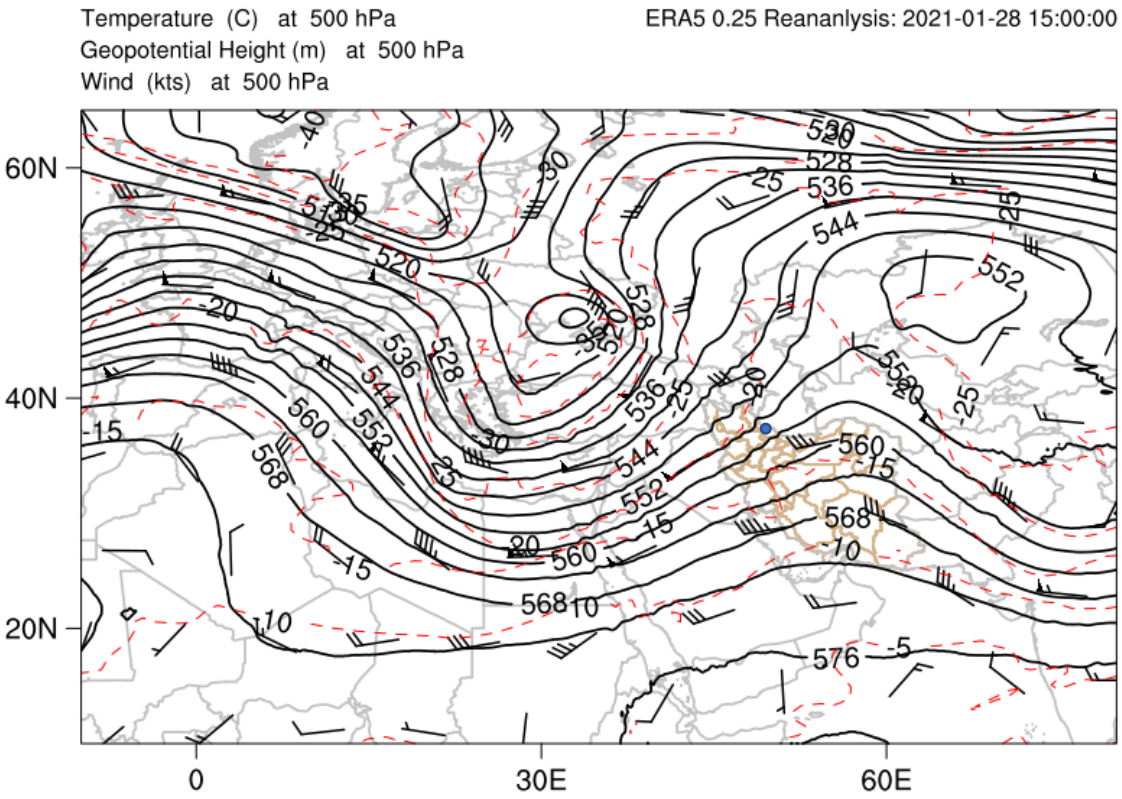
Temperature (C) at 500 hPa
Geopotential Height (m) at 500 hPa
Wind (kts) at 500 hPa
ERA5 0.25 Reananlysis: 2021-01-28 15:00:00
60N
40N
20N
0
30E
60E

(d)

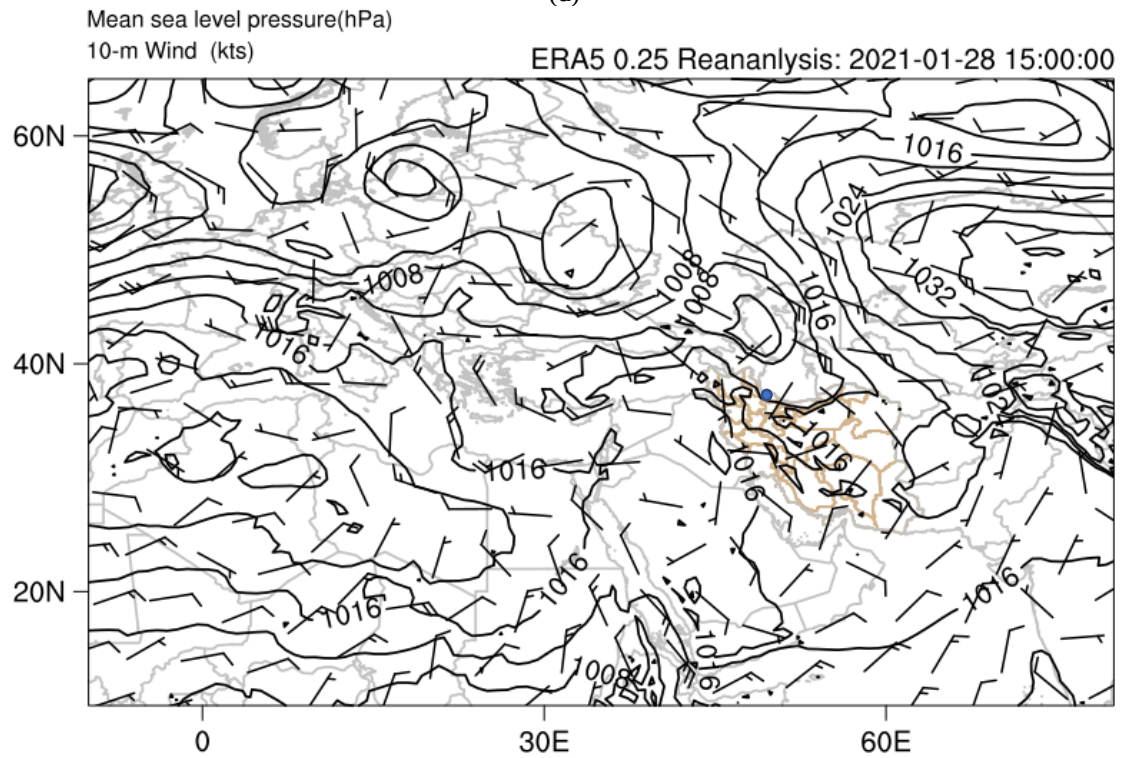
Mean sea level pressure(hPa)
10-m Wind (kts)
ERA5 0.25 Reananlysis: 2021-01-28 15:00:00
60N
40N
20N
0
30E
60E

(e)

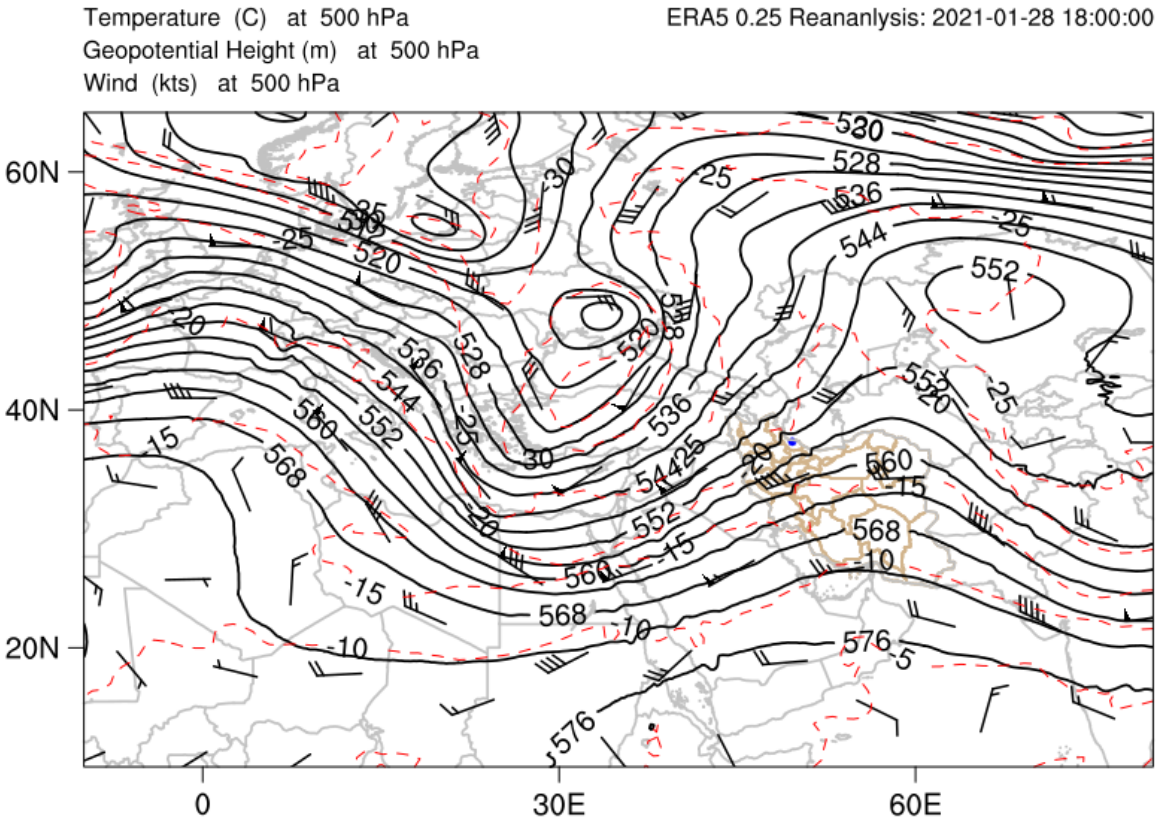
Temperature (C) at 500 hPa
Geopotential Height (m) at 500 hPa
Wind (kts) at 500 hPa
ERA5 0.25 Reananlysis: 2021-01-28 18:00:00
60N
40N
20N
0
30E
60E

(f)

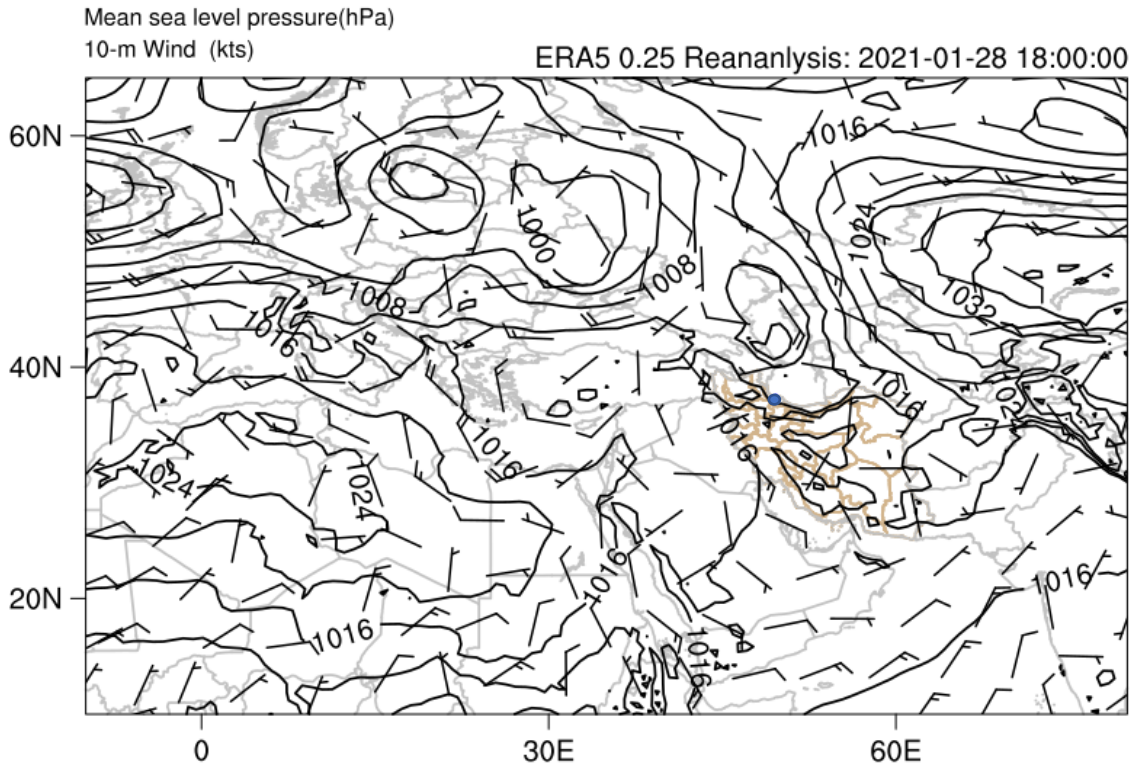
Mean sea level pressure(hPa)
10-m Wind (kts)
ERA5 0.25 Reananlysis: 2021-01-28 18:00:00
60N
40N
20N
0
30E
60E

(g)

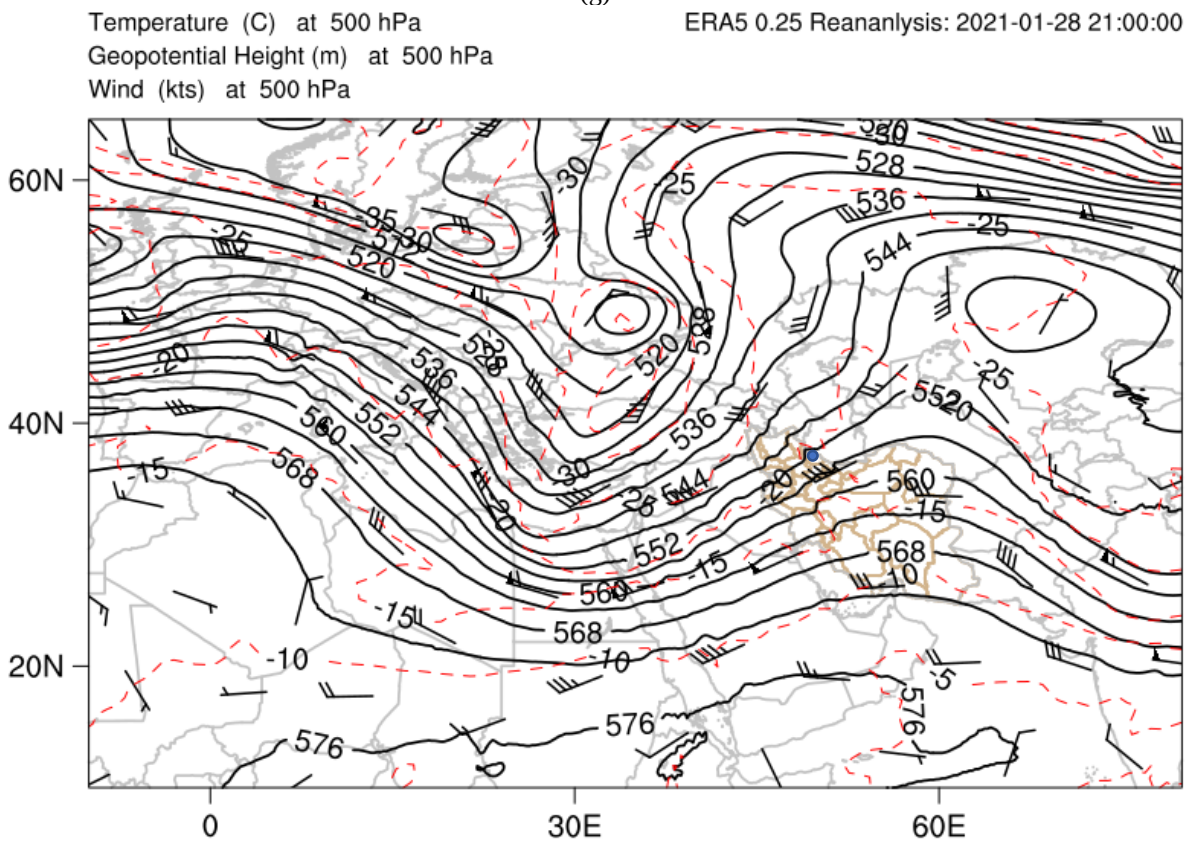
Temperature (C) at 500 hPa
Geopotential Height (m) at 500 hPa
Wind (kts) at 500 hPa
ERA5 0.25 Reananlysis: 2021-01-28 21:00:00
60N
40N
20N
0
30E
60E

(h)

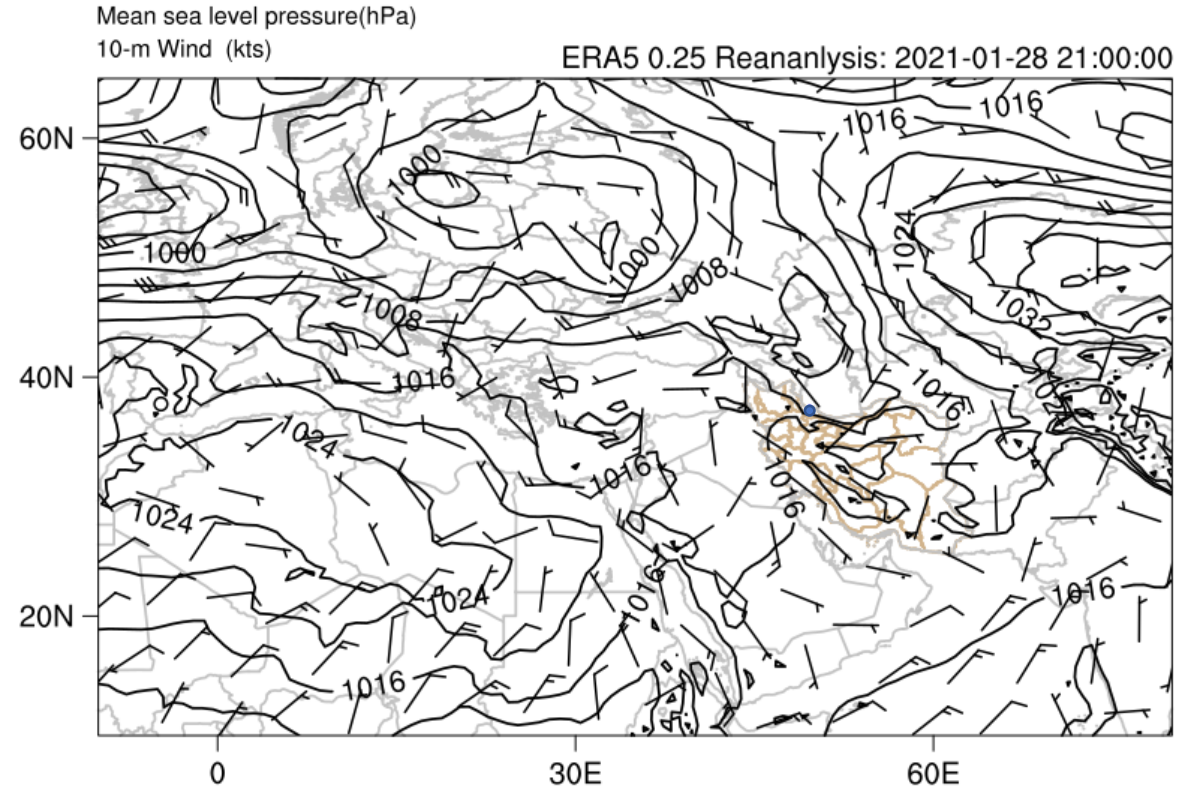
Mean sea level pressure(hPa)
10-m Wind (kts)
ERA5 0.25 Reananlysis: 2021-01-28 21:00:00
60N
40N
20N
0
30E
60E

(i)

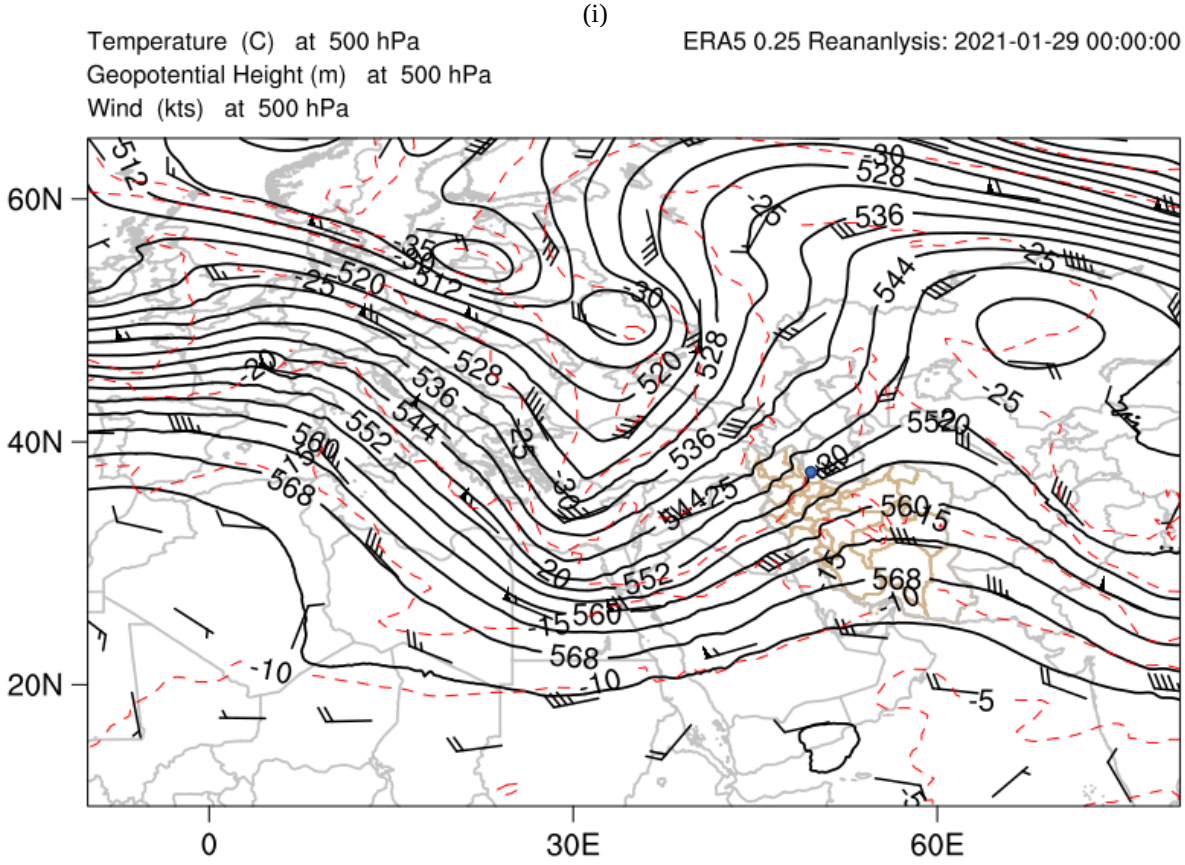
Temperature (C) at 500 hPa
Geopotential Height (m) at 500 hPa
Wind (kts) at 500 hPa
ERA5 0.25 Reananlysis: 2021-01-29 00:00:00
60N
40N
20N
0
30E
60E

(j)

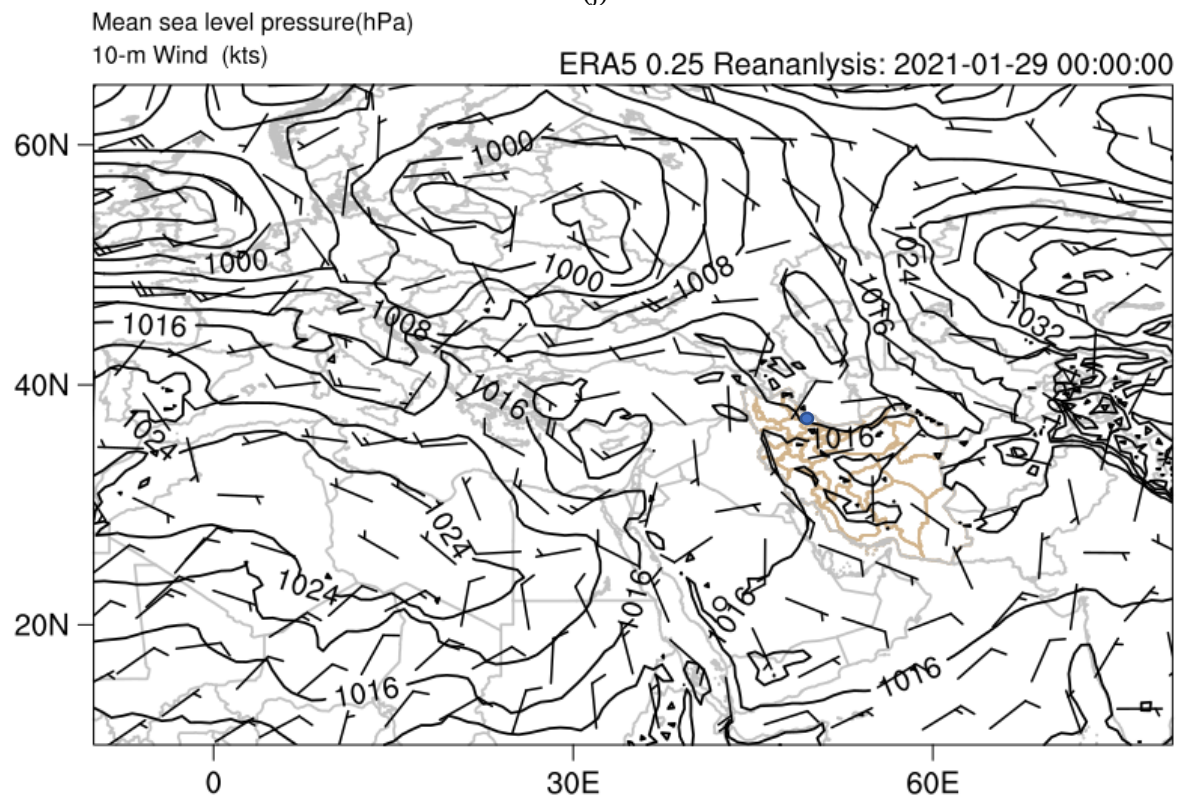
Mean sea level pressure(hPa)
10-m Wind (kts)
ERA5 0.25 Reananlysis: 2021-01-29 00:00:00
60N
40N
20N
0
30E
60E

(k)

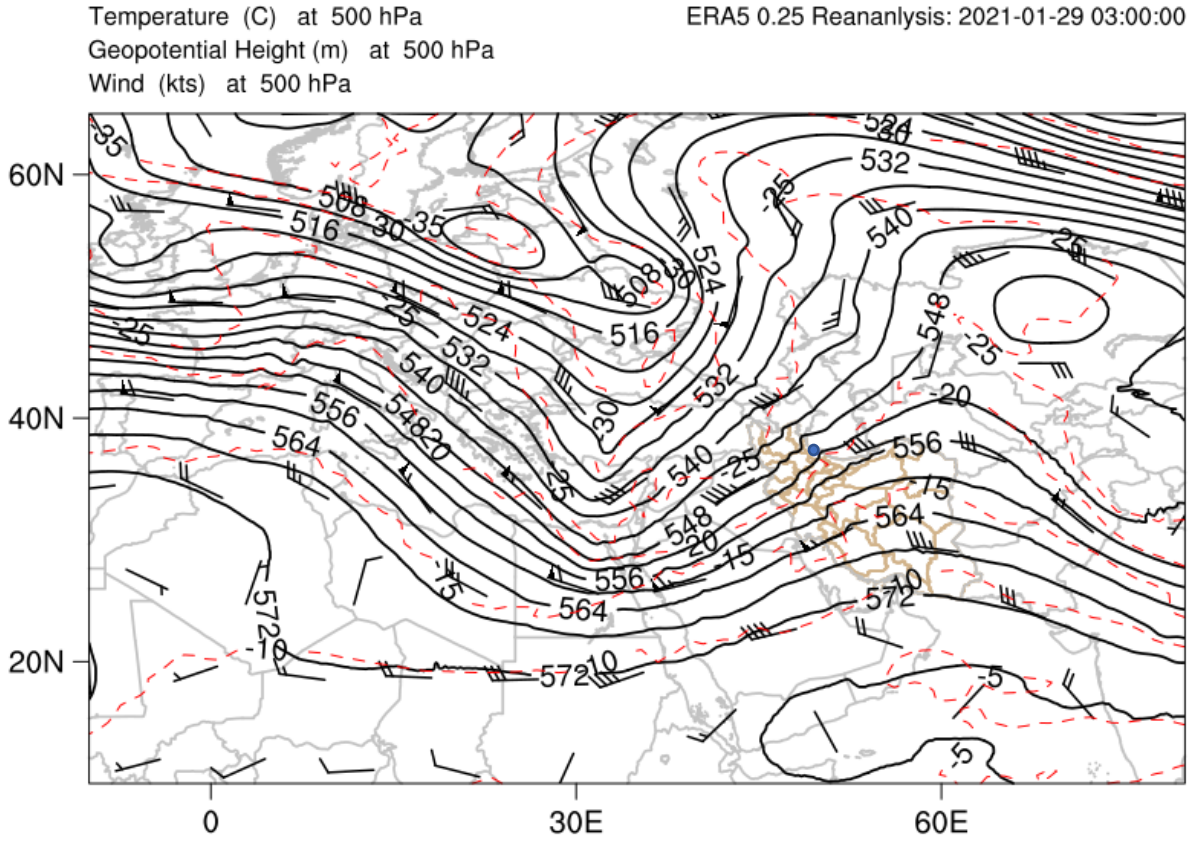
Temperature (C) at 500 hPa
Geopotential Height (m) at 500 hPa
Wind (kts) at 500 hPa
ERA5 0.25 Reananlysis: 2021-01-29 03:00:00
60N
40N
20N
0
30E
60E

(l)

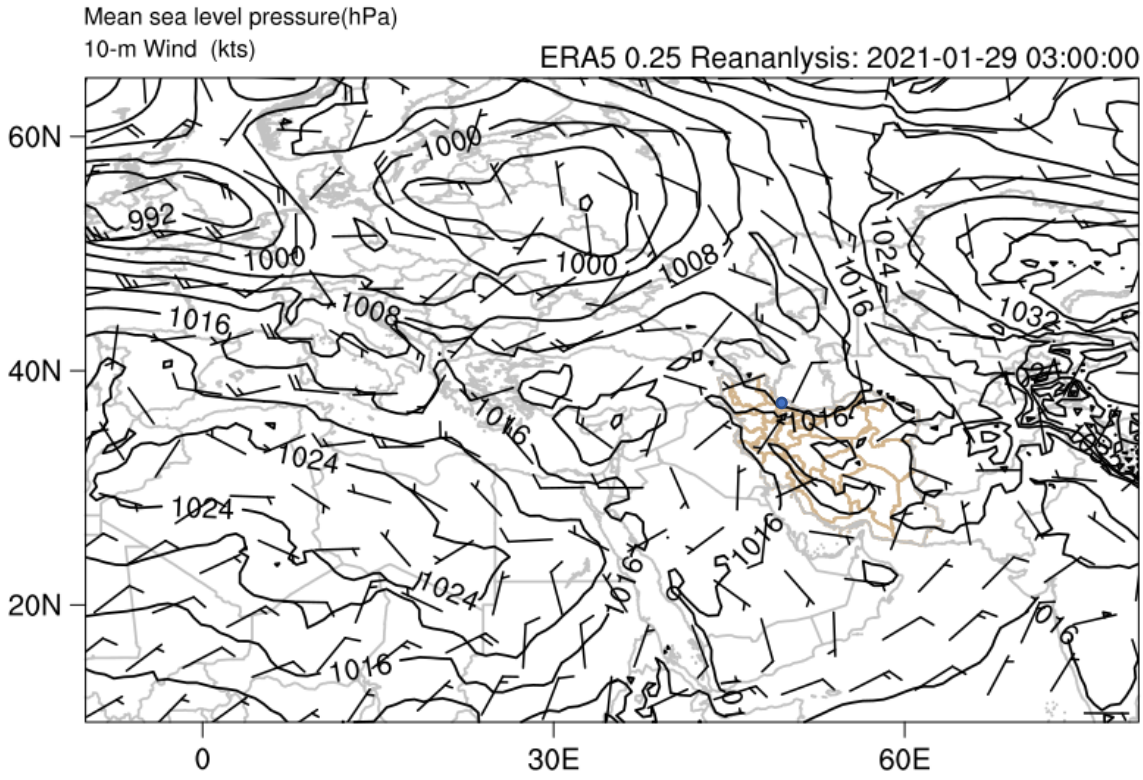
Mean sea level pressure(hPa)
10-m Wind (kts)
ERA5 0.25 Reananlysis: 2021-01-29 03:00:00
60N
40N
20N
0
30E
60E

(m)

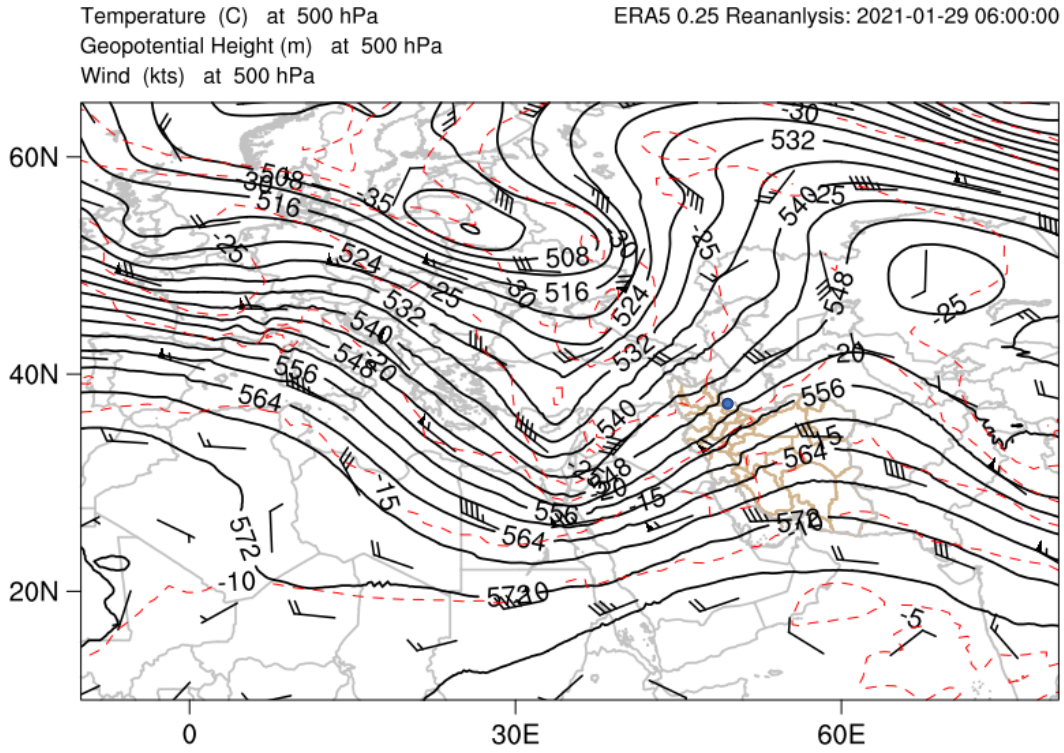

(n)

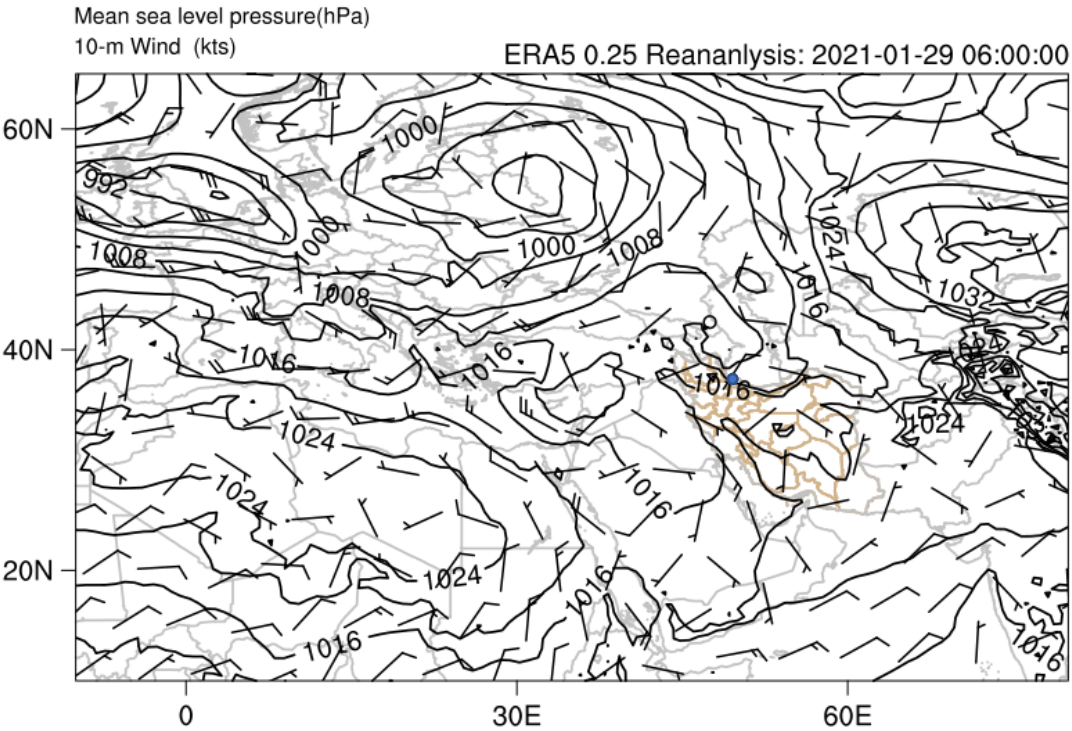

Figure 3-9. Analysis maps for (a, c, e, g, i, k, m) geopotential height (m) (black contours), temperature (°C) (red contoures) and wind barbs at 500 mb pressure level, (b, d, f, h, j, l, n) mean sea level pressure (mb) (black contours) with wind barbs at 10-m height above ground for17-18 January, different hours as the headers.

Skew-T plots for 12:00 UTC January 28 and 00:00 UTC January 29 for Tehran station from University of Wyoming are shown in Figure 3-10. In both diagrams the wind direction through the columns of atmosphere below the 500 hPa was nearly southwesterly to westerly with speed about 40 kt at top of the ridge, representing appropriate conditions for wind crossing over the Alborz Mountains from the south to the north, and providing foehn condition.

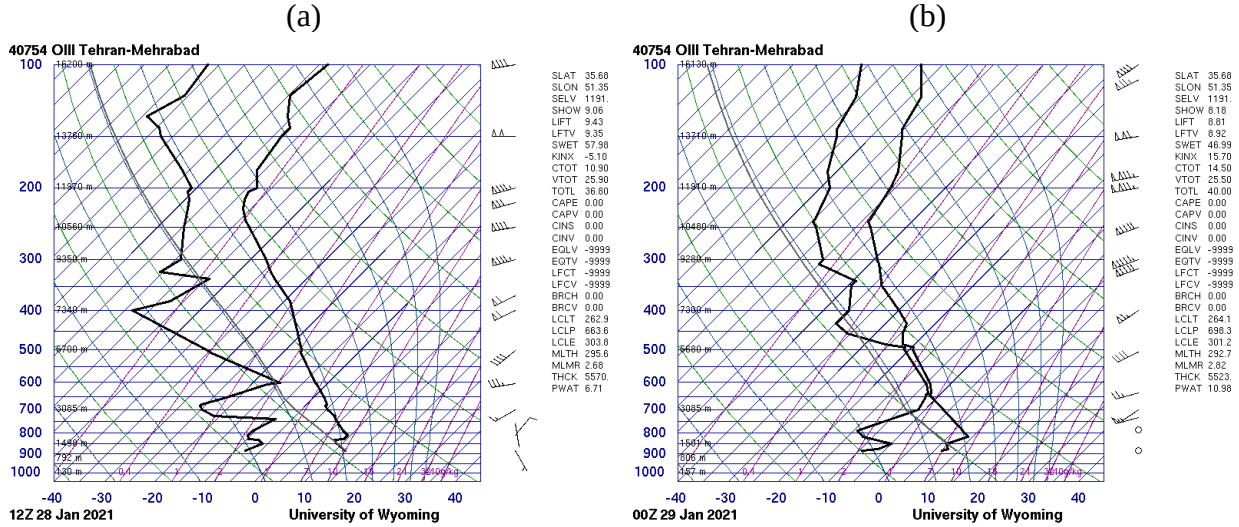

Figure 3-10. Skew-T diagram of Tehran Station (windward) at (a) 12:00 UTC January 28 and (b) 00:00 UTC January 29 derived form Univeristy of Wyoming.

3.2.5 Analysis of foehn event on 5 February 2021

As mentioned in section 3.2 there was another foehn event on 5 February 2021. Same as previous subsections, some characteristics of that would be analyzed here. Some meteorological parameters at Rasht-Airport station were gathered in Table 3-8; foehn times were shaded gray in this table. Based on this table, pressure decreased from 1015 hPa at 21:00 UTC 4 February to 1013 hPa at 00:00 UTC 5 February, then to 1012 hPa at 03:00 UTC and also 1010 hPa at 07:30 UTC 5 February 2021, showing a decreasing trend, which from 21:00 UTC 4 February to 03:00 UTC 5 February is not in accordance with diurnal variations. This decreasing trend would be investigated at analysis maps in the following. With this decreasing trend of pressure, wind speed increased, as till 03:00 UTC 5 February wind was nearly calm, but from 06:00 UTC wind speed reached to 3 m/s, and at 08:00 UTC wind speed reached 10 m/s with southerly direction (150 degree). Temperature rose from 14 ℃ at 07:00 UTC to 25 ℃ at 07:30 UTC 5 February, which shows an 11 ℃ temperature increase in half-hour. At the same time humidity decreased, as dewpoint fell from 10 ℃ to 6 ℃,

then to 3 ℃ at 09:00 UTC 5 February. Visibility improved from 100 m at 03:00 UTC 5 February to 8000 m at 06:00 UTC, then reached to more than 10 km at 08:00 UTC. Finally, low-level cloudiness at 07:30 UTC was about 1-2 oktas with a based at 2000 feet. With these conditions, foehn event can be easily deduced from 07:30 UTC 5 February.

Same conditions continued till 18:00 UTC 5 February, however, from 19:00 UTC pressure took increasing trend, as it was about 1010 hPa at 18:00 UTC, 1011 hPa at 19:00 UTC, and reached 1017 hPa at 21:00 UTC. Wind speed reduced from 5 m/s at 18:00 UTC, to 4 m/s at 19:00 UTC, then was almost calm after 21:00 UTC. Also, wind direction changed from southerly (180 degree) at 18:00 UTC to westerly (270 degree) at 19:00 UTC. The most obvious variations could be seen in temperature with a decrease from 23 ℃ at 18:00 UTC to 14 ℃ at 19:00 UTC, showing about a 9 ℃ temperature drop in one hour. At the same time dewpoint increased by about 7 ℃. Visibility changed from more than 10 km at 18:00 UTC to about 6000 m at 19:00 UTC. Finally, low-level cloudiness at 18:00 UTC was about 3-4 oktas with a base at 2000 feet. At 19:00 UTC the cloud base lowered to 1500 feet and at 21:00 UTC low-level cloud covered 5-7 oktas. So, it can be said that foehn conditions were removed from 19:00 UTC 5 February. Times with foehn condition shaded gray at Table 3-8.

Table 3-8. Same as Table 3 1 except from 00:00 UTC 4 February to 21:00 UTC 6 February 2021. Foehn conditions were shaded gray.

Date	Wind direction (degree)	Wind speed (m/s)	Temperature (℃)	Dewpoint (℃)	Visibility (m)	Cloudiness	Pressure (mb)
2/4/2021 00:00	0	0	7.8	7.8	300	VV002	1019
2/4/2021 03:00	0	0	7.6	7.6	1200	BKN004	1019
2/4/2021 06:00	180	2	7.4	7.4	3000	OVC006	1020
2/4/2021 09:00	240	2	8.6	8.2	4000	OVC009	1019
2/4/2021 12:00	0	0	11.6	7.9	4000	SCT010	1018
2/4/2021 15:00	0	0	8.6	8.6	2000	SCT010	1018
2/4/2021 18:00	90	2	8.2	8.2	2000	SCT010	1016
2/4/2021 21:00						SCT009	
	0	0	8.0	8.0	1800	SCT180	1015
2/5/2021 00:00	0	0	8.4	8.4	100	VV005	1013
2/5/2021 03:00	0	0	8.4	8.4	100	VV004	1012
						FEW020	
2/5/2021 06:00	210	3	14.6	7.8	8000	SCT080	1011

2/5/2021 07:00	300	3	14	10	7000	FEW020 BKN080	1011
2/5/2021 07:30	300	3	25	6	7000	FEW020 BKN080	1010
2/5/2021 08:00	150	10	26	6	9999	FEW020 BKN080	1010
2/5/2021 09:00	150	8	26.2	3.1	9999	FEW020 SCT080	1009
2/5/2021 12:00	150	8	25.6	3.3	9999	FEW020TCU SCT080 BKN170	1008
2/5/2021 15:00	150	8	23.0	3.1	9999	FEW020 SCT080 BKN170	1008
2/5/2021 18:00	180	5	23.0	3.1	9999	SCT020 SCT080 BKN170	1010
2/5/2021 19:00	270	4	14	10	6000	SCT015 BKN080	1011
2/5/2021 21:00	270	2	13.2	9.7	6000	BKN020 OVC070	1017
2/6/2021 00:00	0	0	12	10.4	8000	BKN025 OVC070	1019
2/6/2021 03:00	0	0	10.8	10.8	7000	SCT025 OVC070	1021
2/6/2021 06:00	0	0	11.6	10.4	9999	FEW025CB SCT035 OVC070	1022
2/6/2021 09:00	250	2	13.8	9.9	9999	FEW040 OVC100	1021
2/6/2021 12:00	10	2	15	9.1	9999	FEW040 BKN100	1019
2/6/2021 15:00	40	2	11.8	9.8	9999	SCT040 OVC150	1019
2/6/2021 18:00	0	0	11	10.6	9999	FEW030 OVC150	1019
2/6/2021 21:00	0	0	9	9	7000	NSC	1017

To compare conditions of the day with foehn event and days without foehn, daily maximum temperature, maximum wind speed and its direction, and minimum pressure for 4-6 February 2021 are shown in Table 3-9. The maximum temperature on 5 February when foehn occurred was more than 12 ℃ higher than 4 and 6 February, which are days without foehn event. Maximum wind speed on 5 February was about 9 m/s higher than 4 and 6 February. Also, direction of maximum wind was almost southerly (150 degree) on 5 February, while at 4 and 6 the direction was nearly northerly (330-40 degree). Minimum pressure on 5 February was about 1008 hPa, and for 4 and 6 was more than 1015 hPa.

Table 3-9. Same as Table 3-3 except from 4 to 6 February 2021.

date	Maximum Temperature (℃)	Maximum wind speed (m/s)	Direction of maximum wind speed	Minimum pressure (mb)
2/4/2021	11.8	2	330	1015
2/5/2021	27.2	11	150	1008
2/6/2021	15	2	40	1017.8

A similar study was done using meteorology data of Anzali station (Table a-4). In Table a-4 foehn times were shaded gray. As Rasht-Airport station, a decreasing trend of surface pressure is seen from February 4 to 5. At 12:00 UTC February 4 surface pressure was about 1017 hPa and at the same time of February 5 was about 1006 hPa. It seems other considered meteorological quantities didn't change as sharpen as at Rasht-airport station, except in 13:00-14:00 UTC February 5. In this one-hour interval wind turned southerly (190 degree), temperature increased by about 6 ℃, however, dewpoint decreased by only 2 ℃. It could be related to the somehow continuous northerly wind (340-30 degree) in the station which brought humidity from the sea. In 14:00-15:00 UTC 5 February, surface pressure increased about 2 mb (from 1006 to 1008 mb); temperature decreased about 8 ℃, from 21 ℃ to 13.5 ℃; wind turned from southerly (190 degree) to northwesterly (300 degree). It seems foehn conditions affected Anzali station for only 1-2 hours.

Weather reports of Tehran station for 4-6 February was collected in Table a-8. Again, in this table foehn times were shaded gray. Surface pressure of the station on February 4 was about 1018-1021 hPa. Comparing surface pressure over Rasht-Airport (Table 3-8) and Anzali stations (Table a-4), pressure gradient from south to north of the Alborz Mountains was not significant in February

4. Decreasing surface pressure over the leeward stations from 21:00 UTC February 4, producing a pressure gradient. From 06-18:00 UTC February 5 surface pressure over Tehran station was 1015-1020 hPa (Table a-8), however over leeward stations pressure was about 1006-1011 hPa (Table 3-8 and Table a-4). The cloudiness of sky over Tehran station was started about 03:00 UTC February 5, besides, rain phenomenon was reported after 10:00 UTC. Weather condition over Zanjan station for 4-6 February, confirms the pressure gradient, shows cloudiness of sky over the station during foehn event with southerly to westerly wind (Table a-12). Times with foehn event were shaded gray in Table a-12.

Analysis maps produced by IRIMO are shown in Figure 3-11. Weather condition reported by meteorological stations have been exhibited by weather symbols at these figures. Some cloudiness of sky over windward stations can be seen at 00:00 UTC February 5 (Figure 3-11(a)). It is worth noting some stations windward (south) of Alborz Mountains, reported cloudiness (the shaded circle symbol) and rainfall (• and ∇ icons) at 06:00 and 12:00 UTC 5 February, on the other hand, there is no rainfall report at leeward stations (north of Alborz Mountains), which is consistent with foehn condition.

(a)

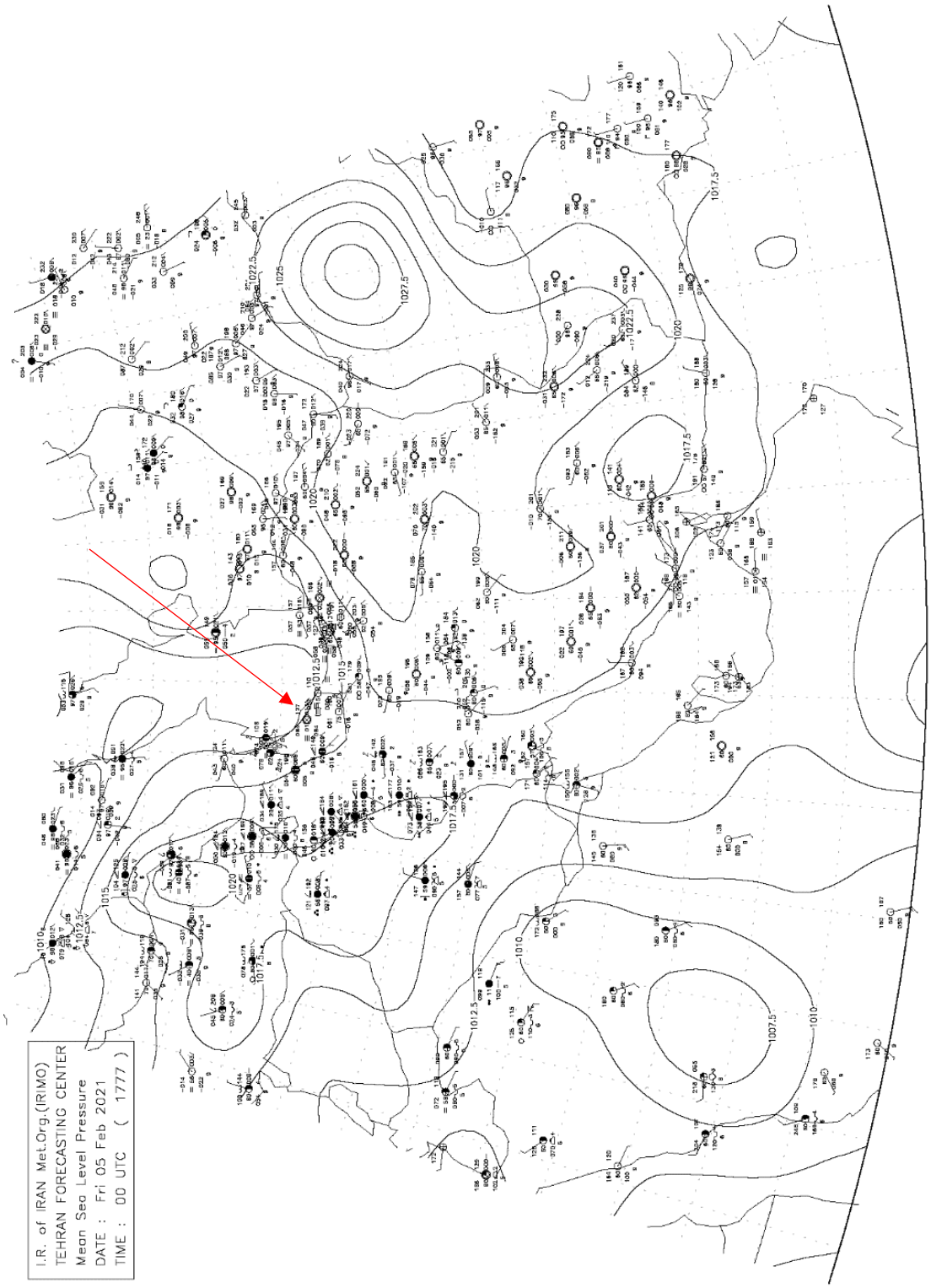
I.R. of IRAN Met.Org.(IRIMO)
TEHRAN FORECASTING CENTER
Mean Sea Level Pressure
DATE : Fri 05 Feb 2021
TIME : 00 UTC (1777)

(b)

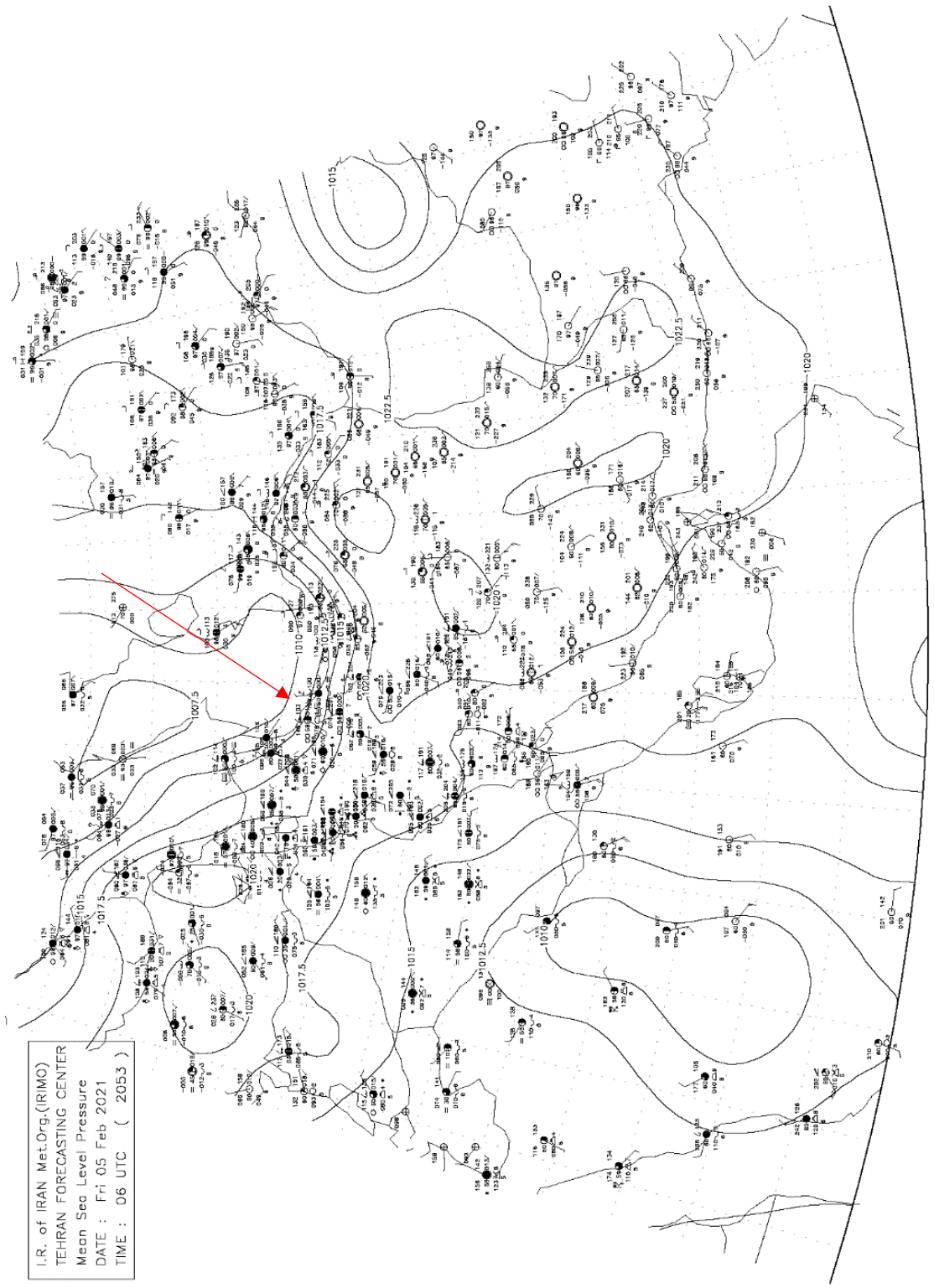
I.R. of IRAN Met.Org.(IRIMO)
TEHRAN FORECASTING CENTER
Mean Sea Level Pressure
DATE : Fri 05 Feb 2021
TIME : 06 UTC (2053)

(c)

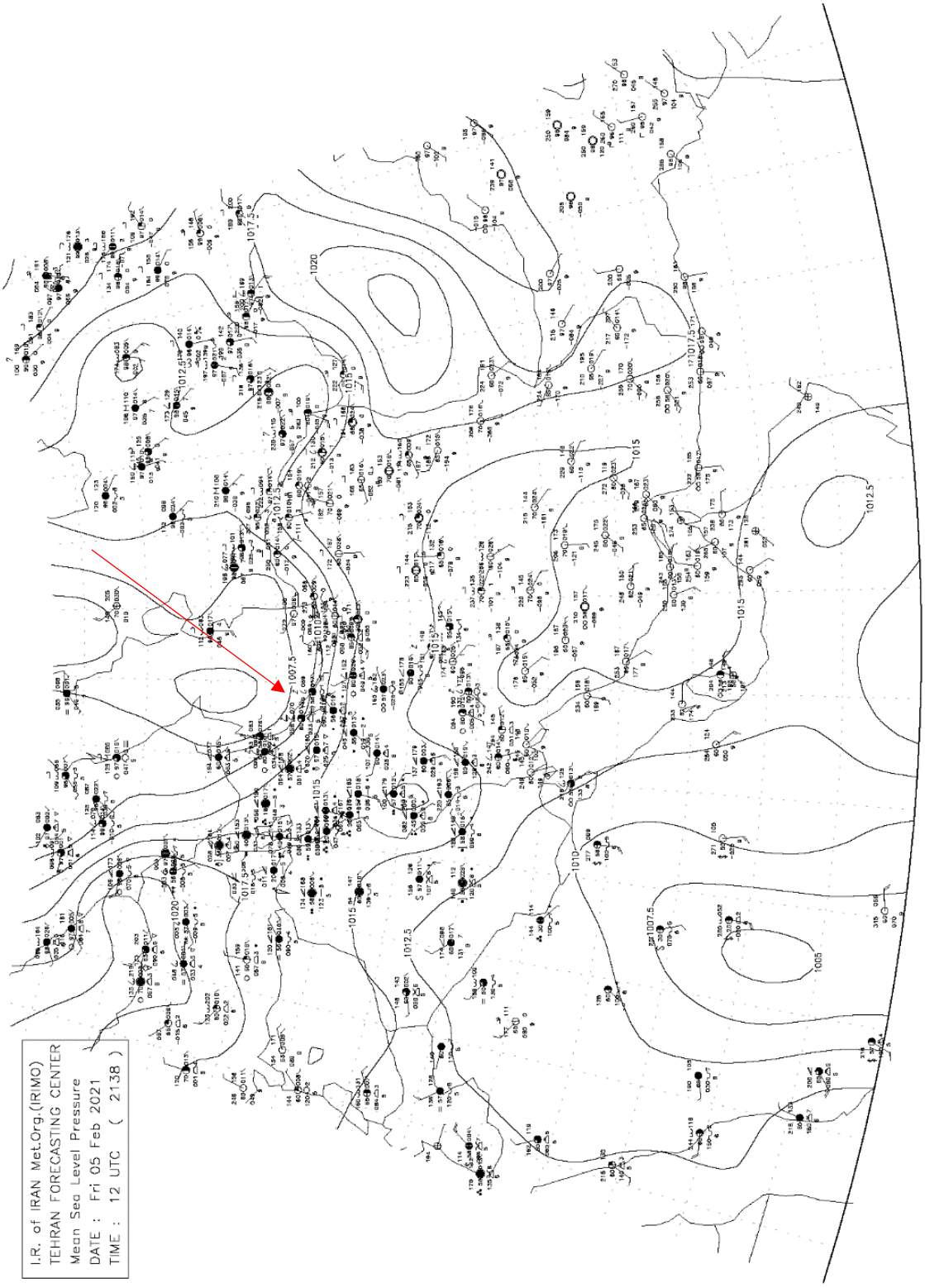

Figure 3-11. Analysis maps of mean sea level pressure provided by IRIMO for (a) 00:00, (b) 06:00 and (c) 12:00 UTC 5 February. The weather condition for stations have been exhibited at this figure with weather symbols.

As in previous sections, reanalysis maps of the foehn event are considered. In the map of geopotential height of the 500 hPa level at 21:00 UTC 4 February an elongated trough can be seen from the north of Russia with closed height contour and value of 496 m to north of the Black Sea (Figure 3-12(a)). Downstream of this trough, developing of a low pressure can be seen where its tongue stretched north of the Caspian Sea, as the 1012 hPa contour touched the Caspian Sea. On the other hand, a 1016 hPa pressure contour could be seen over the south coasts of the Caspian Sea (Figure 3-12(b)).

At 00:00 UTC, the mentioned trough moved eastward (Figure 3-12(c)), and 1012 hPa contour reached over the south coast of Caspian Sea (Figure 3-12(d)), as affirmation of the above mentioned decreasing trend of pressure at Rasht-Airport station from 1015 hPa at 21:00 UTC 4 February to 1013 hPa at 00:00 UTC 5 February (Table 3-8).

The eastward movement of the trough could also be seen at 03:00-06:00 UTC 5 February ((Figure 3-12(e) and (g))), and resulted in more penetration of low pressure over the Caspian Sea, as the 1008 hPa contour reached the Caspian Sea ((Figure 3-12(f) and (h))), and the 1011 hPa pressure value reported by Rash-Airport station (Table 3-8). On the other hand, a 1016 hPa contour over the Alborz Mountains and 1020 hPa over the south of Alborz Mountains could provide the necessary mechanism for initialization of a foehn event (Figure 3-12(f) and (h)), as the foehn event started from 07:30 UTC 5 February.

For the following times (09:00-15:00 UTC), the eastward movement of the trough axis at 500 hPa level continued (Figure 3-12(i), (k) and (m)). At surface level, penetration of the low pressure over the Caspian Sea continued, as a 1008 hPa pressure contour reached over the south coasts (Figure 3-12(j), (l) and (n)) and 1009-1008 hPa pressure values were reported by Rasht-Airport station at 09:00-15:00 UTC (Table 3-8). The pressure difference of about 8 hPa between south and north of Alborz mountains caused the relatively high wind speed, 8-11 m/s, at Rasht-Airport station during the foehn event.

At 18:00 UTC, the trough at 500 hPa level reached the neighborhood of the Caspian Sea (Figure 3-12(o)), and at surface level the 1008 hPa contour moved away from the south coast of the Caspian Sea (Figure 3-12(p)). The pressure value at Rasht-Airport station at this time rose to 1010 hPa (Table 3-8), corresponding to the abovementioned increasing trend of pressure. Also, wind speed reduced from 8 m/s at 15:00 UTC to 5 m/s at 18:00 UTC. At 21:00 UTC, the analysis map of the 500 hPa level shows the axis of trough located north-south along the Caspian Sea (Figure

3-12(q)), and at surface level, 1012 hPa moved away from west coast of Caspian Sea in Iran (Figure 3-12(r)), as 1017 hPa reported at this time by the Rasht-Airport station. By removing the pressure gradient between south and north of Alborz Mountains, the wind speed decreased, and its direction changed, too, as wind speed 2 m/s with westerly (270 degree) direction reported. So, it seems foehn condition has not remained longs. At 00:00 UTC 6 February, by continuing of eastward movement of the axis of trough, the Caspian Sea was located at the upstream and subsidence region of the trough (Figure 3-12(s)), causing rising pressure and also a pressure gradient decreasing over the studied area (Figure 3-12(t)).

(a)

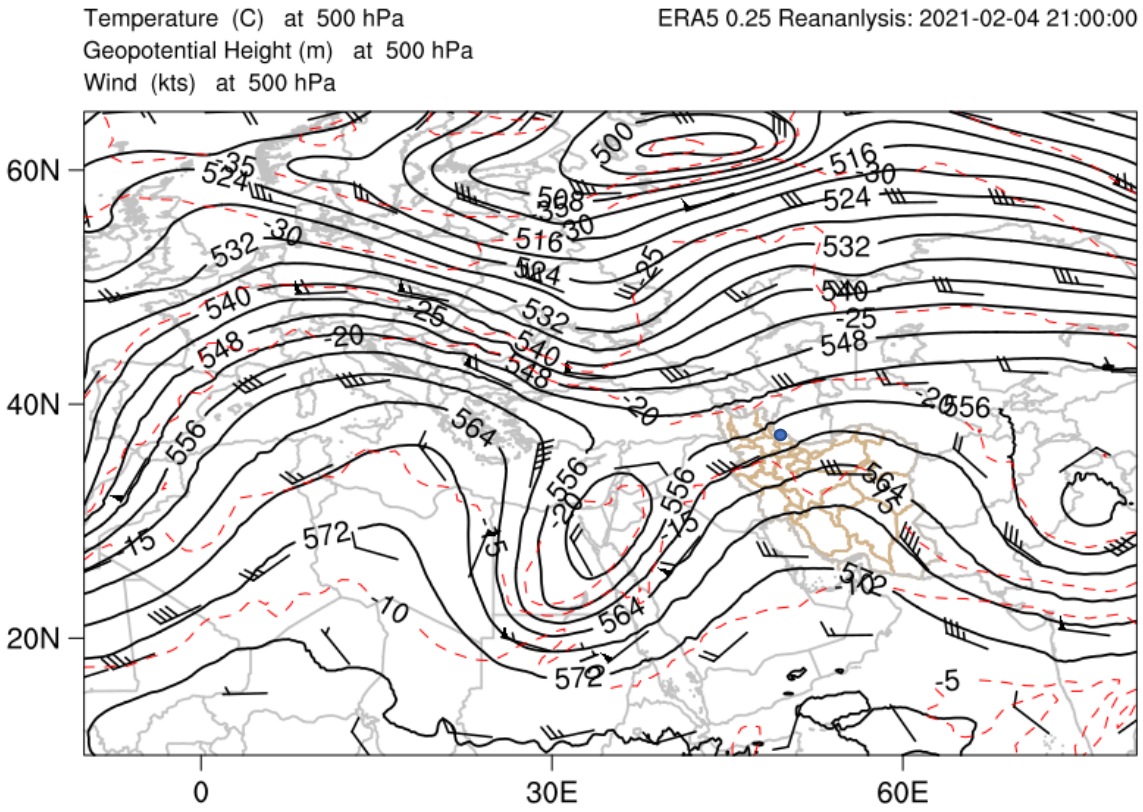

(b)

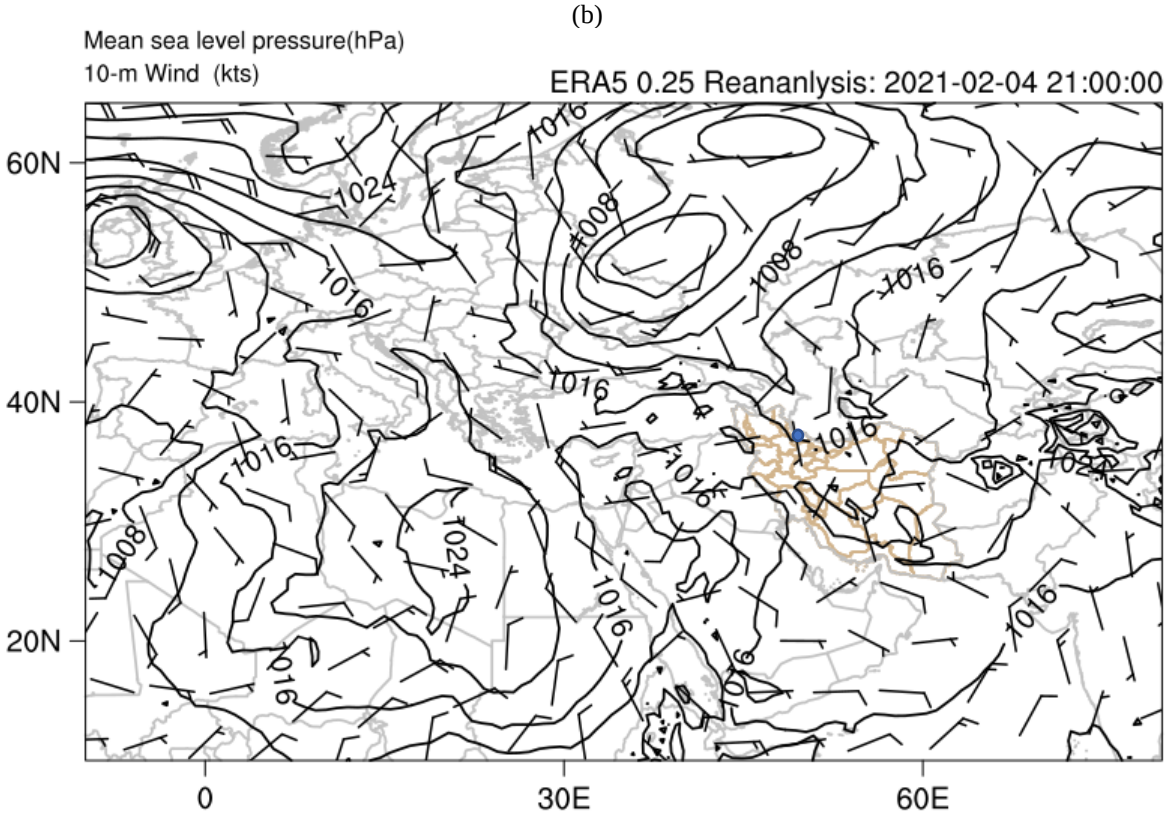
Mean sea level pressure(hPa)
10-m Wind (kts)
ERA5 0.25 Reananlysis: 2021-02-04 21:00:00
60N
40N
20N
0
30E
60E

(c)

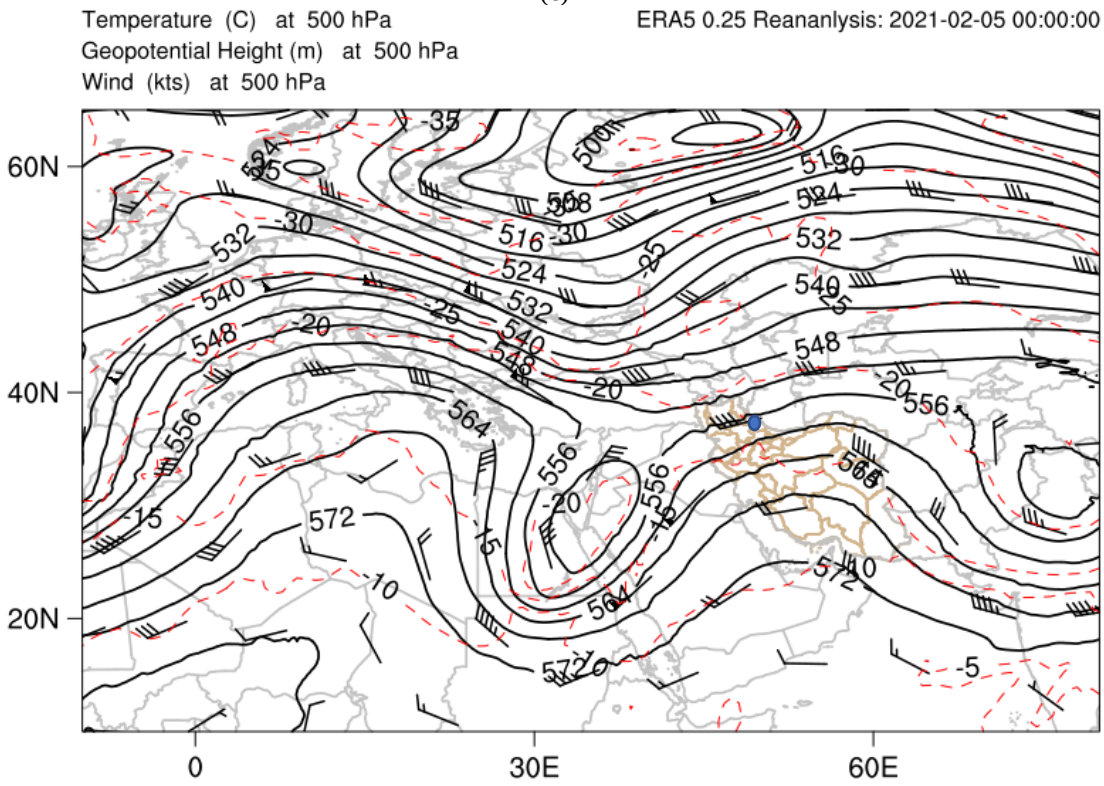
Temperature (C) at 500 hPa
Geopotential Height (m) at 500 hPa
Wind (kts) at 500 hPa
ERA5 0.25 Reananlysis: 2021-02-05 00:00:00
60N
40N
20N
0
30E
60E

(d)

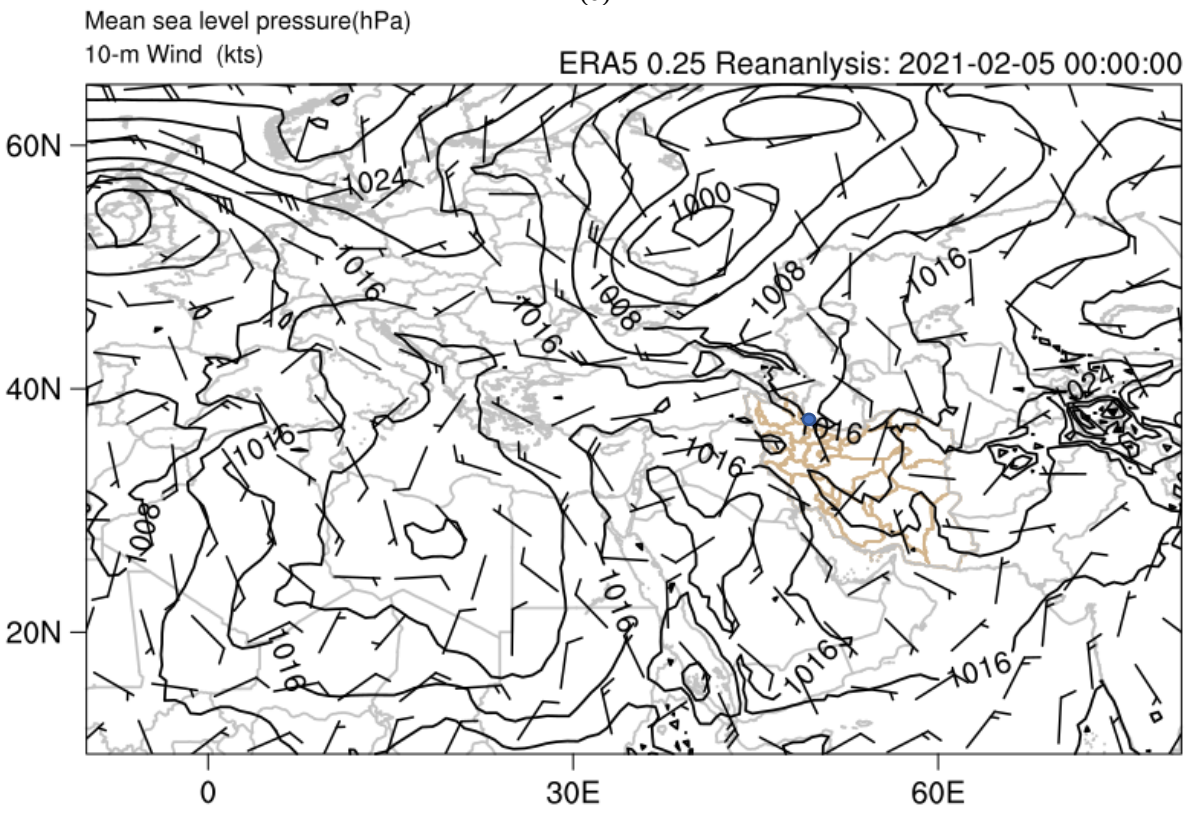
Mean sea level pressure(hPa)
10-m Wind (kts)
ERA5 0.25 Reananlysis: 2021-02-05 00:00:00
60N
40N
20N
0
30E
60E

(e)

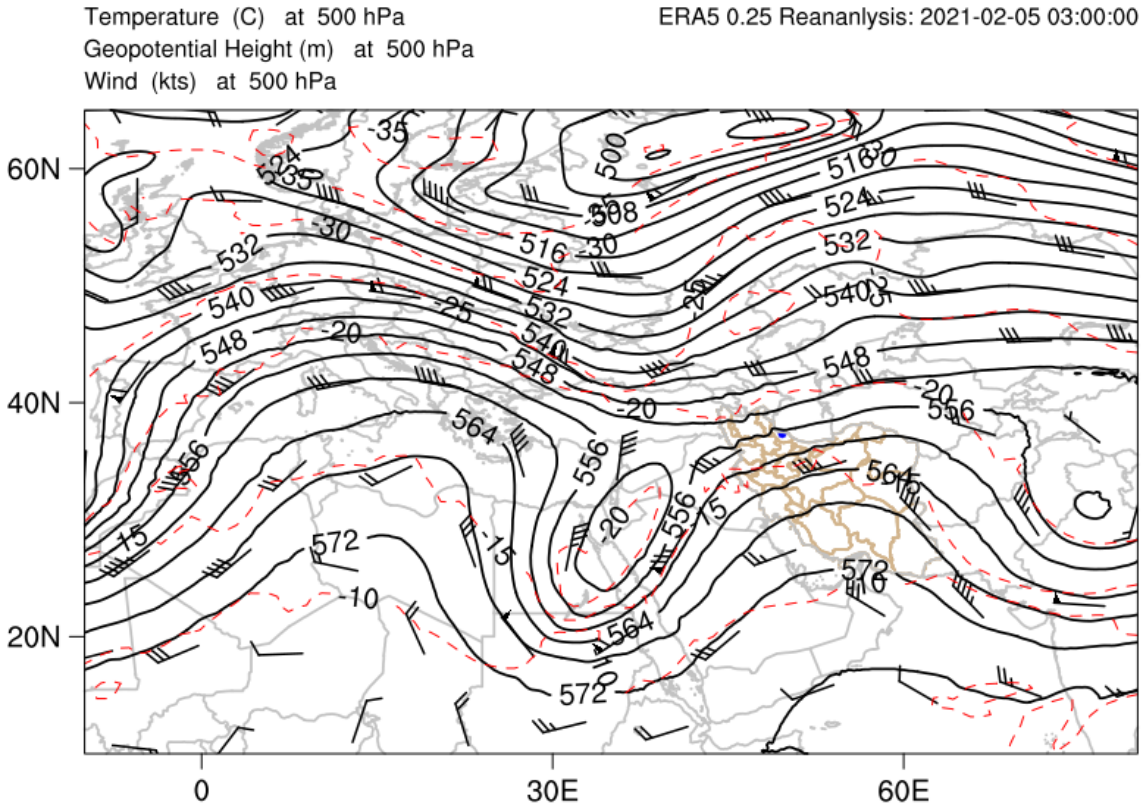
Temperature (C) at 500 hPa
Geopotential Height (m) at 500 hPa
Wind (kts) at 500 hPa
ERA5 0.25 Reananlysis: 2021-02-05 03:00:00
60N
40N
20N
0
30E
60E

(f)

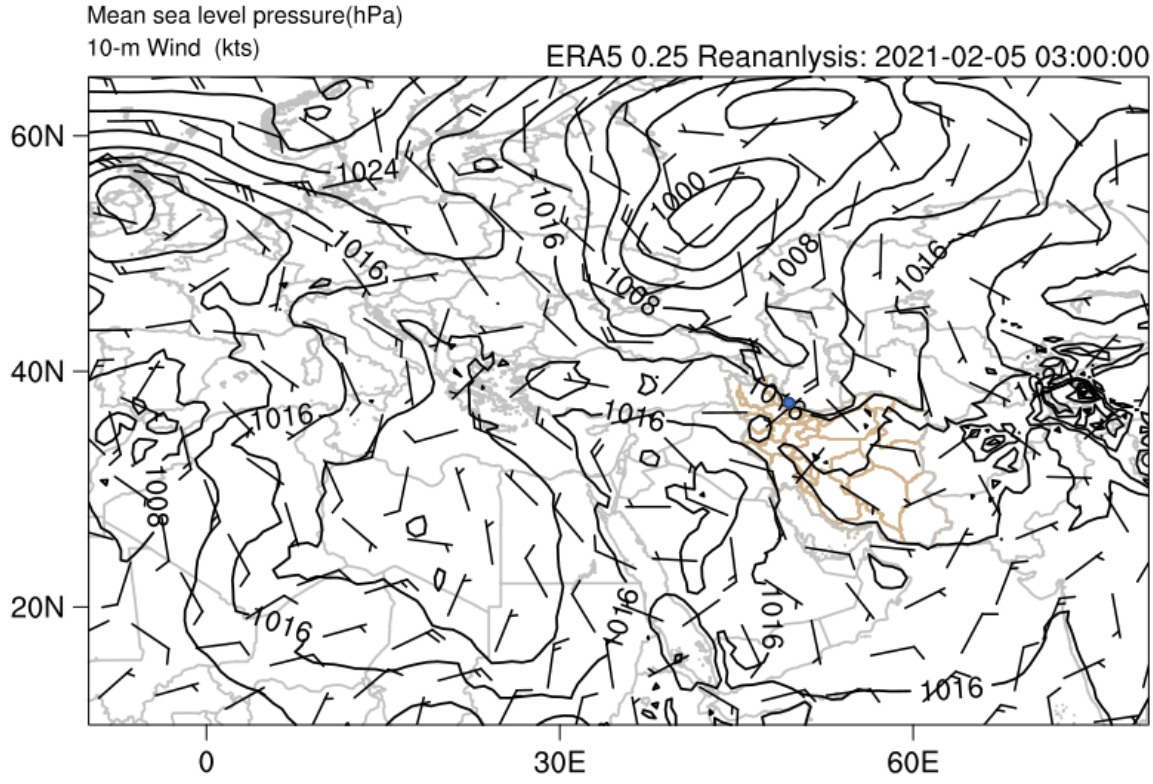
Mean sea level pressure(hPa)
10-m Wind (kts)
ERA5 0.25 Reananlysis: 2021-02-05 03:00:00
60N
40N
20N
0
30E
60E
1024
1016
1008
1000

(g)

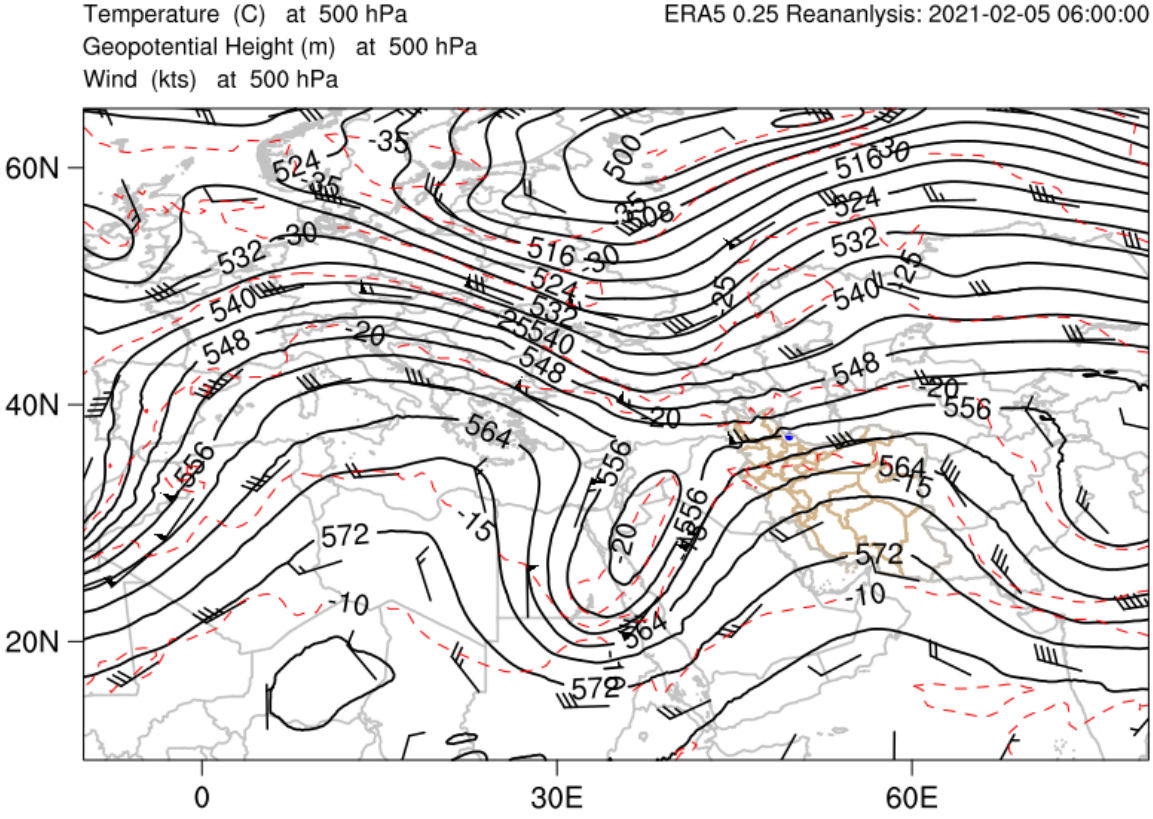
Temperature (C) at 500 hPa
Geopotential Height (m) at 500 hPa
Wind (kts) at 500 hPa
ERA5 0.25 Reananlysis: 2021-02-05 06:00:00
60N
40N
20N
0
30E
60E

(h)

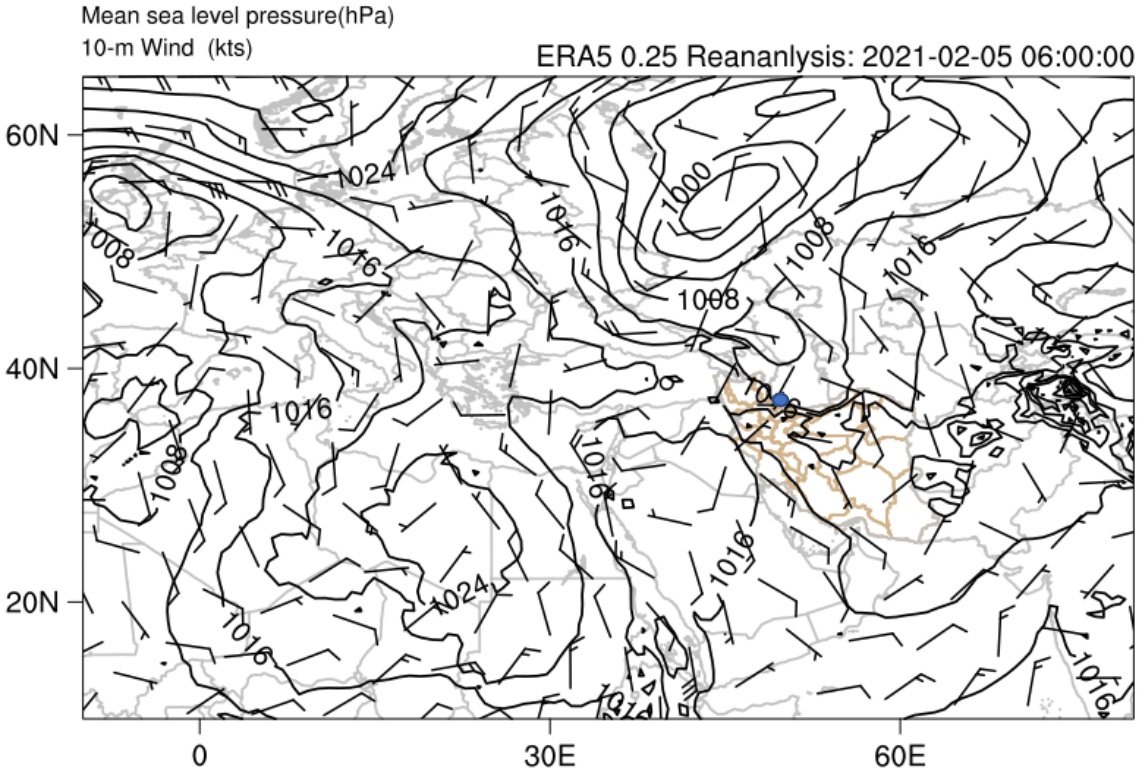
Mean sea level pressure(hPa)
10-m Wind (kts)
ERA5 0.25 Reananlysis: 2021-02-05 06:00:00
60N
40N
20N
0
30E
60E

(i)

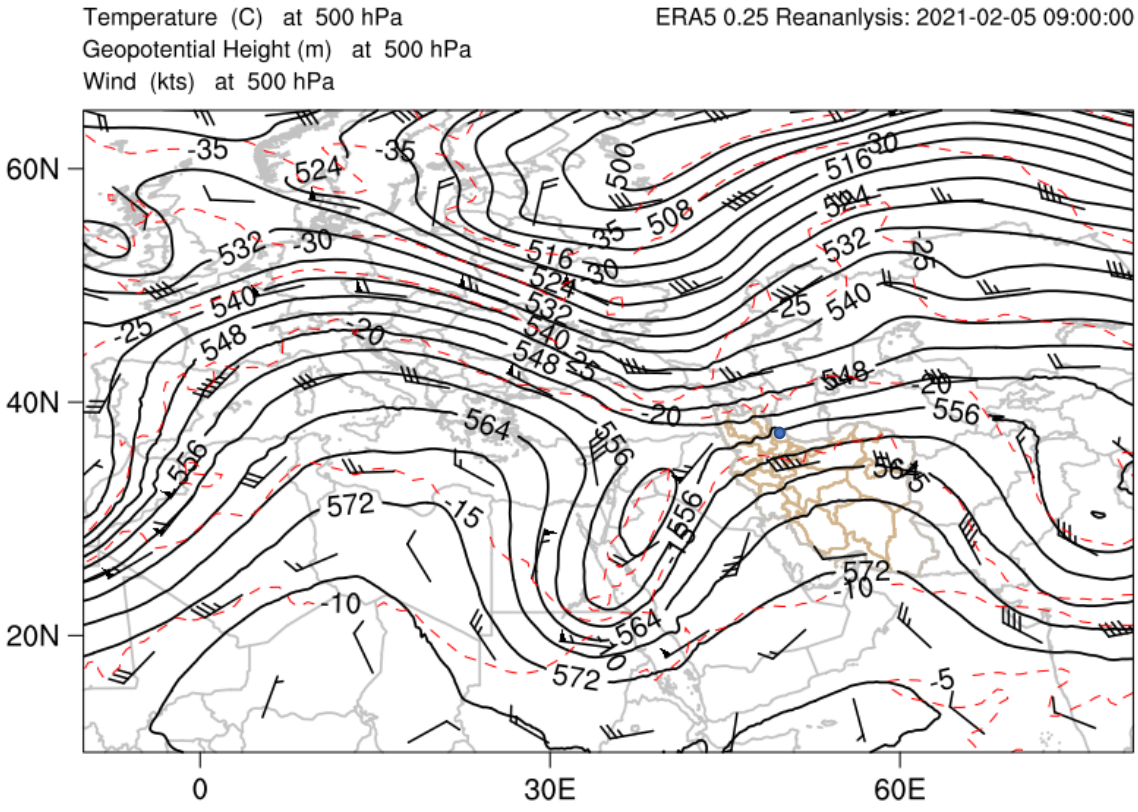
Temperature (C) at 500 hPa
Geopotential Height (m) at 500 hPa
Wind (kts) at 500 hPa
ERA5 0.25 Reananlysis: 2021-02-05 09:00:00
60N
40N
20N
0
30E
60E

(j)

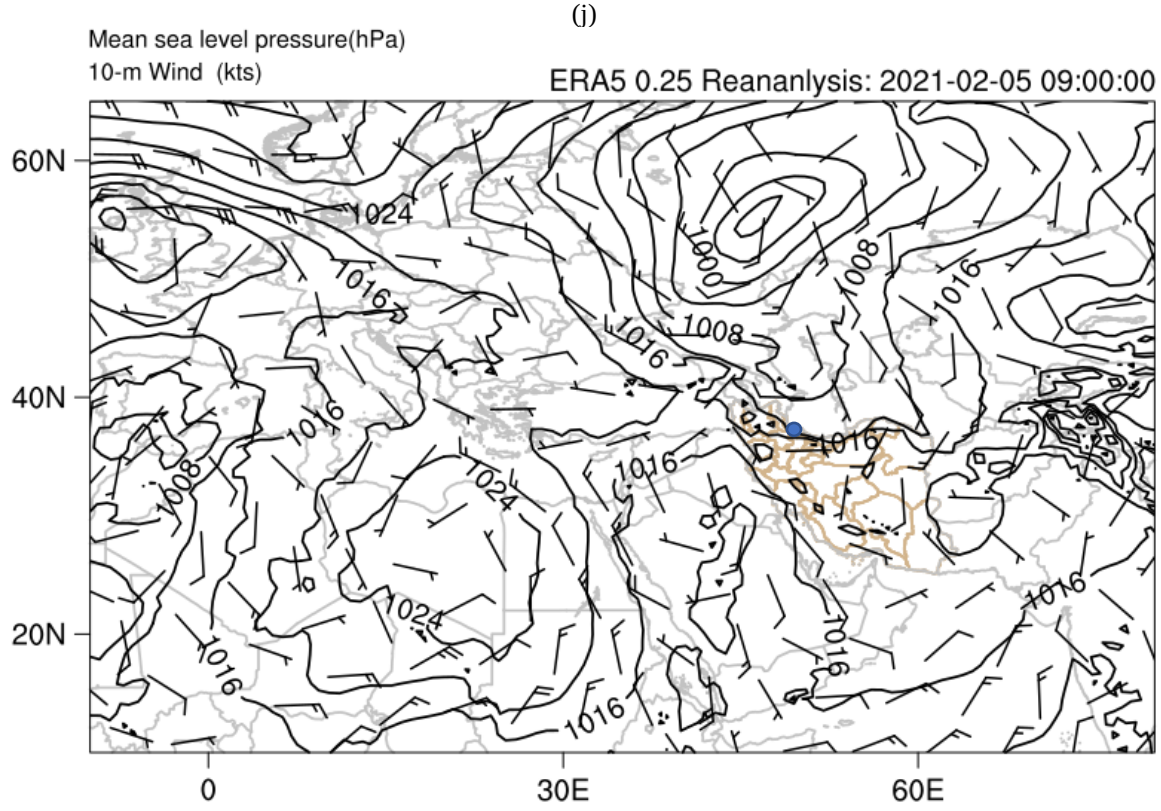
Mean sea level pressure(hPa)
10-m Wind (kts)
ERA5 0.25 Reananlysis: 2021-02-05 09:00:00
60N
40N
20N
0
30E
60E

(k)

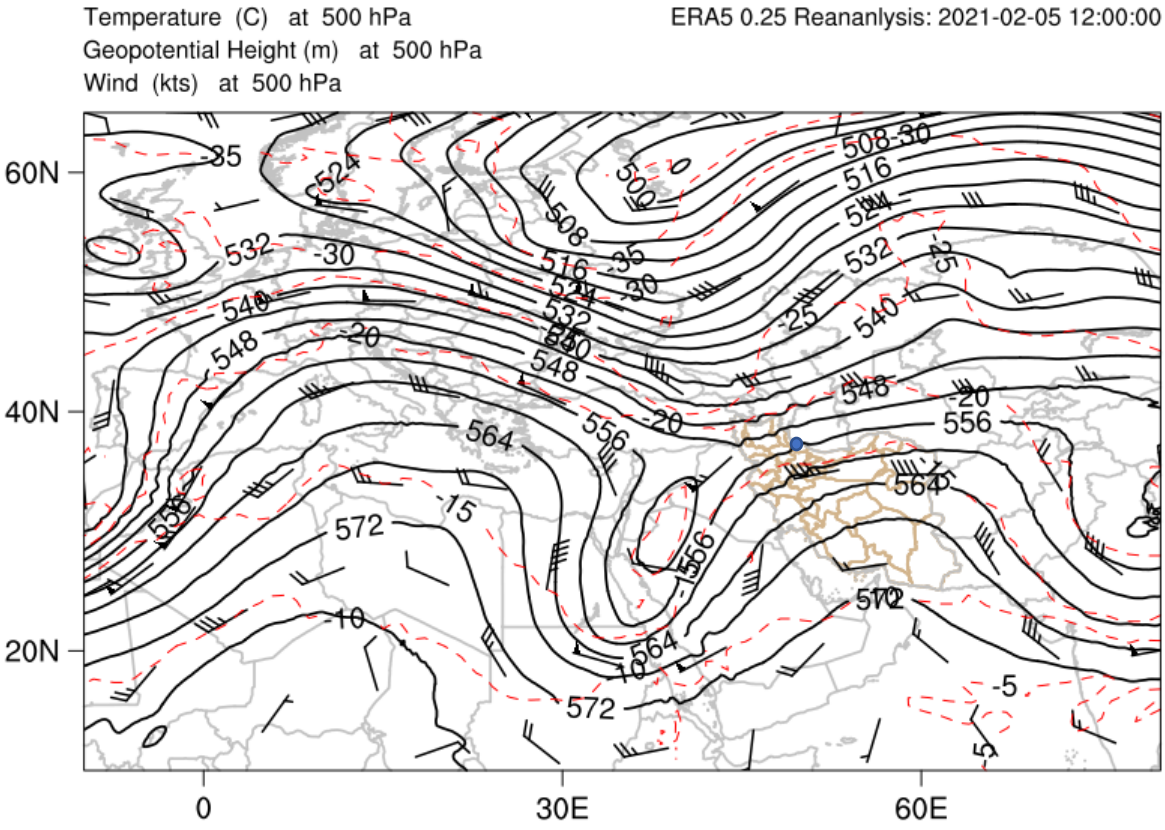
Temperature (C) at 500 hPa
Geopotential Height (m) at 500 hPa
Wind (kts) at 500 hPa
ERA5 0.25 Reananlysis: 2021-02-05 12:00:00
60N
40N
20N
0
30E
60E

(l)

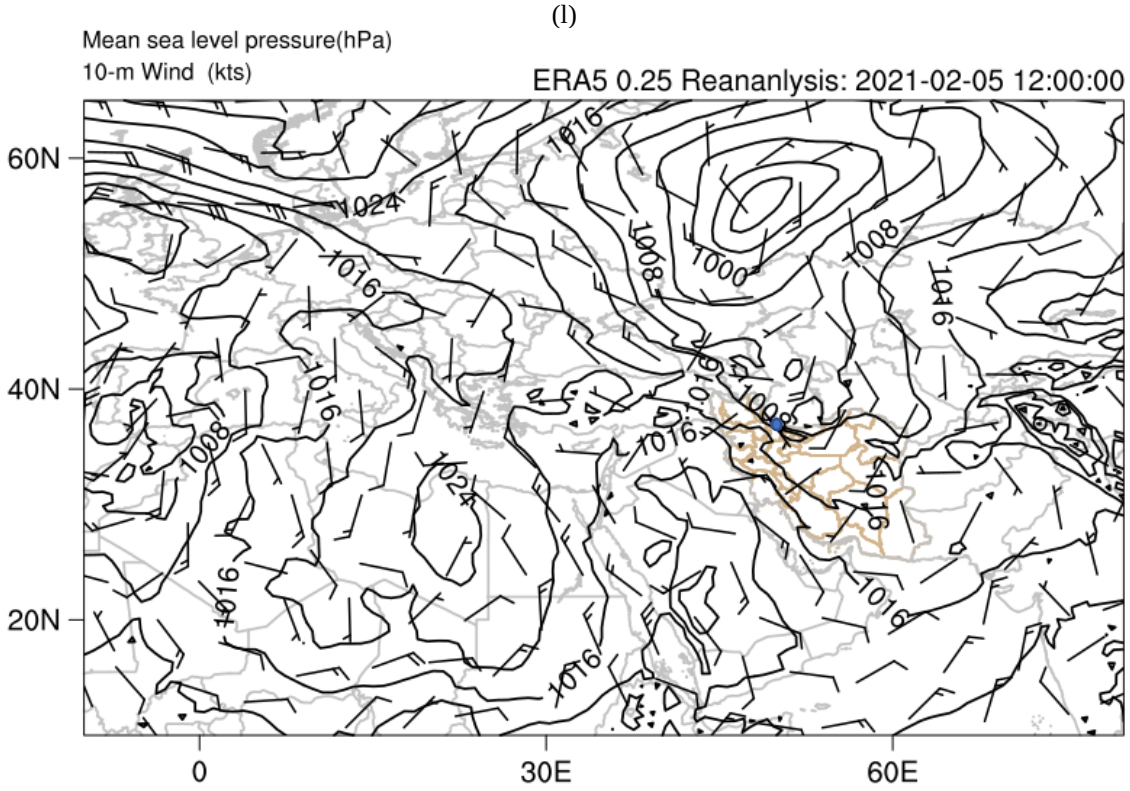
Mean sea level pressure(hPa)
10-m Wind (kts)
ERA5 0.25 Reananlysis: 2021-02-05 12:00:00
60N
40N
20N
0
30E
60E

(m)

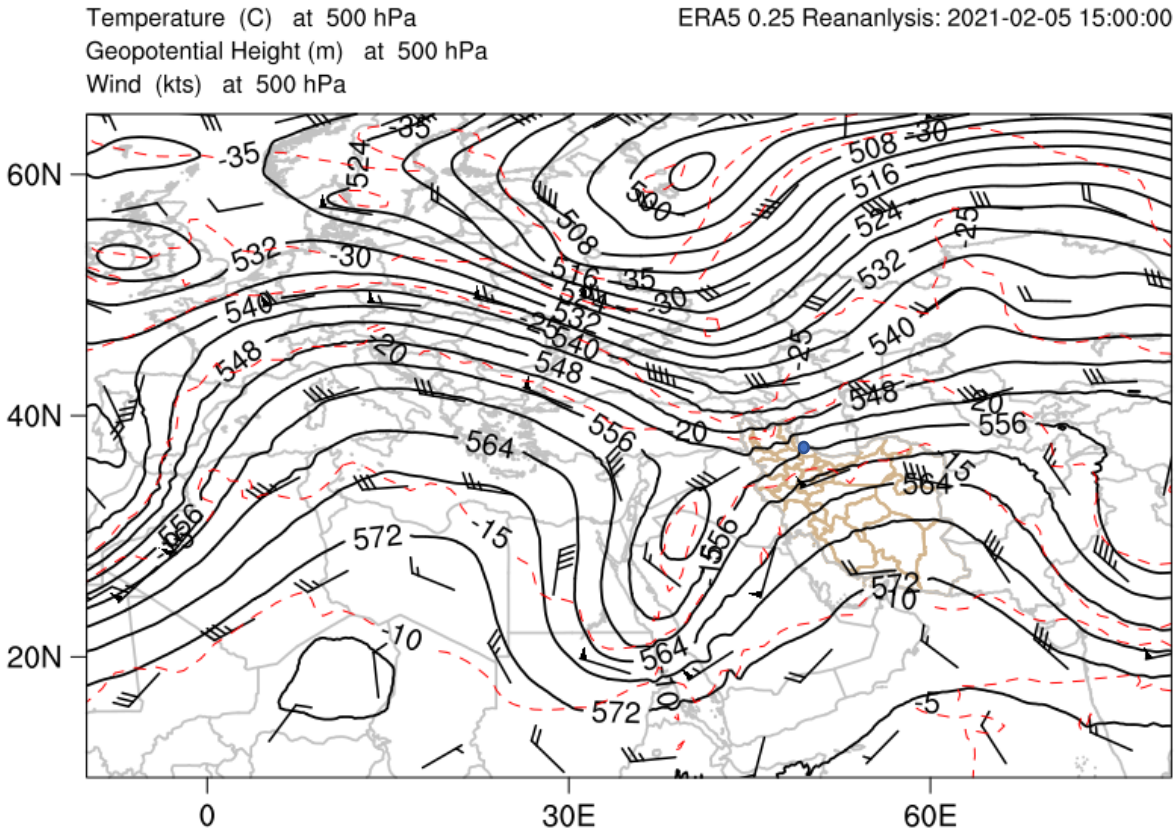
Temperature (C) at 500 hPa
Geopotential Height (m) at 500 hPa
Wind (kts) at 500 hPa
ERA5 0.25 Reananlysis: 2021-02-05 15:00:00
60N
40N
20N
0
30E
60E

(n)

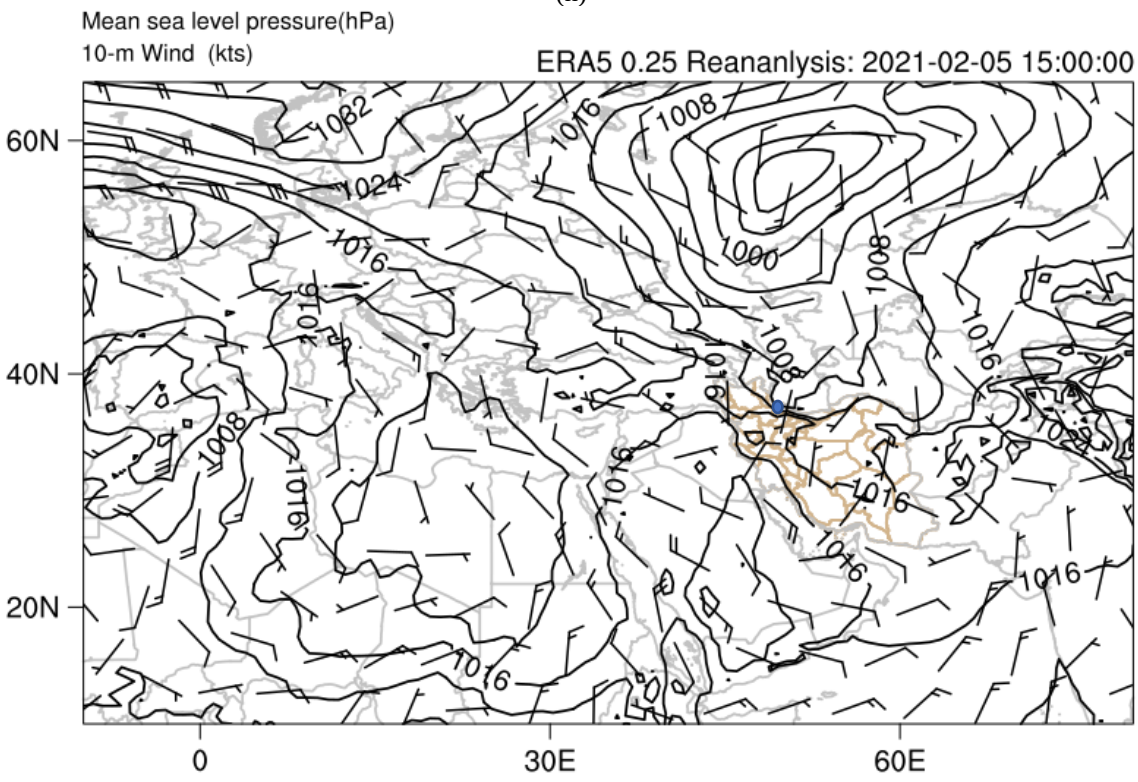
Mean sea level pressure(hPa)
10-m Wind (kts)
ERA5 0.25 Reananlysis: 2021-02-05 15:00:00
60N
40N
20N
0
30E
60E

(o)

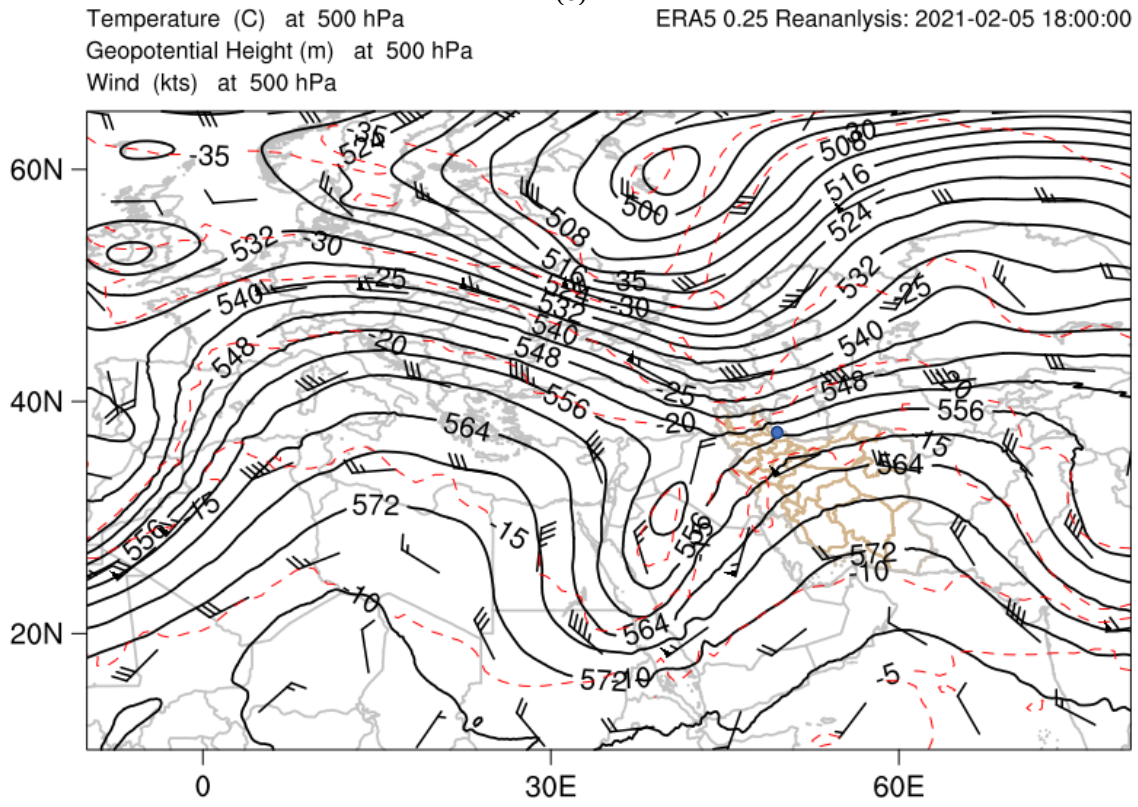
Temperature (C) at 500 hPa
Geopotential Height (m) at 500 hPa
Wind (kts) at 500 hPa
ERA5 0.25 Reananlysis: 2021-02-05 18:00:00
60N
40N
20N
0
30E
60E

(p)

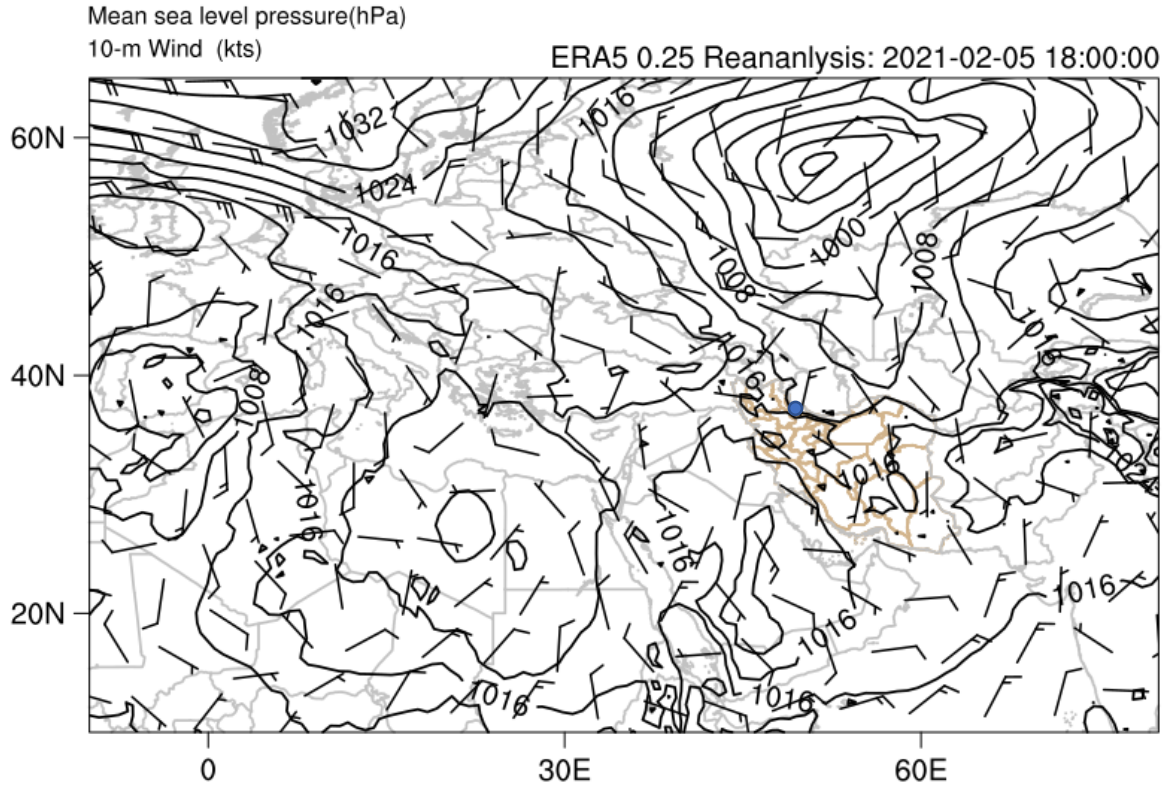
Mean sea level pressure(hPa)
10-m Wind (kts)
ERA5 0.25 Reananlysis: 2021-02-05 18:00:00
60N
40N
20N
0
30E
60E

(q)

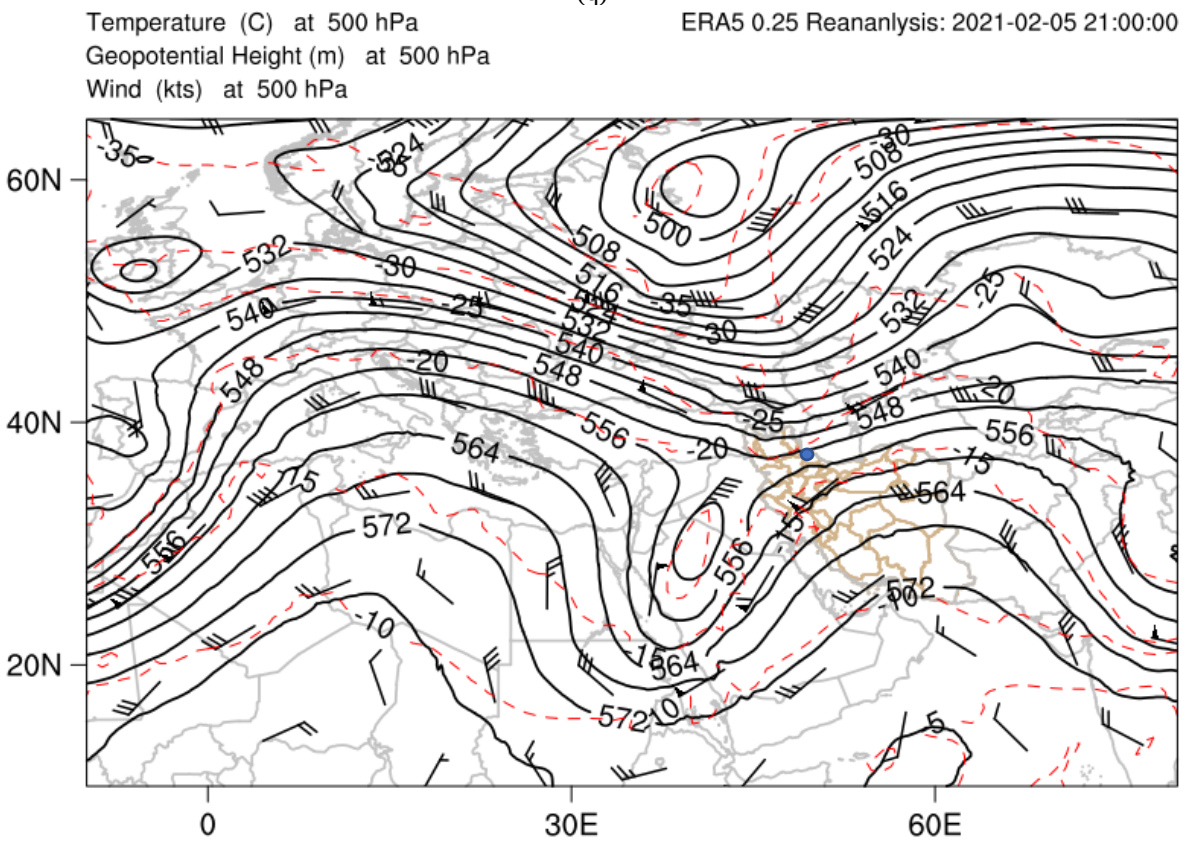
Temperature (C) at 500 hPa
Geopotential Height (m) at 500 hPa
Wind (kts) at 500 hPa
ERA5 0.25 Reananlysis: 2021-02-05 21:00:00
60N
40N
20N
0
30E
60E

(r)

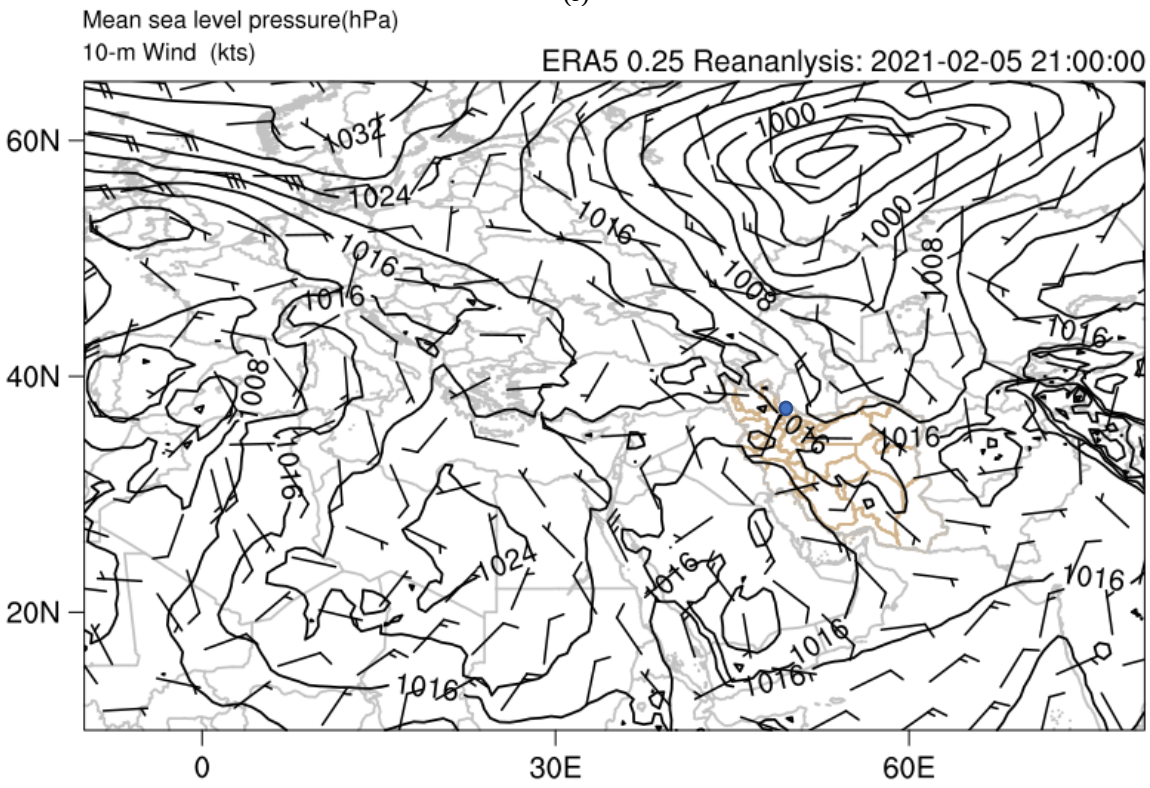
Mean sea level pressure(hPa)
10-m Wind (kts)
ERA5 0.25 Reananlysis: 2021-02-05 21:00:00
60N
40N
20N
0
30E
60E

(s)

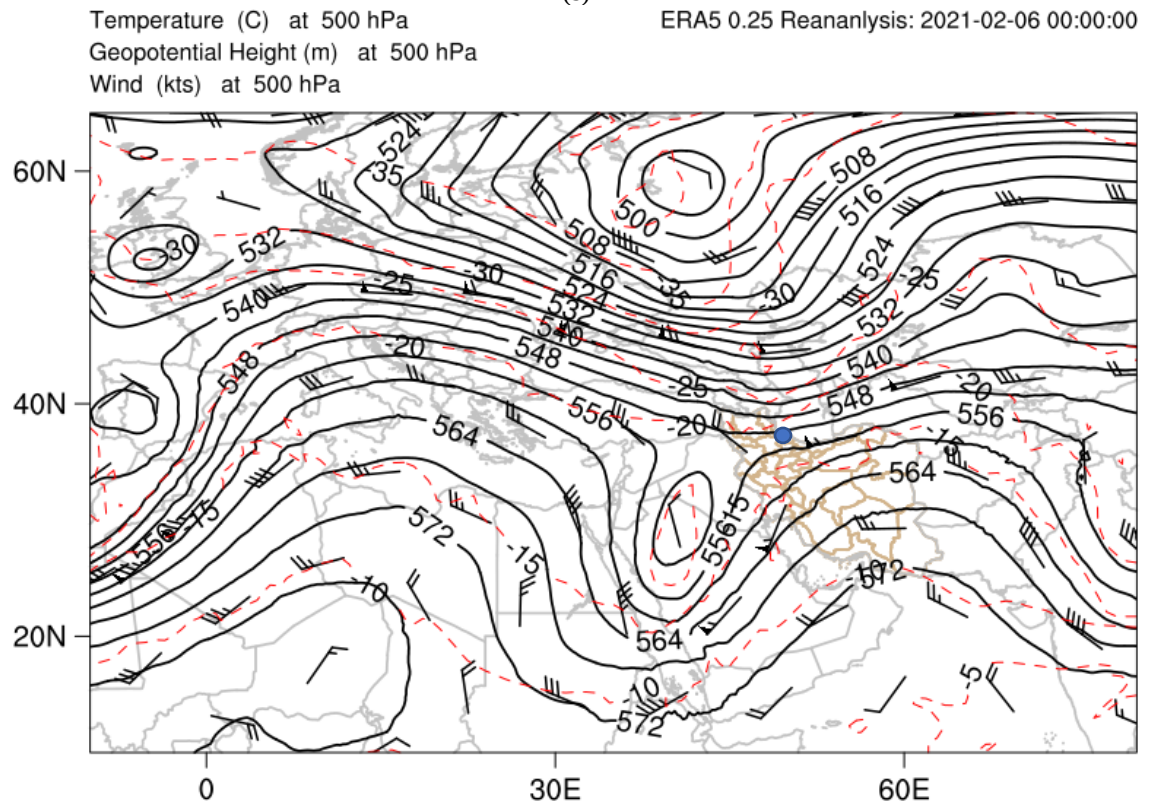
Temperature (C) at 500 hPa
Geopotential Height (m) at 500 hPa
Wind (kts) at 500 hPa
ERA5 0.25 Reananlysis: 2021-02-06 00:00:00
60N
40N
20N
0
30E
60E

(t)

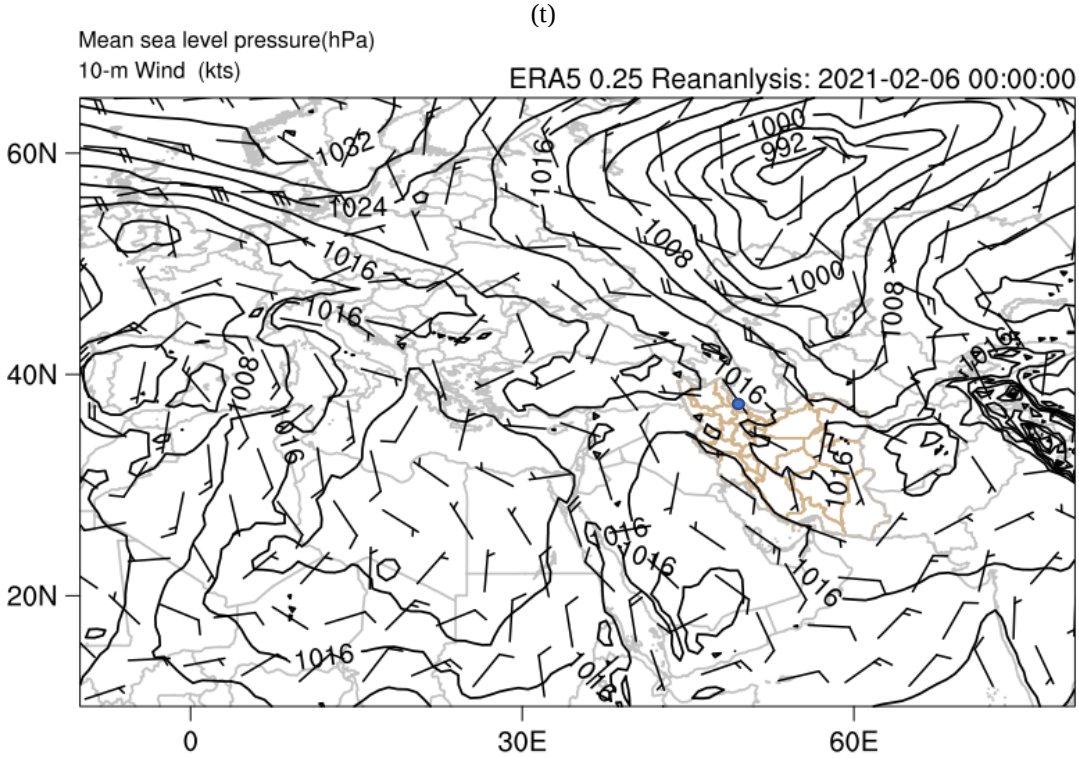

Figure 3-12. Analysis maps for (a, c, e, g, i, k, m, o, q, s) geopotential height (m) (black contours), temperature (℃) (red contoures) and wind barbs at 500 mb pressure level, (b, d, f, h, j, l, n, p, r, t) mean sea level pressure (mb) (black contours) with wind barbs at 10-m height above ground for4-6 January, different hours as the headers.

Skew-T plots over Tehran station for 00:00 and 12:00 UTC February 4 and 00:00 UTC February 5 from University of Wyoming were shown in Figure 3-13. The wind direction at 00:00 and 12:00 UTC February 4 (Figure 3-13(a-b)) from surface to approximately 700 hPa was about southwesterly to northwesterly. In both times from 700 to 500 hPa wind direction was about southwesterly to westerly. For 12:00 UTC February 5 the skew-T diagram was not completed, even though somehow southwesterly from 700 hPa can be seen.

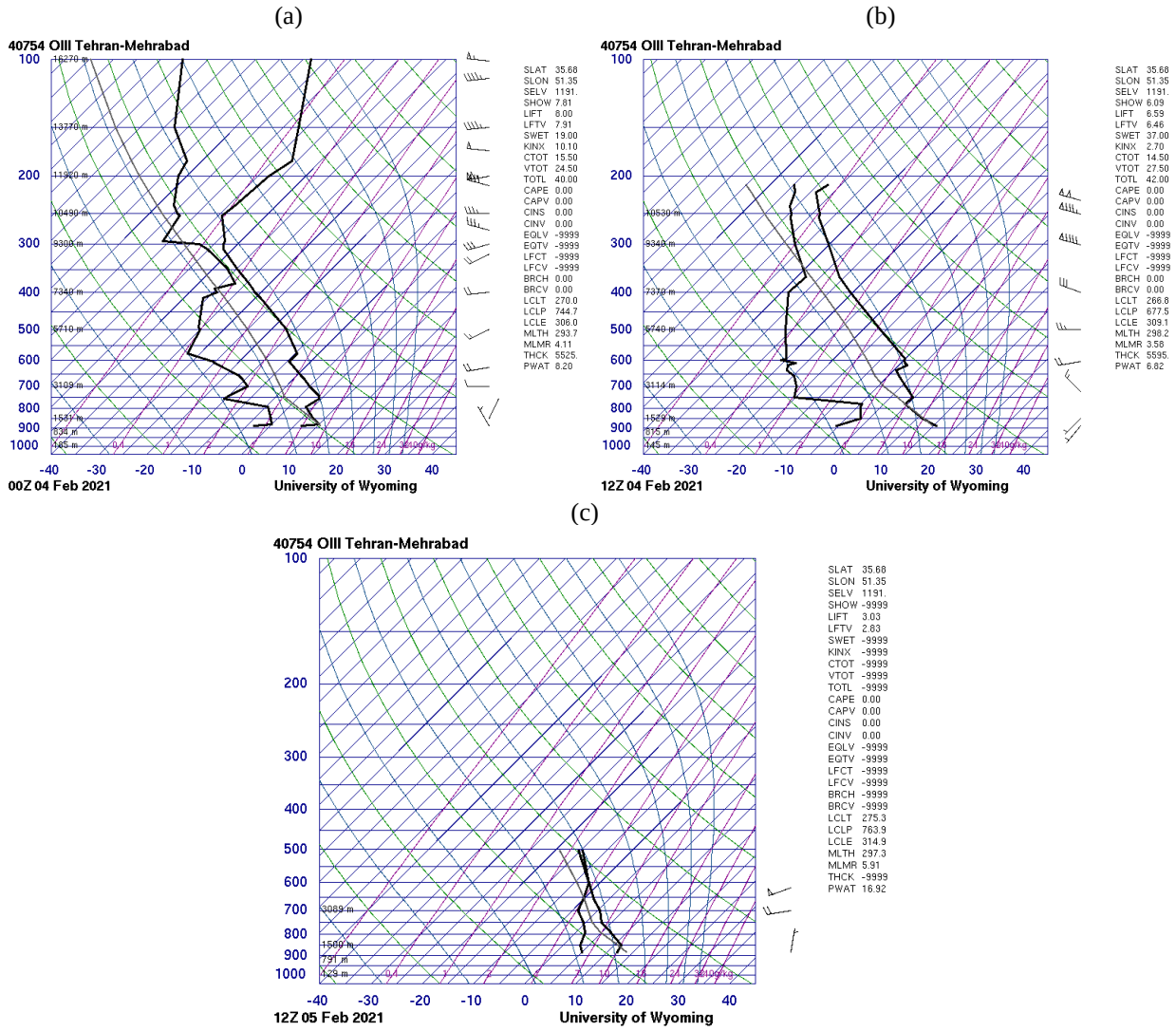

Figure 3-13. Skew-T diagram of Tehran Station over (windward) at (a) 00:00 UTC February 4, (b) 12:00 UTC February 4 and (c) 00:00 UTC February 5 derived form Univeristy of Wyoming.

In summary, the position of a trough at the upper level (500 hPa) and its low pressure at the surface level is a determining factor for foehn events over the south coast of the Caspian Sea. Foehn can be expected that if low pressure is located over the Caspian Sea and high pressure exists south of the Alborz Mountains. The pressure gradient between south and north of Alborz Mountains is an ideal situation for initialization of a foehn event. Also, the occurred foehn event continues as long as this pressure gradient exists. With changing the position of the upper trough and, as a result, changing the position of the low pressure over the Caspian Sea, or even high pressure over the south of Alborz Mountains, the pressure gradient could also be changed (decreased) and then the condition for foehn event be weakened.

Chapter 4

Simulation

4.1 Introduction

In this section results of numerical modeling of one of the studied foehn events in previous chapter are presented. By undertaking high-resolution modeling with the Weather and Research Forecasting (WRF) model, the possibility of foehn prediction was assessed. The WRF model is widely used in numerical studies and operational weather forecast in Iran (Khashjan, 2019; Mofidi et al., 2015). Prediction of sudden changes in meteorological quantities are basis of this chapter.

4.2 WRF Model and Setup2

For the high-resolution simulation of atmospheric processes during foehn events, WRF model version 4.0 was applied. The WRF model is a numerical weather prediction and atmospheric simulation system designed for both research and operational applications (Skamarock et al., 2019).

In this study, the model was set up using three domains centered on northern area of Iran (Figure 4-1). This approach increased the horizontal resolution from 45 km in the parent domain (d01) to 15 km and 5 km in the nested domains d02 and d03. Due to the complex topography at the study site, the high resolution of the innermost domain was necessary to enable a realistic simulation and an analysis of the small-scale processes influencing a foehn event. In the vertical, 30 levels were used with a model top of 50 hPa. The initial and boundary conditions were provided by forecasts of GFS 0.5 degree at three-hourly intervals. Model parameterizations and grid spacing were set based on the expertise from many years of modeling experience (Azadi et al., 2013; Ghader et al., 2015; Rezazadeh et al., 2020) and its setup is summarized in Table 4-1. Full namelists for both WRF Preprocessing System (WPS) and WRF (namelist.wps and namelist.input, respectively) have been written in the appendix (Table a-13 and Table a-14, respectively).

In order to examine foehn event, four studied cases in the previous chapter have been selected. The temporal resolution of the model output is 3-hourly in the parent domain and hourly in the nested domains. In order to produce a realistic simulation, WRF model surface variables were compared qualitatively and statistically with in-situ observations.

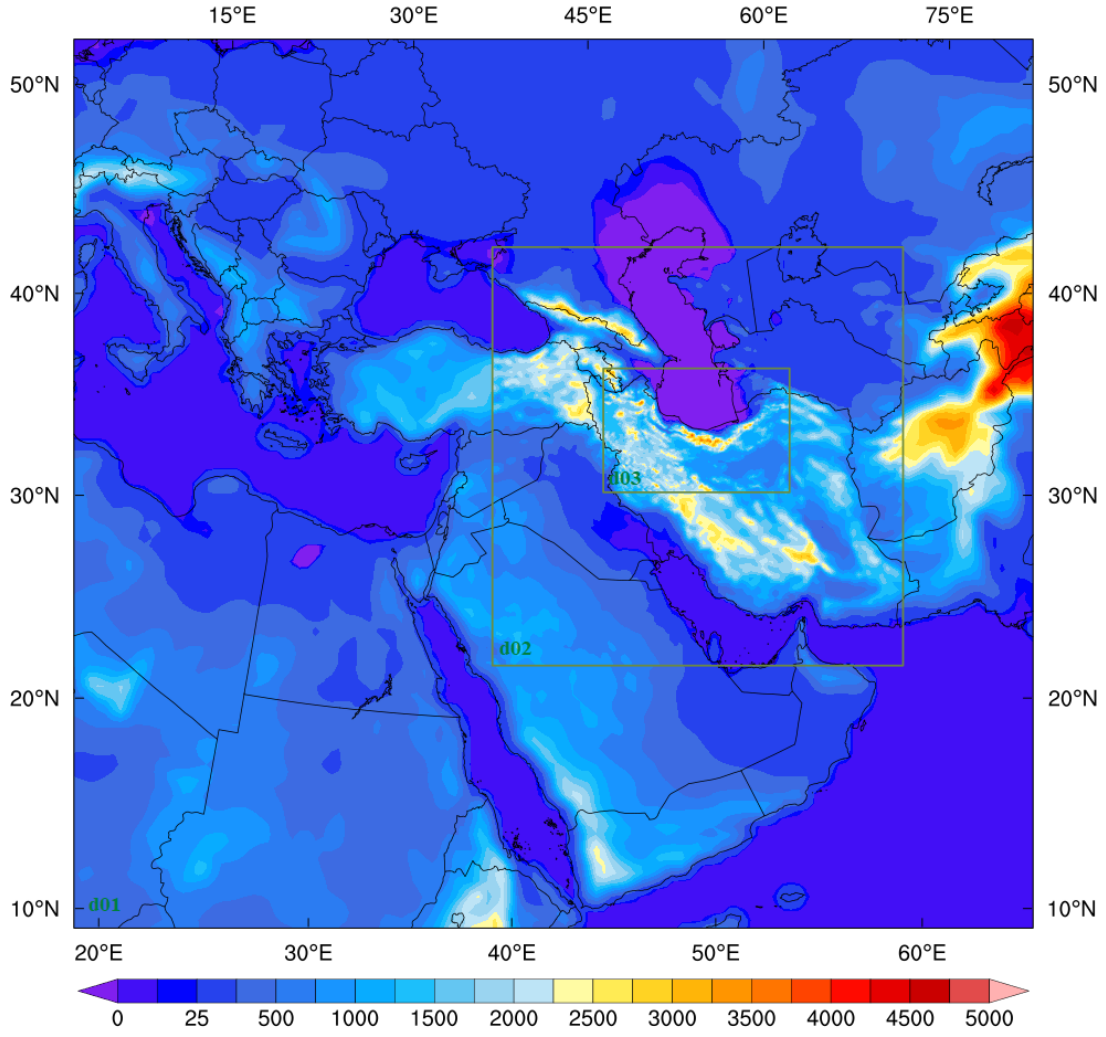

Figure 4-1. WRF model domains considered in this study and topography.

Table 4-1. WRF model setup.

Parameter	Selection
Horizontal resolution	d01: 45 km, d02: 15 km, d03: 5 km
Vertical resolution	30 levels
Land surface physics	unified Noah land surface model
Microphysics	Purdue Lin scheme
Longwave radiation	Rapid Radiative Transfer Model (RRTM) scheme
Shortwave radiation	Dudhia scheme
Surface layer physics	Monin-Obukhov (Janjic Eta) scheme
Planetary boundary layer	Mellor-Yamada Nakanishi and Niino (MYNN) 2.5 level TKE
Convection	Kain-Fritsch (new Eta) scheme

4.3 Model Evaluation

Since the foehn response in the lee is one of the main interests in this study and has been reported to strongly challenge WRF in former foehn studies (Turton et al., 2017; Temme et al., 2020), this section has focused on the lee station Rasht Airport (Figure 4-3) (49.62E, 37.32N, -8.6 m), where measurements are most reliable and include the largest number of variables, that is showed an obvious foehn event. To comparison of grid data with station data, NCL interpolation function was used to interpolate of WRF data to the station point.

In order to give a concise insight into the model skills, three commonly used scalar measures of accuracy consisted of root mean square error (RMSE), mean absolute error (MAE), mean error (ME) have been calculated. Besides, the correlation coefficient *r* were used to investigate the linear correlation between observation and estimation (Table 4-2). In Table 4-2, (y_k, o_k) is the kth of n pairs of quantity estimate by the WRF and observations, $\bar{y}$ and $\bar{x}$ are the average values of WRF and observation quantity. The *r* value varies from -1 to +1, where +1 indicates a perfect skill score and -1 indicates a perfect negative linear correlation.

Surface meteorological variables considered to evaluate are sea level pressure (SLP), temperature at 2 m height (T2m), dewpoint temperature at 2 m height (TD2m), wind speed and direction at 10 m height (WS10m and WD10m, respectively). It should be pointed out, all observation and estimated variables rounded without decimal point; simulated WD10m was rounded to ten factors, same as station reports.

Table 4-2. Statistical scores used in the evlaluation of WRF.

Metric	Calculation	Range	Optimal value
Correlation Coefficient	$r = \frac{\frac{1}{n-1}\sum_{k=1}^{n}[(x_k-\bar{x})(y_k-\bar{y})]}{\left[\frac{1}{n-1}\sum_{k=1}^{n}(x_k-\bar{x})^2\right]^{1/2}\left[\frac{1}{n-1}\sum_{k=1}^{n}(y_k-\bar{y})^2\right]^{1/2}}$	-1 to +1	1
Root Mean Square Error	$RMSE = \sqrt{\frac{1}{n}\sum_{k=1}^{n}(y_k-o_k)^2}$	0 to ∞	0
Mean Absolute Error	$MAE = \frac{1}{n}\sum_{k=1}^{n}\lvert y_k-o_k\rvert$	0 to ∞	0

Mean Error	$ME = \frac{1}{n}\sum_{k=1}^{n}(y_k - o_k)$	-∞ to ∞	0

4.3.1 Simulation of foehn event on 14-15 January 2021

It should be reminded foehn conditions were observed about 05:00-22:00 UTC 14 and 05:00-15:00 UTC 15 January 2021. WRF was run for 72 h, from 12:00 UTC 13 January to 12:00 UTC 16 January 2021; 6 h of this run were considered as spin-up and the evaluation has been done from 18:00 UTC 13 January 2021. Time series of the SLP, T2m, TD2m, WS10m and WD10m have been shown in Figure 4-2 and some statistical scores have been gathered in Table 4-3.

Figure 4-2(a) shows WRF could simulated sea level pressure falling during foehn event. However, it couldn't be adopted with real conditions, soon. WRF have MAE about 2 hPa for SLP in this period. Negative value of ME (~0.3 hPa) could be related to the underestimating of WRF for SLP after terminating of foehn event. It should be noted to good correlation of simulated and observed values of SLP, which *r* is about 0.7 (Table 4-3).

Figure 4-2(b) shows time series of T2m extracted from WRF and its observed values. It seems WRF could capture increasing of T2m. However, it has lag to adopt with conditions after finishing foehn events, as it has overestimation of T2m between 23:00 UTC January 14 and 05:00 UTC January 15, which foehn conditions were removed. This is, also, true after 16:00 UTC January 15, which foehn event had been finished. MAE for T2m in this period is more than 5 ℃ (Table 4-3), which positive value of ME (~ 3 ℃), confirms overestimation of WRF for T2m in this period.

In Figure 4-2(c), time series estimated by WRF and observed values of TD2m has been shown. WRF could simulated decreasing of TD2m with starting of foehn event at 05:00 UTC January 14, but it couldn't match with conditions after removing of foehn conditions, soon. It estimated smaller values of TD2m for some times after finishing foehn events, resulted to negative value of ME with relatively high amount about -4 ℃ (Table 4-3). Also, *r* with value about 0.2 shows weak correlation between estimated and observed TD2m.

WS10m time series extracted from WRF and station reports, has been shown Figure 4-2(d). It seems WRF could estimate high wind speed during foehn event, however, it has overestimation for wind speed, as ME for WS10m is about 4 m/s (Table 4-3). It took times for WRF to match with conditions after finishing of foehn event.

An interesting result could be seen in time series of WD10m, as WRF could simulate southerly

wind during foehn events (from 05:00 UTC January 14 to 22:00 UTC January 14 and from 05:00 UTC January 15 to 15:00 UTC January 15). However, after finishing foehn events, WRF kept southerly wind for a few hours (Figure 4-2(e)).

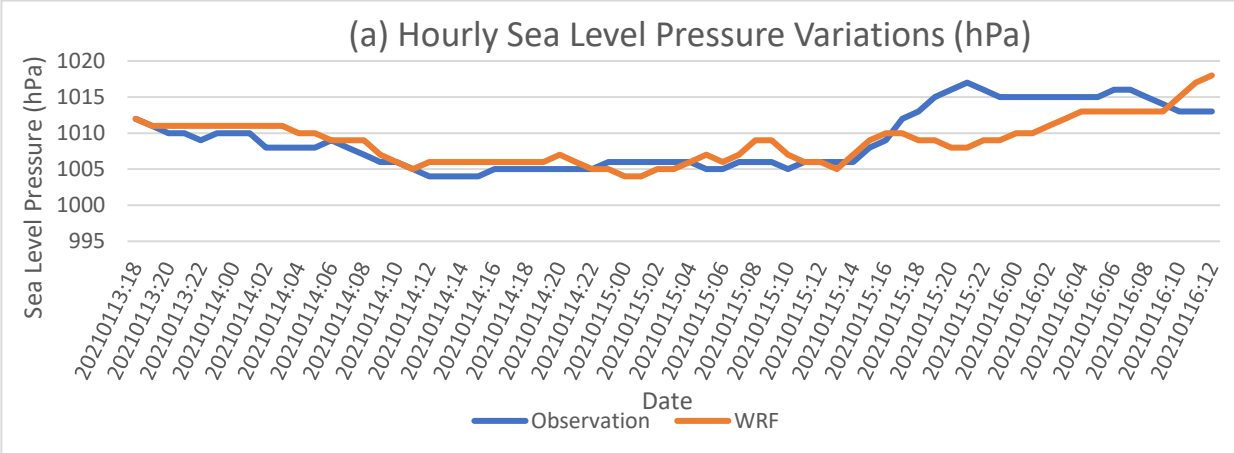

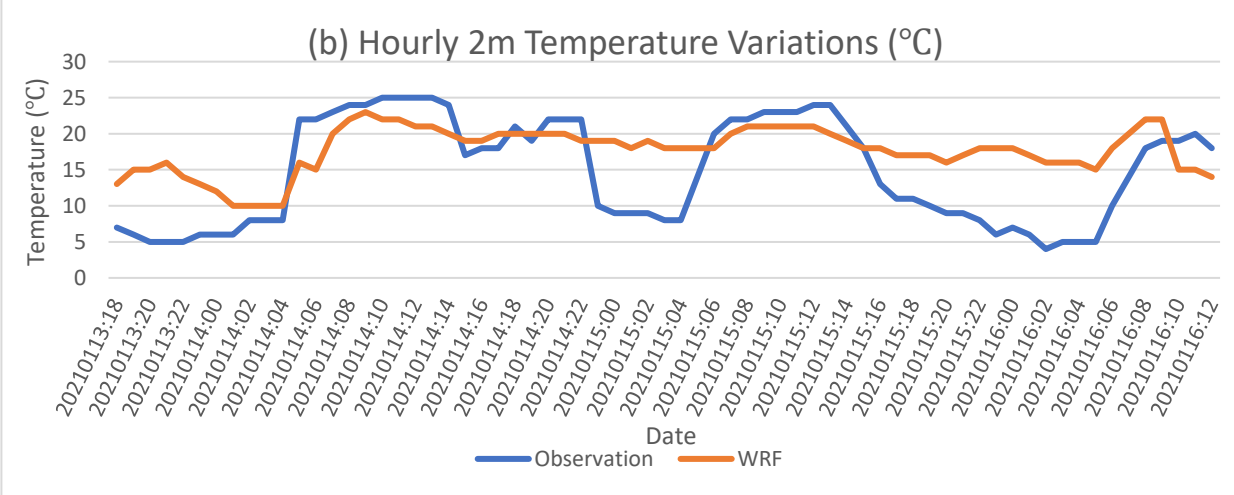

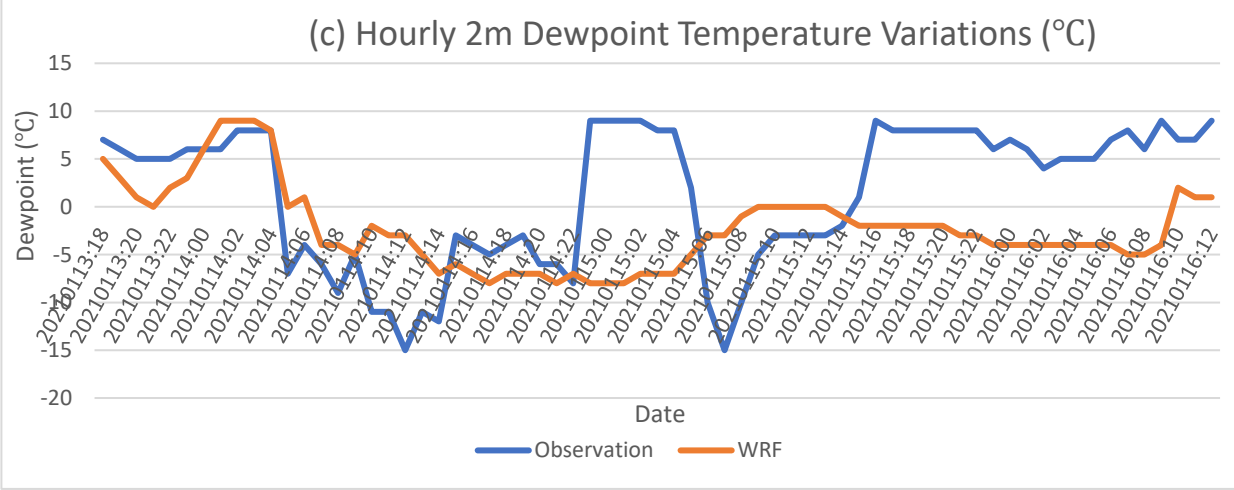

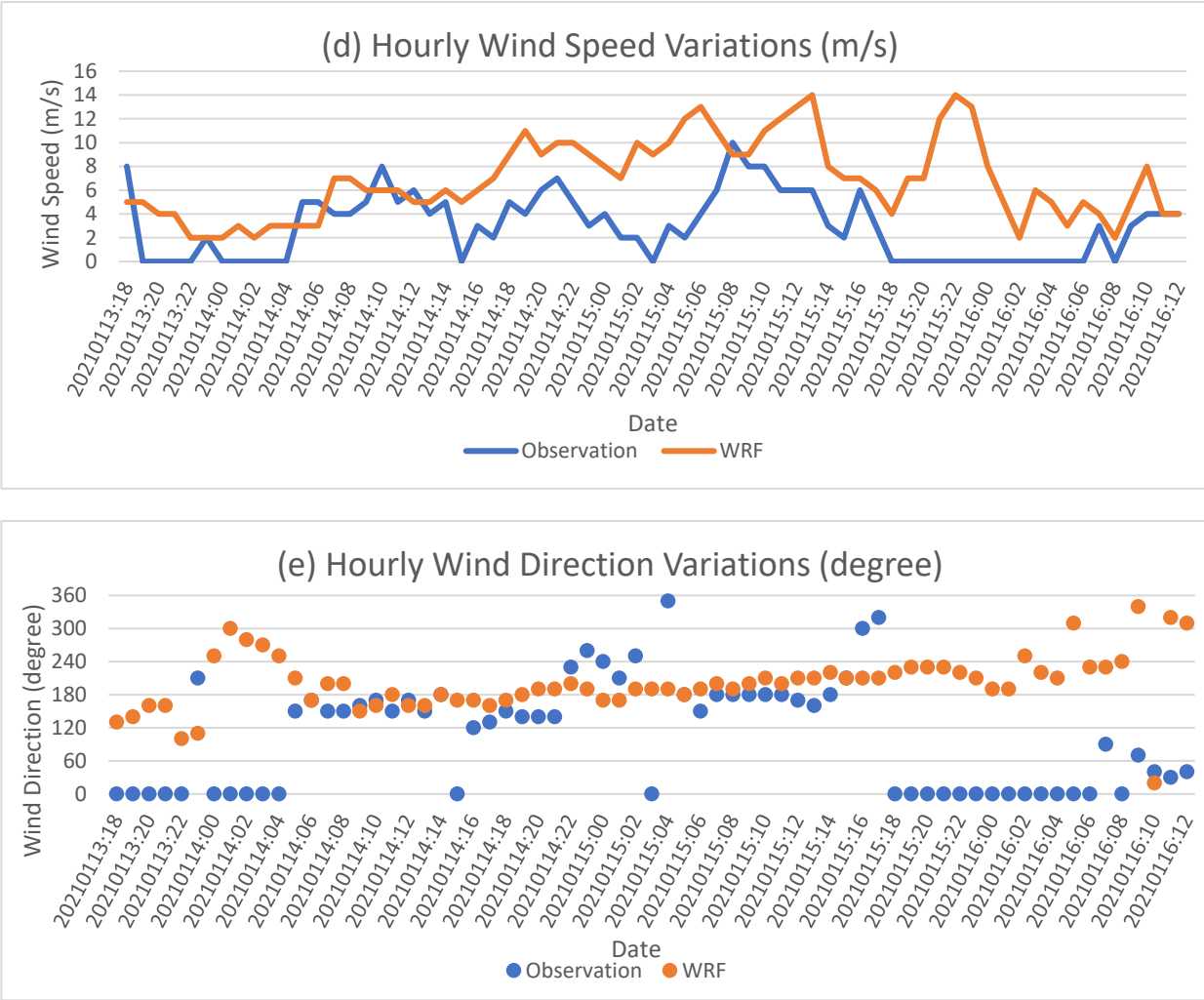

Figure 4-2. Comparison of the modeled (dashed line) meteorological surface variables interpolated over the stations with measurements (solid line) at the OIGG station from 18:00 UTC 13 January to 12:00 UTC 16 January 2021.

Table 4-3. Statistics of the model evaluation (root mean square error: RMSE, mean absolute error: MAE, mean error: ME) at OIGG station for foehn events in 14-15 January. Considered meteorological quantities are included sea level pressure (SLP), 2m temperature (T2m), 2m dewpoint temperature (TD2m), 10m wind speed (WS10m) and wind direction (WD10m).

Statistic / Quantity	RMSE	MAE	ME	r
SLP (hPa)	2.85	2.12	-0.27	0.72
T2m (℃)	6.43	5.40	3.07	0.67
TD2m (℃)	8.34	6.91	-3.60	0.23
WS10m (m/s)	5.24	4.27	3.94	0.36
WD10m (degree)	61.62	47.86	-1.19	

4.3.2 Simulation of foehn event on 18 January 2021

It is worth noting that the foehn condition in this date, was started approximately from 22:00 UTC 17 January and continued to 15:00 UTC 18 January 2021. The duration of simulation is 48 h, 12:00 UTC 17-19 January 2021, in which 6 h are considered as spin-up and the evaluation has been done at 42 h. Figure 4-3(a-e) shows time series of surface meteorological quantities measured in station (solid line) and simulated by WRF (dashed line) from 18:00 UTC January 17 to 12:00 UTC January 19. Besides, the statistical performance of the WRF simulation at this event was summarized in Table 4-4. SLP has been shown in Figure 4-3(a), modeled very well having r = 0.98, RMSE and MAE about 1 hPa. The simulated SLP seems to have smaller values respect to the real ones some hours after finishing of foehn event. In other words, foehn conditions were removed after 15:00 UTC January 18, however, WRF simulated smaller SLP than observation till 21:00 UTC January 18.

Another surface meteorological quantities which were extracted from WRF is T2m, which has been shown in Figure 4-3(b). It seems the WRF increased T2m a little before the starting of foehn event (23:00 UTC January 18) and kept the higher temperature some hours after termination of the event (15:00 UTC January 18). The early onset of foehn simulated by WRF prohibited ~~of~~ capturing the observed sharp increasing of temperature. Also, during foehn event temperature simulated by WRF were smaller than observations. The other considered quantity was dewpoint; decreasing of TD2m before onset of the foehn event and keeping the smaller values respect to the measured TD2m, again shows timing offset of the event (Figure 4-3(c)). The simulated TD2m has little r (0.09) which could be related to the position of the Rasht-Airport station and its proximity to the sea, also, some parameterization of WRF should be checked. On the other hand, it could be related to comparison of a local point vs 5 km grid.

WS10m and WD10m were also extracted from WRF output. WS10m output of WRF shows higher values respect to the observation some hours before of the event (Figure 4-3(d)) and WD10m was southerly (Figure 4-3(e)) in WRF again before foehn was started. Although simulating of surface wind speed is challenging in most of NWP models, the r values of WS in this time series is about 0.7 and error is about 2 m/s, indicating acceptable results.

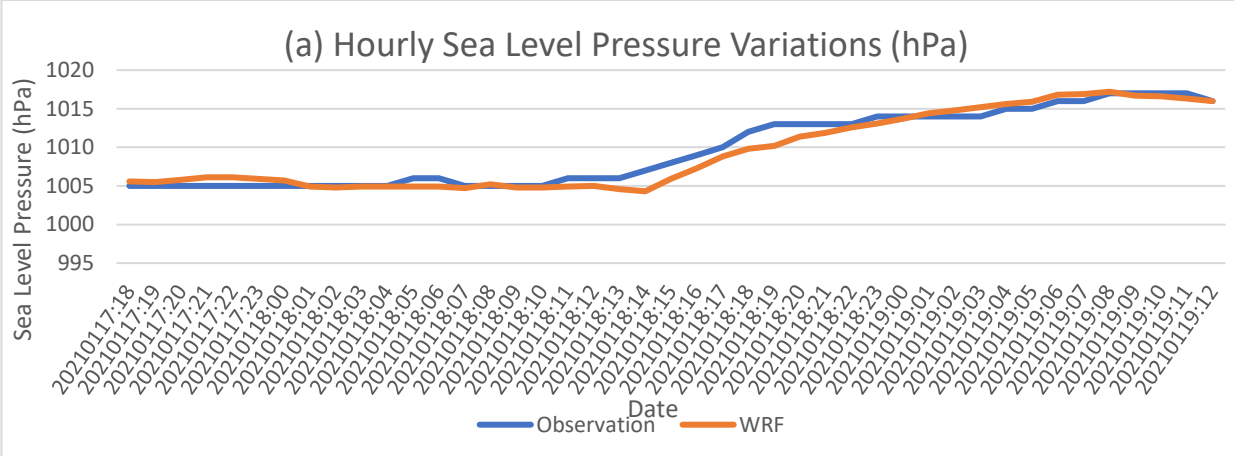
(a) Hourly Sea Level Pressure Variations (hPa)
Sea Level Pressure (hPa)
1020
1015
1010
1005
1000
995
Date
Observation
WRF

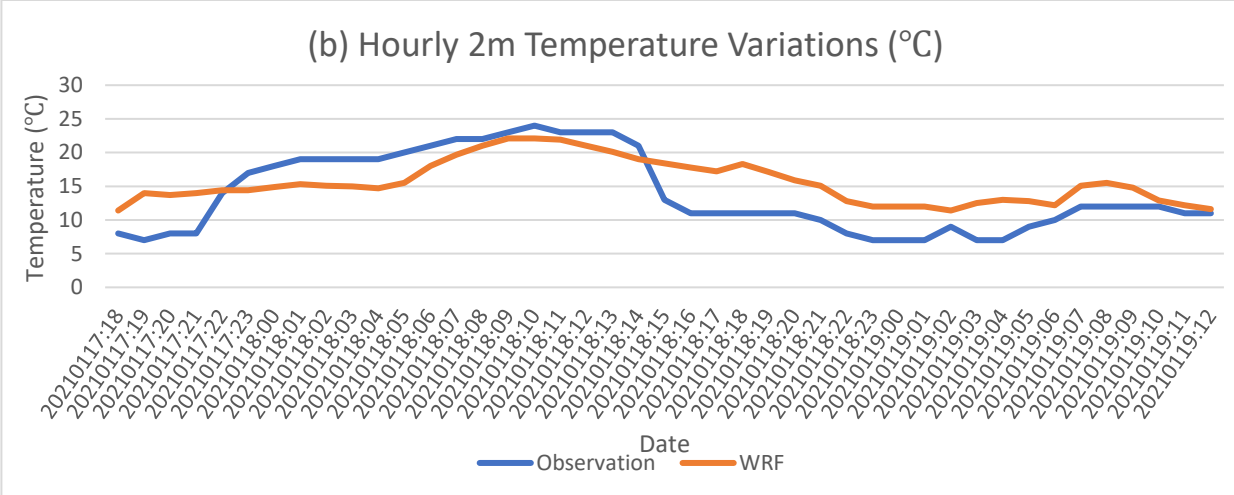
(b) Hourly 2m Temperature Variations (°C)
Temperature (°C)
30
25
20
15
10
5
0
Date
Observation
WRF

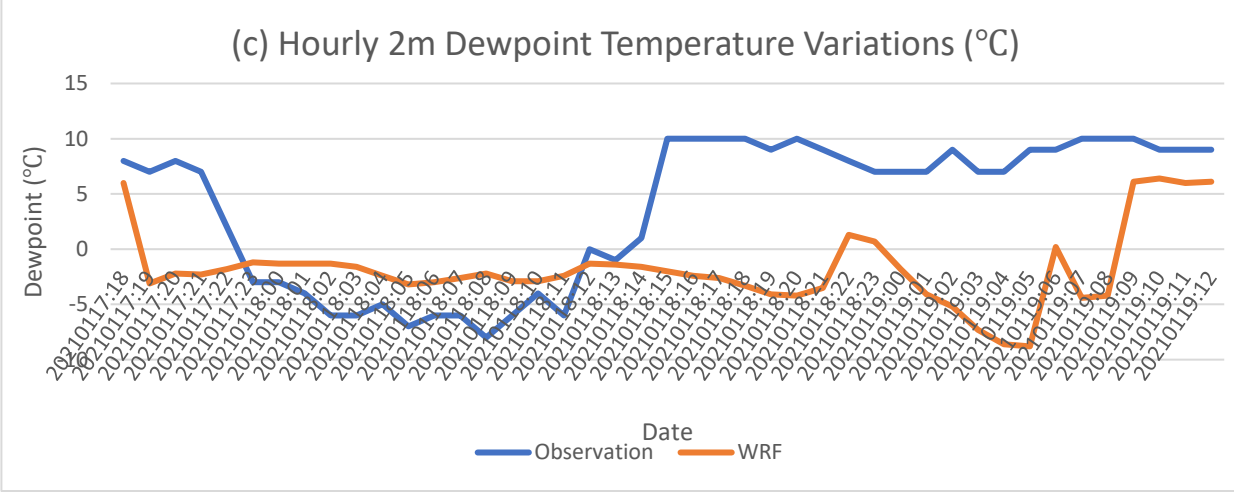
(c) Hourly 2m Dewpoint Temperature Variations (°C)
Dewpoint (°C)
15
10
5
0
-5
Date
Observation
WRF

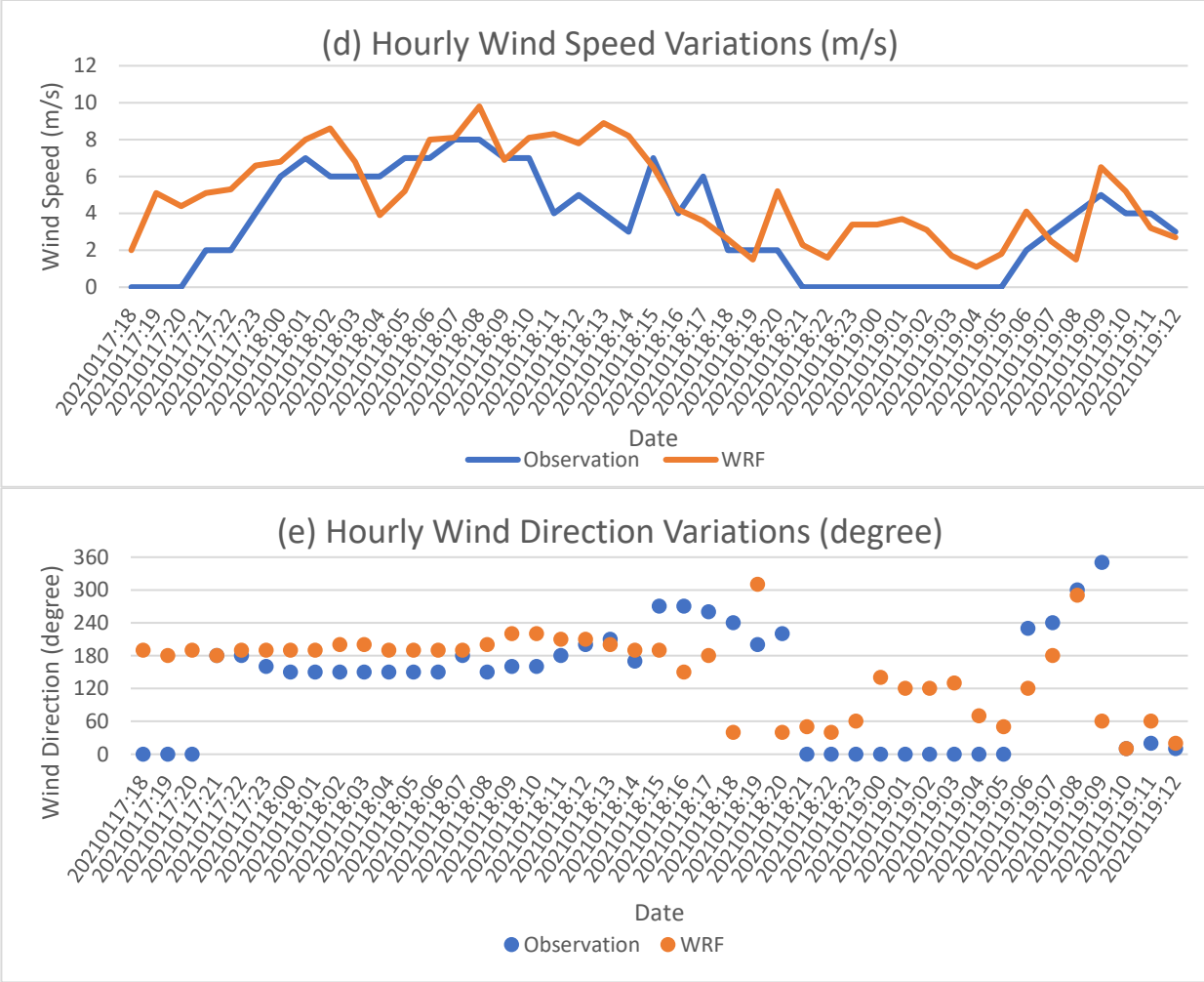

Figure 4-3. Comparison of the modeled (dashed line) meteorological surface variables interpolated over the stations with measurements (solid line) at the OIGG station from 18:00 UTC 17 January to 12:00 UTC 19 January 2021.

Table 4-4. Same as Table 4-3 but for foehn event in January 18.

Statistic / Quantity	RMSE	MAE	ME	r
SLP (hPa)	1.09	0.86	-0.32	0.98
T2m (℃)	4.16	3.70	1.70	0.78
TD2m (℃)	8.91	7.35	-5.41	0.09
WS (m/s)	2.51	2.08	1.54	0.71
WD (degree)	68.41	52.27	10.34	

4.3.3 Simulation of foehn event on 28-29 January 2021

In this subsection, the results of foehn event occurred from 18:00 UTC 28 January to 05:00 UTC

29 January 2021 have been presented. WRF was run for 48 h, 12:00 UTC 27-29 January 2021. Considering 6 h as spin-up, the evaluation has been done from 18:00 UTC 27 January. It seems WRF could simulated the trend of SLP variations well, with a few hours delay (Figure 4-4(a)). The sharp T2m increasing in the station occurred in 17:00-18:00 UTC January 28, with about 8 ℃ increasing; WRF increased temperature about 5 ℃ in 19:00-20:00 UTC January 28 (Figure 4-4(b)). Almost same behavior could be seen for TD2m; in station reports TD2m was decreased about 8 ℃ in 17:00-18:00 UTC January 28, however, WRF simulated the falling of humidity in 19:00-20:00 UTC January 28. On the other hand, the high underestimation of WRF for TD2m should be mentioned in 04:00-14:00 UTC January 28 (Figure 4-4(c)).

WS10m in station was increased in 17:00-19:00 UTC January 28 from 2 to 7 m/s. WRF increased WS10m in 22:00-24:00 UTC January 28 from 3 to 7 m/s (Figure 4-4(d)). Also, southerly wind, related to foehn event, reported from 18:00 UTC January 28 and continued to about 24:00 UTC January 28 (00:00 UTC January 29); WRF simulated southerly wind from about 22:00 UTC January 28 (Figure 4-4(e)). The statistical performance of the WRF was summarized in Table 4-5 in order to give a concise insight into the model skills. The high correlation in SLP quantity (~0.85) and relatively low correlation in TD2m (~0.24) could be seen in this table.

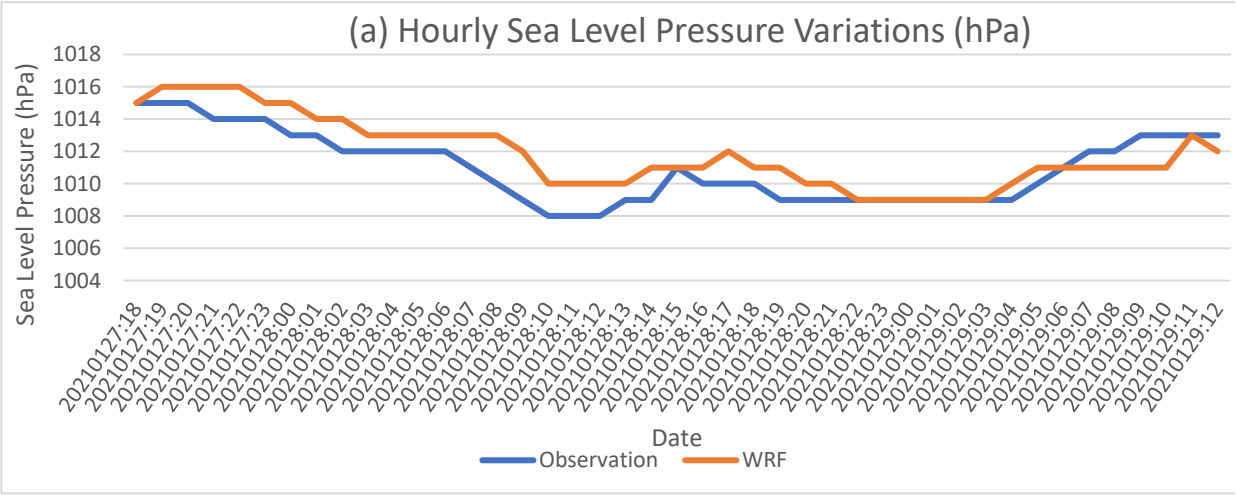

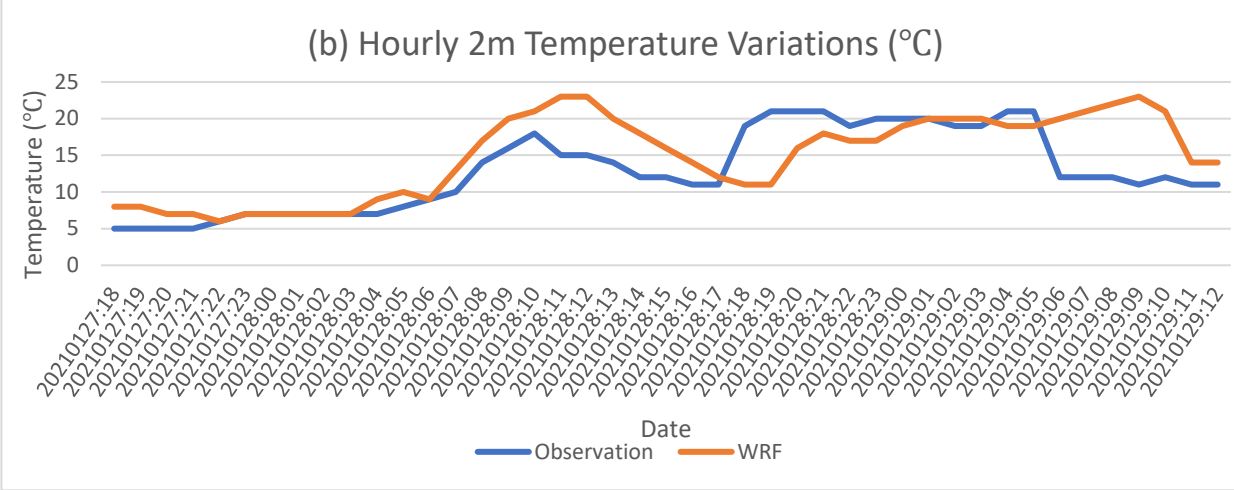
(b) Hourly 2m Temperature Variations (°C)
Temperature (°C)
25
20
15
10
5
0
Date
Observation
WRF

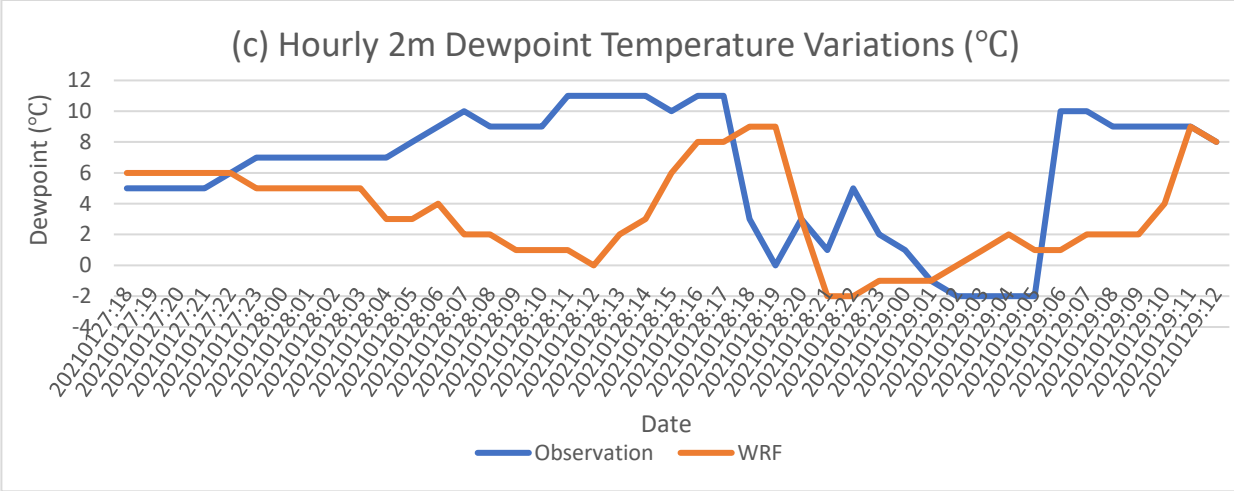
(c) Hourly 2m Dewpoint Temperature Variations (°C)
Dewpoint (°C)
12
10
8
6
4
2
0
-2
-4
Date
Observation
WRF

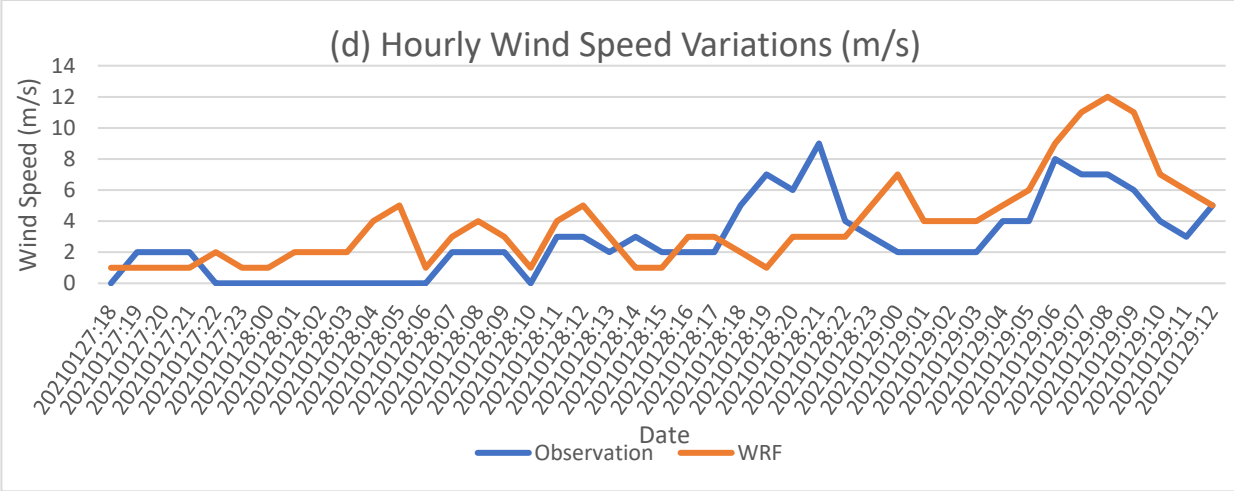
(d) Hourly Wind Speed Variations (m/s)
Wind Speed (m/s)
14
12
10
8
6
4
2
0
Date
Observation
WRF

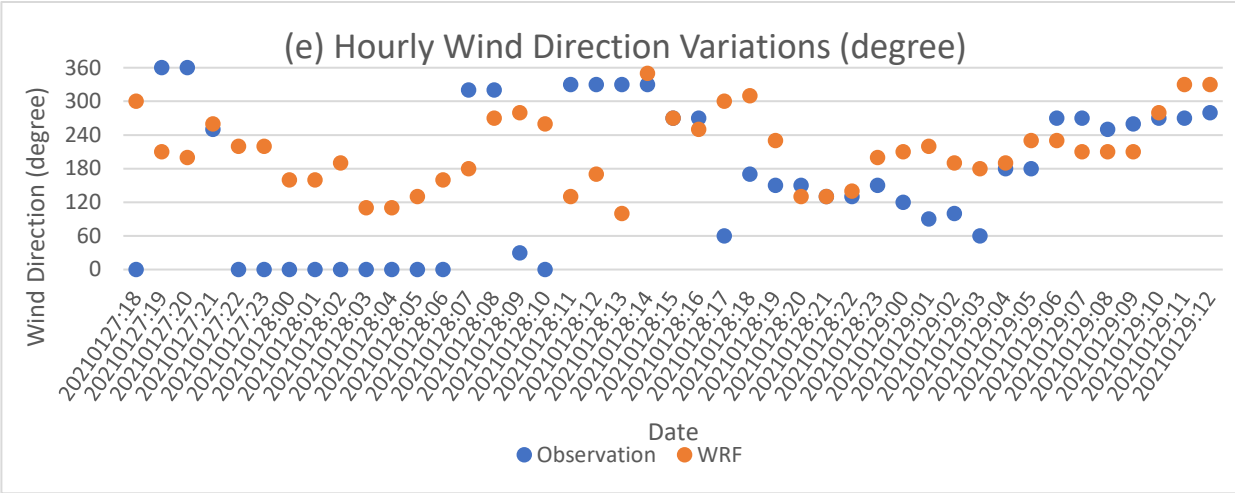

Figure 4-4. Comparison of the modeled (dashed line) meteorological surface variables interpolated over the stations with measurements (solid line) at the OIGG station from 18:00 UTC 27 January to 12:00 UTC 29 January 2021.

Table 4-5. Same as Table 4-3 but for foehn event in January 28.

Quantity \ Statistic	RMSE	MAE	ME	r
SLP (hPa)	1.43	1.16	0.84	0.85
T2m (℃)	4.85	3.60	1.93	0.67
TD2m (℃)	5.34	4.30	-2.86	0.24
WS (m/s)	2.67	2.19	1.02	0.57
WD (degree)	90.19	72.81	2.81	

4.3.4 Simulation of foehn event on 5 February 2021

For the last simulation, foehn event occurred in 07:00-18:00 UTC 5 February 2021 was selected. WRF was run from 12:00 UTC 4 February to 12:00 UTC 5 February 2021; 6 h was considered as spin-up. It seems WRF could simulate SLP and Td2m well (Figure 4-5(a-b)); *r* for SLP is around 0.9 and for T2 is more than 0.8 (Table 4-6). However, in simulation TD2m WRF was not very successful, as it could be some inverse trend between observed and simulated values (Figure 4-5(c)) and *r* is only about 0.15. The simulation of WS10m is acceptable; *r* is about 0.59 and MAE is about 2 m/s (Table 4-6). It seems WRF could approximately capture southerly wind during foehn event (Table 4-6).

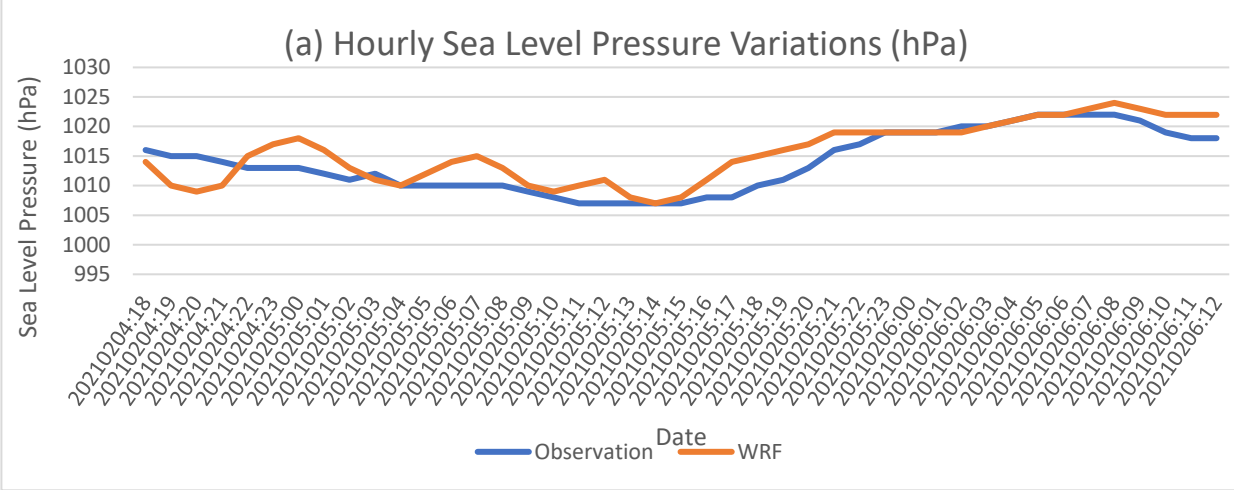
(a) Hourly Sea Level Pressure Variations (hPa)
Sea Level Pressure (hPa)
1030
1025
1020
1015
1010
1005
1000
995
Date
Observation
WRF

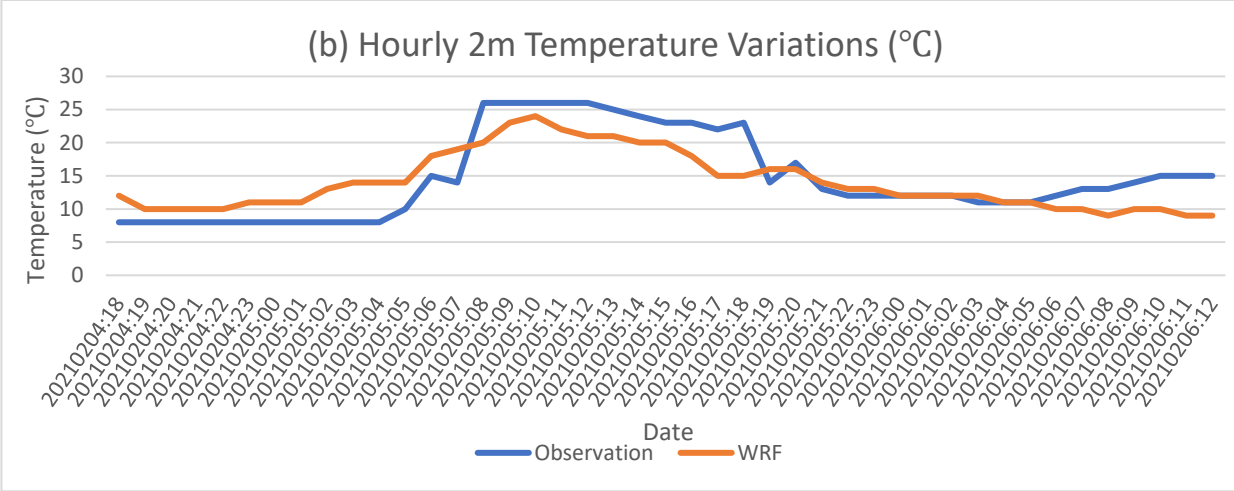
(b) Hourly 2m Temperature Variations (°C)
Temperature (°C)
30
25
20
15
10
5
0
Date
Observation
WRF

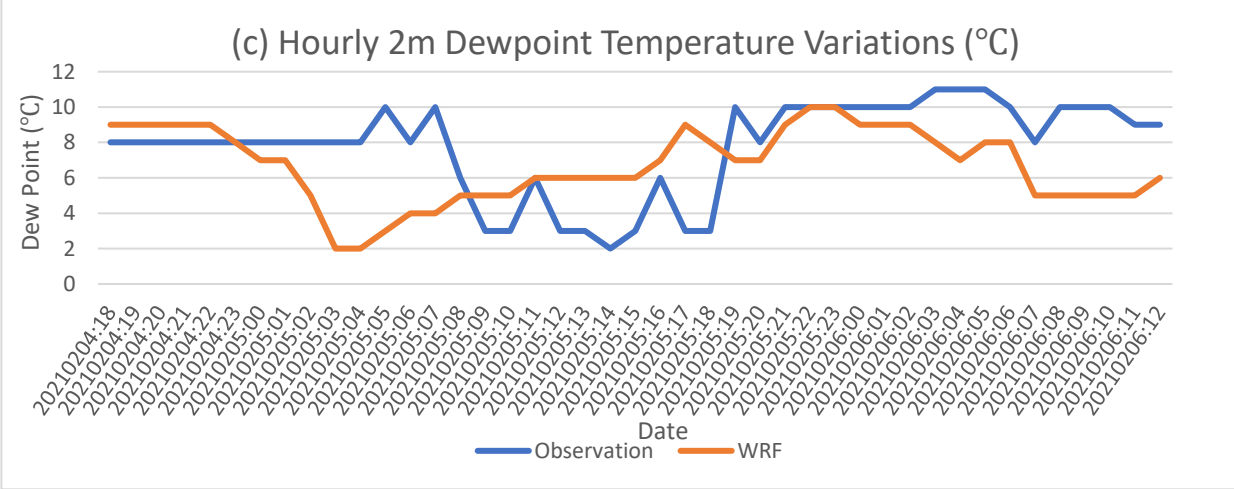
(c) Hourly 2m Dewpoint Temperature Variations (°C)
Dew Point (°C)
12
10
8
6
4
2
0
Date
Observation
WRF

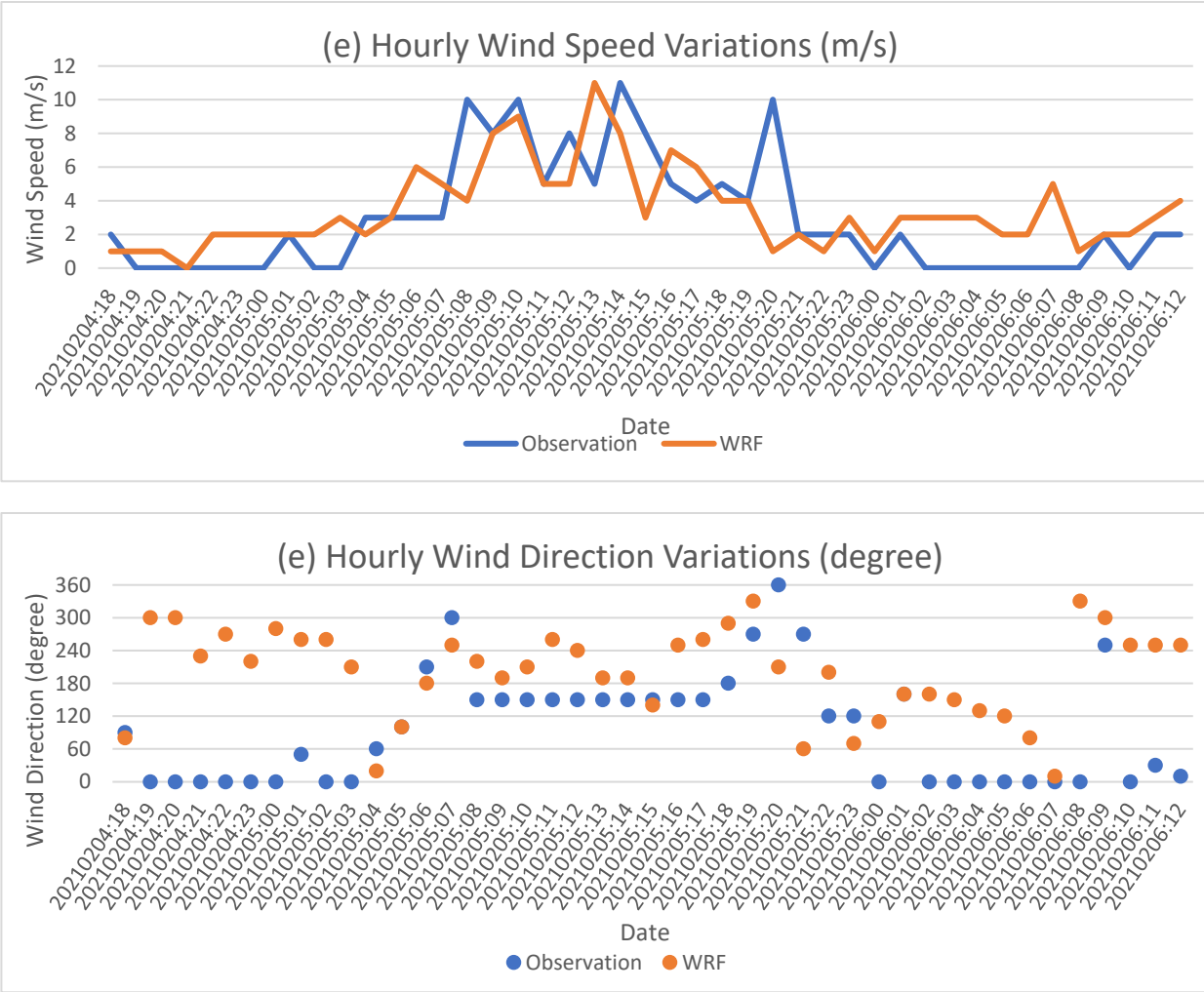

Figure 4-5. Comparison of the modeled (dashed line) meteorological surface variables interpolated over the stations with measurements (solid line) at the OIGG station from 18:00 UTC 4 February to 12:00 UTC 6 February 2021.

Table 4-6. Same as Table 4-3 but for foehn event in February 5.

Statistic / Quantity	RMSE	MAE	ME	r
SLP (hPa)	3.07	2.44	1.56	0.86
T2m (℃)	3.82	3.21	-0.60	0.81
TD2m (℃)	3.28	2.65	-1.07	0.15
WS (m/s)	2.74	2.00	0.56	0.59
WD (degree)	85.35	71.54	13.85	

Chapter 5

Conclusion

5.1 Introduction

“The two most well-known mechanisms responsible for heating and drying the foehn air are thermodynamic warming and isentropic drawdown”, as Elvidge et al. (2016) described in more detail. The former describes an air parcel orographically lifted over a mountain barrier and cooling at the saturated adiabatic lapse rate, which causes the formation of clouds and precipitation on the windward side of the mountains. After the obstacle is passed, the air descends and warms dry adiabatically, leading to drier and warmer air masses in the lee compared with upstream of the range. The second mechanism suggests that, with stable stratification, the mountain blocks the low-level flow. Hence, potentially warmer air is isentropically advected from upwind and subsides down the lee slope, warming at the dry adiabatic lapse rate.

This study focuses on a region in Iran between 34.5-38.5° N and 48-52° E, including areas north and south of the Western Alborz Mountains. We used observational data from IRIMO meteorological stations along a south-north transect across the Alborz chain in the northern part of Iran.

5.2 Summary

On the synoptic scale, the foehn events that we studied here occurred due to the presence of high pressure over the interior regions of Iran and lee cyclones over the southern Caspian Sea, with a strong south-north pressure gradient across the Alborz Mountains. A trough, approaching from the west and crossing the Caspian Sea could change the meteorological conditions north and south of the Alborz Mountains, causing a foehn event over the northern coasts of Iran.

In an interesting case, pressure variations with a trough approaching the study area and its position relative to the Caspian Sea created, reduced and again created foehn conditions north of Alborz Mountains.

The wind rose plots confirm southerly/southeasterly and sometimes southwesterly wind during foehn conditions over the Rasht-Airport station located leeward of the Alborz Mountain.

When foehn occurred north of the Alborz Mountains, a pressure gradient could be concluded between the leeward and windward sides, causing appropriate conditions for the wind to cross the mountain. In this situation, the cloudiness of windward stations could be expected. However, rainfall did not necessarily occur windward, although in some cases, it happened.

In foehn conditions, the wind below 500 hPa, which is approximately ridge height, mostly crossed the mountain with higher speed than at times without upstream conditions for foehn development.

It should be mentioned that the altitude difference between the south (windward) and north (leeward) sides of the Alborz Mountains is considerable for the studied area. That may increase the chance of a foehn event on the leeward side since descending air parcels on the leeward increased temperature as they descend at the dry adiabatic rate. It is worth noting that maximum temperature in Iran usually occurred before 15:00 UTC and so is reported at this time. However, foehn could cause temperature increase after that time, also at night or morning times.

The statistical performance of WRF simiulation of foehn situations was summarized by root mean square error (RMSE), mean absolute error (MAE), mean error (ME) and Pearson correlation coefficient (r). Overall, the atmospheric fields were realistically simulated by the WRF model. The main issues were: (i) the WRF model simulated the foehn onset early, which was similarly found in Turton (2017) and Temme, (2020), and (ii) 2m dew point temperature was not simulated well, suggesting consideration of changing the WRF model selected. This could also be related to the effect of being close to the sea, (iii) adaptation of WRF with conditions after foehn event takes time.

Bibliography

Albergel, C., E. Dutra, S. Munier, J.C Calvet, J. Munoz-Sabater, P. de Rosnay, G. Balsamo, 2018: ERA-5 and ERA-Interim driven ISBA land surface model simulations: Which one performs better? *Hydrol. Earth Syst. Sci.,* **22,** 3515–3532.

Armi, L., G.J. Mayr, 2007: Continuously stratified flows across an Alpine crest with a pass: Shallow and deep föhn. *Q. J. R. Meteorol. Soc.* **133,** 459–477.

Azadi, M., E. Taghizadeh, M.H. Memarian, and L.R. Dmitrieva-Arrago, 2013: Comparing the results of precipitation forecast based on mesoscale models on the territory of Iran during the cold season. *Russ. Meteorol. Hydrol.,* **38(9),** 605-613.

Barry, R.G., 1992: *Mountain Weather and Climate*. 2nd ed. Routledge, 402 pp.

Barry, R.G., 2008: *Mountain Weather and Climate.* 3 rd edition, Cambridge University Press. 506 pp.

Baumann, K., H. Maurer, G. Rau, M. Piringer, U. Pechinger, A. Pr´evˆot, M. Furger, B. Neininger, and U. Pellegrini, 2001: The influence of south Foehn on the ozone distribution in the Alpine Rhine valley – results from the MAP field phase. *Atmos. Environ.,* **35,** 6379–6390.

Beer, T., 1974: *Atmospheric Waves*. John Wiley and Sons, 300 pp.

Brinkmann, W.A.R., 1970: *The Chinook at Calgary*. *Theor. Appl. Climatol.*, 18, 269-278.

Brinkmann, W.A.R., 1971; *What is a Foehn*? *Weather*, 26, 230-239.

Brinkmann, W.A.R.,1973: A climatological study of strong downslope winds in the Boulder area. NCAR Cooperative Thesis 27/INSTARR Occasional Paper 7, University of Colorado, 229 pp.

Brinkmann, W.A.R., 1974: Strong downslope winds at Boulder, Colorado. *Mon. Wea. Rev.,* **102,** 592–602.

Burri K., P. Hächler, M. Schüepp, and R. Werner, 1999: *Der Föhnfall vom April 1993.* Arbeitsbericht 196, MeteoSchweiz, 193 pp.

Cape, M.R., M. Vernet, P. Skvarca, S. Marinsek, T. Scambos, E. Domack, 2015: Foehn winds link climate-driven warming to ice shelf evolution in Antarctica. *J. Geophys. Res. Atmos.,* **120,** 11037–11057.

Carrega, P., 1991: A meteorological index for forest fire hazard in Mediterranean France. *Int. J. Wildland Fire,* **1,** 79–86.

Cook, A. W., and A. G. Topil, 1952: Some examples of chinooks east of the mountains in Colorado. *Bull. Amer. Meteor. Soc.,* **33,** 42–47.

Cooke, L.J., M.S. Rose, and W.J. Becker, 2000: Chinook winds and migraine headache. *Neurology,* **54,** 302

Conedera,M., P.Marxer, C. Hoffmann,W. Tinner, and B. Amman, 1996: Forest fire research in Switzerland. Part 1: Fire ecology and history research in the Southern part of Switzerland. *Int. For. Fire News,* **15,** 13–21.

Conedera,M., P.Marxer, P. Ambrosetti, G. Della Bruna, and F. Spinedi, 1998: The 1997 forest fire season in Switzerland. *Int. For. Fire News,* **18,** 85–88.

Drechsel, S., and G. J. Mayr, 2008: Objective forecasting of foehn winds for a subgrid-scale alpine valley. *Wea. Forecasting,* **23,** 205–218.

Drobinski, P., and Coauthors, 2007: Foehn in the Rhine Valley during MAO: A review of its multiscale dynamics in complex valley geometry. *Quart. J. Roy. Meteor. Soc.,* **133,** 897-916.

Elvidge, A.D. and I.A. Renfrew, 2016: The causes of Foehn Warning in the lee of Mountains. *Bull. Am. Meteorol. Soc.*, **97(3),** pp. 455-466.

Field, T.S. and M.D. Hill, 2002:Weather, Chinook, and Stroke Occurrence. *Stroke,* **33,** 1751–1758.

Franssila, M., 1959: *Kulovaaran ja säätekijöiden välisestä riippuvuudesta* (in Finnish, summary in English, "*The dependence of forest fire danger on meteorological factors*"). Acta Forestalia Fennica 67.

Frey, K., 1957: Zur diagnose des Foehns. Meteor. Rundsch., 10(6), 181-185.

Gaffin, D.M., 2007. Foehn winds that produced large temperature differences near the southern Appalachian Mountains. Weather Forecast, 22(1), pp. 145-159.

Garreaud, R. 2009: The Andes climate and weather. *Adv. Geosci.,* **7,** 1–9.

Ghader, S., D. Yazegi, M. Soltanpour, and M.H. Nemati, 2015: Using an Ensemble Prediction System Developed for the WRF Model to Predict Surface Wind Over Persian Gulf. *Hydrophysics,* **1(1),** 41-54.

Golvani, F., H. Lashkari, 2011: The analysis and prediction of the Foehn wind on the forest fires in Gilan province. SEPEHR, 20(79), pp. 31-36, (Persian).

Gorski, C.J. and A. Farnsworth, 2000: Fire weather and smoke management. Mountain meteorology fundamentals and applications. Oxford University Press, New York.

Gohm, A., G.J. Mayr, 2004: Hydraulic aspects of föhn winds in an Alpine valley. *Q. J. R. Meteorol. Soc.,* **130,** 449–480.

Gohm, A., G. Zangl, G.J. Mayr, 2004: South Foehn in the Wipp Valley on October 24, 1999 (MAP IOP 10): Verification of high-resolution numerical simulations with observations. Mon. Wea. Rev., **132,** 78-102.

Gohm, A., G.J. Mayr, A. Fix, A. Giez, 2008: On the onset of bora and the formation of rotors and jumps near a mountain gap. *Q. J. R. Meteorol. Soc.,* **134,** 21–46.

Gosai, A., and J. Salinger, 2003: Seasonal fire weather outlook March – May 2003. NIWA Client Rep. AKL2003-028, National Institute of Water and Atmospheric Research, Auckland, New Zealand, 17 pp.

Gosai, A., and J. Salinger, 2004: Seasonal fire weather outlook March – May 2004. NIWA Client Rep. AKL2004-20, National Institute of Water and Atmospheric Research, Auckland, New Zealand, 18 pp.

Gosai, A., and J. Salinger, 2005: Seasonal fire weather outlook March – May 2005. NIWA Client Rep. AKL2005-018, National Institute of Water and Atmospheric Research, Auckland, New Zealand, 19 pp.

Hann, J., 1866: Zur Frage über den Ursprung des Föhn. *Z. Österr. Ges. Meteor.,* **1,** 257–263.

Hann, J., 1867: Der Föhn in den österreichischen Alpen. *Z. Österr. Ges. Meteor.,* **2,** 433–445.

Hann, J., 1901: *Lehrbuch der Meteorologie*. Tauchnitz, Leipzig, 805 pp.

Hersbach, H., B. Bell, P. Berrisford, G. Biavati, A. Horányi, J. Muñoz Sabater, J. Nicolas, C. Peubey, R. Radu, I. Rozum, D. Schepers, A. Simmons, C. Soci, D. Dee, J-N. Thépaut, 2018a: ERA5 hourly data on single levels from 1959 to present. *Copernicus Climate Change Service (C3S) Climate Data Store (CDS).* (Accessed on 18-Nov-2021), DOI: 10.24381/cds.adbb2d47.

Hersbach, H., B. Bell, P. Berrisford, G. Biavati, A. Horányi, J. Muñoz Sabater, J. Nicolas, C. Peubey, R. Radu, I. Rozum, D. Schepers, A. Simmons, C. Soci, D. Dee, J-N. Thépaut, 2018b: ERA5 hourly data on pressure levels from 1959 to present. *Copernicus Climate Change Service (C3S) Climate Data Store (CDS).* (Accessed on 18-Nov-2021), DOI: 10.24381/cds.bd0915c6.

Hersbach, H., B. Bell, P. Berrisford, A. Horányi, J.M. Sabater, J. Nicolas, R. Radu, D. Schepers, A. Simmons, C. Soci, et al., 2019: Global reanalysis: Goodbye ERA-Interim, hello ERA5. *ECMWF Newsl.,* **159,** 17–24.

Hersbach, H., B. Bell, P. Berrisford, S. Hirahara, A. Horányi, J. Muñoz-Sabater, J. Nicolas, C. Peubey, R. Radu, D. Schepers, and A. Simmons, 2020: The ERA5 global reanalysis. *Q. J. R.*

Meteorol. Soc., **146(730),** 1999-2049.
Hoinka, K.P., 1985a: Observation of airflow over the Alps during a Foehn event. *Q. J. R. Meteorol. Soc.,* **111,** 199-224.
Hoinka, K.P., 1985b: What is a foehn clearance?. *Bull. Am. Meteorol. Soc.,* **66(9),** pp.1123-1132.
Huschke, R. E., 1959: *Glossary of Meteorology.* Amer. Meteor. Soc., 638 pp.
Jazirehei M.H., 1995: Forest and fires. *J. For Pasture*, **29,** 1–6. [In Persian]
Keeley, J. E., 2004: Impact of antecedent climate on fire regimes in coastal California. *Int. J. Wildland Fire*, **13 (2),** 173–182.
Khashjan, S.H., 2019: *The influence of Meteorological Factors and Foehn wind on Zagros Forests Fire.* M.S. Thesis, University of Tehran, Institute of Geophysics, Tehran. [In Persian]
Kondo, J., and T. Kuwagata, 1992: Enhancement of forest fires over northeastern Japan due to atypical strong dry wind. *J. Appl. Meteor.,* **31,** 386–396.
Lim, J.-H., 2002: Fire situation in Republic of Korea. *Int. For. Fire News,* **26,** 61–65.
Lin, Y.-1., 2007: Mesoscale Dynamics. Cambridge University Press, 630 pp.
Lockwood, J. G., 1962: Occurrence of föhn winds in the British Isles. *Meteor. Mag.,* **91,** 57–65.
Marsh, L., 1987: Fire weather forecasting in Tasmania. Meteorological Note 171, Bureau of Meteorology, 47 pp.
Mayr, G.J., D. Plavcan, L. Armi, A. Elvidge, B. Grisogono, K. Horvath, P. Jackson, A. Neururer, P. Seibert, J.W. Steenburgh, and I. Stiperski, 2018: The community Foehn Classification Experiment. *Bull. Am. Meteorol. Soc.,* **99(11),** pp. 2229-2235.
McGowan, H.A., A.P. Sturman, 1996: Regional and local scale characteristics of Foehn wind events over the South Island of New Zealand. Meteor. Atmos. Ohus., 58, 151-164.
McGowan, H.A., A.P. Sturman, M. Kossmann, P. Zawar-Reza, 2002: Observations of foehn onset in the Southern Alps, New Zealand. Meteorol. *Atmos. Phys.,* **79,** 215–230.
Mofidi, A., I. Soltanzadeh, Y. Yousefi, A. Zarrin, M. Soltani, J.M. Samakosh, G. Azizi, and S.T. Miller, 2015: Modeling the exceptional south Foehn event (Garmij) over the Alborz Mountains during the extreme forest fire of December 2005. Natural Hazards, 75(3), pp.2489-2518.
NCAR Command Language (Version, 6.6.2) [Software], (2019). Boulder, Colorado: UCAR/NCAR/CISL/TDD. http://dx.doi.org/10.5065/D6WD3XH5.
Nesterov, V.G., 1949: *Combustibility of the forest and methods for its determination (in Russian)*. USSR State Industry Press.
Ninomiya, K., Y. Yamagishi, H. Ohno, and N. Miura, 1985: Analysis and numerical prediction experiment of extremely strong dry wind occurred over the northeastern Japan on 27 April 1983. *J. Meteor. Soc. Japan,* **63,** 589–604.
Norte, F.A. 2015: Understanding and Forecasting ZondaWind (Andean Foehn) in Argentina: A Review. *Atmospheric and Climate Sciences,* **5,** 163–193.
Olafsson, H., 2005: The heat source of the Foehn. Hrvat. Meteor. Casopis, 40, 542-545
Olauson, J., 2018: ERA5: The new champion of wind power modelling? *Renew. Energy,* **126,** 322–331.
Osmond, H.L., 1941: The Chinook wind east of the Canadian Rokies. Can. J. Res. A, 19(4), 57-66.
Parnian A., 1999: *Foehn formation conditions over the Gilan and Mazandaran provinces.* M.S. Thesis, Islamic Azad University—North Tehran branch, Faculty of Marine Sciences, Department of Physics, Tehran. [In Persian]
Plavcan, D., G.J. Mayr, and A. Zeileis, 2014: Automatic and probabilistic Foehn diagnosis with a statistical mixture model. J. Appl. Meteorol. Clim., 53(3), pp. 652-659.

Rezazadeh, M., F. Moradian, and S. Ghader, 2020: Evaluation of a WRF model multi-physics ensemble forecasting system for simulation of precipitation over central region of Iran. *Iranian Journal of Geophysics,* **14(1),** 13-38.

Richner, H., Hächler, P., 2013: Understanding and Forecasting Alpine Foehn. In Mountain Weather Research and Forecasting: Recent Progress and Current Challenges, Eds. Chow, F.K., de Wekker, S.F.J., and B.J. Snyder, Springer, Netherlands, pp 219-260.

Salinger, J., and A. Porteous, 2002: Seasonal fire weather outlook January - March 2002. NIWA Rep. AK02003, National Institute of Water and Atmospheric Research, Auckland, New Zealand, 17 pp.

Salinger, J., A. Porteous, and J. Renwick, 2000: Seasonal fire weather outlook September – November 2000. NIWA Rep. AK00102, National Institute of Water and Atmospheric Research, Auckland, New Zealand, 13 pp.

Scorer, R.S., 1978: *Environmental Aerodynamics*. Vol. 815. Ellis Horwood, 488 pp.

Seibert, P., 1990: South Foehn studies since the ALPEX experiment. *Meteor. Atoms. Phys.,* **43,** 91-103.

Seibert, P., 2005: Hann's Thermodynamic Foehn Theory and its Presentation in Meteorological Textbooks in the Course of Time. *From Beaufort to Bjerknes and Beyond, Algorismus,* Issue **52,** 169–180; ISBN 978-3936905-13-7.

Sharples, J.J., 2009: An overview of mountain meteorological effects relevant to fire behaviour and bushfire risk. International Journal of Wildland Fire, 18(7), pp.737-754.

Sharples, J.J., G.A. Mills, R.H.D. McRae, R.O. Weber, 2010: Foehn-Like Winds and Elevated Fire Danger Conditions in Southeastern Australia. J. Appl. Meteorol. Clim., 49, 1067-1095.

Shirzadi, H., 1992: *The study of physical and synoptic condition of Foehn events and its destructive effects in Iran.* M.S. Thesis, University of Tehran, Institute of Geophysics, Tehran. [In Persian]

Skamarock, W. C., J.B. Klemp, J. Dudhia, D.O. Gill, Z. Liu, J. Berner, W. Wang, J.G. Powers, M.G. Duda, D.M. Barker, and X.-Y. Huang, 2019: A Description of the Advanced Research WRF Version 4. *NCAR Tech. Note NCAR/TN-556+STR,* 145 pp.

Smith, R.B., 1990: Why can't stably stratified air rise over high ground? Atmospheric Processes over Complex Terrain. Meteor. Monographs, W. Blumen, Ed., *Amer. Meteor. Soc.,* **23,** 105-107.

Speirs, J.C., D.F. Steinho, H.A. McGowan, D.H. Bromwich, A.J. Monaghan, 2010: Foehn Winds in the McMurdo Dry Valleys, Antarctica: The Origin of Extreme Warming Events. *J. Clim.,* **23,** 3577–3598.

Sprenger, M., S. Schemm, R. Oechslim, and J. J enkner, 2017: Nowcasting Foehn wind events using the adaboost machine learning algorithm. *Weather Forecast,* **32(3),** 1079-1099.

Taghavi, F., M. Mard Azad, A.A. Aliakbari Bidokhti, 2015: Investigation of Multiscale and Unsteady Characteristics of Deep Foehn Events Over Alborz Mountains. *AMS 16th Conference on Mesoscale Processes,* Boston.

Taghizadeh, E., F. Ahmadi-Givi, L. Brocca, and E. Sharifi, 2021: Evaluation of satellite/reanalysis precipitation products over Iran. *Int. J. Remote Sens.,* **42(9),** 3474-3497.

Temme, F., J.V. Turton, T. Mölg, and T. Sauter, T., 2020: Flow regimes and föhn types characterize the local climate of Southern Patagonia. *Atmosphere,* **11(9),** p.899.

Turton, J.V., A. Kirchgaessner, A.N. Ross, and J.C. King, 2017: Does high-resolution modelling improve the spatial analysis of föhn flow over the Larsen C Ice Shelf?. *Weather,* **72(7),** 192-196.

Turton, J.V., A. Kirchgaessner, A.N. Ross, J.C. King, 2018: The spatial distribution and temporal

variability of föhn winds over the Larsen C ice shelf, Antarctica. *Q. J. R. Meteorol. Soc.* **144,** 1169–1178.

Ustrnul, Z., 1992: Influence of foehn winds on air temperature and humidity in the Polish Carpathians. *Theor. Appl. Climatol.*, **45 (1),** 43–47.

Vergeiner, I., 1971: Comments on: The Chinook at Calgary (Canada) by Waltraud A.R. Brinkmann. Theor. Appl. Climatol., 19, 339-341.

Whiteman, C. D., 2000: *Mountain Meteorology: Fundamentals and Applications.* Oxford University Press, 355 pp.

WMO, 1992: *International Meteorological Vocabulary.* 2nd ed. World Meteorological Organization, 784 pp.

WRPLOT View Version 8.0.2: Wind Rose Plots for Meteorological Data [Software], 2018. Waterloo, Canada: Lakes Environmental. http://www.weblakes.com/products/wrplot/index.html.

Appendix

A

Table a-1. 3-hourly and some hourly temperature, dewpoint temperature, wind speed and wind direction over Anzali station (Lon 49.46E, Lat 37.48N; leeward) from 00:00 UTC 13 January to 21:00 UTC 16 January 2021. Foehn conditions were shaded gray.

Date	Wind direction (degree)	Wind speed (m/s)	Temperature (°C)	Dewpoint (°C)	Visibility (m)	Pressure (mb)
1/13/2021 00:00	0	0	7.2	7.2	3000	1020
1/13/2021 03:00	0	0	7.0	7.0	7000	1020
1/13/2021 06:00	160	2	7.1	7.1	100	1020
1/13/2021 09:00	160	1	11.0	8.5	4000	1016
1/13/2021 12:00	310	1	11.2	8.8	9999	1014
1/13/2021 15:00	0	0	8.8	7.9	7000	1013
1/13/2021 18:00	280	1	9.3	8.5	7000	1011
1/13/2021 21:00	340	3	9.7	9.4	7000	1009
1/14/2021 00:00	290	2	9.5	9.2	7000	1009
1/14/2021 03:00	250	2	9.4	8.8	7000	1007
1/14/2021 04:00		0	9	9	7000	1007
1/14/2021 05:00	0	0	9	9	7000	1007
1/14/2021 06:00	210	3	19.6	3.7	9999	1007
1/14/2021 09:00	190	4	23.2	-1	9999	1005
1/14/2021 11:00	170	5	24	-2	9999	1002
1/14/2021 12:00	160	5	23.6	-1.4	9999	1002
1/14/2021 15:00	180	4	22.5	-2.3	9999	1003
1/14/2021 18:00	180	4	20.9	-1.6	9999	1004
1/14/2021 19:00	190	2	20	-1	9999	1004
1/14/2021 20:00	180	3	19	-1	9999	1004
1/14/2021 21:00	300	4	11.3	10.5	9999	1005
1/14/2021 22:00	320	6	11	11	3000	1005
1/14/2021 23:00	310	5	11	11	1500	1006
1/15/2021 00:00	310	6	10.5	10.3	100	1006
1/15/2021 03:00	290	3	10.0	9.7	1500	1005
1/15/2021 04:00	260	1	9	9	4000	1005
1/15/2021 05:00	210	2	8	8	8000	1004
1/15/2021 06:00	200	3	10.8	6.5	8000	1004
1/15/2021 07:00	190	5	20	-1	9999	1004
1/15/2021 08:00	200	5	21	-1	9999	1004
1/15/2021 09:00	210	7	23.5	1.8	9999	1004
1/15/2021 12:00	210	4	24.1	2.8	9999	1004

1/15/2021 13:00	190	2	23	5	9999	1005
1/15/2021 14:00	330	2	16	8	9999	1006
1/15/2021 15:00	60	1	14.9	6.7	9999	1008
1/15/2021 16:00	30	6	12	10	9999	1010
1/15/2021 17:00	20	8	12	9	9999	1011
1/15/2021 18:00	40	2	11.9	8.9	9999	1013
1/15/2021 21:00	210	2	10.1	8.2	9999	1015
1/16/2021 00:00	150	1	8.4	7.2	9999	1015
1/16/2021 03:00	150	2	7.4	6.5	7000	1015
1/16/2021 06:00	150	3	11.5	7.4	7000	1015
1/16/2021 09:00	50	1	15.5	9.8	9999	1013
1/16/2021 12:00	330	6	13.0	11.4	9999	1013
1/16/2021 15:00	360	4	11.9	11.3	9999	1015
1/16/2021 18:00	300	2	11.3	10.7	9999	1014
1/16/2021 21:00	310	1	11.2	9.9	8000	1012

Table a-2. 3-hourly and some hourly temperature, dewpoint temperature, wind speed and wind direction over Anzali station (Lon 49.46E, Lat 37.48N; leeward) from 00:00 UTC 17 January to 21:00 UTC 19 January 2021. Foehn conditions were shaded gray.

Date	Wind direction (degree)	Wind speed (m/s)	Temperature (°C)	Dewpoint (°C)	Visibility (m)	Pressure (mb)
1/17/2021 00:00	290	1	10.9	9.3	9999	1011
1/17/2021 03:00	320	2	11	9.1	9999	1010
1/17/2021 06:00	250	1	12.5	9.3	9999	1010
1/17/2021 09:00	360	2	13.9	10.1	9999	1007
1/17/2021 12:00	360	2	13.0	10.2	9999	1006
1/17/2021 15:00	160	2	11.0	9.9	9999	1006
1/17/2021 17:00	170	2	10	9	9999	1005
1/17/2021 18:00	0	0	9.3	8.8	9999	1005
1/17/2021 19:00	150	2	10	9	9999	1004
1/17/2021 20:00	0	0	9	9	9999	1004
1/17/2021 21:00	200	2	10.4	7.3	9999	1004
1/17/2021 22:00	200	2	12	6	9999	1004
1/17/2021 23:00	200	3	15	3	9999	1004
1/18/2021 00:00	180	3	13.6	2.8	9999	1004
1/18/2021 01:00	170	2	15	3	9999	1003

1/18/2021 02:00	200	2	15	3	9999	1003
1/18/2021 03:00	200	2	15.5	2.3	9999	1003
1/18/2021 04:00	170	3	16	1	9999	1003
1/18/2021 05:00	200	4	17	2	9999	1004
1/18/2021 06:00	200	3	17.9	2.2	9999	1005
1/18/2021 09:00	230	4	24.4	1.3	9999	1004
1/18/2021 12:00	240	3	24.0	1.0	9999	1005
1/18/2021 13:00	210	2	23	1	9999	1005
1/18/2021 14:00	250	2	13	11	9999	1006
1/18/2021 15:00	340	5	11.5	10.5	9999	1009
1/18/2021 18:00	360	3	11.4	10.0	9999	1012
1/18/2021 21:00	60	2	10.8	9.5	9999	1013
1/19/2021 00:00	40	3	10.3	9.0	9999	1014
1/19/2021 03:00	170	2	8.8	8.2	9999	1015
1/19/2021 06:00	10	1	12.6	9.4	9999	1016
1/19/2021 09:00	50	4	12.2	9.7	8000	1017
1/19/2021 12:00	90	3	11.3	8.8	8000	1016
1/19/2021 15:00	290	3	9.2	9.0	3000	1016
1/19/2021 18:00	320	3	9.8	9.3	7000	1016
1/19/2021 21:00	350	6	8.4	8.1	4000	1017

Table a-3. 3-hourly and some hourly temperature, dewpoint temperature, wind speed and wind direction over Anzali station (Lon 49.46E, Lat 37.48N; leeward) from 00:00 UTC 27 January to 21:00 UTC 30 January 2021. Foehn conditions were shaded gray.

Date	Wind direction	Wind speed (m/s)	Temperature (°C)	Dewpoint (°C)	Visibility (m)	Pressure (mb)
1/27/2021 00:00	170	1	3.6	3.4	800	1021
1/27/2021 03:00	290	1	4.3	4.3	500	1020
1/27/2021 06:00	210	1	5.2	4.7	1000	1020
1/27/2021 09:00	310	3	10.6	8.0	9999	1018
1/27/2021 12:00	320	2	12	9.2	9999	1017
1/27/2021 15:00	320	1	9.3	8.4	9999	1016
1/27/2021 18:00	0	0	5.9	5.7	6000	1015
1/27/2021 21:00	290	2	8.0	8.0	2000	1014
1/28/2021 00:00	320	1	8.1	7.9	2000	1012
1/28/2021 03:00	200	1	7.8	7.3	6000	1012

1/28/2021 06:00	280	1	9.7	8.4	6000	1011
1/28/2021 09:00	10	2	12.8	10.3	9999	1009
1/28/2021 12:00	340	2	12.0	10.2	9999	1008
1/28/2021 15:00	250	1	11.7	10.6	7000	1011
1/28/2021 16:00	120	2	11	10	6000	1010
1/28/2021 17:00	160	1	11	10	4000	1009
1/28/2021 18:00	200	1	11.2	9.4	7000	1009
1/28/2021 19:00	10	2	12	9	7000	1008
1/28/2021 20:00	190	3	19	6	9999	1008
1/28/2021 21:00	240	1	14.6	6.2	9999	1008
1/28/2021 22:00	190	1	12	8	9999	1008
1/28/2021 23:00	190	1	14	8	9999	1008
1/29/2021 00:00	170	2	14.1	6.4	9999	1008
1/29/2021 03:00	210	3	19.1	3.7	9999	1008
1/29/2021 04:00	200	3	19	3	9999	1008
1/29/2021 05:00	310	6	11	10	9999	1010
1/29/2021 06:00	330	9	10.7	10.1	5000	1012
1/29/2021 09:00	350	4	11.4	9.3	5000	1013
1/29/2021 12:00	340	3	10.6	8.8	6000	1012
1/29/2021 15:00	320	2	9.8	8.5	8000	1013
1/29/2021 18:00	350	1	9.6	8.2	9999	1013
1/29/2021 21:00	360	1	9.6	7.9	9999	1011
1/30/2021 00:00	0	0	9.2	8.3	9999	1010
1/30/2021 03:00	310	1	9.2	8.3	9999	1009
1/30/2021 06:00	300	1	9.8	8.7	6000	1008
1/30/2021 09:00	350	2	12.3	9.5	9999	1008
1/30/2021 12:00	360	2	12.6	9.4	9999	1008
1/30/2021 15:00	120	3	10.5	8.9	9999	1010
1/30/2021 18:00	350	3	10.0	9.4	9999	1012
1/30/2021 21:00	250	2	8.7	7.8	9999	1012

Table a-4. 3-hourly and some hourly temperature, dewpoint temperature, wind speed and wind direction over Anzali station (Lon 49.46E, Lat 37.48N; leeward) from 00:00 UTC 4 February to 21:00 UTC 6 February 2021. Foehn conditions were shaded gray.

Date	Wind direction (degree)	Wind speed (m/s)	Temperature (°C)	Dewpoint (°C)	Visibility (m)	Pressure (mb)

2/4/2021 00:00	10	1	8.1	7.8	4000	1018
2/4/2021 03:00	0	0	7.8	7.3	4000	1019
2/4/2021 06:00	170	1	8.4	7.5	1000	1019
2/4/2021 09:00	100	1	9.5	7.8	3000	1018
2/4/2021 12:00	10	1	10.3	8.2	4000	1017
2/4/2021 15:00	100	1	9.2	8.4	5000	1017
2/4/2021 18:00	130	2	9.1	8.5	5000	1016
2/4/2021 21:00	170	1	8.9	8.4	7000	1013
2/5/2021 00:00	200	1	7.8	7.8	3000	1012
2/5/2021 03:00	120	2	8.6	8.6	100	1010
2/5/2021 06:00	340	3	10.6	10.6	400	1011
2/5/2021 07:00	0	0	12	12	500	1010
2/5/2021 08:00	0	0	15	12	1000	1009
2/5/2021 09:00	30	2	15	12.1	4000	1009
2/5/2021 12:00	10	1	17.2	11.0	6000	1006
2/5/2021 13:00	0	0	15	11	6000	1006
2/5/2021 14:00	190	2	21	9	6000	1006
2/5/2021 15:00	300	3	13.5	11	6000	1008
2/5/2021 18:00	310	4	12.4	11.1	5000	1010
2/5/2021 21:00	340	3	12.3	10.8	5000	1016
2/6/2021 00:00	210	1	11.5	10.7	7000	1018
2/6/2021 03:00	190	2	11.2	10.9	5000	1020
2/6/2021 06:00	200	2	11.4	10.5	8000	1021
2/6/2021 09:00	190	2	15	9.8	9999	1020
2/6/2021 12:00	90	2	13.9	10.9	9999	1018
2/6/2021 15:00	90	3	11.8	10.2	9999	1018
2/6/2021 18:00	120	1	11.3	10.5	9999	1018
2/6/2021 21:00	0	0	10.0	9.7	9999	1016

Table a-5. 3-hourly temperature, dewpoint temperature, wind speed and wind direction over Tehran station (Lon 51.31E, Lat 35.69N; windward) from 00:00 UTC 13 January to 21:00 UTC 16 January 2021. Foehn conditions were shaded gray.

Date	Wind direction (degree)	Wind speed (m/s)	Temperature (°C)	Dewpoint (°C)	Visibility (m)	Cloudiness	Pressure (mb)
1/13/2021 00:00	0	0	2.2	-5.2	3500	NSC	1025.9
1/13/2021 03:00	310	2	1.1	-5.2	3500	NSC	1027.4

1/13/2021 06:00	0	0	5.5	-5.2	5000	NSC	1027.6
1/13/2021 09:00	0	0	9.5	-5.2	3000	NSC	1024.4
1/13/2021 12:00	160	3	10.6	-5.4	2500	NSC	1022.4
1/13/2021 15:00	170	2	7.0	-6.0	4000	NSC	1023.8
1/13/2021 18:00	210	2	4.5	-5.0	5000	NSC	1023.1
1/13/2021 21:00	340	2	3.7	-4.7	5000	NSC	1021.4
1/14/2021 00:00	280	2	2.2	-4.8	4000	NSC	1020.8
1/14/2021 03:00	0	0	2.2	-4.3	4000	NSC	1021.0
1/14/2021 06:00	150	2	5.9	-5.4	5000	FEW100 BKN190	1021.5
1/14/2021 09:00	200	3	9.8	-6.5	4000	FEW100 SCT190	1018.5
1/14/2021 12:00	180	3	9.2	-5.1	3000	SCT100 BKN190	1016.9
1/14/2021 15:00	170	3	6.8	-5.9	3000	SCT100 BKN190	1017.4
1/14/2021 18:00	270	3	5.9	-7.3	4000	SCT100 BKN190	1017.7
1/14/2021 21:00	290	3	5.8	-6.8	4000	SCT100 BKN190	1016.2
1/15/2021 00:00	0	0	5.7	-7.5	5000	SCT100 BKN190	1015.5
1/15/2021 03:00	0	0	4.6	-6/0	6000	BKN100 BKN190	1016.0
1/15/2021 06:00	230	2	7.8	-8.7	6000	FEW110 SCT190	1016.4
1/15/2021 09:00	240	3	9.8	-9.3	5000	BKN100	1014.8
1/15/2021 12:00	150	2	11.7	-12.5	6000	FEW040 BKN100	1013.7
1/15/2021 15:00	210	3	8.3	-9.6	4000	FEW040 SCT100	1016.8
1/15/2021 18:00	300	2	6.6	-7.8	8000	FEW040	1017.2
1/15/2021 21:00	330	2	6.0	-6.9	9999	NSC	1016.7
1/16/2021 00:00	310	2	5.4	-5.3	9999	NSC	1017.1
1/16/2021 03:00	310	2	4.4	-5.4	9999	NSC	1018.7
1/16/2021 06:00	220	2	10.8	-8.4	8000	NSC	1019.3
1/16/2021 09:00	150	2	14.7	-5.6	5000	NSC	1016.2

1/16/2021 12:00	240	3	14.8	-8.6	9999	NSC	1014.6
1/16/2021 15:00	130	4	11.3	-5.6	9999	NSC	1016.3
1/16/2021 18:00	180	2	8.9	-4.3	9999	NSC	1015.3
1/16/2021 21:00	320	2	5.8	-3.8	8000	NSC	1013.5

Table a-6. 3-hourly temperature, dewpoint temperature, wind speed and wind direction over Tehran station (Lon 51.31E, Lat 35.69N; windward) from 00:00 UTC 17 January to 21:00 UTC 19 January 2021. Foehn conditions were shaded gray.

Date	Wind direction (degree)	Wind speed (m/s)	Temperature (°C)	Dewpoint (°C)	Visibility (m)	Cloudiness	Pressure (mb)
1/17/2021 00:00	0	0	4.7	-4.3	9999	NSC	1011.3
1/17/2021 03:00	300	3	5.9	-6.7	8000 6000	BKN100 FEW040	1012.1
1/17/2021 06:00	0	0	7.6	-5.1	5000	BKN100 FEW040	1012.5
1/17/2021 09:00	270	2	10	-6.8	6000	BKN100 FEW035 FEW040CB	1010.8
1/17/2021 12:00	260	5	10.8	-4.8		BKN100	1010.1
1/17/2021 15:00	270	2	7.4	-1.8	9999	FEW035	1011.1
1/17/2021 18:00	270	2	6.9	-3.3	9999	FEW035 SCT100	1011.4
1/17/2021 21:00	290	3	6.1	-2	9999	FEW035 SCT100	1010.5
1/18/2021 00:00	300	3	6.8	-6.9	9999	FEW035	1010.1
1/18/2021 03:00	270	5	3.9	-4.8	9999	FEW035	1012.7
1/18/2021 06:00	160	2	10.1	-4.3	9999	FEW035 SCT100	1013.1
1/18/2021 09:00	280	8	12.9	-7.2	9999	FEW035	1011.4
1/18/2021 12:00	270	10	12.7	-5.3	9999	FEW035TCU	1011.3
1/18/2021 15:00	320	3	10.3	-5.7	9999	FEW035 SCT100	1014.2
1/18/2021 18:00	300	3	9.3	-5.4	9999	FEW040	1013.9
1/18/2021 21:00	300	5	9.3	-5.8	9999	FEW040	1013.8
1/19/2021 00:00	280	4	7.5	-4.3	9999	SCT040	1015.8
1/19/2021 03:00	280	5	7.3	-8.3	9999	FEW040	1017.3

1/19/2021 06:00	60	2	10.4	-9.3	9999	NSC	1018
1/19/2021 09:00	220	6	12.2	-8.3	9999	NSC	1016.2
1/19/2021 12:00	210	3	12.7	-9.7	9999	FEW040	1014.9
1/19/2021 15:00	140	2	10.8	-7.9	9999	NSC	1016
1/19/2021 18:00	0	0	8.9	-7.3	9999	NSC	1016.4
1/19/2021 21:00	0	0	6.6	-7.0	9999	NSC	1015.9

Table a-7. 3-hourly temperature, dewpoint temperature, wind speed and wind direction over Tehran station (Lon 51.31E, Lat 35.69N; windward) from 00:00 UTC 27 January to 21:00 UTC 30 January 2021. Foehn conditions were shaded gray.

Date	Wind direction	Wind speed (m/s)	Temperature (°C)	Dewpoint (°C)	Visibility (m)	Cloudiness	Pressure (mb)
1/27/2021 00:00	0	0	1.4	-7.6	7000	NSC	1022.8
1/27/2021 03:00	280	2	0.6	-7.4	7000	NSC	1023.7
1/27/2021 06:00	0	0	7.0	-7.8	6000	NSC	1024.1
1/27/2021 09:00	180	2	10.3	-9.6	3500	NSC	1023.1
1/27/2021 12:00	200	2	13.2	-13.7	5000	NSC	1020.4
1/27/2021 15:00	0	0	9.2	-10.9	8000	NSC	1021.8
1/27/2021 18:00	0	0	5.7	-7.9	8000	NSC	1022.2
1/27/2021 21:00	0	0	4.6	-6.9	8000	NSC	1020.8
1/28/2021 00:00	270	2	2.8	-6.6	8000	NSC	1020.0
1/28/2021 03:00	0	0	3.8	-5.4	8000	FEW100 SCT200	1020.1
1/28/2021 06:00	180	2	7.6	-7.6	5000	NSC	1020.2
1/28/2021 09:00	180	3	11.2	-7.6	5000	NSC	1018.4
1/28/2021 12:00	120	4	12.7	-8.5	7000	NSC	1016.9
1/28/2021 15:00	0	0	9.0	-7.6	6000	SCT100	1018.0
1/28/2021 18:00	170	2	7.4	-8.6	6000	SCT040 BKN100	1018.5
1/28/2021 21:00	290	2	6.7	-8.4	6000	SCT040 BKN100	1017.6
1/29/2021 00:00	290	2	6.8	-7.6	7000	SCT040 OVC100	1016.9
1/29/2021 03:00	0	0	7.0	-9.4	8000	SCT040 BKN100	1017.6
1/29/2021 06:00	250	3	7.3	-7.9	8000	FEW035CB	1018.7

						SCT040 BKN100	
1/29/2021 09:00	0	0	12	-8	4000	FEW040 SCT100	1016.0
1/29/2021 12:00	170	3	12.7	-4.9	4000	FEW040 SCT100 BKN180	1013.4
1/29/2021 15:00	130	3	9.8	-8.3	6000	SCT040 BKN100	1016.2
1/29/2021 18:00	60	4	8.2	3.3	6000	SCT035 OVC090	1015.5
1/29/2021 21:00	50	4	7.4	2.5	9999	SCT035 BKN090	1011.4
1/30/2021 00:00	110	3	9.4	3.2	9999	SCT035 BKN100	1008.9
1/30/2021 03:00	320	2	6.2	4.5	4000	FEW025 FEW030CB SCT035 OVC080	1012.6
1/30/2021 06:00	120	3	9.0	3.2	9999	SCT030 BKN090	1012.8
1/30/2021 09:00	230	2	11.3	2.3	9999	FEW030TCU FEW035 BKN090	1011.6
1/30/2021 12:00	250	10	10.9	-2.5	9999	SCT030 FEW035CB SCT090	1011.8
1/30/2021 15:00	220	3	9.3	-0.3	9999	SCT035 SCT200	1011.6
1/30/2021 18:00	300	9	8.3	-8.7	9999	FEW035	1013.7
1/30/2021 21:00	280	6	5.3	-7.9	9999	NSC	1013.4

Table a-8. 3-hourly temperature, dewpoint temperature, wind speed and wind direction over Tehran station (Lon 51.31E, Lat 35.69N; windward) from 00:00 UTC 4 February to 21:00 UTC 6 February 2021. Foehn conditions were shaded gray.

Date	Wind direction	Wind speed	Temperature (°C)	Dewpoint (°C)	Visibility (m)	Cloudiness	Pressure (mb)

	(degree)	(m/s)					
2/4/2021 00:00	330	2	6.2	-2.9	5000	NSC	1020.0
2/4/2021 03:00	300	2	7.3	-4.4	5000	NSC	1020.7
2/4/2021 06:00	0	0	12.2	-4.9	7000	NSC	1021.1
2/4/2021 09:00	190	3	13.6	-5.0	7000	NSC	1020.5
2/4/2021 12:00	240	4	15.7	-5.4	8000	NSC	1018.7
2/4/2021 15:00	180	3	13.4	-4.3	8000	NSC	1018.8
2/4/2021 18:00	80	2	11.4	-4.7	8000	NSC	1019.4
2/4/2021 21:00	0	0	9.2	-4.4	8000	NSC	1019.1
2/5/2021 00:00	310	2	8.1	-4.7	8000	NSC	1017.9
2/5/2021 03:00	0	0	8.9	-4.0	8000	SCT100 BKN200	1018.1
2/5/2021 06:00	310	3	10.2	-2.5	5000	FEW040 SCT100 BKN200	1020.4
2/5/2021 09:00	300	2	15.0	-0.3	8000	SCT035 BKN090	1017.5
2/5/2021 12:00	330	2	12.7	4.9	9999	SCT030 FEW035CB BKN090	1015.2
2/5/2021 15:00	260	2	9.8	5.6	6000	SCT030 OVC090	1017.3
2/5/2021 18:00	0	0	9.6	6.9	5000	SCT035 OVC090	1017.3
2/5/2021 21:00	350	2	9.2	5.4	7000	SCT035 OVC090	1015.1
2/6/2021 00:00	270	3	9.8	4.6	8000	FEW030CB SCT035 OVC090	1015.2
2/6/2021 03:00	300	4	11.5	3.0	9999	SCT035 OVC100	1015.5
2/6/2021 06:00	280	6	11.1	2.9	9999	FEW030CB SCT035 OVC100	1017.7
2/6/2021 09:00	310	4	12.2	2.9	9999	FEW030CB SCT035 BKN100	1016.3

	330	3	11.2	3.3	9999	SCT035	1016.2
2/6/2021 12:00						OVC100	
	340	3	9.3	5.1	8000	FEW030CB	1016.7
						SCT035	
2/6/2021 15:00						OVC100	
2/6/2021 18:00	0	0	10.0	4.2	9999	SCT035	1016.3
						BKN090	
2/6/2021 21:00	260	2	9.2	5.6	9999	SCT040	1015.5
						BKN090	

Table a-9. 3-hourly temperature, dewpoint temperature, wind speed and wind direction over Zanjan station (Lon 48.52E, Lat 36.66N; windward) from 00:00 UTC 13 January to 21:00 UTC 16 January 2021. Foehn conditions were shaded gray.

Date	Wind direction (degree)	Wind speed (m/s)	Temperature (°C)	Dewpoint (°C)	Visibility (m)	Cloudiness	Pressure (mb)
1/13/2021 00:00	100	1	-1	-4.2	9999	NSC	1023.1
1/13/2021 03:00	80	2	-1.1	-3.9	9999	NSC	1026.4
1/13/2021 06:00	90	1	5.2	-2.9	9999	NSC	1025.8
1/13/2021 09:00	110	3	12.9	-1.1	9999	NSC	1020.5
1/13/2021 12:00	80	3	14.3	-1.0	9999	NSC	1018.6
1/13/2021 15:00	100	2	5.9	-0.8	9999	NSC	1021.6
1/13/2021 18:00	90	2	2.9	-2.8	9999	NSC	1020.1
1/13/2021 21:00	100	2	0.9	-3.4	9999	NSC	1017.1
1/14/2021 00:00	90	2	1.9	-3.4	9999	NSC	1014.7
1/14/2021 03:00	100	2	1.8	-3.9	9999	NSC	1017.2
1/14/2021 06:00	100	1	6.3	-3.4	9999	NSC	1017.1
1/14/2021 09:00	110	2	14.5	-10.3	9999	NSC	1012.4
1/14/2021 12:00	120	2	12.2	-4.9	9999	NSC	1009.6
1/14/2021 15:00	100	2	5.3	-5.1	9999	NSC	1013.2
1/14/2021 18:00	110	2	3.0	-4.5	9999	NSC	1013.5
1/14/2021 21:00	110	1	2.0	-7.1	9999	NSC	1010.0
1/15/2021 00:00	70	1	3.4	-12.6	9999	NSC	1010.0
1/15/2021 03:00	110	1	2.3	-9.0	9999	NSC	1011.6
1/15/2021 06:00	200	3	6.2	-7.4	9999	FEW020	1013.0
						SCT035	
						BKN080	

1/15/2021 09:00	200	6	7.4	-1.8	9999	SCT035	1010.5
1/15/2021 12:00	240	5	9.0	-1.7	9999	SCT035	1010.4
1/15/2021 15:00	220	1	4.7	-1.1	9999	FEW035	1016.2
1/15/2021 18:00	200	1	3.3	-2.1	9999	NSC	1016.8
1/15/2021 21:00	0	0	1.1	-2.3	9999	NSC	1017.6
1/16/2021 00:00	90	1	0.1	-2.4	9999	FEW035	1017.4
1/16/2021 03:00	80	1	0.5	-2.6	9999	NSC	1019.6
1/16/2021 06:00	110	1	6.3	-2.1	9999	FEW035 SCT200	1019.2
1/16/2021 09:00	130	2	9.7	-1.4	9999	FEW035 BKN200	1017.5
1/16/2021 12:00	200	2	9.7	-3.3	9999	FEW035 BKN200	1015.5
1/16/2021 15:00	110	1	2.8	-3.5	9999	FEW035 BKN200	1017.5
1/16/2021 18:00	90	2	1.6	-2.4	9999	NSC	1015.0
1/16/2021 21:00	90	1	0.9	-2.8	9999	NSC	1012.8

Table a-10. 3-hourly temperature, dewpoint temperature, wind speed and wind direction over Zanjan station (Lon 48.52E, Lat 36.66N; windward) from 00:00 UTC 17 January to 21:00 UTC 19 January 2021. Foehn conditions were shaded gray.

Date	Wind direction (degree)	Wind speed (m/s)	Temperature (°C)	Dewpoint (°C)	Visibility (m)	Cloudiness	Pressure (mb)
1/17/2021 00:00	90	1	0	-3.6	9999	NSC	1011.8
					9999	FEW030CB SCT035	
1/17/2021 03:00	90	2	0.9	-2.8		BKN090	1013.0
					9999	SCT035	
1/17/2021 06:00	130	1	5.0	-1.7		SCT080	1012.3
					9999	FEW030CB SCT035	
1/17/2021 09:00	230	4	7.1	-2.4		SCT080	1010.2
					9999	FEW030CB SCT035	
1/17/2021 12:00	260	4	6.3	-4.5		SCT080	1010.1
1/17/2021 15:00	200	1	3.4	-4.1	9999	FEW035	1011.5

1/17/2021 18:00	0	0	-0.5	-4.8	9999	FEW035	1012.3
1/17/2021 21:00	240	3	3.7	-3.1	9999	FEW035	1009.8
1/18/2021 00:00	130	1	2.3	-4.0	9999	FEW035 SCT080	1011.6
1/18/2021 03:00	210	2	2.7	-4.8	9999	FEW035 SCT080	1013.1
1/18/2021 06:00	210	2	5.6	-3.0	9999	FEW035 SCT080	1014.0
1/18/2021 09:00	220	4	6.0	-2.1	9999	FEW025 SCT030CB SCT080	1011.6
1/18/2021 12:00	230	3	9.8	-3.2	9999	FEW025 FEW030CB SCT035	1010.9
1/18/2021 15:00	210	6	4.8	-3.5	9999	FEW030CB SCT035	1014.0
1/18/2021 18:00	210	1	3.0	-3.0	9999	FEW030CB FEW035	1014.7
1/18/2021 21:00	220	2	3.5	-3.8	9999	FEW030CB FEW035	1015.1
1/19/2021 00:00	180	1	1.4	-3.3	9999	FEW035	1016.8
1/19/2021 03:00	140	1	1.7	-3.8	9999	FEW035	1019.1
1/19/2021 06:00	130	2	4.8	-4.0	9999	FEW035	1018.7
1/19/2021 09:00	170	3	7.8	-4.3	9999	FEW015 FEW030CB	1015.6
1/19/2021 12:00	180	3	7.0	-6.4	9999	FEW030CB SCT035	1014.4
1/19/2021 15:00	200	3	5.2	-6.4	9999	FEW035	1014.8
1/19/2021 18:00	180	1	1.1	-6.5	9999	FEW035	1016.9
1/19/2021 21:00	0	0	0.7	-7.1	9999	FEW035	1015.7

Table a-11. 3-hourly temperature, dewpoint temperature, wind speed and wind direction over Zanjan station (Lon 48.52E, Lat 36.66N; windward) from 00:00 UTC 27 January to 21:00 UTC 30 January 2021. Foehn conditions were shaded gray.

Date	Wind direction	Wind speed (m/s)	Temperature (°C)	Dewpoint (°C)	Visibility (m)	Cloudiness	Pressure (mb)

1/27/2021 00:00	90	1	-5.8	-8.7	9999	NSC	1026.1
1/27/2021 03:00	0	0	-7.7	-10.0	9999	NSC	1030.2
1/27/2021 06:00	130	1	-0.8	-6.4	9999	NSC	1028.9
1/27/2021 09:00	110	2	9.0	-6.4	9999	NSC	1024.5
1/27/2021 12:00	140	1	10.0	-8.1	9999	NSC	1021.9
1/27/2021 15:00	250	2	2.1	-3.8	9999	NSC	1026.3
1/27/2021 18:00	110	1	-1.2	-5.1	9999	NSC	1024.8
1/27/2021 21:00	80	2	0.8	-6.1	9999	NSC	1019.6
1/28/2021 00:00	80	1	1.7	-6.4	9999	NSC	1018.0
1/28/2021 03:00	90	2	1.2	-6.8	9999	NSC	1020.2
1/28/2021 06:00	100	2	4.3	-6.0	9999	FEW040 SCT080 BKN180	1020.7
1/28/2021 09:00	110	2	12.6	-3.3	9999	FEW035TCU SCT035	1014.8
1/28/2021 12:00	190	3	11.5	-3.4	9999	FEW035TCU SCT035	1013.9
1/28/2021 15:00	120	3	3.6	2.1	7000	FEW020 BKN035 OVC080	1018.9
1/28/2021 18:00	0	0	3.0	1.4	9999	FEW020 SCT035 BKN080	1017.9
1/28/2021 21:00	40	2	4.9	0.7	9999	FEW015 FEW030CB BKN035	1013.3
1/29/2021 00:00	0	0	5.2	0.4	9999	FEW020 BKN035	1012.6
1/29/2021 03:00	100	1	4.1	0.1	9999	FEW020 BKN035	1015.3
1/29/2021 06:00	190	3	6.6	1.1	9999	FEW020 FEW030CB SCT035	1015.6
1/29/2021 09:00	210	6	9.8	0.7	9999	FEW020 FEW030CB SCT035	1012.0
1/29/2021 12:00	220	6	11.2	-3.7	9999	FEW030CB	1009.4

						FEW035	
1/29/2021 15:00	0	0	4.0	-5.0	9999	FEW030	1012.7
1/29/2021 18:00	100	1	4.4	-2.3	9999	FEW030	1011.1
1/29/2021 21:00	110	2	3.1	1.3	7000	FEW030CB	1008.9
						SCT035	
						OVC080	
1/30/2021 00:00	80	2	1.4	1.1	7000	FEW030CB	1008.4
						SCT035	
						OVC080	
1/30/2021 03:00	0	0	3.0	-4.6	9999	SCT020	1009.4
						BKN035	
						BKN080	
1/30/2021 06:00	210	4	3.2	-2.3	9999	FEW020	1011.9
						FEW030CB	
						SCT030	
1/30/2021 09:00	230	4	3.7	-3.8	9999	FEW030CB	1012.4
						SCT030	
1/30/2021 12:00	250	6	3.6	-6.7	9999	FEW030CB	1013.5
						BKN030	
1/30/2021 15:00	240	6	0.6	-7.9	9999	FEW025	1014.7
1/30/2021 18:00	230	3	-1.3	-7.2	9999	FEW035	1017.9
1/30/2021 21:00	30	1	-2.8	-7.7	9999	FEW035	1018.2

Table a-12. 3-hourly temperature, dewpoint temperature, wind speed and wind direction over Zanjan (Lon 48.52E, Lat 36.66N; windward) station from 00:00 UTC 4 February to 21:00 UTC 6 February 2021. Foehn conditions were shaded gray.

Date	Wind direction (degree)	Wind speed (m/s)	Temperature (°C)	Dewpoint (°C)	Visibility (m)	Cloudiness	Pressure (mb)
2/4/2021 00:00	100	1	-0.5	-3.5	9999	NSC	1019.9
2/4/2021 03:00	100	1	-1.3	-4.3	9999	NSC	1023.7
2/4/2021 06:00	90	2	4.4	-1.6	9999	NSC	1024.2
2/4/2021 09:00	0	0	12.4	-4.8	9999	NSC	1021.4
2/4/2021 12:00	230	1	15	-3.4	9999	NSC	1018.8
2/4/2021 15:00	240	1	7.9	-0.8	9999	NSC	1021.8
2/4/2021 18:00	90	1	5.6	-2.5	9999	NSC	1020.6
2/4/2021 21:00	120	1	5.2	-2.2	9999	NSC	1016.7

					9999	SCT035	
2/5/2021 00:00	130	1	4.8	-1.6		BKN080	1014.9
					8000	SCT035	
2/5/2021 03:00	180	2	6.1	2.2		BKN080	1016.8
					9999	SCT025	
						SCT035	
2/5/2021 06:00	0	0	7.1	2.0		OVC090	1018.5
					9999	SCT025	
						FEW030CB	
						SCT035	
2/5/2021 09:00	210	2	8.1	3.4		OVC080	1017.3
						SCT025	
						FEW030CB	
						SCT035	
2/5/2021 12:00	300	2	7.0	2.5	7000	OVC070	1016.0
					9999	SCT025	
						FEW030CB	
						SCT035	
2/5/2021 15:00	110	3	5.8	2.4		OVC070	1015.9
2/5/2021 18:00	90	3	6.7	2.6	9999	SCT025	1015.6
						FEW030CB	
						SCT035	
						BKN070	
2/5/2021 21:00	170	2	6.3	2.4	9000	SCT025	1015.1
						FEW030CB	
						SCT035	
						BKN070	
	260	2	5.5	2.7	7000	SCT017	1016.0
						FEW030CB	
						SCT035	
2/6/2021 00:00						OVC070	
	0	0	2.9	2.2	4000	SCT017	1018.2
						FEW030CB	
						SCT035	
2/6/2021 03:00						OVC070	
	250	1	0.5	0.5	4000	SCT015	1021.3
2/6/2021 06:00						FEW030CB	

						SCT035	
						OVC060	
	100	1	2.4	2.0	8000	SCT015	1020.0
						FEW030CB	
						SCT035	
2/6/2021 09:00						OVC060	
	120	1	4.6	2.9	8000	SCT015	1017.9
						FEW030CB	
						SCT035	
2/6/2021 12:00						OVC060	
	0	0	4.0	2.6	9999	SCT020	1019.5
						BKN035	
2/6/2021 15:00						BKN080	
2/6/2021 18:00	0	0	3.5	2.8	9999	SCT020	1021.0
						BKN035	
						BKN080	
2/6/2021 21:00	110	1	3.2	2.6	9999	SCT020	1019.7
						BKN035	
						BKN080	

Table a-13. Namelist of WPS (namelist.wps) used in this study.

```
&share
 wrf_core = 'ARW',
 max_dom =3,
 start_date = '2021-01-17_12:00:00','2021-01-17_12:00:00','2021-01-17_12:00:00'
 end_date   = '2021-01-19_12:00:00','2021-01-19_12:00:00','2021-01-19_12:00:00'
 interval_seconds =10800
 io_form_geogrid = 2,
/

&geogrid
 parent_id         =   1,   1,  2,
 parent_grid_ratio =   1,   3,  3,
 i_parent_start    = 1,55,44,
 j_parent_start    = 1,35,68,
 e_we          = 125,160,217,
 e_sn          = 116,163,145,
 geog_data_res     = '10m','2m', '30s',
 dx = 45000,
 dy = 45000,
 map_proj = 'lambert',
 ref_lat   = 34.183,
 ref_lon   = 42.022,
 truelat1  = 34.183,
```

```
 truelat2  = 34.183,
 stand_lon = 42.022,
 geog_data_path = '/home/sepehr64/geog_data',
/

&ungrib
 out_format = 'WPS',
 prefix = 'FILE',
/

&metgrid
 fg_name = 'FILE'
 io_form_metgrid = 2,
/
```

Table a-14. Namelist of WRF (namelist.input) used in this study.

```
&time_control
 run_days                            =0,
 run_hours                           = 48,
 run_minutes                         = 0,
 run_seconds                         = 0,
 start_year     =        2021 2021,2021
 start_month    =         01,01,01
 start_day      =        17,17,17
 start_hour     =        12,12,12
 start_minute                  = 00,   00,   00,
 start_second                  = 00,   00,   00,
 end_year     =          2021 2021,2021
 end_month    =           01,01,01
 end_day      =          19,19,19
 end_hour     =          12,12,12
 end_minute                    = 00,   00,   00,
 end_second                    = 00,   00,   00,
 interval_seconds              =10800
 input_from_file               = .true.,.true.,.true.,
 history_interval              =180,60,60,
 frames_per_auxhist2 = 1000,1000,
 frames_per_outfile            = 1000, 1000, 1000,
 restart                       = .false.,
 restart_interval              = 5000,
 io_form_history               = 2
 io_form_restart               = 2
 io_form_input                 = 2
 io_form_boundary              = 2
 debug_level                   = 0
 /

 &domains
 time_step                     = 150,
 time_step_fract_num           = 0,
 time_step_fract_den           = 1,
 max_dom                       =3,
e_we                = 125,     160,     217,
```

```
e_sn                    = 116,      163,      145,
e_vert                  = 30,       30,       30,
p_top_requested         = 5000,
num_metgrid_levels      = 34,
num_metgrid_soil_levels  = 4,
dx                      = 45000,    15000,     5000,
dy                      = 45000,    15000,     5000,
grid_id                  = 1,        2,        3,
parent_id                = 1,        1,        2,
i_parent_start           = 1,       55,       44,
j_parent_start           = 1,       35,       68,
parent_grid_ratio        = 1,        3,        3,
parent_time_step_ratio   = 1,        3,        3,
feedback                 = 1,
smooth_option            = 0,
/

 &physics
 mp_physics                     = 2,     2,     2,
 ra_lw_physics                   = 1,     1,     1,
 ra_sw_physics                   = 1,     1,     1,
 radt                           = 30,    30,    30,
 sf_sfclay_physics               = 2,     2,     2,
 sf_surface_physics              = 2,     2,     2,
 bl_pbl_physics                  = 5,     5,     5,
 bldt                           = 0,     0,     0,
 cu_physics                      = 1,     1,     0,
 cudt                           = 5,     5,     5,
 isfflx                         = 1,
 ifsnow                          = 1,
 icloud                          = 1,
 surface_input_source            = 1,
 num_soil_layers                 = 4,
 sf_urban_physics                = 0,     0,     0,
 /

 &fdda
 /

 &dynamics
 w_damping                       = 0,
 diff_opt                       = 1,      1,      1,
 km_opt                         = 4,      4,      4,
 diff_6th_opt                    = 0,      0,      0,
 diff_6th_factor                 = 0.12,   0.12,   0.12,
 base_temp                       = 290.
 damp_opt                        = 0,
 zdamp                          = 5000.,  5000.,  5000.,
 dampcoef                        = 0.2,    0.2,    0.2
 khdif                          = 0,      0,      0,
 kvdif                          = 0,      0,      0,
 non_hydrostatic                 = .true., .true., .true.,
 moist_adv_opt                   = 1,      1,      1,
 scalar_adv_opt                  = 1,      1,      1,
 /
```

```
&bdy_control
spec_bdy_width                = 5,
spec_zone                     = 1,
relax_zone                    = 4,
specified                     = .true., .false.,.false.,
nested                        = .false., .true., .true.,
/

&grib2
/

&namelist_quilt
nio_tasks_per_group = 0,
nio_groups = 1,
/
```